



Strål
säkerhets
myndigheten

Swedish Radiation Safety Authority

Authors:

Digby D. Macdonald
Samin Sharifi-Asl

Research

2011:09

Is Copper Immune to Corrosion
When in Contact With Water
and Aqueous Solutions?

SSM perspective

Background

The KBS-3 concept implies that spent nuclear fuel is placed in copper canisters surrounded by clay and finally placed approximately 500 m down from surface into granitic bedrock, in order to isolate the spent nuclear fuel from humans and environment for very long time scales (i.e. millions of years). The concept is based on the multi-barrier principle, in this respect the barriers are the copper canister, clay material and finally the granitic bedrock. All barriers will work alone and together in order to retard the spent nuclear fuel to enter into the biosphere. In this report it is only degradation of the first barrier, the copper canister that is considered.

The mechanisms of copper corrosion in the planned repository for spent nuclear fuel according to the KBS-3 concept need to be fully understood in order to review the license application in an authoritative way. Copper as a canister material was chosen by SKB already 1978 in the KBS-2 report. The main reasons for selecting copper were 1) copper is thermodynamically immune in the presence of pure anoxic water, and 2) copper has sufficient mechanical strength to resist all plausible mechanical loads present in the repository. Thermodynamically, immunity of copper in pure anoxic water implies that copper will not corrode in the presence of pure anoxic water. The reason for why copper cannot corrode in the immune state is that this will cause a positive change in the Gibbs Energy. This contradicts the second law of thermodynamics, which states that for a spontaneous reaction to occur the change in Gibbs Energy has to be negative.

The water present at the repository depth in the proposed site at Forsmark is of course not pure water. At repository depth different dissolved species like sulphide in the water will cause corrosion of copper. It is a fact that the reaction between copper and sulphide occurs under a negative change in Gibbs Energy, this was also recognized by SKB in the KBS-2 report. The rate of copper corrosion at repository depth will hence be controlled by either the rate of transport of corroding species to the canister or the rate of transport of corrosion products from the copper surface, or both.

Objectives

The aim of this project has been to increase knowledge and to contribute to the research community in the area of copper corrosion in a repository environment. For SSM, the most important subject is to provide better conditions for a science based evaluation of a repository for spent nuclear fuel. In this respect, this project aimed at conducting a comprehensive theoretical study on corrosion of copper in repository environment based on an expected composition of dissolved species in the groundwater in the Forsmark area. In addition the thermodynamic immunity of copper in pure anoxic water has been especially addressed as this was one of the initial conditions made by SKB for selecting copper as canister material.

Results

The authors have shown, in so-called corrosion Domain Diagrams, that copper in a thermodynamic sense can be considered as immune in pure anoxic water (without dissolved oxygen) only under certain conditions. It is shown that copper will corrode in pure anoxic water with very low concentrations of $[Cu^+]$ and very low partial pressures of hydrogen gas. At higher concentrations of $[Cu^+]$ and partial pressures of hydrogen, copper is found to be thermodynamically immune and will not corrode. The rate of copper corrosion in the repository water environment will thus depend on the transport of corrosion products away from the copper surface or the transport of corroding species to the copper surface. The degree to which this affects the corrosion of copper canisters in the repository environment has not been further studied. Still, the result shows that copper cannot be considered as thermodynamically immune in the presence of pure anoxic water, this implicate that one of SKB:s initial conditions for selecting copper as a canister material can be questioned. To what degree this may influence the corrosion of copper canisters in the repository environment still needs to be investigated.

Of other species present in the water at repository depth in Forsmark, different sulphur species was found to be most deleterious causing copper to corrode in an anoxic environment under hydrogen gas evolution. In order to find out what species that can be present in a repository environment a Gibbs Energy Minimisation algorithm was employed. By this method it was concluded that (S^{2-} , HS^- and H_2S) are predicted to be present in the entire anoxic period at sufficient concentrations to cause corrosion of copper. It is finally concluded that the corrosion rate of copper canisters will be determined by the very complex interaction between copper, buffer material and bedrock in order to reduce corrosion of copper to an acceptable level.

Need for further research

In order to provide a better understanding of copper corrosion processes more work is needed to understand the system that forms complexes with copper in an expanded concentration interval of species in groundwater. The evolution of corrosion damage during the lifetime of the repository need to be understood more in detail before a realistic assessment of copper corrosion in repository environment can be made.

Project information

Contact person SSM: Jan Linder

Reference: SSM 2010/531



Strål
säkerhets
myndigheten

Swedish Radiation Safety Authority

Authors: Digby D. Macdonald and Samin Sharifi-Asl
Center for Electrochemical Science and Technology
Department of Materials Science and Engineering
Pennsylvania State University, USA

2011:09

Is Copper Immune to Corrosion When in Contact With Water and Aqueous Solutions?

Date: March 2011

Report number: 2011:09 ISSN: 2000-0456

Available at www.stralsakerhetsmyndigheten.se

This report concerns a study which has been conducted for the Swedish Radiation Safety Authority, SSM. The conclusions and viewpoints presented in the report are those of the author/authors and do not necessarily coincide with those of the SSM.

Table of Contents

Executive Summary.....	7
I. Introduction.....	12
II. Thermodynamic Data for Copper and Sulfur Species.....	13
III. Corrosion Domain Diagrams.....	15
IV. Volt-Equivalent Diagrams	30
V. Hydrogen Pressure.....	34
VI. Simulation of the Repository-Gibbs Energy Minimization Studies.....	66
VII. Definition of the Corrosion Evolutionary Path.....	95
VIII. Summary and Conclusions.....	115
Appendix I: Corrosion Domain Diagrams.....	120
Appendix II: Volt-Equivalent Diagrams.....	203

List of Figures

Figure 1: Corrosion domain diagram for copper in water as a function of temperature.....	16
Figure 2: Corrosion domain diagram for copper in water + HS^- as a function of temperature.....	18
Figure 3: Corrosion Domain Diagram for copper in the presence of the polysulfide, S_3^{2-}	20
Figure 4: Structure of the trithiosulfate anion.....	20
Figure 5: Corrosion Domain Diagram for copper in the presence of $HS_3O_3^-$. Note that this species is a powerful activator of copper.....	22
Figure 6: Corrosion Domain Diagram for copper in the presence of $S_4O_3^{2-}$. Note that this species is predicted not to activate copper.....	23
Figure 7: Volt-Equivalent Diagram for sulfur in Forsmark ground water, $pH = 7$, $[S] = 10$ ppm, $25^\circ C$. The red point represents elemental sulfur.....	32
Figure 8: VED for the sulfur-water system at $125^\circ C$, $pH = 9$, $[S] = 0.001$ ppm.....	34
Figure 9: Calculated hydrogen pressure from the reaction, $3Fe_2SiO_4(F)+2H_2O(l)=2Fe_3O_4+3SiO_2+2H_2(g)$	37
Figure 10: Calculated hydrogen pressure from the reaction, $3Fe(OH)_2=Fe_3O_4+2H_2O(l)+H_2(g)$	38
Figure 11: Calculated hydrogen pressure from the reaction, $Cu + H(+) = Cu(+) + 0.5H_2(g)$, $m(Cl)=0.169$	43
Figure 12: Calculated hydrogen pressure from the reaction, $Cu + H(+) = Cu(+) + 0.5H_2(g)$, $m(Cl)=0.338$	43
Figure 13: Calculated hydrogen pressure from the reaction, $Cu+H(+a)+Cl(-a) = CuCl(s) + 0.5H_2(g)$, $m(Cl)=0.169$	44
Figure 14: Calculated hydrogen pressure from the reaction, $Cu + H(+a)+Cl(-a) = CuCl(s) + 0.5H_2(g)$, $m(Cl)=0.338$	44
Figure 15: Calculated hydrogen pressure from the reaction, $Cu + H(+a)+Cl(-a) = CuCl(a) + 0.5H_2(g)$, $m(Cl)=0.169$	45
Figure 16: Calculated hydrogen pressure from the reaction, $Cu + H(+a)+Cl(-a) = CuCl(a) + 0.5H_2(g)$, $m(Cl)=0.338$	45
Figure 17: Calculated hydrogen pressure from the reaction, $Cu + H(+a)+2Cl(-a) = CuCl_2(-a) + 0.5H_2(g)$, $m(Cl)=0.169$	46
Figure 18: Calculated hydrogen pressure from the reaction, $Cu + H(+a)+2Cl(-a) = CuCl_2(-a) + 0.5H_2(g)$, $m(Cl)=0.338$	46

Figure 19: Calculated hydrogen pressure from the reaction, $2Cu + 2H(+a)+4Cl(-a) = Cu_2Cl_4(-2a) + H_2(g)$, $m(Cl)=0.169$47

Figure 20: Calculated hydrogen pressure from the reaction, $2Cu + 2H(+a)+4Cl(-a) = Cu_2Cl_4(-2a) + H_2(g)$, $m(Cl)=0.338$47

Figure 21: Calculated hydrogen pressure from the reaction, $3Cu + 3H(+a)+6Cl(-a) = Cu_3Cl_6(-3a) + 3/2H_2(g)$, $m(Cl)=0.169$48

Figure 22: Calculated hydrogen pressure from the reaction, $3Cu + 3H(+a)+6Cl(-a) = Cu_3Cl_6(-3a) + 3/2H_2(g)$, $m(Cl)=0.338$48

Figure 23: Calculated hydrogen pressure from the reaction, $Cu + H_2O(l) = CuOH(a) + 1/2H_2(g)$49

Figure 24: Calculated hydrogen pressure from the reaction, $Cu + 2H_2O(l) = Cu(OH)_2(-3a)+H(+a) + 1/2H_2(g)$, $m(Cl)=0.169$50

Figure 25: Calculated hydrogen pressure from the reaction, $Cu + 2H_2O(l) = Cu(OH)_2(-3a) + H(+a)+1/2H_2(g)$, $m(Cl)=0.338$50

Figure 26: Calculated hydrogen pressure from the reaction, $2Cu + H_2O(l) = Cu_2O + H_2(g)$51

Figure 27: Calculated hydrogen pressure from the reaction, $Cu + 2H(+a) = Cu(+2a) + H_2(g)$, $m(Cl)=0.169$52

Figure 28: Calculated hydrogen pressure from the reaction, $Cu + 2H(+a) = Cu(+2a) + H_2(g)$, $m(Cl)=0.338$52

Figure 29: Calculated hydrogen pressure from the reaction, $Cu + 2H(+a) + Cl(-a) = CuCl(+a) + H_2(g)$, $m(Cl)=0.169$53

Figure 30: Calculated hydrogen pressure from the reaction, $Cu + 2H(+a) + Cl(-a) = CuCl(+a) + H_2(g)$, $m(Cl)=0.338$53

Figure 31: Calculated hydrogen pressure from the reaction, $Cu + 2H(+a) + 2Cl(-a) = CuCl_2(a) + H_2(g)$, $m(Cl)=0.169$54

Figure 32: Calculated hydrogen pressure from the reaction, $Cu + 2H(+a) + 2Cl(-a) = CuCl_2(a) + H_2(g)$, $m(Cl)=0.338$54

Figure 33: Calculated hydrogen pressure from the reaction, $Cu + 2H_2O(l) = Cu(OH)_2(a) + H_2(g)$55

Figure 34: Calculated hydrogen pressure from the reaction, $Cu + H_2O(l) + H(+a) = CuOH(+a) + H_2(g)$, $m(Cl)=0.169$56

Figure 35: Calculated hydrogen pressure from the reaction, $Cu + H_2O(l) + H(+a) = CuOH(+a) + H_2(g)$, $m(Cl)=0.169$56

Figure 36: Calculated hydrogen pressure from the reaction, $Cu + H_2O(l) + H(+a) = CuOH(+a) + H_2(g)$, $m(Cl)=0.169$57

Figure 37: Calculated hydrogen pressure from the reaction, $Cu + H_2O(l) + H(+a) = CuOH(+a) + H_2(g)$, $m(Cl)=0.338$	57
Figure 38: Calculated hydrogen pressure from the reaction, $Cu + 3H_2O(l) = Cu(OH)_3(-a) + H(+a) + H_2(g)$, $m(Cl)=0.169$	58
Figure 39: Calculated hydrogen pressure from the reaction, $Cu + 3H_2O(l) = Cu(OH)_3(-a) + H(+a) + H_2(g)$, $m(Cl)=0.338$	58
Figure 40: Calculated hydrogen pressure from the reaction, $Cu + 4H_2O(l) = Cu(OH)_4(-2a) + 2H(+a) + H_2(g)$, $m(Cl)=0.169$	59
Figure 41: Calculated hydrogen pressure from the reaction, $Cu + 4H_2O(l) = Cu(OH)_4(-2a) + 2H(+a) + H_2(g)$, $m(Cl)=0.338$	59
Figure 42: Calculated hydrogen pressure from the reaction, $2Cu + 2H_2O(l) + 2H(+a) = Cu_2(OH)_2(+2a) + 2H_2(g)$, $m(Cl)=0.169$	60
Figure 43: Calculated hydrogen pressure from the reaction, $2Cu + 2H_2O(l) + 2H(+a) = Cu_2(OH)_2(+2a) + 2H_2(g)$, $m(Cl)=0.338$	60
Figure 44: Calculated hydrogen pressure from the reaction, $3Cu + 4H_2O(l) + 2H(+a) = Cu_3(OH)_4(+2a) + 3H_2(g)$, $m(Cl)=0.169$	61
Figure 45: Calculated hydrogen pressure from the reaction, $3Cu + 4H_2O(l) + 2H(+a) = Cu_3(OH)_4(+2a) + 3H_2(g)$, $m(Cl)=0.338$	61
Figure 46: Calculated hydrogen pressure from the reaction, $6Cu + S_3(-2a) + 2H(+a) = 3Cu_2S(s) + H_2(g)$	62
Figure 47: Calculated hydrogen pressure from the reaction, $8Cu + S_4(-2a) + 2H(+a) = 4Cu_2S(s) + H_2(g)$	62
Figure 48: Calculated hydrogen pressure from the reaction, $10Cu + S_5(-2a) + 2H(+a) = 5Cu_2S(s) + H_2(g)$	63
Figure 49: Calculated hydrogen pressure from the reaction, $12Cu + S_6(-2a) + 2H(+a) = 6Cu_2S(s) + H_2(g)$	63
Figure 50: Calculated hydrogen pressure from the reaction, $2Cu + H_2S(a) = Cu_2S(s) + H_2(g)$	64
Figure 51: Calculated hydrogen pressure from the reaction, $Cu + Br(-a) + H(+a) = CuBr(s) + 0.5H_2(g)$...	64
Figure 52: Calculated hydrogen pressure from the reaction, $Cu + F(-a) + H(+a) = CuF(s) + 0.5H_2(g)$	65
Figure 53: Calculated hydrogen pressure from the reaction, $Cu + I(-a) + H(+a) = CuI(s) + 0.5H_2(g)$	65
Figure 54: CDD for the reaction of Cu with S_2^{2-} as a function of temperature for conditions that are predicted to exist in the Forsmark repository.....	93
Figure 55: Concentrations of species versus temperature as predicted by GEMS	93
Figure 56: Concentrations of sulfur-containing species as a function of temperature as predicted by GEMS.....	94

Figure 57: Relative concentrations of sulfur-containing species as predicted by GEMS	94
Figure 58: Schematic of the envisioned granitic rock repository for the final storage of spent nuclear fuel in Sweden[35].....	95
Figure 59: Schematic of an emplaced canister in the Swedish envisioned granitic rock repository, according to the <i>KBS-3</i> plan for the isolation of High Level Nuclear Waste. ([35]).....	96
Figure 60: The thermal evolution for a number of locations in a canister at mid-height in a granitic repository. ([34]).....	98
Figure 61: Predicted E_h versus time data along the Corrosion Evolutionary Path (<i>CEP</i>) defined by the temperature of the inner surface of the buffer versus time profile shown in Figure 59.....	114
Figure 62: Variation of predicted pH versus time data along the Corrosion Evolutionary Path (<i>CEP</i>) defined by the temperature of the inner surface of the buffer versus time profile shown in Figure 59.....	114

List of Tables

Table 1: Thermodynamic data for polysulfides and polythiooxyanions taken from the literature.....	13
Table 2: Calculated P values for different reactions at $T=42^{\circ}\text{C}$	24
Table 3: Calculated P values for different reactions at $T=58^{\circ}\text{C}$	26
Table 4: Calculated P values for different reactions at $T=80^{\circ}\text{C}$	28
Table 5: Reactions and formula for calculating hydrogen pressure in the <i>Cu-H-O-S-Cl</i> system.....	39
Table 6: Input material in Anoxic condition.....	71
Table 7: Parameters of Dependent Components (DC, Species) at 18°C	73
Table 8: Parameters of Dependent Components (DC, Species) at 42°C	75
Table 9: Parameters of Dependent Components (DC, Species) at 45°C	78
Table 10: Parameters of Dependent Components (DC, Species) at 58°C	81
Table 11: Parameters of Dependent Components (DC, Species) at 65°C	83
Table 12: Parameters of Dependent Components (DC, Species) at 70°C	86
Table 13: Parameters of Dependent Components (DC, Species) at 80°C	88
Table 14: Composition of deep granitic ground water ([35]).....	97
Table 15: Parameters of Dependent Components (DC, Species) at 80°C	99
Table 16: Parameters of Dependent Components (DC, Species) at 65°C	101
Table 17: Parameters of Dependent Components (DC, Species) at 42°C	104
Table 18: Parameters of Dependent Components (DC, Species) at 18°C	107
Table 19: Experimentally-determined composition, E_h , and pH data for the Forsmark repository	109

Executive Summary

This report addresses a central issue of the KBS-2 and KBS-3 plans for the disposal of high level nuclear waste (HLNW) in Sweden; that copper metal in pure water under anoxic conditions will exist in the thermodynamically-immune state and hence will not corrode. An implied assumption in these plans is that the copper container may also be thermodynamically immune to corrosion, under certain circumstances, by virtue of the electrochemical properties of the repository near-field environment and upon the basis that native copper deposits are found in granitic geological formations around the world. However, SKB recognizes that in practical repository environments, such as that which exists at Forsmark, copper is no longer immune, because of the presence of sulfide ion, and will corrode at a rate that is controlled by the rate of transport of sulfide ion to the canister surface. This rate is estimated by SKB to be about 10 nm/year, corresponding to a loss of copper over a 100,000 year storage period of approximately 1 mm, which is well within the 5-cm corrosion allowance of the current canister design. However, it is important to note that native copper deposits have existed for geological time (presumably, billions of years), which can only be explained if the metal has been thermodynamically more stable than any product that may form via the reaction of the metal with the environment over much of that period. Nevertheless, even the assumption of immunity of copper in pure water has been recently questioned by Swedish scientists (Hultqvist and Szakalos [1-3]), who report that copper corrodes in oxygen-free, pure water with the release of hydrogen. While this finding is controversial, it is not at odds with thermodynamics, provided that the concentration of Cu^+ and the partial pressure of hydrogen are suitably low, as we demonstrate in this report. The fact that others are experiencing difficulty in repeating these experiments may simply reflect that the initial values of $[Cu^+]$ and p_{H_2} in their experiments are so high that the quantity $P = [Cu^+]p_{H_2}^{1/2}$ is greater than the equilibrium value, P^e , as expressed in a Corrosion Domain Diagram (plots of P and P^e versus pH). Under these conditions, corrosion is thermodynamically impossible, and no hydrogen is released, because its occurrence would require a positive change in the Gibbs energy of the reaction, and the copper is therefore said to be “thermodynamically immune”. If, on the other hand, $P < P^e$ corrosion will proceed and the value of P will rise as Cu^+ and H_2 accumulate at the interface. It is postulated that this condition was met in the Hultqvist and Szakalos [1-3] experiments, thereby leading to a successful result. Eventually, however, as the corrosion products build up in the system, P increases until $P = P^e$ and the rate of corrosion occurs under “quasi-equilibrium” conditions. Under these conditions, the reaction can occur no faster than the rate of transport of the corroding species (e.g., H^+ in the reaction $Cu + H^+ \rightarrow Cu^+ + 1/2H_2$) to, or corrosion products (Cu^+ , H_2) from, the copper surface. These rates may be sufficiently low that the assumption of immunity is unnecessary to qualify copper as a suitable canister material. Thus, if the corrosion rate can be maintained at a value of less than 10^{-8} m/year (0.01 μ m/year), the canister will lose only 1 mm of metal over a one hundred thousand year storage period, which is well within the designed corrosion allowance of 5-cm. However, if the rate of transport through the bentonite buffer is, indeed, that low, then it begs the question: “Why is it necessary to use copper or would a less expensive alternative (e.g., carbon steel) suffice?”

Prior to beginning extensive calculations, it was recognized that the most deleterious species toward copper are sulfur-containing entities, such as sulfide, and various polysulfides, poly thiosulfates, and polythionates, particularly those species that readily transfer atomic sulfur

to a metal surface (e.g. $2Cu + S_2O_3^{2-} \rightarrow Cu_2S + SO_3^{2-}$). Accordingly, we performed a very thorough literature search and successfully located extensive thermodynamic data for sulfur-containing species, primarily from studies performed in Israel, that are not contained in established databases. These data are now included in the database developed in this study.

The environment within the proposed repository is not pristine, pure water, but instead is brine containing a variety of species, including halide ions, sulfur-containing species, and iron oxidation products, as well as small amounts of hydrogen (determined to be about 10^{-11} M by bore-hole sampling). Some of these species are known to activate copper by forming reaction products at potentials that are more negative than in their absence, thereby leading to a much larger value for P^e . For example, in the case of sulfide, whence $2Cu + HS^- \rightarrow Cu_2S + 1/2H_2$, the value of P^e rises by more than twenty-five orders of magnitude at ambient temperature, compared with that for the formation of Cu^+ , for sulfide concentrations that are typical of the repository. Since sulfide species are ubiquitous in groundwater in Sweden, and elsewhere, the controversy raging around whether copper corrodes in pure water is moot, at least with regard to the isolation of High Level Nuclear Waste in Sweden. In this study, we have derived CDDs for copper in the presence of a large number of species that are known or suspected to exist in the repositories. We show that a wide variety of sulfur-containing species and non-sulfur-containing entities activate copper, thereby destroying the immunity assumed for copper in pure water. For example, in addition to the sulfide species (S^{2-} , HS^- , H_2S) the polysulfides (S_x^{2-} , $x = 2 - 8$), polythionates ($S_xO_6^{2-}$) and thiosulfate ($S_2O_3^{2-}$) are all found to be powerful activators of copper. Interestingly, the poly thiosulfates ($S_xO_3^{2-}$, $x = 3 - 6$) are found not to activate copper. The reason for this unexpected result is not yet known and may require determination of electron densities on the atoms in these species, in order to resolve this issue. Chloride ion, which is also ubiquitous in groundwater systems is found to be a mild activator, but the other halide ions (F^- , Br^- , I^-) are generally not activators, except at low pH .

Because of their propensity to activate copper, and because some, at least, are present in the repository ground waters, sulfur species were singled out for a more intensive study. It is well-known that, except for carbon, sulfur displays the richest chemistry of any element in the periodic table. Sulfur-containing species display oxidation states ranging from -2 to +8, with a multitude of fractional oxidation states. The species are generally labile with little kinetic inhibition to interconversion. We summarize this redox chemistry in the form of volt-equivalent diagrams, in which the equilibrium potential of the species with respect to elemental sulfur multiplied by the average oxidation state of sulfur in the species is plotted against the average sulfur oxidation state for a given temperature (ranging from 25 °C to 125 °C) and pH . These diagrams provide a set of rules that indicate which pairs of species will react and which species undergo disproportionation, with the products being indicated in both instances. The diagrams have been developed to match the conditions that are found in the proposed repository. The diagrams reveal that those sulfur compounds, for example, the polythiosulfates ($S_xO_3^{2-}$, $x = 3 - 6$), that are found not to activate copper, are characterized by excessively low (negative) volt-equivalent values. While this is seen to be an important factor, it is not considered to be decisive and we continue with our search for a rational electrochemical thermodynamic explanation as to why the polythiosulfates ($S_xO_3^{2-}$, $x = 3 - 6$) are found not to activate copper. The VEDs developed in this study represent one of the most comprehensive analyses reported to date on the redox chemistry of sulfur and provides a wealth of data for predicting the fate of sulfur in repository environments.

One of the surprising findings of Phase I was the non-activating behavior of $S_xO_3^{2-}$, $x \geq 3$. Thus, our preliminary explanation is that adsorption of this ion onto the metal surface occurs via the three oxygen atoms in a pyramid configuration, with the polysulfur chain extending from the apex. It is further postulated that this configuration occurs, because of a high electron density on the oxygen atoms, compared with that of activating species, such that a partial covalent bond is formed between each oxygen atom and copper. In this configuration, it is reasoned that the sulfur atoms would not have access to the metal surface, in order to react and form Cu_2S , and hence would be non-activating. Resolution of this issue requires determination of the atomic electron densities in activating and non-activating polysulfur species and the configurations of the adsorbed species on copper. We will attempt to resolve this important issue in the next phase of this work by using Density Functional Theory to estimate atomic electron densities and to identify the most favorable configurations for the adsorbed species on copper. An important goal will be to explain why thiosulfate ($S_2O_3^{2-}$) is a powerful activator but the higher homologues are non-activating. In the thiosulfate case, it is possible that the electron density on the sulfur is higher than that on the oxygen and hence that the ion adsorbs in a configuration that allows the sulfur to react with the copper.

Under anoxic conditions the activation of copper produces hydrogen and the relationship between the equilibrium hydrogen pressure from the reaction and the hydrogen pressure in the repository is another indicator of whether copper will corrode. Thus, if the equilibrium hydrogen pressure for a reaction is greater than the hydrogen pressure in the repository, the reaction will proceed in the forward (hydrogen-producing and corrosion) direction, whereas if the equilibrium hydrogen pressure is less than that of the repository the reaction is spontaneous in the reverse direction. It is this latter situation that represents immunity to corrosion. Not unexpectedly, the results of this analysis are in accord with the findings from the Corrosion Domain Diagrams, and, again, the propensity of the sulfur-containing species to activate copper is demonstrated. Chloride ion is, again, found to be a weak activator in accordance with the CDDs. This work was also performed to more closely define the conditions of the Szakalos and Hultqvist [1-3] experiments, which have detected the formation of hydrogen when copper is in contact with highly pure, deoxygenated water. As with the CDDs, the hydrogen pressure calculations predict that the reaction of copper with water under these conditions is only spontaneous if the pressure of hydrogen and the concentration (activity) of Cu^+ are both exceptionally low, providing further corroboration that the lack of agreement between the various sets of experiments reflects differences in the initial states of the experiment with respect to the quantity $P = [Cu^+]p_{H_2}^{1/2}$ compared to the equilibrium value, P^e . In carrying out this analysis, it was necessary to consider the processes that might establish the hydrogen partial pressure in the repository. From a review of the geochemical literature, it appears that the hydrogen partial pressure is established by the hydrolysis of Fayalite [$3Fe_2SiO_4 + 2H_2O \rightarrow 2Fe_3O_4 + 3SiO_2 + 2H_2$] and/or the Schikorr reaction [$3Fe(OH)_2 \rightarrow Fe_3O_4 + 2H_2O + H_2$]. We carried out a thermodynamic analysis of these reactions and found that the Fayalite hydrolysis reaction is, theoretically, capable of producing only a fraction of an atmosphere of H_2 , while the Schikorr reaction is predicted to produce an equilibrium hydrogen pressure of the order of 1000 atm. Realization of this pressure would require that $Fe(OH)_2$ and/or Fe_2SiO_4 and the reaction products (Fe_3O_4 and SiO_2) be present in the system. However, if $Fe(OH)_2$ and Fe_2SiO_4 are minor components of the rock, they will be quickly depleted and, recognizing that hydrogen is continually lost from the system, the hydrogen concentration will be much lower than that indicated by thermodynamic calculation, which assumes a closed system. This expectation is in keeping with the measured concentration of hydrogen from bore-hole sampling programs at Forsmark and elsewhere, which show that the

H_2 concentration is of the order of 10^{-11} M, corresponding to a partial pressure of about 10^{-14} atm. This low concentration, compared with the thermodynamically predicted value, indicates that the rate of loss of hydrogen from the geological formation is much greater than the rate of generation. However, it is important to recognize that sampling indicates a wide range of hydrogen concentration, with values ranging up to 10^{-6} M. This figure is still so much lower than the thermodynamic predictions that it raises the question as to whether the measured values are accurate or whether neither of the two reactions identified above actually occur in the repository. Certainly, if the Schikorr reaction controls the hydrogen pressure in geological formations, explaining the existence of native copper is straight forward, provided sulfur-containing species that can activate copper are at a suitably low concentration. Even if Fayalite hydrolysis is the operative hydrogen-control mechanism, the existence of native copper is, again, readily explained, but it requires a correspondingly lower (by a factor of about 10^4) sulfide concentration than in the Schikorr reaction case. The discrepancy between the calculated hydrogen pressure and that sampled from bore-holes is disturbing and needs to be resolved, in spite of this issue being studied extensively by SKB (SKB R-08-85). Resolution of this issue is necessary, because hydrogen has a huge impact on the redox potential of the repository and hence upon the corrosion properties of the canisters. An accurate prediction of the evolution of corrosion damage along the Corrosion Evolutionary Path (CEP) will require accurate estimation of hydrogen fugacity in the repository over at least one hundred thousand years after it has been closed.

Currently, there exist data on the chemical composition of the ground water that are the result of analyzing “grab” samples from bore holes. While this procedure is notoriously unreliable, particularly when volatile gases are involved, it does provide good measures of dissolved components, provided that precipitation does not occur during the sampling process. Frequently, solid phases will precipitate in response to the loss of volatile gases, and unless the sampling capsule is tightly sealed considerable error may ensue. Given these caveats, as well as the fact that some of the techniques measure the total concentration of an element (e.g., sulfur as sulfate by oxidizing all sulfur species in the system to SO_4^{2-} with a strong oxidizing agent, such as H_2O_2), we accept the analysis of the concentrations of the ionic species, because they are measured using the normally reliable method of ion chromatography. However, these anions (e.g., Cl^- , Br^- , CO_3^{2-} , etc) are generally not particularly strong activators and hence are of only secondary interest in determining the corrosion behavior of copper. Accordingly, we decided to employ a modern, sophisticated Gibbs Energy Minimization algorithm to predict the composition of the repository environment, as a function of temperature and redox condition, with the latter being adjusted by changing the relative concentrations of hydrogen and oxygen inputs to the code, in order to obtain the desired outputs. Note that the input concentrations are much greater than the output concentrations, because these gases react with components in the system as the system comes to equilibrium. After evaluating several codes, we chose GEMS, which was developed in Switzerland by Prof. Dmitrii Kulik. This code is designed specifically to model complex geochemical systems, contains a large database of compounds, and is in general use in the geochemical community. Prior to using the code to model the repository, we upgraded the database by adding thermodynamic data for various polysulfur species (polysulfides, polythiosulfates, and polythionates) that had been developed earlier in this program. However, the code became ill-behaved when the data for $S_xO_3^{2-}$, $x = 3 - 7$ was added. Consultation with the code developer, Prof. Dmitrii Kulik of the Paul Scherrer Institute in Switzerland failed to identify and isolate the problem and, accordingly, it was necessary to

remove those species from the database. The reader will recall that these are the very species that, anomalously, do not activate copper. With the code in its present form, we have modeled the repository under both oxic and anoxic conditions with the greatest emphasis being placed on the latter, because the great fraction of the storage time is under anoxic conditions. The most important finding to date is that the concentrations of the polysulfur species (polysulfides, polythiosulfates, and polythionates) under anoxic conditions are predicted to be very low, but it is still not possible, because of the uncertainty in the calculations, to ascertain with unequivocally whether these species will activate copper in the repository. However, the point may be moot, because sulfide species (S^{2-} , HS^- , and H_2S) are predicted to be present in sufficient concentration to activate copper and cause the metal to corrode under simulated repository conditions.

Finally, we have initiated work to define the corrosion evolutionary path (CEP) in preparation for modeling the corrosion of the canisters in the next phase of this program. The task of defining the CEP essentially involves predicting the redox potential (E_h), pH , and granitic groundwater composition, as defined by the variation of temperature (note that the temperature decreases roughly exponentially with time, due to radioactive decay of the short-lived isotopes), and then applying Gibbs energy minimization to predict speciation at selected times along the path. At each step, the CDD for copper is derived and the value of P is compared to P^e to ascertain whether copper is active or thermodynamically immune. Although the polysulfur species (e.g., HS_2^- and S_2^{2-}) are generally predicted to be present at very low concentrations, or are predicted to be absent altogether (e.g., polysulfuroxyanions), some are predicted to be present at sufficient concentration (e.g., S_2^{2-}) that they might activate copper. Thus, in the case of S_2^{2-} , the CDDs indicate that this species need be present at only miniscule concentrations (10^{-44} M) for activation to occur. In any event, as noted above, sulfide (H_2S , HS^- , and/or S^{2-}) are predicted to be present during the entire anoxic period at sufficiently high concentrations to activate copper, so that activation by the polysulfur species seemingly is not an important issue.

The assumption that copper is unequivocally immune in pure water under anoxic conditions is strictly untenable, and it is even more so in the presence of activating species, such as sulfide. Thus, it appears that two conditions must be met in order to explain the existence of the native deposits of copper that occur in granitic formations: (1) A suitably high hydrogen fugacity (partial pressure) and; (2) A suitably high cuprous ion activity, as shown in this report. Accordingly, the success of the KBS-3 program must rely upon the multiple barriers being sufficiently impervious to the transport of activating species and corrosion products that the corrosion rate is reduced to an acceptable level.

I. Introduction

Sweden's KBS-3 plan for the disposal of high level nuclear waste (HLNW) is partly predicated upon the assumption that copper, the material from which the canisters will be fabricated, was thermodynamically immune to corrosion when in contact with pure water under anoxic conditions. In other words, copper was classified as being a noble metal like gold. In the immune state, corrosion cannot occur, because any oxidation process of the copper is characterized by a positive change in the Gibbs energy, rather than a negative change demanded by the Second Law of Thermodynamics for a spontaneous process. Accordingly, "immunity" is a thermodynamic state that must be characterized upon the basis of thermodynamic arguments. This immunity postulate was apparently intriguing, because of the occurrence of deposits of native (metallic) copper in various geological formations throughout the World (e.g., in the upper Michigan peninsula in the USA, and in Sweden). Accordingly, it was reasoned that, during the anoxic period, when all of the oxygen that was present during the initial oxic period, due to exposure to air upon placement of the waste, had been consumed and the redox potential, E_h , had fallen to a sufficiently low value, copper might become thermodynamically immune and corrosion might not occur, even over geological times, provided the environment remained conducive to that condition. We now understand that this condition can be realized only if hydrogen is present at a suitably high fugacity, if activating species, such as sulfide, are present at suitably low concentrations, and if the activity of Cu^+ is suitably high. We also understand that these conditions cannot be met in any practical repository environment, particularly with regard to the concentrations of activating species. In that case, the corrosion of copper is thermodynamically spontaneous and the safe isolation of HLNW requires inhibiting corrosion to the extent that the waste will be safely contained over the designated storage period.

The issue of copper immunity in pure water under anoxic conditions has developed into one of considerable controversy within both the scientific and lay communities in Sweden, because direct experimentation has failed to achieve resolution. Thus, experiments by Hultqvist, et. al. [1-3] have reported detection of hydrogen evolution when copper metal is exposed to deoxygenated, pure water, while other experiments appear to refute those claims [4-6]. The experiments were all carried out to the highest of scientific standards using hydrogen detection techniques that were more than adequate for the task of quantitatively detecting and measuring the gas, and each group reports internally-consistent results that, nevertheless, appear to be diametrically opposite from one group to the other. While the work reported in Refs. 1 to 6 is of great scientific interest, it is perhaps moot, when viewed in light of the environment that is present at Forsmark, the site of the initial HLNW repository in Sweden. Nevertheless, resolution of the scientific controversy underlying the experiments of Hultqvist, et.al. [1-3], and those in refute, is important, because it would remove one aspect of uncertainty in the assessment of the KBS-3 plan for storing High Level Nuclear Waste (HLNW) in Sweden.

In this study, we report a comprehensive thermodynamic study of copper in contact with anoxic pure water and granitic groundwater of the type and composition that is expected in the Forsmark repository in Sweden. Our primary objective was to ascertain whether copper would exist in the thermodynamically immune state, when in contact with pure water under anoxic conditions, and to provide a thermodynamic basis for assessing the corrosion behavior of copper in the repository. In spite of the fact that metallic copper is known to exist for geological times in granitic, geological formations, copper is well-known to be activated from the immune state, and to corrode, by specific species that may exist in the environment. The principal activator of

copper is known to be sulfur in its various forms, including sulfide (H_2S , HS^- , S^{2-}), polysulfide (H_2S_x , HS_x^- , S_x^{2-}), poly sulfurthiosulfate ($S_xO_3^{2-}$), and polythionates ($S_xO_6^{2-}$). A comprehensive study of this aspect of copper chemistry has never been reported, and yet an understanding of this issue is vital for assessing whether copper is a suitable material for fabricating canisters for the disposal of HLNW. Our study identifies and explores those species that activate copper; these species include sulfur-containing entities as well as other, non-sulfur species that may be present in the repository. In order to explore these issues, we have introduced new, innovative techniques, such as corrosion domain diagrams (CDDs) and Volt-Equivalent Diagrams (VEDs), as well as traditional Gibbs energy minimization algorithms, in order to display the chemical implications of copper activation and the electrochemical properties of the activating species, in a manner that allows a reader to discern the issues and follow their resolution. No new experiments are performed, but considerable analysis of the thermodynamic data for copper metal in contact with the environments of interest is reported. From this analysis the question of copper corrosion in pure water under anoxic conditions and in HLNW repositories is readily addressed.

II. Thermodynamic Data for Copper and Sulfur Species

The initial task in the present investigation was to review various databases and the literature for thermodynamic data. Of particular interest was assessing the consistency of the data from one database to another. High consistency was expected, because the Gibbs energies of formation, the third law entropies, and the heat capacity are commonly taken from a common source. Of course, that does not ensure accuracy, because the original measurements themselves may have been in error. A better assessment method is to compare predicted phenomena with direct experiment, by first making sure that the phenomenon that is being predicted was not used for the original derivation of the data. For example, common comparisons include calculated and observed solubility, acid/base dissociation constants, volatility, and electrode potentials. However, doing this effectively for all of the species in the database is an enormous task that is well beyond the scope of the present study. Instead, this approach is being used to assess the data for only those species for which we have doubts of appropriate accuracy. Since this task is on-going, the final results will be reported in a later report.

The second objective of this task was to develop a more comprehensive database for the polysulfide and polythiooxyanions by carefully reviewing the more recent literature than that included in the older databases. This proved to be highly fruitful and successful, as we were able to locate several recent papers that reported thermodynamic data for a variety of partially oxidized/reduced sulfur species, including the polysulfides, polythiosulfates, and the polythionates (Table 1). To our knowledge, Table 1 represents the most comprehensive compilation of thermodynamic data for sulfur-containing species. Even so, and recognizing the complexity of the *S-O-H* system, the database is far from complete, particularly with respect to the acid species.

Table 1: Thermodynamic data for polysulfides and polythiooxyanions taken from the literatures.

Species	$\Delta_f G^\circ / \text{kJmol}^{-1}$	$\Delta_f H^\circ / \text{kJmol}^{-1}$	$S^\circ / \text{J.K}^{-1}.\text{mol}^{-1}$	$C_p^\circ / \text{J.K}^{-1}.\text{mol}^{-1}$	Source
S_2^{2-}	77.685	13.040	28.451	-221.635	Kamyshny et. al.[7]
S_3^{2-}	71.564	6.600	9.000	-222.744	Kamyshny et. al.[7]
S_4^{2-}	56.394	9.000	100.000	-226.000	Kamyshny et. al.[7]

S_5^{2-}	66.666	21.338	139.000	-227.395	Kamysny et. al.[7]
S_6^{2-}	68.189	13.300	139.000	-227.395	Kamysny et. al.[7]
S_7^{2-}	80.951	16.500	139.000	-227.395	Kamysny et. al.[7]
S_8^{2-}	88.272	23.800	171.000	-228.540	Kamysny et. al.[7]
S^{2-}	85.973	33.095	-14.602	-137.154	NBS[4], Helgeson[13]
$S_2O_3^{2-}$	-518.646	-648.52	66.944	-237.631	Shock[8], NBS[10]
$S_4O_6^{2-}$	-1040.253	-1224.238	257.316	-109.153	Shock[9], NBS[10]
$S_2O_4^{2-}$	-600.567	-753.538	92.048	-207.684	Shock[9], NBS[10]
$S_2O_5^{2-}$	-790.876	-970.688	104.600	-200.199	Shock[9], Kivialo[15]
$S_2O_6^{2-}$	-969.037	-1173.194	125.520	-187.730	Shock[9], Kivialo[15]
$S_2O_7^{2-}$	-795.090	-1011.101	188.334	-75.969	Williamson[11]
$S_2O_8^{2-}$	-1114.868	-1344.763	244.346	-103.318	Shock[8], NBS[10]
$S_3O_3^{2-}$	-827.187	-951.400	118.001	-198.747	Williamson[11]
$S_3O_6^{2-}$	-957.360	-1167.336	138.072	-180.243	Shock[9], Kivialo[15], Rossini[16]
$S_4O_3^{2-}$	-957.384	-1085.099	138.323	-163.272	Williamson[11]
$S_5O_3^{2-}$	-1030.080	-1159.700	164.004	-118.441	Williamson[11]
$S_5O_6^{2-}$	-955.337	-1175.704	167.360	-162.782	Shock[9], Kivialo[15]
$S_6O_3^{2-}$	-1074.377	-1205.201	192.037	-69.505	Williamson[11]
$S_6O_6^{2-}$	-1196.975	-1381.000	321.323	156.185	Williamson[11]
$S_7O_3^{2-}$	-1104.774	-1236.401	221.413	-18.224	Williamson[11]
HS^-	12.082	-16.108	68.199	-93.618	Shock[8], NBS[10], Helgeson[13]
HS_2^-	11.506	-267.902	-742.317	-195.115	Williamson[11]
HS_3^-	20.510	-352.402	-1023.862	-185.042	Williamson[11]
HS_4^-	27.714	-394.401	-1156.822	-180.285	Williamson[11]
HS_5^-	33.017	-419.601	-1227.058	-177.772	Williamson[11]
HS_6^-	36.228	-436.299	-1261.765	-176.530	Williamson[11]
$H_2S(a)$	-28.6	-39.706	125.5	183.667	Plyasunov[14]
$H_2S_2O_4(a)$	-616.66	-733.455	213.384	155.905	Shock[9]
$HS_2O_4^-$	-614.471	-749.354	152.716	56.282	Shock[9], Williamson[11]
$H_2SO_3(a)$	-537.86	-608.898	232.212	0.000	NBS[10]
$H_2S_2O_3(a)$	-535.576	-629.274	188.280	114.724	Shock[9]
HSO_3^-	-527.613	-626.219	139.746	-5.304	Shock[8], NBS[10]
$H_2SO_4(a)$	-744.526	-909.392	20.083	-176.410	NBS[10]
HSO_4^-	-755.67	-889.1	125.52	22.589	Shock[8], NBS[10]
HSO_5^-	-637.440	-775.630	212.129	154.047	Shock[9]
$HS_2O_3^-$	-532.132	-643.918	127.612	15.095	Shock[9]
SO_3^{2-}	-486.546	-635.55	-29.288	-280.022	Shock[9], Phillips[12]
SO_4^{2-}	-744.361	-909.602	18.828	-264.944	Shock[8], NBS[10]
$SO_2(a)$	-300.555	-323.005	161.921	311.612	NBS[10], Shock[8]
$SO_3(a)$	-525.637	-635.591	-28.995	0.000	NBS[10]
$HS_2O_5^-$	-998.490	-1218.799	-31.229	-532.911	Williamson[11]
$HS_2O_6^-$	-1073.389	-739.798	1929.134	6013.290	Williamson[11]
$HS_2O_7^-$	-1372.589	-1253.798	1311.266	3950.056	Williamson[11]
$HS_2O_8^-$	-1510.289	-1253.798	1875.687	5834.817	Williamson[11]
$HS_3O_3^-$	-471.386	-718.899	-295.549	-1415.549	Williamson[11]
$HS_4O_3^-$	-477.382	-760.898	-384.233	-1711.690	Williamson[11]
$HS_5O_3^-$	-480.179	-786.098	-427.308	-1855.527	Williamson[11]

$HS_6O_3^-$	-481.378	-802.801	-447.236	-1922.074	Williamson[11]
$HS_7O_3^-$	-481.974	-815.001	-454.085	-1944.945	Williamson[11]

III. Corrosion Domain Diagrams

The objective of deriving Corrosion Domain Diagrams is to present the consequences of the Second Law of Thermodynamics in the clearest form possible, when assessing the immunity and activation of copper. Traditionally, this subject has been addressed using potential- pH (or Pourbaix) diagrams, but this form of presentation fails to emphasize the importance of species at very low concentrations and the impact that they may have in determining the thermodynamic properties of a metal. We stress, however, that all forms of presentation essentially employ the same thermodynamic data, so that the message that needs to be relayed is in the very form of the presentation itself. In order to illustrate this feature, we need to explore the derivation of Corrosion Domain Diagrams (CDDs).

Consider the most basic corrosion reaction in the copper/water system:



The change in Gibbs energy for this reaction can be written as

$$\Delta G = \Delta G^0 + 2.303RT \log(f_{H_2}^{1/2} a_{Cu^+} / a_{H^+}) \quad (2)$$

which, upon rearrangement yields

$$\log(f_{H_2}^{1/2} a_{Cu^+}) = \frac{\Delta G - \Delta G^0}{2.303RT} - pH \quad (3)$$

where ΔG^0 is the change in standard Gibbs energy; i.e., the change in Gibbs energy when all components of the reaction are in their standard state with the fugacity of hydrogen, f_{H_2} , and the activity of cuprous ion, a_{Cu^+} , being equal to one. At equilibrium, $\Delta G = 0$, and designating the equilibrium values of f_{H_2} and a_{Cu^+} with superscripts “e” we may write

$$P^e = f_{H_2}^{e,1/2} a_{Cu^+}^e = 10^{-\left(\frac{\Delta G^0}{2.303RT} + pH\right)} \quad (4)$$

where P^e is termed the “partial equilibrium reaction quotient”. We now define the partial reaction quotients, P , for non-equilibrium conditions as follows

$$P = f_{H_2}^{1/2} a_{Cu^+} \quad (5)$$

The condition for spontaneity of Reaction (1) then becomes $P < P^e$ and immunity is indicated by $P > P^e$.

Below, we present various CDDs for the *Cu-O-S-H* system, in order to display the power of the method for addressing the immunity issue and for identifying those species that will activate copper. Other CDDs for wide ranges of conditions and species are given in Appendix 1. In the first instance, we consider the CDD for copper in contact with pure water under anoxic conditions (Figure 1).

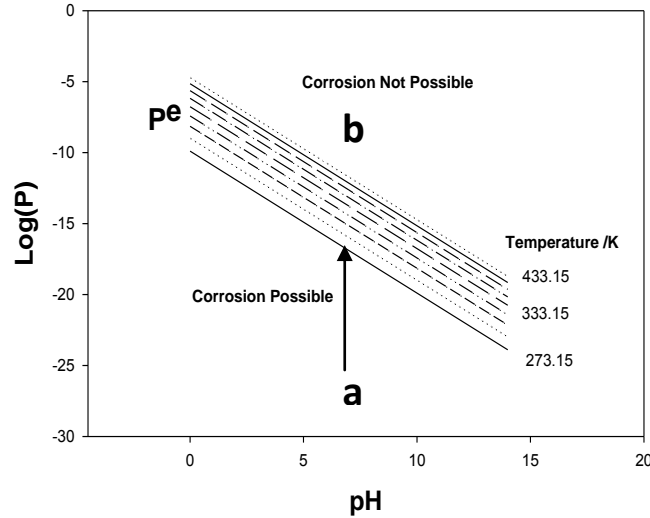


Figure 1: Corrosion domain diagram for copper in water as a function of temperature.

The quantity P^e has been calculated for Reaction (1) using Equation (4) and is plotted as a function of pH in Figure 1. These plots divide the $\log(P)$ versus pH domain into regions of immunity (upper region) and corrosion (lower region), with the regions being separated by $\log(P^e)$ versus pH for different temperatures. These plots clearly demonstrate that whether copper is immune (thermodynamically stable) depends sensitively upon the value of P , which is a property of the environment ($P = f_{H_2}^{1/2} a_{Cu^+}$), and hence upon the initial conditions in the system (fugacity of hydrogen and activity of Cu^+). Thus, if P is small (e.g., at Point a, Figure 1), $P < P^e$ and the corrosion of copper is spontaneous as written in Equation (1). On the other hand, if the system is located at Point (b), Figure 1), because the initial value of $f_{H_2}^{1/2} a_{Cu^+}$ is sufficiently high, $P > P^e$ and corrosion is not possible, thermodynamically, and hence the metal is “immune”. Returning now to the case described by Point a, we note that as the corrosion reaction proceeds, the concentration of Cu^+ and the fugacity of hydrogen at the interface will increase, particularly in a medium of restricted mass transport (e.g., in the bentonite buffer surrounding a canister), such that P will steadily increase with time until it meets the value of P^e at the corresponding temperature. At this point, the metal may be classified as being “quasi-immune”; “quasi” only because transport of Cu^+ and H_2 away from the canister surface, through the bentonite buffer must be matched by corrosion, in order to maintain $P = P^e$ at the metal surface. Accordingly, the corrosion rate ultimately becomes controlled by the diffusion of Cu^+ , H^+ , and H_2 (in this case) through the adjacent bentonite buffer. Thus, we conclude that, for any system starting at a point below the P^e versus pH for the relevant temperature, copper metal is not thermodynamically immune and will corrode in the repository at a rate that is governed by the rate of transport of the reactants (H^+) to, and the corrosion products away from, the metal surface. Of course, this rate is

readily predicted by solving the mass transport equations for the system, if the diffusivities of Cu^+ and H_2 in bentonite are known. Note that a system can never cross from the corrosion region to the immune region spontaneously as the change in Gibbs energy would become positive. That transition can be affected, however, by imposing a higher value of $f_{H_2}^{1/2} a_{Cu^+}$ by the addition of hydrogen and/or Cu^+ ; this is equivalent to performing work, which is the condition for reversing an irreversible process (the “refrigerator principle”).

As noted above, for any system whose initial conditions (value of P) lie above the relevant P^e versus pH line, copper is unequivocally immune and corrosion cannot occur, as corrosion would violate the Second Law of Thermodynamics. However, it is evident, that the conditions for immunity might be engineered in advance by doping the bentonite with a $Cu(I)$ salt and a suitable reducing agent to simulate the reducing power of hydrogen, such that the initial conditions lie above P^e versus pH . It is suggested that cuprous sulfite, Cu_2SO_3 , might be a suitable material, with the cation providing the suitably high Cu^+ activity and the anion establishing the required reducing conditions that, otherwise, would be established by hydrogen. Of course, the dopant will slowly diffuse out of the bentonite and into the external environment, but it is expected to be sufficiently slow that the conditions of immunity may be maintained for a considerable period. Thus, in a “back-of-the-envelope” calculation,

$$t = L^2 / D \quad (7)$$

we choose $L = 10$ cm and $D = 10^{-9}$ cm²/s to yield a diffusion time of 10^{11} seconds or 316,456 years, considerably longer than the generally recognized storage horizon of 100,000 yrs. At a time of this order, the value of P at the canister surface will have been reduced to P^e and corrosion will have initiated at a rate that is determined by the transport of reactants and products through the bentonite buffer. It is important to note that the above calculation is only a rough estimate and that a more accurate value can be obtained by solving the transport equation with experimentally determined values for the diffusivities of the reactants and products. The important point is that immunity may be maintained for a sufficiently long period that the more active components of the HLNW will have decayed away and will no longer represent a threat to the biosphere.

The analysis presented above is largely predicated on the corrosion of copper in contact with pure water (Figure 1). However, groundwater is far from pure, and a common contaminant is sulfide as H_2S , HS^- , or S^{2-} . Sulfide species arises from dissolution of sulfur-containing minerals in the host rock of the repository, from dissolution of pyrite in the bentonite, from the decomposition of organic (plant) material, and even from the action of sulfate-reducing bacteria (SRBs). It is fair to conclude that sulfide, and other sulfur-containing species are ubiquitous in groundwater environments at concentration ranging up to a few ppm, at least. It is also well-known that sulfide species (H_2S , HS^- , or S^{2-}) activate copper by giving rise to the formation of Cu_2S at potentials that are significantly more negative than the potential for the formation of Cu_2O or Cu^+ from water. Thus, in the presence of bisulfide, the lowest corrosion reaction of copper may be written as:



for which the change in Gibbs energy is written as

$$\Delta G = \Delta G^0 + 2.303RT \log(f_{H_2} / a_{HS^-} \cdot a_{H^+}) \quad (9)$$

As before, we define an equilibrium value of P and P^e as

$$P = f_{H_2} / a_{HS^-} \text{) and } P^e = f_{H_2}^e / a_{HS^-}^e \text{)}$$

$$(10)$$

where

$$f_{H_2}^e / a_{HS^-}^e = 10^{-\left(\frac{\Delta G^0}{2.303RT} + pH\right)} \quad (11)$$

The value of P under non-equilibrium conditions is simply $P = f / a_{HS^-}$, where f_{H_2} is the actual fugacity of hydrogen and a_{HS^-} is the actual activity of HS^- in the repository environment.

Values of P^e versus pH are plotted in Figure 2 as a function of temperature for temperatures ranging from 0 °C to 160 °C in steps of 20 °C. Again, P^e versus pH divides the diagram into two regions corresponding to spontaneous corrosion (lower region) and immunity (upper region). The reader will note that the P^e values for the lines are more positive than those for the Cu – pure water case by a factor of about 10^{25} , demonstrating that immunity is much more difficult to achieve in the presence of bisulfide.

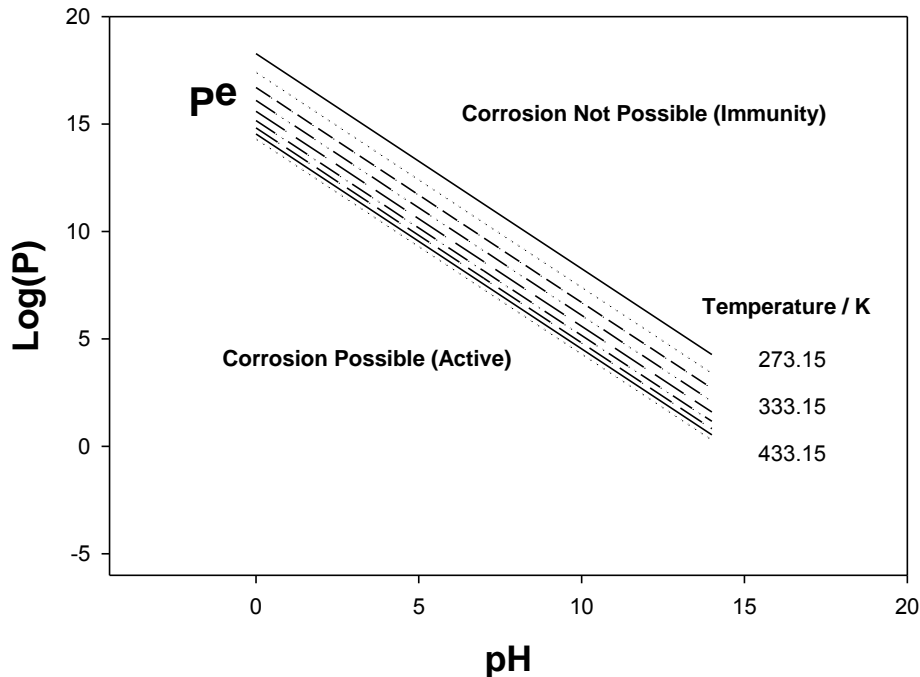


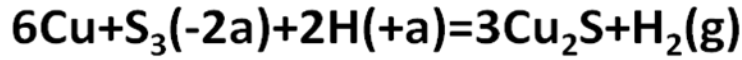
Figure 2: Corrosion domain diagram for copper in water + HS^- as a function of temperature.

In order to illustrate the difficulties posed by small amounts of sulfide species in the environment, we note that if $[HS^-] = 10^{-12}$ M (3.3×10^{-8} ppm) and $p_{H_2} = 10^{-6}$ atm (0.02 ppb), the environment is characterized by a $\log(P)$ value of -10.854, which lies well below P^e in Figure 2. Note that the range of P indicated in Figure 3 corresponds to ranges in f_{H_2} of 7.06×10^{-11} to 7.05×10^{-17}

atm and in $a_{S_3^{2-}}$ is calculated based on the concentration of SO_4^{2-} of 38.3 to 547 mg/L that are believed to describe the variability of the environment, based upon data from Forsmark [31]. Accordingly, under these conditions, copper will corrode and hence cannot be considered to be immune. Noting again that immunity is achieved only if $P > P^e$, we emphasize, again, that the desired immune condition could only be achieved by having extraordinarily low concentrations of HS^- and/or extraordinarily high partial pressures of hydrogen. For example, the following two sets of conditions are predicted to yield immunity, $[HS^-]$ and p_{H_2} combinations of 3.3×10^{-10} ppm and 10^{-6} atm (about a factor of 10^8 greater than the actual value from Forsmark) and 0.033 ppm and 10^{10} atm, respectively. In the first case, the concentration of HS^- is orders of magnitude lower than the sulfide concentration in ground water (a few ppb to a few ppm), particularly in the presence of bentonite, which commonly contains pyrite, FeS_2 , and hence is an unrealistic scenario. In the second case, the required partial pressure of hydrogen (10^{10} atm) is impossibly high to be achieved and maintained practically in the repository, and hence is also unrealistic. Accordingly, the prospects for achieving immunity of copper in a repository in which the ground water contains a significant concentration of sulfide species must be judged as being remote or even non-existent, at least in terms of the ground water environment that is naturally present in the system. Of course, these thermodynamic predictions can be easily checked by experiment, and experiments to do so should be performed at the earliest opportunity.

Let us now explore the feasibility of engineering the near field environment to induce immunity by the addition of $CuSO_3$ to the bentonite buffer. In this “scoping” calculation, we assume that the activity and fugacity coefficients are unity and we accept the SO_3^{2-}/SO_4^{2-} equivalent hydrogen pressure as being 5988 atm. From Figure 2, for $pH = 7$, we see that P^e has a value of 10^{10} , so that the concentration of HS^- must be below 20 ppb for the copper to be immune (i.e. for $P > P^e$). This number may be compared with the concentration of HS^- modeled using a Gibbs energy minimization code from LLNL, which gives values for various boreholes ranging from $(6.68 \times 10^{-5} \text{ M to } 1.27 \times 10^{-10} \text{ M or } 2200 \text{ ppb to } 4.19 \times 10^{-3} \text{ ppb})$ [21]. Actual borehole analyses yield much higher total sulfur concentrations (101 to 547 ppm), because the analytical technique oxidizes all sulfur species to SO_4^{2-} prior to determining the concentration [21]. Of course, much of the total sulfur probably existed as sulfate ion in the original grab sample. The calculated immunity value lies within the range estimated range for HS^- concentration, demonstrating that theoretically, at least, it may be possible to engineer immunity of the copper by suitably modifying the composition of the buffer. The effect may be enhanced (i.e., the critical HS^- concentration may be increased) by incorporating a copper salt having a more powerful reducing anion into the bentonite buffer and/or by increasing the salt loading. Thus, the strategy of engineering the redox conditions in the bentonite buffer appears to be a most promising approach.

It is likely that a great variety of partially oxidized/reduced sulfur species may exist in the repository, due to the oxidation of pyrite during the initial oxic period (first 100 years or so after resaturation of the buffer by groundwater) or due to the action of Sulfate Reducing Bacteria (SRBs) acting upon sulfate present in the groundwater or as Gypsum in the bentonite. The species produced are expected to include the polysulfides, $(H_2S_x, HS_x^-, S_x^{2-})$, polythiosulfates $(H_2S_xO_3, HS_xO_3^-, S_xO_3^{2-})$, and the polythionates $(H_2S_xO_6, HS_xO_6^-, S_xO_6^{2-})$ amongst others. Corrosion Domain Diagrams for copper in the presence of these species with $\log(P)$ being typical of repository conditions have been derived in this study and an example is shown in Figure 3.



$$\log\left(\frac{P_{\text{H}_2(\text{g})}}{a_{\text{S}_3^{2-}}}\right) = \frac{-\Delta G^0}{2.303RT} - 2\text{pH}$$

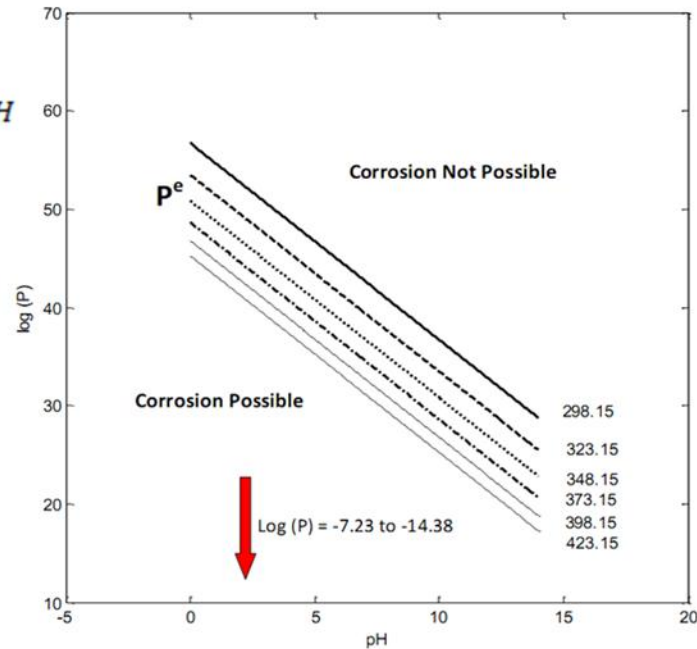


Figure 3: Corrosion Domain Diagram for copper in the presence of the polysulfide, S_3^{2-} . The red arrow indicates the range of P calculated from the expected variability in the composition of the ground water.

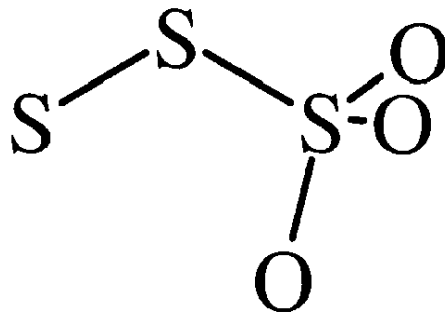
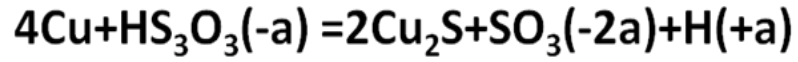


Figure 4: Structure of the trithiosulfate anion. Note that the two terminal sulfur atoms are prevented from being donated to reactive sites on a metal surface, thereby activating the metal toward corrosion, by the postulated adsorption of the species on the surface via the three oxygen atoms.

Note that $\log(P)$ for the repository, which was calculated using $P = f_{\text{H}_2} / a_{\text{HS}^-}$ lies well below $\log(P^e)$ for any of the temperatures considered, and hence S_3^{2-} is considered to be a powerful activator of metallic copper. In fact, the same conclusion is arrived at for all of the

polysulfides (H_2S_x , HS_x^- , S_x^{2-} , $x = 2 - 8$), polythiosulfates ($H_2S_xO_3$, $HS_xO_3^-$, $S_xO_3^{2-}$, $x = 2$), and the polythionates ($H_2S_xO_6$, $HS_xO_6^-$, $S_xO_6^{2-}$, $x = 2 - 6$), with the exception of $S_xO_3^{2-}$, $x \geq 3$. Thus, the CDD for *Cu* in contact with $HS_3O_3^-$, Figure 5, shows that this species is a powerful activator of copper, with the value of $\log(P)$ for the environment being estimated to be -0.47, indicating a very large driving force in terms of ΔG for the corrosion process. On the other hand, the oxyanion $S_3O_3^{2-}$, and higher members of the polythiosulfates homologous series, $S_xO_3^{2-}$ ($x \geq 3$), e.g., Figure 6 and the Appendix, are predicted not to activate copper at all, as summarized in Tables 2 to 4. In these cases, the value of $\log(P)$ for the environment lies well above $\log(P^e)$ for the activating reaction. The origin of this loss in activating ability by the higher polythiosulfates remains unknown, but it is postulated to lie in the electron density on the terminal sulfur atom versus that on the three oxygen atoms (Figure 4). Thus, our preliminary explanation is that adsorption of this ion onto the metal surface occurs via the three oxygen atoms in a pyramid configuration, with the polysulfur chain extending from the apex. It is further postulated that this configuration occurs, because of a high electron density on the oxygen atoms, compared with that of activating species, such that a partial covalent bond is formed between each oxygen atom and copper. In this configuration, it is reasoned that the sulfur atoms would not have access to the metal surface, in order to react and form Cu_2S , and hence would be non-activating. Resolution of this issue requires determination of the atomic electron densities in activating and non-activating polysulfur species and the configurations of the adsorbed species on copper. We will attempt to resolve this important issue in the next phase of this work by using Density Functional Theory to estimate atomic electron densities and to identify the most favorable configurations for the adsorbed species on copper. An important goal will be to explain why thiosulfate ($S_2O_3^{2-}$) is a powerful activator but the higher homologues are non-activating. In the thiosulfate case, it is possible that the electron density on the sulfur is higher than that on the oxygen and hence that the ion adsorbs in a configuration that (a pyramid "on its side") allows the sulfur to react with the copper.



$$\log\left(\frac{a_{\text{SO}_3(2-)}}{a_{\text{HS}_3\text{O}_3(1-)}}\right) = \frac{-\Delta G^0}{2.303RT} + pH$$

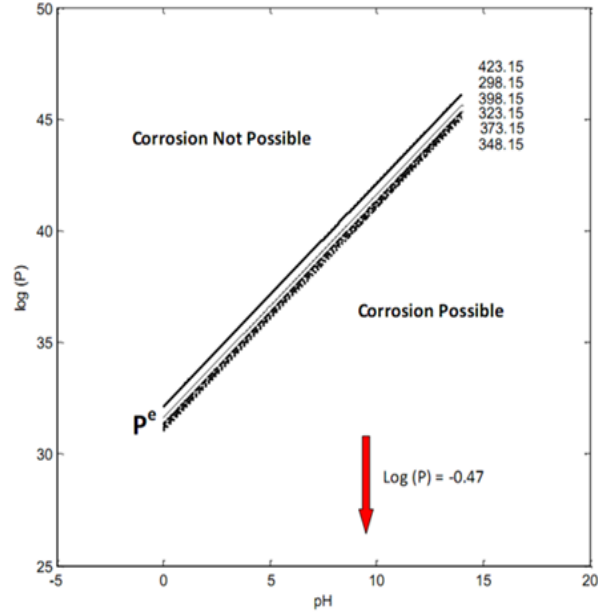
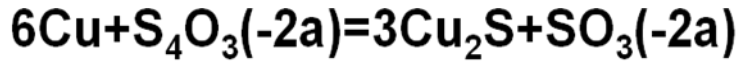


Figure 5: Corrosion Domain Diagram for copper in the presence of HS_3O_3^- . Note that this species is a powerful activator of copper. The red arrow indicates the range of P calculated from the documented composition of the ground water.



$$\log\left(\frac{a_{\text{SO}_3^{2-}}}{a_{\text{S}_4\text{O}_3^{2-}}}\right) = \frac{-\Delta G^0}{2.303RT}$$

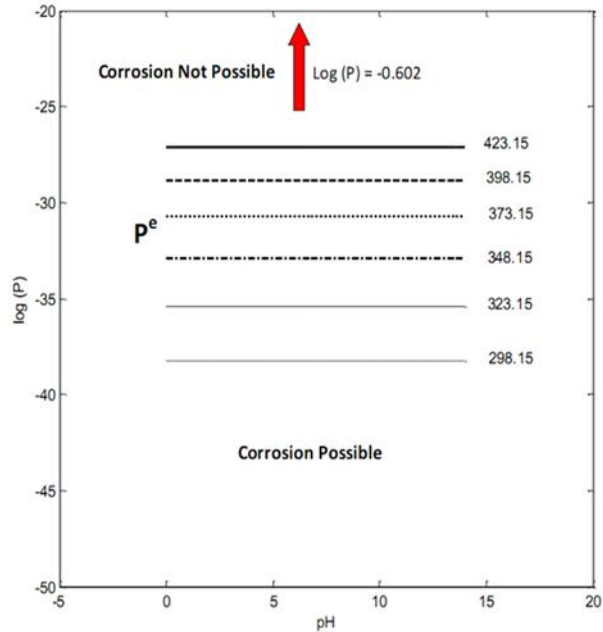


Figure 6: Corrosion Domain Diagram for copper in the presence of $\text{S}_4\text{O}_3^{2-}$. Note that this species is predicted not to activate copper. The red arrow indicates the range of P calculated from the documented composition of the ground water.

A comprehensive listing of reactions involving various activating species is presented in Tables 2 to 4. In these tables, calculated P values for those compounds that are predicted to be present in the system (based on the GEMS output results) are shown and they are compared with the equilibrium P^e value presented on the CDD for each reaction. As a result, possible corrosion relationships in the systems were predicted. (Please note that blank cells indicate that the corrosion prediction is not possible, because the components involved in the reactions are predicted not to be present in the system, based upon the GEMS results).

Table-2- a-Calculated *P* values for different reactions at T = 42 °C

Reaction	Log (P)	Corrosion possible?
$2\text{Cu} + \text{H}_2\text{O} (\text{l}) = \text{Cu}_2\text{O} + \text{H}_2(\text{g})$	-13.65	No-Near the Eq. line
$2\text{Cu} + \text{H}_2\text{S}_2\text{O}_3(\text{a}) = \text{Cu}_2\text{S} + \text{SO}_3(-2\text{a}) + 2\text{H}(+\text{a})$	---	---
$2\text{Cu} + \text{H}_2\text{S}_2\text{O}_4(\text{a}) = \text{Cu}_2\text{S} + \text{SO}_4(-2\text{a}) + 2\text{H}(+\text{a})$	---	---
$2\text{Cu} + \text{HS}_2\text{O}_3(-\text{a}) = \text{Cu}_2\text{S} + \text{SO}_3(-2\text{a}) + \text{H}(+\text{a})$	---	---
$2\text{Cu} + \text{HS}_2\text{O}_4(-\text{a}) = \text{Cu}_2\text{S} + \text{SO}_4(-2\text{a}) + \text{H}(+\text{a})$	---	---
$2\text{Cu} + \text{S}(-2\text{a}) + 2\text{H}(+\text{a}) = \text{Cu}_2\text{S} + \text{H}_2(\text{g})$	4.75	Yes
$2\text{Cu} + \text{H}_2\text{S} = \text{Cu}_2\text{S} + \text{H}_2(\text{g})$	-4.44	Yes
$2\text{Cu} + \text{S}_2\text{O}_3(-2\text{a}) = \text{Cu}_2\text{S} + \text{SO}_3(-2\text{a})$	---	---
$2\text{Cu} + \text{S}_2\text{O}_4(-2\text{a}) = \text{Cu}_2\text{S} + \text{SO}_4(-2\text{a})$	---	---
$4\text{Cu} + \text{S}_2(-2\text{a}) + 2\text{H}(+\text{a}) = 2\text{Cu}_2\text{S} + \text{H}_2(\text{g})$	---	---
$4\text{Cu} + \text{S}_3\text{O}_3(-2\text{a}) = 2\text{Cu}_2\text{S} + \text{SO}_3(-2\text{a})$	---	---
$4\text{Cu} + \text{S}_4\text{O}_6(-2\text{a}) = 2\text{Cu}_2\text{S} + \text{SO}_3(-2\text{a}) + \text{SO}_3(\text{a})$	---	---
$6\text{Cu} + \text{S}_3(-2\text{a}) + 2\text{H}(+\text{a}) = 3\text{Cu}_2\text{S} + \text{H}_2(\text{g})$	---	---
$6\text{Cu} + \text{S}_4\text{O}_3(-2\text{a}) = 3\text{Cu}_2\text{S} + \text{SO}_3(-2\text{a})$	---	---
$6\text{Cu} + \text{S}_5\text{O}_6(-2\text{a}) = 3\text{Cu}_2\text{S} + \text{SO}_3(-2\text{a}) + \text{SO}_3(\text{a})$	---	---
$8\text{Cu} + \text{S}_4(-2\text{a}) + 2\text{H}(+\text{a}) = 4\text{Cu}_2\text{S} + \text{H}_2(\text{g})$	---	---
$8\text{Cu} + \text{S}_5\text{O}_3(-2\text{a}) = 4\text{Cu}_2\text{S} + \text{SO}_3(-2\text{a})$	---	---
$8\text{Cu} + \text{S}_6\text{O}_6(-2\text{a}) = 4\text{Cu}_2\text{S} + \text{SO}_3(-2\text{a}) + \text{SO}_3(\text{a})$	---	---
$10\text{Cu} + \text{S}_5(-2\text{a}) + 2\text{H}(+\text{a}) = 5\text{Cu}_2\text{S} + \text{H}_2(\text{g})$	---	---
$10\text{Cu} + \text{S}_6\text{O}_3(-2\text{a}) = 5\text{Cu}_2\text{S} + \text{SO}_3(-2\text{a})$	---	---
$10\text{Cu} + \text{S}_7\text{O}_6(-2\text{a}) = 5\text{Cu}_2\text{S} + \text{SO}_3(-2\text{a}) + \text{SO}_3(\text{a})$	---	---
$12\text{Cu} + \text{S}_6(-2\text{a}) + 2\text{H}(+\text{a}) = 6\text{Cu}_2\text{S} + \text{H}_2(\text{g})$	---	---
$12\text{Cu} + \text{S}_7\text{O}_3(-2\text{a}) = 6\text{Cu}_2\text{S} + \text{SO}_3(-2\text{a})$	---	---
$\text{Cu} + \text{Br}(-\text{a}) + \text{H}(+\text{a}) = \text{CuBr} + 0.5\text{H}_2(\text{g})$	---	---
$\text{Cu} + \text{Cl}(-\text{a}) + \text{H}(+\text{a}) = \text{CuCl} + 0.5\text{H}_2(\text{g})$	---	---
$\text{Cu} + \text{F}(-\text{a}) + \text{H}(+\text{a}) = \text{CuF} + 0.5\text{H}_2(\text{g})$	---	---
$\text{Cu} + \text{I}(-\text{a}) + \text{H}(+\text{a}) = \text{CuI} + 0.5\text{H}_2(\text{g})$	---	---
$4\text{Cu} + \text{HS}_3\text{O}_3(-\text{a}) = 2\text{Cu}_2\text{S} + \text{SO}_3(-2\text{a}) + \text{H}(+\text{a})$	---	---
$\text{Cu} + 2\text{NH}_3(\text{a}) + \text{H}(+\text{a}) = \text{Cu}(\text{NH}_3)_2(+\text{a}) + 1/2\text{H}_2(\text{g})$	3.71	No
$\text{Cu} + 2\text{NH}_3(\text{a}) + 2\text{H}(+\text{a}) = \text{Cu}(\text{NH}_3)_2(+2\text{a}) + \text{H}_2(\text{g})$	---	---
$\text{Cu} + \text{CO}_3^{2-} + 2\text{H}^+ = \text{CuCO}_3(\text{a}) + \text{H}_2$	---	---
$\text{Cu} + 2\text{CO}_3^{2-} + 2\text{H}^+ = \text{Cu}(\text{CO}_3)_2(-2\text{a}) + \text{H}_2$	---	---
$\text{Cu} + \text{Cl}^- + \text{H}^+ = \text{CuCl}(\text{a}) + 1/2 \text{H}_2$	---	---
$\text{Cu} + 2\text{Cl}^- + 2\text{H}^+ = \text{CuCl}_2(\text{a}) + \text{H}_2$	---	---
$\text{Cu} + 2\text{Cl}^- + \text{H}^+ = \text{CuCl}_2(-\text{a}) + 1/2 \text{H}_2$	---	---
$\text{Cu} + 3\text{Cl}^- + 2\text{H}^+ = \text{CuCl}_3(-\text{a}) + \text{H}_2$	---	---
$\text{Cu} + 4\text{Cl}^- + 2\text{H}^+ = \text{CuCl}_4(-2\text{a}) + \text{H}_2$	---	---
$2\text{Cu} + 4\text{Cl}^- + 2\text{H}^+ = \text{Cu}_2\text{Cl}_4(-2\text{a}) + \text{H}_2$	---	---
$3\text{Cu} + 6\text{Cl}^- + 3\text{H}^+ = \text{Cu}_3\text{Cl}_6(-3\text{a}) + 1.5\text{H}_2$	---	---
$\text{Cu} + \text{F}^- + 2\text{H}^+ = \text{CuF}(\text{a}) + \text{H}_2$	---	---
$\text{Cu} + \text{HCO}_3^- + 2\text{H}^+ = \text{Cu}(\text{HCO}_3)(+\text{a}) + \text{H}_2$	---	---
$\text{Cu} + \text{HPO}_4^{2-} + 2\text{H}^+ = \text{CuHPO}_4(\text{a}) + \text{H}_2$	---	---
$\text{Cu} + \text{H}_2\text{PO}_4^- + \text{H}^+ = \text{CuH}_2\text{PO}_4(\text{a}) + 1/2 \text{H}_2$	---	---

Table-2- b- Calculated *P* values for different reactions at T = 42 °C

Reaction	Log (P)	Corrosion possible?
$Cu + H_2PO_4^- + 2H^+ = Cu(H_2PO_4)(+a) + H_2$	---	---
$Cu + 2HPO_4^{2-} + 2H^+ = Cu(HPO_4)_2(-2a) + H_2$	---	---
$Cu + HPO_4^{2-} + H_2PO_4^- + 2H^+ = Cu(HPO_4)(H_2PO_4)(-a) + H_2$	---	---
$Cu + HPO_4^{2-} + H_2PO_4^- + H^+ = Cu(HPO_4)(H_2PO_4)(-2a) + \frac{1}{2} H_2$	---	---
$2Cu + HS^- + H^+ = Cu_2S + H_2$	-1.9	YES
$Cu + 2HS^- + H^+ = Cu(HS)_2(-a) + \frac{1}{2} H_2$	---	---
$Cu + NH_3(a) + 2H^+ = Cu(NH_3)(+2a) + H_2$	---	---
$Cu + 2NH_3 + 2H^+ = Cu(NH_3)_2(+2a) + H_2$	---	---
$Cu + 2NH_3 + H^+ = Cu(NH_3)_2(+a) + \frac{1}{2} H_2$	---	---
$Cu + 3NH_3 + 2H^+ = Cu(NH_3)_3(+2a) + H_2$	4.77	No
$Cu + 4NH_3 + 2H^+ = Cu(NH_3)_4(+2a) + H_2$	23.09	No
$Cu + 2NO_2^- + 2H^+ = Cu(NO_2)_2(a) + H_2$	---	---
$Cu + 2NO_3^- + 2H^+ = Cu(NO_3)_2(ia) + H_2$	---	---
$Cu + NO_2^- + 2H^+ = Cu(NO_2)(+a) + H_2$	---	---
$Cu + NO_3^- + 2H^+ = Cu(NO_3)(+a) + H_2$	---	---
$Cu + 2H_2O = Cu(OH)_2(ia) + H_2$	---	---
$Cu + H_2O + H^+ = CuOH(+a) + H_2$	---	---
$Cu + 2H_2O = Cu(OH)_2(-a) + H^+ + \frac{1}{2} H_2$	-23.65	Yes
$Cu + 3H_2O = Cu(OH)_3(-a) + H^+ + H_2$	---	---
$Cu + 4H_2O = Cu(OH)_4(-2a) + 2H^+ + H_2$	---	---
$2Cu + 2H_2O + 2H^+ = Cu_2(OH)_2(+2a) + 2H_2$	---	---
$3Cu + 4H_2O + 2H^+ = Cu_3(OH)_4(+2a) + 3H_2$	---	---
$2Cu + 3HS^- + H^+ = Cu_2S(HS)_2(-2a) + H_2$	---	---
$Cu + SO_4^{2-} + 2H^+ = CuSO_4(ia) + H_2$	---	---
$Cu + S_2O_3^{2-} + H^+ = Cu(S_2O_3)(-a) + \frac{1}{2} H_2$	---	---
$2Cu + H_2S_2O_3(a) + H_2O(l) = Cu_2S + SO_4(-2a) + 2H(+a) + H_2(g)$	---	---
$2Cu + H_2S_2O_4(a) + H_2(g) = Cu_2S + SO_3(-2a) + 2H(+a) + H_2O(l)$	---	---
$2Cu + HS_2O_3(-a) + H_2O(l) = Cu_2S + SO_4(-2a) + H(+a) + H_2(g)$	---	---
$2Cu + HS_2O_4(-a) + H_2(g) = Cu_2S + SO_3(-2a) + H(+a) + H_2O(l)$	---	---
$2Cu + S_2O_3(-2a) + H_2O(l) = Cu_2S + SO_4(-2a) + H_2(g)$	---	---
$2Cu + S_2O_4(-2a) + H_2(g) = Cu_2S + SO_3(-2a) + H_2O(l)$	---	---
$4Cu + S_3O_3(-2a) + H_2O(l) = 2Cu_2S + SO_4(-2a) + H_2(g)$	---	---
$4Cu + S_4O_6(-2a) + H_2O(l) = 2Cu_2S + SO_4(-2a) + SO_3(a) + H_2(g)$	---	---
$6Cu + S_4O_3(-2a) + H_2O(l) = 3Cu_2S + SO_4(-2a) + H_2(g)$	---	---
$6Cu + S_5O_6(-2a) + H_2O(l) = 3Cu_2S + SO_4(-2a) + SO_3(a) + H_2(g)$	---	---
$8Cu + S_5O_3(-2a) + H_2O(l) = 4Cu_2S + SO_4(-2a) + H_2(g)$	---	---
$8Cu + S_6O_6(-2a) + H_2O(l) = 4Cu_2S + SO_4(-2a) + SO_3(a) + H_2(g)$	---	---
$10Cu + S_6O_3(-2a) + H_2O(l) = 5Cu_2S + SO_4(-2a) + H_2(g)$	---	---
$10Cu + S_7O_6(-2a) + H_2O(l) = 5Cu_2S + SO_4(-2a) + SO_3(a) + H_2(g)$	---	---
$12Cu + S_7O_3(-2a) + H_2O(l) = 6Cu_2S + SO_4(-2a) + H_2(g)$	---	---
$4Cu + HS_3O_3(-a) + H_2O(l) = 2Cu_2S + SO_4(-2a) + H(+a) + H_2(g)$	---	---

Table-3-a- Calculated *P* values for different reactions at T = 58 °C.

Reaction	Log (P)	Corrosion possible?
$2\text{Cu} + \text{H}_2\text{O} (\text{l}) = \text{Cu}_2\text{O} + \text{H}_2(\text{g})$	-13.42	No-Near the Eq. line
$2\text{Cu} + \text{H}_2\text{S}_2\text{O}_3(\text{a}) = \text{Cu}_2\text{S} + \text{SO}_3(-2\text{a}) + 2\text{H}(+\text{a})$	---	---
$2\text{Cu} + \text{H}_2\text{S}_2\text{O}_4(\text{a}) = \text{Cu}_2\text{S} + \text{SO}_4(-2\text{a}) + 2\text{H}(+\text{a})$	---	---
$2\text{Cu} + \text{HS}_2\text{O}_3(-\text{a}) = \text{Cu}_2\text{S} + \text{SO}_3(-2\text{a}) + \text{H}(+\text{a})$	---	---
$2\text{Cu} + \text{HS}_2\text{O}_4(-\text{a}) = \text{Cu}_2\text{S} + \text{SO}_4(-2\text{a}) + \text{H}(+\text{a})$	---	---
$2\text{Cu} + \text{S}(-2\text{a}) + 2\text{H}(+\text{a}) = \text{Cu}_2\text{S} + \text{H}_2(\text{g})$	4.17	Yes
$2\text{Cu} + \text{H}_2\text{S} = \text{Cu}_2\text{S} + \text{H}_2(\text{g})$	-4.76	Yes
$2\text{Cu} + \text{S}_2\text{O}_3(-2\text{a}) = \text{Cu}_2\text{S} + \text{SO}_3(-2\text{a})$	---	---
$2\text{Cu} + \text{S}_2\text{O}_4(-2\text{a}) = \text{Cu}_2\text{S} + \text{SO}_4(-2\text{a})$	---	---
$4\text{Cu} + \text{S}_2(-2\text{a}) + 2\text{H}(+\text{a}) = 2\text{Cu}_2\text{S} + \text{H}_2(\text{g})$	---	---
$4\text{Cu} + \text{S}_3\text{O}_3(-2\text{a}) = 2\text{Cu}_2\text{S} + \text{SO}_3(-2\text{a})$	---	---
$4\text{Cu} + \text{S}_4\text{O}_6(-2\text{a}) = 2\text{Cu}_2\text{S} + \text{SO}_3(-2\text{a}) + \text{SO}_3(\text{a})$	---	---
$6\text{Cu} + \text{S}_3(-2\text{a}) + 2\text{H}(+\text{a}) = 3\text{Cu}_2\text{S} + \text{H}_2(\text{g})$	---	---
$6\text{Cu} + \text{S}_4\text{O}_3(-2\text{a}) = 3\text{Cu}_2\text{S} + \text{SO}_3(-2\text{a})$	---	---
$6\text{Cu} + \text{S}_5\text{O}_6(-2\text{a}) = 3\text{Cu}_2\text{S} + \text{SO}_3(-2\text{a}) + \text{SO}_3(\text{a})$	---	---
$8\text{Cu} + \text{S}_4(-2\text{a}) + 2\text{H}(+\text{a}) = 4\text{Cu}_2\text{S} + \text{H}_2(\text{g})$	---	---
$8\text{Cu} + \text{S}_5\text{O}_3(-2\text{a}) = 4\text{Cu}_2\text{S} + \text{SO}_3(-2\text{a})$	---	---
$8\text{Cu} + \text{S}_6\text{O}_6(-2\text{a}) = 4\text{Cu}_2\text{S} + \text{SO}_3(-2\text{a}) + \text{SO}_3(\text{a})$	---	---
$10\text{Cu} + \text{S}_5(-2\text{a}) + 2\text{H}(+\text{a}) = 5\text{Cu}_2\text{S} + \text{H}_2(\text{g})$	---	---
$10\text{Cu} + \text{S}_6\text{O}_3(-2\text{a}) = 5\text{Cu}_2\text{S} + \text{SO}_3(-2\text{a})$	---	---
$10\text{Cu} + \text{S}_7\text{O}_6(-2\text{a}) = 5\text{Cu}_2\text{S} + \text{SO}_3(-2\text{a}) + \text{SO}_3(\text{a})$	---	---
$12\text{Cu} + \text{S}_6(-2\text{a}) + 2\text{H}(+\text{a}) = 6\text{Cu}_2\text{S} + \text{H}_2(\text{g})$	---	---
$12\text{Cu} + \text{S}_7\text{O}_3(-2\text{a}) = 6\text{Cu}_2\text{S} + \text{SO}_3(-2\text{a})$	---	---
$\text{Cu} + \text{Br}(-\text{a}) + \text{H}(+\text{a}) = \text{CuBr} + 0.5\text{H}_2(\text{g})$	---	---
$\text{Cu} + \text{Cl}(-\text{a}) + \text{H}(+\text{a}) = \text{CuCl} + 0.5\text{H}_2(\text{g})$	---	---
$\text{Cu} + \text{F}(-\text{a}) + \text{H}(+\text{a}) = \text{CuF} + 0.5\text{H}_2(\text{g})$	---	---
$\text{Cu} + \text{I}(-\text{a}) + \text{H}(+\text{a}) = \text{CuI} + 0.5\text{H}_2(\text{g})$	---	---
$4\text{Cu} + \text{HS}_3\text{O}_3(-\text{a}) = 2\text{Cu}_2\text{S} + \text{SO}_3(-2\text{a}) + \text{H}(+\text{a})$	---	---
$\text{Cu} + 2\text{NH}_3(\text{a}) + \text{H}(+\text{a}) = \text{Cu}(\text{NH}_3)_2(+\text{a}) + 1/2\text{H}_2(\text{g})$	4.75	Yes
$\text{Cu} + 2\text{NH}_3(\text{a}) + 2\text{H}(+\text{a}) = \text{Cu}(\text{NH}_3)_2(+2\text{a}) + \text{H}_2(\text{g})$	---	---
$\text{Cu} + \text{CO}_3^{2-} + 2\text{H}^+ = \text{CuCO}_3(\text{a}) + \text{H}_2$	---	---
$\text{Cu} + 2\text{CO}_3^{2-} + 2\text{H}^+ = \text{Cu}(\text{CO}_3)_2(-2\text{a}) + \text{H}_2$	---	---
$\text{Cu} + \text{Cl}^- + \text{H}^+ = \text{CuCl}(\text{a}) + 1/2 \text{H}_2$	---	---
$\text{Cu} + 2\text{Cl}^- + 2\text{H}^+ = \text{CuCl}_2(\text{a}) + \text{H}_2$	---	---
$\text{Cu} + 2\text{Cl}^- + \text{H}^+ = \text{CuCl}_2(-\text{a}) + 1/2 \text{H}_2$	---	---
$\text{Cu} + 3\text{Cl}^- + 2\text{H}^+ = \text{CuCl}_3(-\text{a}) + \text{H}_2$	---	---
$\text{Cu} + 4\text{Cl}^- + 2\text{H}^+ = \text{CuCl}_4(-2\text{a}) + \text{H}_2$	---	---
$2\text{Cu} + 4\text{Cl}^- + 2\text{H}^+ = \text{Cu}_2\text{Cl}_4(-2\text{a}) + \text{H}_2$	---	---
$3\text{Cu} + 6\text{Cl}^- + 3\text{H}^+ = \text{Cu}_3\text{Cl}_6(-3\text{a}) + 1.5\text{H}_2$	---	---
$\text{Cu} + \text{F}^- + 2\text{H}^+ = \text{CuF}(\text{a}) + \text{H}_2$	---	---
$\text{Cu} + \text{HCO}_3^- + 2\text{H}^+ = \text{Cu}(\text{HCO}_3)(+\text{a}) + \text{H}_2$	---	---
$\text{Cu} + \text{HPO}_4^{2-} + 2\text{H}^+ = \text{CuHPO}_4(\text{a}) + \text{H}_2$	---	---
$\text{Cu} + \text{H}_2\text{PO}_4^- + \text{H}^+ = \text{CuH}_2\text{PO}_4(\text{a}) + 1/2 \text{H}_2$	---	---

Table-3-b- Calculated *P* values for different reactions at T = 58 °C.

Reaction	Log (P)	Corrosion possible?
$Cu + H_2PO_4^- + 2H^+ = Cu(H_2PO_4)(+a) + H_2$	---	---
$Cu + 2HPO_4^{2-} + 2H^+ = Cu(HPO_4)_2(-2a) + H_2$	---	---
$Cu + HPO_4^{2-} + H_2PO_4^- + 2H^+ = Cu(HPO_4)(H_2PO_4)(-a) + H_2$	---	---
$Cu + HPO_4^{2-} + H_2PO_4^- + H^+ = Cu(HPO_4)(H_2PO_4)(-2a) + \frac{1}{2} H_2$	---	---
$2Cu + HS^- + H^+ = Cu_2S + H_2$	-2.24	YES
$Cu + 2HS^- + H^+ = Cu(HS)_2(-a) + \frac{1}{2} H_2$	---	---
$Cu + NH_3(a) + 2H^+ = Cu(NH_3)(+2a) + H_2$	---	---
$Cu + 2NH_3 + 2H^+ = Cu(NH_3)_2(+2a) + H_2$	---	---
$Cu + 2NH_3 + H^+ = Cu(NH_3)_2(+a) + \frac{1}{2} H_2$	---	---
$Cu + 3NH_3 + 2H^+ = Cu(NH_3)_3(+2a) + H_2$	6.56	No
$Cu + 4NH_3 + 2H^+ = Cu(NH_3)_4(+2a) + H_2$	25.24	No
$Cu + 2NO_2^- + 2H^+ = Cu(NO_2)_2(a) + H_2$	---	---
$Cu + 2NO_3^- + 2H^+ = Cu(NO_3)_2(ia) + H_2$	---	---
$Cu + NO_2^- + 2H^+ = Cu(NO_2)(+a) + H_2$	---	---
$Cu + NO_3^- + 2H^+ = Cu(NO_3)(+a) + H_2$	---	---
$Cu + 2H_2O = Cu(OH)_2(ia) + H_2$	---	---
$Cu + H_2O + H^+ = CuOH(+a) + H_2$	---	---
$Cu + 2H_2O = Cu(OH)_2(-a) + H^+ + \frac{1}{2} H_2$	-23.52	Yes
$Cu + 3H_2O = Cu(OH)_3(-a) + H^+ + H_2$	---	---
$Cu + 4H_2O = Cu(OH)_4(-2a) + 2H^+ + H_2$	---	---
$2Cu + 2H_2O + 2H^+ = Cu_2(OH)_2(+2a) + 2H_2$	---	---
$3Cu + 4H_2O + 2H^+ = Cu_3(OH)_4(+2a) + 3H_2$	---	---
$2Cu + 3HS^- + H^+ = Cu_2S(HS)_2(-2a) + H_2$	---	---
$Cu + SO_4^{2-} + 2H^+ = CuSO_4(ia) + H_2$	---	---
$Cu + S_2O_3^{2-} + H^+ = Cu(S_2O_3)(-a) + \frac{1}{2} H_2$	---	---
$2Cu + H_2S_2O_3(a) + H_2O(l) = Cu_2S + SO_4(-2a) + 2H(+a) + H_2(g)$	---	---
$2Cu + H_2S_2O_4(a) + H_2(g) = Cu_2S + SO_3(-2a) + 2H(+a) + H_2O(l)$	---	---
$2Cu + HS_2O_3(-a) + H_2O(l) = Cu_2S + SO_4(-2a) + H(+a) + H_2(g)$	---	---
$2Cu + HS_2O_4(-a) + H_2(g) = Cu_2S + SO_3(-2a) + H(+a) + H_2O(l)$	---	---
$2Cu + S_2O_3(-2a) + H_2O(l) = Cu_2S + SO_4(-2a) + H_2(g)$	---	---
$2Cu + S_2O_4(-2a) + H_2(g) = Cu_2S + SO_3(-2a) + H_2O(l)$	---	---
$4Cu + S_3O_3(-2a) + H_2O(l) = 2Cu_2S + SO_4(-2a) + H_2(g)$	---	---
$4Cu + S_4O_6(-2a) + H_2O(l) = 2Cu_2S + SO_4(-2a) + SO_3(a) + H_2(g)$	---	---
$6Cu + S_4O_3(-2a) + H_2O(l) = 3Cu_2S + SO_4(-2a) + H_2(g)$	---	---
$6Cu + S_5O_6(-2a) + H_2O(l) = 3Cu_2S + SO_4(-2a) + SO_3(a) + H_2(g)$	---	---
$8Cu + S_5O_3(-2a) + H_2O(l) = 4Cu_2S + SO_4(-2a) + H_2(g)$	---	---
$8Cu + S_6O_6(-2a) + H_2O(l) = 4Cu_2S + SO_4(-2a) + SO_3(a) + H_2(g)$	---	---
$10Cu + S_6O_3(-2a) + H_2O(l) = 5Cu_2S + SO_4(-2a) + H_2(g)$	---	---
$10Cu + S_7O_6(-2a) + H_2O(l) = 5Cu_2S + SO_4(-2a) + SO_3(a) + H_2(g)$	---	---
$12Cu + S_7O_3(-2a) + H_2O(l) = 6Cu_2S + SO_4(-2a) + H_2(g)$	---	---
$4Cu + HS_3O_3(-a) + H_2O(l) = 2Cu_2S + SO_4(-2a) + H(+a) + H_2(g)$	---	---

Table-4-a- Calculated P values for different reactions at $T = 80\text{ }^{\circ}\text{C}$.

Reaction	Log (P)	Corrosion possible?
$2\text{Cu} + \text{H}_2\text{O} (\text{l}) = \text{Cu}_2\text{O} + \text{H}_2(\text{g})$	-13.15	No-Near the Eq. line
$2\text{Cu} + \text{H}_2\text{S}_2\text{O}_3(\text{a}) = \text{Cu}_2\text{S} + \text{SO}_3(-2\text{a}) + 2\text{H}(+\text{a})$	---	---
$2\text{Cu} + \text{H}_2\text{S}_2\text{O}_4(\text{a}) = \text{Cu}_2\text{S} + \text{SO}_4(-2\text{a}) + 2\text{H}(+\text{a})$	---	---
$2\text{Cu} + \text{HS}_2\text{O}_3(-\text{a}) = \text{Cu}_2\text{S} + \text{SO}_3(-2\text{a}) + \text{H}(+\text{a})$	---	---
$2\text{Cu} + \text{HS}_2\text{O}_4(-\text{a}) = \text{Cu}_2\text{S} + \text{SO}_4(-2\text{a}) + \text{H}(+\text{a})$	---	---
$2\text{Cu} + \text{S}(-2\text{a}) + 2\text{H}(+\text{a}) = \text{Cu}_2\text{S} + \text{H}_2(\text{g})$	3.47	Yes
$2\text{Cu} + \text{H}_2\text{S} = \text{Cu}_2\text{S} + \text{H}_2(\text{g})$	-5.17	Yes
$2\text{Cu} + \text{S}_2\text{O}_3(-2\text{a}) = \text{Cu}_2\text{S} + \text{SO}_3(-2\text{a})$	---	---
$2\text{Cu} + \text{S}_2\text{O}_4(-2\text{a}) = \text{Cu}_2\text{S} + \text{SO}_4(-2\text{a})$	---	---
$4\text{Cu} + \text{S}_2(-2\text{a}) + 2\text{H}(+\text{a}) = 2\text{Cu}_2\text{S} + \text{H}_2(\text{g})$	5.99	Yes
$4\text{Cu} + \text{S}_3\text{O}_3(-2\text{a}) = 2\text{Cu}_2\text{S} + \text{SO}_3(-2\text{a})$	---	---
$4\text{Cu} + \text{S}_4\text{O}_6(-2\text{a}) = 2\text{Cu}_2\text{S} + \text{SO}_3(-2\text{a}) + \text{SO}_3(\text{a})$	---	---
$6\text{Cu} + \text{S}_3(-2\text{a}) + 2\text{H}(+\text{a}) = 3\text{Cu}_2\text{S} + \text{H}_2(\text{g})$	---	---
$6\text{Cu} + \text{S}_4\text{O}_3(-2\text{a}) = 3\text{Cu}_2\text{S} + \text{SO}_3(-2\text{a})$	---	---
$6\text{Cu} + \text{S}_5\text{O}_6(-2\text{a}) = 3\text{Cu}_2\text{S} + \text{SO}_3(-2\text{a}) + \text{SO}_3(\text{a})$	---	---
$8\text{Cu} + \text{S}_4(-2\text{a}) + 2\text{H}(+\text{a}) = 4\text{Cu}_2\text{S} + \text{H}_2(\text{g})$	---	---
$8\text{Cu} + \text{S}_5\text{O}_3(-2\text{a}) = 4\text{Cu}_2\text{S} + \text{SO}_3(-2\text{a})$	---	---
$8\text{Cu} + \text{S}_6\text{O}_6(-2\text{a}) = 4\text{Cu}_2\text{S} + \text{SO}_3(-2\text{a}) + \text{SO}_3(\text{a})$	---	---
$10\text{Cu} + \text{S}_5(-2\text{a}) + 2\text{H}(+\text{a}) = 5\text{Cu}_2\text{S} + \text{H}_2(\text{g})$	---	---
$10\text{Cu} + \text{S}_6\text{O}_3(-2\text{a}) = 5\text{Cu}_2\text{S} + \text{SO}_3(-2\text{a})$	---	---
$10\text{Cu} + \text{S}_7\text{O}_6(-2\text{a}) = 5\text{Cu}_2\text{S} + \text{SO}_3(-2\text{a}) + \text{SO}_3(\text{a})$	---	---
$12\text{Cu} + \text{S}_6(-2\text{a}) + 2\text{H}(+\text{a}) = 6\text{Cu}_2\text{S} + \text{H}_2(\text{g})$	---	---
$12\text{Cu} + \text{S}_7\text{O}_3(-2\text{a}) = 6\text{Cu}_2\text{S} + \text{SO}_3(-2\text{a})$	---	---
$\text{Cu} + \text{Br}(-\text{a}) + \text{H}(+\text{a}) = \text{CuBr} + 0.5\text{H}_2(\text{g})$	---	---
$\text{Cu} + \text{Cl}(-\text{a}) + \text{H}(+\text{a}) = \text{CuCl} + 0.5\text{H}_2(\text{g})$	---	---
$\text{Cu} + \text{F}(-\text{a}) + \text{H}(+\text{a}) = \text{CuF} + 0.5\text{H}_2(\text{g})$	---	---
$\text{Cu} + \text{I}(-\text{a}) + \text{H}(+\text{a}) = \text{CuI} + 0.5\text{H}_2(\text{g})$	---	---
$4\text{Cu} + \text{HS}_3\text{O}_3(-\text{a}) = 2\text{Cu}_2\text{S} + \text{SO}_3(-2\text{a}) + \text{H}(+\text{a})$	---	---
$\text{Cu} + 2\text{NH}_3(\text{a}) + \text{H}(+\text{a}) = \text{Cu}(\text{NH}_3)_2(+\text{a}) + 1/2\text{H}_2(\text{g})$	6.07	No
$\text{Cu} + 2\text{NH}_3(\text{a}) + 2\text{H}(+\text{a}) = \text{Cu}(\text{NH}_3)_2(+2\text{a}) + \text{H}_2(\text{g})$	---	---
$\text{Cu} + \text{CO}_3^{2-} + 2\text{H}^+ = \text{CuCO}_3(\text{a}) + \text{H}_2$	---	---
$\text{Cu} + 2\text{CO}_3^{2-} + 2\text{H}^+ = \text{Cu}(\text{CO}_3)_2(-2\text{a}) + \text{H}_2$	---	---
$\text{Cu} + \text{Cl}^- + \text{H}^+ = \text{CuCl}(\text{a}) + 1/2\text{H}_2$	---	---
$\text{Cu} + 2\text{Cl}^- + 2\text{H}^+ = \text{CuCl}_2(\text{a}) + \text{H}_2$	---	---
$\text{Cu} + 2\text{Cl}^- + \text{H}^+ = \text{CuCl}_2(-\text{a}) + 1/2\text{H}_2$	---	---
$\text{Cu} + 3\text{Cl}^- + 2\text{H}^+ = \text{CuCl}_3(-\text{a}) + \text{H}_2$	---	---
$\text{Cu} + 4\text{Cl}^- + 2\text{H}^+ = \text{CuCl}_4(-2\text{a}) + \text{H}_2$	---	---
$2\text{Cu} + 4\text{Cl}^- + 2\text{H}^+ = \text{Cu}_2\text{Cl}_4(-2\text{a}) + \text{H}_2$	---	---
$3\text{Cu} + 6\text{Cl}^- + 3\text{H}^+ = \text{Cu}_3\text{Cl}_6(-3\text{a}) + 1.5\text{H}_2$	---	---
$\text{Cu} + \text{F}^- + 2\text{H}^+ = \text{CuF}(\text{a}) + \text{H}_2$	---	---
$\text{Cu} + \text{HCO}_3^- + 2\text{H}^+ = \text{Cu}(\text{HCO}_3)(+\text{a}) + \text{H}_2$	---	---
$\text{Cu} + \text{HPO}_4^{2-} + 2\text{H}^+ = \text{CuHPO}_4(\text{a}) + \text{H}_2$	---	---
$\text{Cu} + \text{H}_2\text{PO}_4^- + \text{H}^+ = \text{CuH}_2\text{PO}_4(\text{a}) + 1/2\text{H}_2$	---	---

Table-4-b- Calculated *P* values for different reactions at T = 80 °C.

Reaction	Log (P)	Corrosion possible?
$Cu + H_2PO_4^- + 2H^+ = Cu(H_2PO_4)(+a) + H_2$	---	---
$Cu + 2HPO_4^{2-} + 2H^+ = Cu(HPO_4)_2(-2a) + H_2$	---	---
$Cu + HPO_4^{2-} + H_2PO_4^- + 2H^+ = Cu(HPO_4)(H_2PO_4)(-a) + H_2$	---	---
$Cu + HPO_4^{2-} + H_2PO_4^- + H^+ = Cu(HPO_4)(H_2PO_4)(-2a) + \frac{1}{2} H_2$	---	---
$2Cu + HS^- + H^+ = Cu_2S + H_2$	-2.6	YES
$Cu + 2HS^- + H^+ = Cu(HS)_2(-a) + \frac{1}{2} H_2$	---	---
$Cu + NH_3(a) + 2H^+ = Cu(NH_3)(+2a) + H_2$	---	---
$Cu + 2NH_3 + 2H^+ = Cu(NH_3)_2(+2a) + H_2$	---	---
$Cu + 3NH_3 + 2H^+ = Cu(NH_3)_3(+2a) + H_2$	8.82	No
$Cu + 4NH_3 + 2H^+ = Cu(NH_3)_4(+2a) + H_2$	27.98	No
$Cu + 2NO_2^- + 2H^+ = Cu(NO_2)_2(a) + H_2$	---	---
$Cu + 2NO_3^- + 2H^+ = Cu(NO_3)_2(ia) + H_2$	---	---
$Cu + NO_2^- + 2H^+ = Cu(NO_2)(+a) + H_2$	---	---
$Cu + NO_3^- + 2H^+ = Cu(NO_3)(+a) + H_2$	---	---
$Cu + 2H_2O = Cu(OH)_2(ia) + H_2$	---	---
$Cu + H_2O + H^+ = CuOH(+a) + H_2$	---	---
$Cu + 2H_2O = Cu(OH)_2(-a) + H^+ + \frac{1}{2} H_2$	-23.40	Yes
$Cu + 3H_2O = Cu(OH)_3(-a) + H^+ + H_2$	---	---
$Cu + 4H_2O = Cu(OH)_4(-2a) + 2H^+ + H_2$	---	---
$2Cu + 2H_2O + 2H^+ = Cu_2(OH)_2(+2a) + 2H_2$	---	---
$3Cu + 4H_2O + 2H^+ = Cu_3(OH)_4(+2a) + 3H_2$	---	---
$2Cu + 3HS^- + H^+ = Cu_2S(HS)_2(-2a) + H_2$	---	---
$Cu + SO_4^{2-} + 2H^+ = CuSO_4(ia) + H_2$	---	---
$Cu + S_2O_3^{2-} + H^+ = Cu(S_2O_3)(-a) + \frac{1}{2} H_2$	---	---
$2Cu + H_2S_2O_3(a) + H_2O(l) = Cu_2S + SO_4(-2a) + 2H(+a) + H_2(g)$	---	---
$2Cu + H_2S_2O_4(a) + H_2(g) = Cu_2S + SO_3(-2a) + 2H(+a) + H_2O(l)$	---	---
$2Cu + HS_2O_3(-a) + H_2O(l) = Cu_2S + SO_4(-2a) + H(+a) + H_2(g)$	---	---
$2Cu + HS_2O_4(-a) + H_2(g) = Cu_2S + SO_3(-2a) + H(+a) + H_2O(l)$	---	---
$2Cu + S_2O_3(-2a) + H_2O(l) = Cu_2S + SO_4(-2a) + H_2(g)$	---	---
$2Cu + S_2O_4(-2a) + H_2(g) = Cu_2S + SO_3(-2a) + H_2O(l)$	---	---
$4Cu + S_3O_3(-2a) + H_2O(l) = 2Cu_2S + SO_4(-2a) + H_2(g)$	---	---
$4Cu + S_4O_6(-2a) + H_2O(l) = 2Cu_2S + SO_4(-2a) + SO_3(a) + H_2(g)$	---	---
$6Cu + S_4O_3(-2a) + H_2O(l) = 3Cu_2S + SO_4(-2a) + H_2(g)$	---	---
$6Cu + S_5O_6(-2a) + H_2O(l) = 3Cu_2S + SO_4(-2a) + SO_3(a) + H_2(g)$	---	---
$8Cu + S_5O_3(-2a) + H_2O(l) = 4Cu_2S + SO_4(-2a) + H_2(g)$	---	---
$8Cu + S_6O_6(-2a) + H_2O(l) = 4Cu_2S + SO_4(-2a) + SO_3(a) + H_2(g)$	---	---
$10Cu + S_6O_3(-2a) + H_2O(l) = 5Cu_2S + SO_4(-2a) + H_2(g)$	---	---
$10Cu + S_7O_6(-2a) + H_2O(l) = 5Cu_2S + SO_4(-2a) + SO_3(a) + H_2(g)$	---	---
$12Cu + S_7O_3(-2a) + H_2O(l) = 6Cu_2S + SO_4(-2a) + H_2(g)$	---	---
$4Cu + HS_3O_3(-a) + H_2O(l) = 2Cu_2S + SO_4(-2a) + H(+a) + H_2(g)$	---	---

The results of the Gibbs energy minimization showed that most of the sulfur based compounds such as polysulfides, polythiosulfates, and polythionates are not present in significant concentrations (i.e. at concentration $> 1 \times 10^{-20}$ M) under the anoxic condition and the temperatures of interest. On the other hand, HS^- , SO_4^{2-} , H_2S (aq), HS_2^- , S^{2-} , HSO_4^- and some other compounds are present at significant levels under these conditions, although their concentrations in the system are still very low. Calculation of P based on the Gibbs energy minimization results (Tables 2-4) and comparing them with P^e values (calculated using the Gibbs energy of formation and the pH value) revealed that H_2S (aq), HS^- , and S^{2-} and the polysulfides, HS_2^- and S_2^{2-} can activate copper at such a low concentration and, especially in the H_2S (aq) case, the P value is found to be far from the equilibrium line (P^e).

Finally, we have derived CDDs for many other systems than those discussed above and the diagrams may be found in the Appendix. These systems include complexing reactions, such as $Cu/CuCl_2^-$, $Cu/Cu(NH_3)_2^{2+}$, and $Cu(H_2PO_4)^+$, and $Cu/Cu(HCO_3)^+$, for example, as well as diagrams for other polysulfur species. The analysis of these diagrams is incomplete, because at the time of their derivation, we did not have reliable values for the concentrations of the activating anions in the repository. However, these data are now becoming available from GEMS simulations of the repository and the analyses will be completed in Phase II of this project.

IV. Volt-Equivalent Diagrams

It is well-known that sulfur is a powerful thermodynamic activator of copper, nickel, and iron through the formation of solid sulfide phases at more active electrochemical potentials than those at which the oxides form; in some cases, by as much as several hundred millivolts. Sulfur is also characterized as having the richest chemistry of any element in the periodic table, except for carbon, and as having the greatest range of oxidation states (-2 to +8), including fractional oxidation states. This richness in chemistry is exploited by nature in biological systems for the metabolism of sulfate, for example, by *Sulfate Reducing Bacteria* (SRB), or by *Thiobacillus Thiooxidans* (TT) in the oxidation of elemental sulfur to sulfate (including concentrated sulfuric acid). Sulfur, in the presence of water and oxygen (air), is also oxidized under UV radiation to sulfuric acid in an abiogenic process [17], the mechanism of which is little understood. In any case, these processes all proceed through sulfur compounds differing in oxidation state as they progress in the $S(-II)$ to $S(VI)$ or $S(VI)$ to $S(-II)$ directions. As our work on CDDs, summarized above, demonstrates, various, but not all, sulfur species activate copper and hence their presence in the groundwater at Forsmark raises the specter of their representing a corrosion threat to copper canisters in the repository. In some cases, the energy gained by reduction of sulfate is used to directly oxidize a metal, as in the case of *Thiobacillus Ferrooxidans* (*Acidithiobacillus ferrooxidans*), but the author knows of no instance where this occurs for copper, which is generally toxic toward micro-organisms. This aerobic species is known to live in pyrite deposits, which is a component of bentonite. It is important to note that the processes that they affect must be thermodynamically viable in the environments of interest and that the bacteria themselves simply act as powerful catalysts. Thus, for SRBs to reduce sulfate to sulfide, the change of Gibbs energy for the reaction $SO_4^{2-} + 4H_2 + 2H^+ \rightarrow H_2S + 4H_2O$ must be negative and must not require the bacteria to be so. This is because of the path-independence requirement of equilibrium thermodynamics. The transition of sulfate to sulfide, as affected chemically or

biochemically (with bacteria as catalysts) is best viewed as occurring through a series of intermediates, as follows:



with the oxidation of sulfide to sulfate occurring via the reverse sequence. Thus, the reaction sequence from left to right can be viewed as discrete reduction in y and increase in x (actually, increase in x/y) and hence a discrete reduction in the sulfur oxidation state.

Equation (12) shows that there are several homologous series of sulfur compounds that are of interest when discussing the rich chemistry of this element. They are:

- Polythionates: $S_xO_6^{2-}$; sulfur oxidation state (z) = $10/x$ ($z < 6$), ranging from $z = 5$ ($S_2O_6^{2-}$, which does not appear to have been synthesized) to 1.67 for $S_6O_6^{2-}$.
- Polythiosulfates: $S_xO_3^{2-}$; sulfur oxidation state (z) = $4/x$ ($z < 4$), ranging from $z = 2$ ($S_2O_3^{2-}$, “thiosulfate”) to 0.57 for $S_7O_3^{2-}$.
- Elemental sulfur, S^0 , $z = 0$.
- Polysulfides: S_x^{2-} ; sulfur oxidation state (z) = $-2/x$ ($z < 0$), ranging from -2 ($x = 1$, S^{2-}) to -0.167 ($x = 6$).

The objectives of the present work are to:

- Develop a rational basis for classifying the chemistry of the various sulfur species with regard to differences in thermodynamic affinities, as determined by their electrochemical reduction potentials and their oxidation states; and
- To ascertain whether an explanation of the abilities of the various sulfur species lies within the thermodynamics of the S - H_2O system.

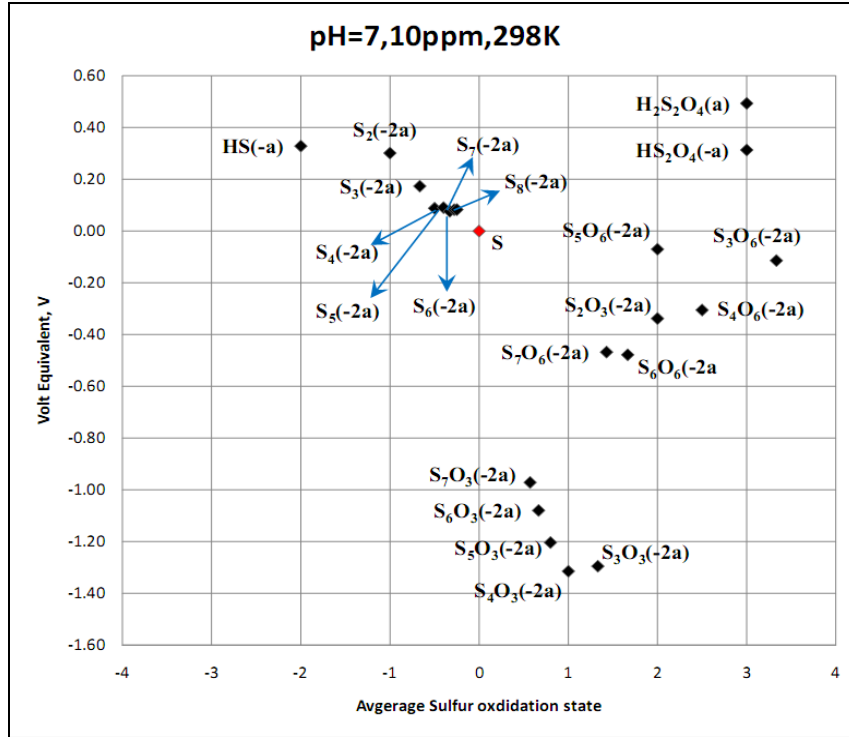


Figure 7: Volt-Equivalent Diagram for sulfur in Forsmark ground water, $pH = 7$, $[S] = 10$ ppm, 25°C . The red point represents elemental sulfur.

The vehicle chosen in this work to explore these issues is the Volt-Equivalent Diagram (VED). The Volt Equivalent for a species is the equilibrium potential for the reduction reaction of the species (e.g., $S_xO_y^{2-}$) to elemental sulfur



multiplied by the average oxidation state of sulfur in the species $[z = 2(y-1)/x]$. The Volt Equivalent Diagram is then formed by plotting the volt-equivalents for the various species versus the average oxidation state. In doing so, we first calculate the standard potential by using

$$E^o = -\Delta_f G^o / 2(y-1)F \quad (14)$$

where $\Delta_f G^o$ is the change in standard Gibbs energy for the cell reaction



The equilibrium potential is then given as

$$E^e = E^o - [2.303RT / (2(y-1))] \log [a_s^{x/8} / (a_{H^+})^{2y}] \quad (16)$$

where a_s is the activity of the sulfur species and a_{H^+} is the corresponding quantity for H^+ . The volt-equivalent (VE) for $S_xO_y^{2-}$ is then simply zE^e .

A typical VED for the sulfur-water system under simulated repository groundwater conditions at 25 °C is presented in Figure 7. The concentrations of dissolved species were set arbitrarily at 10 ppm, but later work will employ actual concentrations as determined by Gibbs energy minimization speciation calculations. The interpretation of the diagrams follows from the following rules:

- Any two species connected by a straight line will tend to react to produce all of the species that lie below that line. Thus, for the reaction of HS^- and $H_2S_2O_4$ is predicted to generate essentially all other species plotted on the diagram.
- If a species lies above the straight line joining two other species, it will tend to disproportionate to produce the latter. Thus S_2^{2-} lies above the line joining S^{2-} and S_3^{2-} , so that the disproportionation reaction, $2S_2^{2-} \rightarrow S^{2-} + S_3^{2-}$, is predicted to occur.
- If several species lie on or close to a straight line joining two terminal species, the solution will contain all species in equilibrium at finite concentrations.
- The reactivity of any given species toward a metal in which a metal sulfide is formed is measured by the value of the VE. The more reactive species are characterized by high (more positive) VE values. Indeed the most reactive species tend to be located in the upper left quadrant, implying high reactivity and high electron density being simultaneously present, followed by species in the upper right quadrant. Species in the lower quadrants tend to be the least reactive toward a metal.

With respect to the activation of copper, which is of specific interest in this work, the activating species all have VE values more positive than $-0.60 V_{she}$, while the non-activating polythiosulfate species, $S_xO_3^{2-}$, $x \geq 3$, all have VE values more negative than $-0.80 V_{she}$. The one species in this homologous series that is activating, thiosulfate, $S_2O_3^{2-}$, has a VE value of $-0.35 V_{she}$, in keeping with this classification. Thus, we conclude that the thermodynamics plays at least a part in determining whether a species is activating and hence is capable of destroying thermodynamic immunity of copper in repository environments. However, we have been unable to identify a thermodynamic “on/off” switch that would account for the activating effects of the various sulfur species, so that some other factor(s) must be involved. On the basis of our present state of knowledge of the chemistry of these systems, we propose that the orientation of the adsorbed species on the Cu surface, as discussed above, is the deciding factor.

A VED for the sulfur- H_2O system at a higher temperature, but at a much lower species concentration (activity) is displayed in Figure 8. The reader will note that Figure 8 is qualitatively similar to Figure 7, with the following notables:

- The data for the polysulfides have moved little in terms of VE values, despite the changes in temperature, concentration, and pH.
- The data for the polythiosulfates, and especially, for the polythionates have shifted sharply in the negative direction, largely eliminating the previously-noted differences between the two homologous series of thiooxyanions. Thus, the VE values for the two series overlap, but still the CDDs predict that the polythionates activate copper, while the polythiosulfates do not. This is a further argument for factors other than thermodynamics being important is the activation of copper.

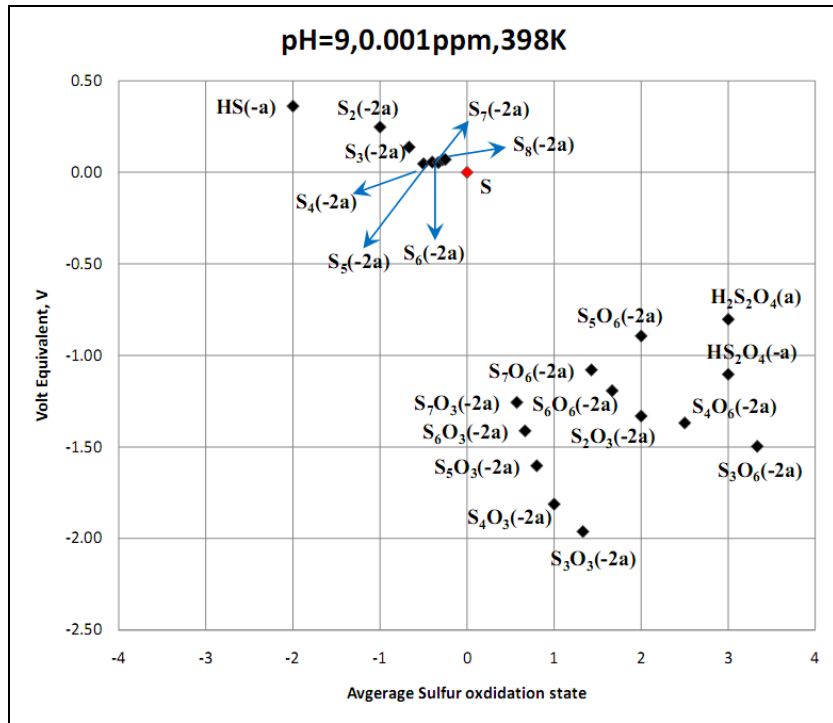


Figure 8: VED for the sulfur-water system at 125°C, $pH = 9$, $[S] = 0.001$ ppm.

More than 100 VEDs have been derived to date and probably an additional 100 or so will need to be derived by the end of this two-year program. When completed, the diagrams will permit a systematic analysis of the impact of each of the independent variables on the redox chemistry of sulfur under repository conditions. A large number of VEDs for various environmental conditions are located in the Appendix to this report.

V. Hydrogen Pressure

As shown by the Corrosion Domain Diagrams, the immunity of copper is intimately related to the partial pressure of hydrogen in the repository through the quantity, P . For the $Cu + H^+ = Cu^+ + 0.5H_2(g)$ reaction, P is defined as

$$P = a_{Cu^+} f_{H_2}^{1/2} \quad (17)$$

where a_{Cu^+} is the activity (“thermodynamic concentration”) of cuprous ion and f_{H_2} is the fugacity (“thermodynamic pressure”) of hydrogen. For a given pH , if $P > P^e$ copper is immune and corrosion cannot occur, regardless of the exposure time. While the KBS-2 and KBS-3 plans for the disposal of HLW in Sweden are not based upon copper being thermodynamically immune to corrosion, the issue of copper immunity is discussed frequently, especially within the context of the existence of native copper deposits in granitic geological formations at various

locations throughout the World (e.g., the Upper Penninsular in Michigan, USA, and in Sweden). These discussions generally end with the question: “What is it about nature that alloys copper to exist for geological time when in contact with some granitic ground waters?” Quite naturally, it is opined by many that, if we had the answer to this question, we might be able to engineer the groundwater environment to simulate what nature, apparently, has achieved, as we have indicated above using “scoping calculations”. However, as shown above, various species, such as sulfide ion and other sulfur-containing species, activate copper and hence destroy immunity. In this section, we estimate the hydrogen pressure that might be generated by a number of reactions in the system. This was partly motivated by the need to address and explain the experimental results of Hultqvist and Szakalos [1-3] that have become so controversial in the HLNW isolation community in Sweden; a controversy that has remained unresolved until now.

In this section, we explore the magnitude of the hydrogen pressure that may be generated by certain reactions between copper and species that are known or thought to exist in the proposed repositories. As noted above, this is done for two reasons:

- To aid in the interpretation of the results of experiments that have been reported by Szakalos and Hultqvist [1-3] that copper corrodes in pure, oxygen-free water with the evolution of hydrogen; and
- As an alternative means of demonstrating whether specific species will activate copper under repository conditions. Thus, if a reaction generates an equilibrium partial pressure of hydrogen that is greater than the repository hydrogen partial pressure (presumably generated by certain geochemical processes in the system) then the reaction will proceed in the forward (hydrogen-producing and corrosion) direction. On the other hand, if the H_2 pressure generated by the reaction under consideration is less than the repository hydrogen pressure then the reaction will proceed in the reverse direction and copper will be thermodynamically immune to corrosion. This is, of course, simply another manifestation of the Second Law of Thermodynamics and delivers the same information, albeit in a different format, as do the Corrosion Domain Diagrams (CDDs) discussed above.

According to SKB R-08-85 [18], “there are at least six possible processes by which crustal hydrogen is generated: (1) reaction between dissolved gases in the C-H-O-S system in magmas, especially in those with basaltic affinities; (2) decomposition of methane to carbon (graphite) and hydrogen at temperatures above 600°C; (3) reaction between CO_2 , H_2O , and CH_4 at elevated temperatures in vapors; (4) radiolysis of water by radioactive isotopes of uranium and thorium and their decay daughters and by radioactive isotopes of potassium; (5) catalysis of silicates under stress in the presence of water; and (6) hydrolysis by ferrous minerals in mafic and ultramafic rocks [19]. The radiolysis of water has been proposed [20] as a possible hydrogen generation process occurring in the granitic system in the Fennoscandian Shield. In addition, hydrogen is biologically produced in microbial fermentation processes. It is important to explore the scale of these processes and the rates at which the produced hydrogen becomes available to deep microbial ecosystems”. At the current time, too little is known of the kinetics of these processes to render an accurate assessment of the source term and, in any event, it is likely that the contributions of the various processes identified above to the overall source term will vary widely from location-to-location, depending upon the local conditions and rock composition. Noting that the steady-state concentration of hydrogen will be determined by the

rate of generation, due to the source term, and the rate of loss, due to the escape of hydrogen from the system by mass transport and reaction with other components in the rock, and assuming that the system will be far from equilibrium, it is evident that the actual concentration of hydrogen in the repository could vary over a wide, essentially unpredictable range. Accordingly, a theoretical approach to calculating the hydrogen concentration does not appear to be particularly fruitful. Thus, it appears that the only recourse in describing the redox conditions in the repository is to employ hydrogen concentrations that are measured in the repository, as summarized by Bath [21], even though the accurate measurement of hydrogen from “grab” samples is fraught with difficulty.

The pressure of hydrogen in the Forsmark repository has been estimated to be about 10^{-14} atm, corresponding to a concentration of about 10^{-11} M, but it is evident that the concentrations widely, being as high as 10^{-6} M in some locations. Indeed, measurements made at Forsmark and reported in SKB TR-06-09[34] set the concentration of H_2 in the repository at 10^{-6} M, five orders of magnitude greater than that reported by Bath [21]. We currently do not know the reason for this discrepancy, which, generally does not change the results of our analysis except in the case of weakly activating species. Once the discrepancy has been resolved, and if it is determined that the SKB results are correct, we will calculate new P values and correct the CDDs. The formation of hydrogen in geological systems has been discussed in the literature [19,22,23] and a comprehensive analysis of this previous work will not be reported here. It is sufficient to note that the formation of hydrogen is commonly attributed to the Schikorr reaction



and/or to the hydrolysis of Fayalite



We have calculated the hydrogen pressures generated from these reactions by noting that $p_{H_2} = K_{18}$ and $p_{H_2} = \sqrt{K_{19}}$ for Reactions (18) and (19), respectively, as a function of temperature, where K_{18} and K_{19} are the equilibrium constants. Plots of the hydrogen pressure from these two reactions are displayed in Figures 9 and 10.

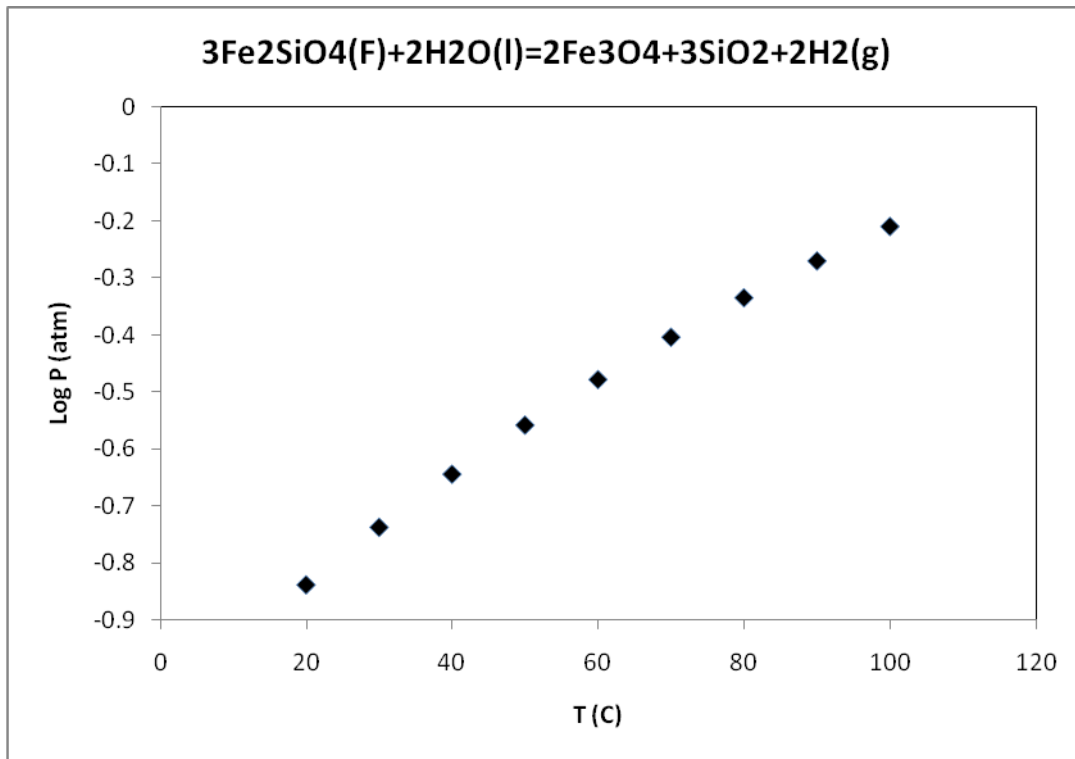


Figure 9: Calculated hydrogen pressure from the reaction, $3\text{Fe}_2\text{SiO}_4(\text{F}) + 2\text{H}_2\text{O}(\text{l}) = 2\text{Fe}_3\text{O}_4 + 3\text{SiO}_2 + 2\text{H}_2(\text{g})$

The data plotted in Figure 9 show that the hydrogen equilibrium pressure from Fayalite hydrolysis varies between about 0.1 atm to 0.6 atm as the temperature increases from 20 °C to 100 °C. In the case of the Schikorr reaction (Figure 10), the calculated equilibrium H_2 pressure varies over the same temperature range from 398 atm to 3981 atm. These numbers are considerably greater than the hydrogen pressures reported for the Forsmark repository in Sweden, which is found to be 10^{-14} atm [21] corresponding to a concentration of about 10^{-11} M (or 10^{-6} M, as reported by SKB TR-06-09[34]) at 25 °C.

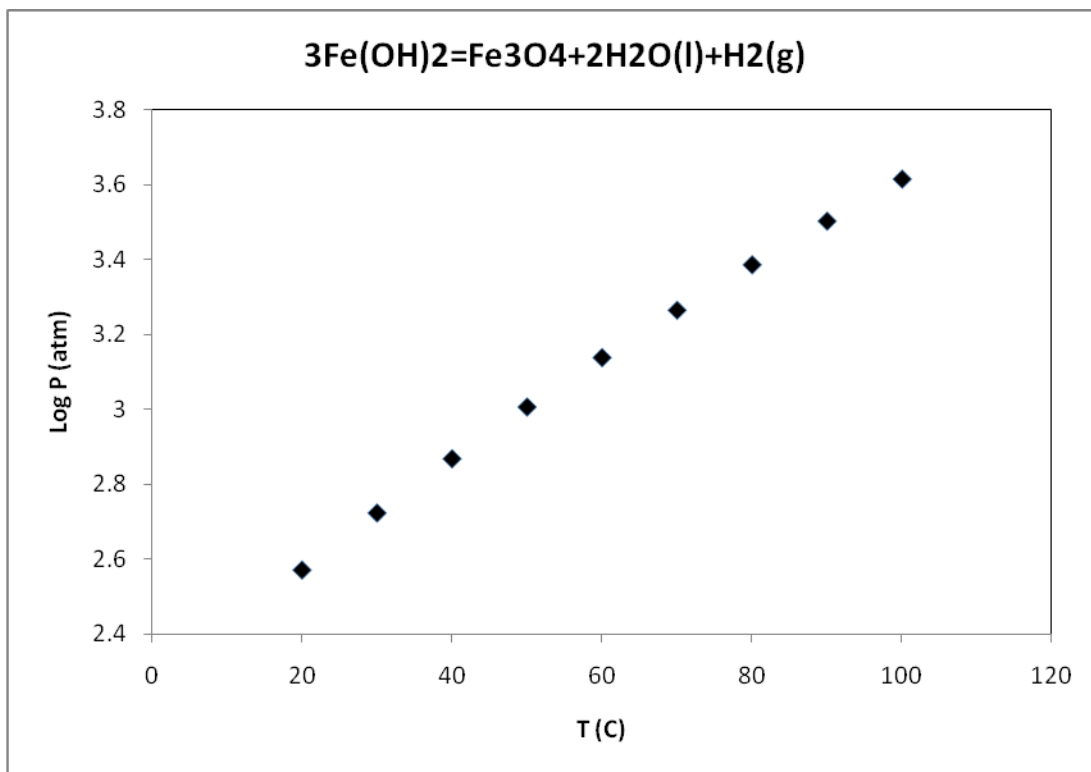


Figure 10: Calculated hydrogen pressure from the reaction, $3Fe(OH)_2=Fe_3O_4+2H_2O(l)+H_2(g)$

Hydrogen pressures for the various copper activation reactions were calculated using the expressions summarized in Table 5. In deriving these expressions, it was assumed that all of the hydrogen was produced by the reaction (i.e., no “background” hydrogen exists). All equilibrium constants were estimated using HSC-5 [24] with our expanded database that includes thermodynamic data for the various sulfur-containing species. Also, in performing these calculations, the non-ideality of the brine and the soluble components was taken into account by estimating activity coefficients using extended Debye-Huckel theory [25] with the ionic strength being established by the NaCl concentration (0.169 m and 0.338 m). However, the activity of water was assumed to be one. Activity coefficient corrections were not large, but were included for completeness. Note that γ_0 , γ_1 , and γ_2 are activity coefficients for uncharged species (e.g., H_2), univalent ions, and divalent ions, respectively. Finally, the activity of hydrogen ion was set equal to that for neutral water, which was calculated as $a_{H^+} = 10^{-pH}$ where the pH for the temperature of interest is estimated as $pH = pK_w / 2$.

In order to illustrate how the equations contained in Table 5 are derived we consider one example, Reaction 38:



The equilibrium constant for this reaction is written as

$$K = \frac{a_{SO_4^{2-}} a_{SO_3} f_{H_2}}{a_{H_2O} a_{S_2O_6^{2-}}}$$

Noting from the stoichiometry of the reaction, and assuming that neither SO_4^{2-} nor $SO_3(a)$ was present initially, we write

$$m_{SO_4^{2-}} = m_{SO_3}(aq)$$

and

$$m_{SO_3}(aq) = m_{H_2} = f_{H_2} / K_H$$

to give

$$f_{H_2} = \left[\frac{KK_H}{\gamma_0} \right]^{1/2}$$

The parameter K_H is Henry's constant from Henry's Law for gas solubility, which is defined here as

$$f_{H_2} = K_H m_{H_2}$$

Table 5: Reactions and formula for calculating hydrogen pressure in the *Cu-H-O-S-Cl* system.

	Reaction	Formula
1	$Cu + H(+a) = Cu(+a) + 0.5H_2(g)$	$f_{H_2} = \left[\frac{KK_H K_W^{1/2}}{2\gamma_1} \right]^{2/3}$
2	$Cu + H(+a) + Cl(-a) = CuCl(s) + 0.5H_2(g)$	$f_{H_2} = \left[\frac{KK_W^{1/2} m_{Cl^-} \gamma_1}{2} \right]^2$
3	$Cu + H(+a) + Cl(-a) = CuCl(a) + 0.5H_2(g)$	$f_{H_2} = \left[\frac{KK_H K_W^{1/2} m_{Cl^-} \gamma_1}{2\gamma_0} \right]^{2/3}$
4	$Cu + H(+a) + 2Cl(-a) = CuCl_2(-a) + 0.5H_2(g)$	$f_{H_2} = \left[\frac{KK_H K_W^{1/2} m_{Cl^-}^2 \gamma_1^2}{2\gamma_0} \right]^{2/3}$

5	$2Cu+2H(+a)+4Cl(-a)=Cu_2Cl_4(-2a)+H_2(g)$	$f_{H_2} = \left[\frac{KK_H K_W m_{Cl^-}^4 \gamma_1^2}{\gamma_2} \right]^{1/2}$
6	$3Cu+3H(+a)+6Cl(-a)=Cu_3Cl_6(-3a)+3/2H_2(g)$	$f_{H_2} = \left[\frac{3KK_H K_W^{3/2} m_{Cl^-}^6 \gamma_1^6}{2\gamma_3} \right]^{2/5}$
7	$Cu+H_2O(l)=Cu(OH)(a)+1/2H_2(g)$	$f_{H_2} = \left[\frac{KK_H}{2\gamma_0} \right]^{2/3}$
8	$Cu+2H_2O(l)=Cu(OH)_2(-a)+H(+a)+1/2H_2(g)$	$f_{H_2} = \left[\frac{KK_H}{2K_W^{1/2} \gamma_1} \right]^{2/3}$
9	$2Cu+H_2O(l)=Cu_2O+H_2(g)$	$f_{H_2} = K$
10	$Cu+2H(+a)=Cu(+2a)+H_2(g)$	$f_{H_2} = \left[\frac{KK_H K_W}{\gamma_2} \right]^{1/2}$
11	$Cu+2H(+a)+Cl(-a)=CuCl(+a)+H_2(g)$	$f_{H_2} = \left[\frac{KK_H K_W m_{Cl^-} \gamma_1}{\gamma_1} \right]^{1/2}$
12	$Cu+2H(+a)+2Cl(-a)=CuCl_2(a)+H_2(g)$	$f_{H_2} = \left[\frac{KK_H K_W m_{Cl^-}^2 \gamma_1^2}{\gamma_0} \right]^{1/2}$
13	$Cu+2H_2O(l)=Cu(OH)_2(ia)+H_2(g)$	$f_{H_2} = \left[\frac{KK_H}{\gamma_0} \right]^{1/2}$
14	$Cu+H_2O(l)+H(+a)=CuOH(+a)+H_2(g)$	$f_{H_2} = \left[\frac{KK_H K_W^{1/2}}{\gamma_1} \right]^{1/2}$
15	$Cu+3H_2O(l)=Cu(OH)_3(-a)+H(+a)+H_2(g)$	$f_{H_2} = \left[\frac{KK_H}{K_W^{1/2} \gamma_1} \right]^{1/2}$
16	$Cu+4H_2O(l)=Cu(OH)_4(-2a)+2H(+a)+H_2(g)$	$f_{H_2} = \left[\frac{KK_H}{K_W \gamma_2} \right]^{1/2}$

17	$2Cu + 2H_2O(l) + 2H^+ = Cu_2(OH)_2^{2+} + 2H_2(g)$	$f_{H_2} = \left[\frac{2KK_H K_W}{\gamma_2} \right]^{1/3}$
18	$3Cu + 4H_2O(l) + 2H^+ = Cu_3(OH)_4^{2+} + 3H_2(g)$	$f_{H_2} = \left[\frac{3KK_H K_W}{\gamma_2} \right]^{1/4}$
19	$2Cu + S^{2-} + 2H^+ = Cu_2S + H_2(g)$	$f_{H_2} = [KK_W \gamma_2 m_{S^{2-}}]$
20	$4Cu + S_2^{2-} + 2H^+ = 2Cu_2S + H_2(g)$	$f_{H_2} = [KK_W \gamma_2 m_{S_2^{2-}}]$
21	$6Cu + S_3^{2-} + 2H^+ = 3Cu_2S + H_2(g)$	$f_{H_2} = [KK_W \gamma_2 m_{S_3^{2-}}]$
22	$8Cu + S_4^{2-} + 2H^+ = 4Cu_2S + H_2(g)$	$f_{H_2} = [KK_W \gamma_2 m_{S_4^{2-}}]$
23	$10Cu + S_5^{2-} + 2H^+ = 5Cu_2S + H_2(g)$	$f_{H_2} = [KK_W \gamma_2 m_{S_5^{2-}}]$
24	$12Cu + S_6^{2-} + 2H^+ = 6Cu_2S + H_2(g)$	$f_{H_2} = [KK_W \gamma_2 m_{S_6^{2-}}]$
25	$2Cu + H_2S(a) = Cu_2S + H_2(g)$	$f_{H_2} = [K\gamma_0 m_{H_2S}]$
26	$Cu + Br^- + H^+ = CuBr + 0.5H_2(g)$	$f_{H_2} = [KK^{1/2}_W \gamma_1 m_{Br^-}]^2$
27	$Cu + F^- + H^+ = CuBr + 0.5H_2(g)$	$f_{H_2} = [KK^{1/2}_W \gamma_1 m_{F^-}]^2$
28	$Cu + I^- + H^+ = CuBr + 0.5H_2(g)$	$f_{H_2} = [KK^{1/2}_W \gamma_1 m_{I^-}]^2$
29	$2Cu + H_2O + H_2S_2O_3(a) = Cu_2S + SO_4^{2-} + 2H^+ + H_2(g)$	$f_{H_2} = \left[\frac{K\gamma_0}{K_W \gamma_2} \right]$
30	$2Cu + H_2S_2O_4(a) + H_2(g) = Cu_2S + SO_3^{2-} + 2H^+ + H_2O$	$f_{H_2} = \left[\frac{K_W \gamma_2}{K\gamma_0} \right]$
31	$2Cu + H_2O + HS_2O_3(-a) = Cu_2S + SO_4^{2-} + 2H^+ + H_2(g)$	$f_{H_2} = \left[\frac{K\gamma_1}{K_W^{1/2} \gamma_2} \right]$
32	$2Cu + HS_2O_4(-a) + H_2(g) = Cu_2S + SO_3^{2-} + 2H^+ + H_2O$	$f_{H_2} = \left[\frac{K_W^{1/2} \gamma_2}{K\gamma_1} \right]$
33	$2Cu + H_2O + S_2O_3(-2a) = Cu_2S + SO_4^{2-} + H_2(g)$	$f_{H_2} = [K]$
34	$2Cu + H_2(g) + S_2O_4(-2a) = Cu_2S + SO_3^{2-} + H_2O$	$f_{H_2} = \left[\frac{1}{K} \right]$

35	$4Cu+H_2O+S_3O_3(-2a)=2Cu_2S+SO_4^{-2}+H_2(g)$	$f_{H_2}=[K]$
36	$4Cu+H_2O+S_4O_6(-2a)=2Cu_2S+SO_4^{-2}+SO_3(a)+H_2(g)$	$f_{H_2}=\left[\frac{KK_H}{\gamma_0}\right]^{1/2}$
37	$6Cu+H_2O+S_4O_3(-2a)=3Cu_2S+SO_4^{-2}+H_2(g)$	$f_{H_2}=[K]$
38	$6Cu+H_2O+S_5O_6(-2a)=3Cu_2S+SO_4^{-2}+SO_3(a)+H_2(g)$	$f_{H_2}=\left[\frac{KK_H}{\gamma_0}\right]^{1/2}$
39	$8Cu+H_2O+S_5O_3(-2a)=4Cu_2S+SO_4^{-2}+H_2(g)$	$f_{H_2}=[K]$
40	$8Cu+H_2O+S_6O_6(-2a)=4Cu_2S+SO_4^{-2}+SO_3(a)+H_2(g)$	$f_{H_2}=\left[\frac{KK_H}{\gamma_0}\right]^{1/2}$
41	$10Cu+H_2O+S_6O_3(-2a)=5Cu_2S+SO_4^{-2}+H_2(g)$	$f_{H_2}=[K]$
42	$10Cu+H_2O+S_7O_6(-2a)=5Cu_2S+SO_4^{-2}+SO_3(a)+H_2(g)$	$f_{H_2}=\left[\frac{KK_H}{\gamma_0}\right]^{1/2}$
43	$12Cu+H_2O+S_7O_3(-2a)=6Cu_2S+SO_4^{-2}+H_2(g)$	$f_{H_2}=[K]$
44	$4Cu+H_2O+HS_3O_3(-a)=2Cu_2S+SO_4^{-2}+H^++H_2(g)$	$f_{H_2}=\left[\frac{K\gamma_1}{K_w^{1/2}\gamma_2}\right]$

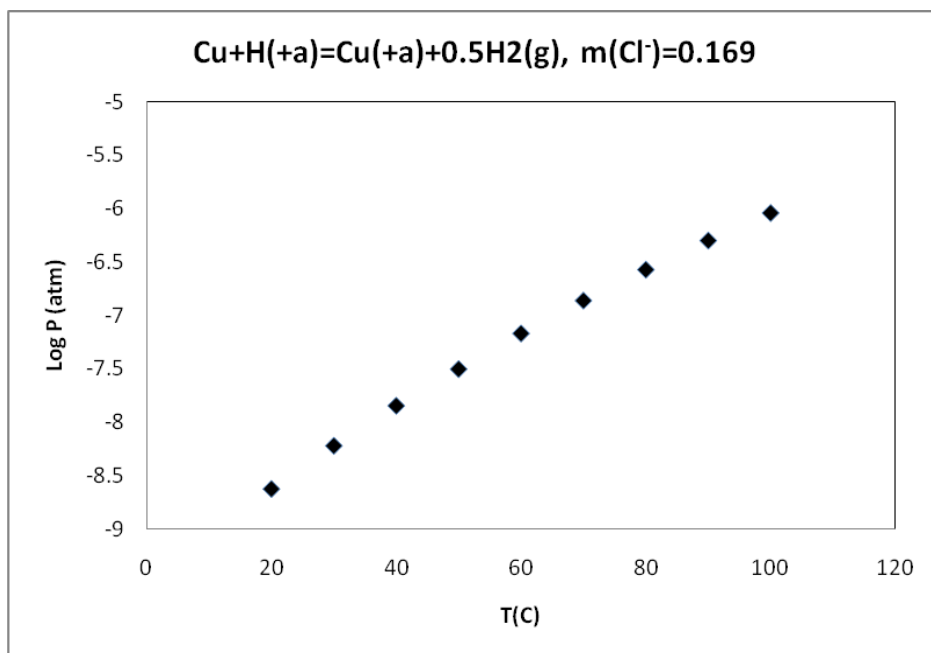


Figure 11: Calculated hydrogen pressure from the reaction, $Cu + H(+) = Cu(+) + 0.5H_2(g)$, in *pH*-neutral *NaCl* solution. $[Cl^-] = 0.169$ m.

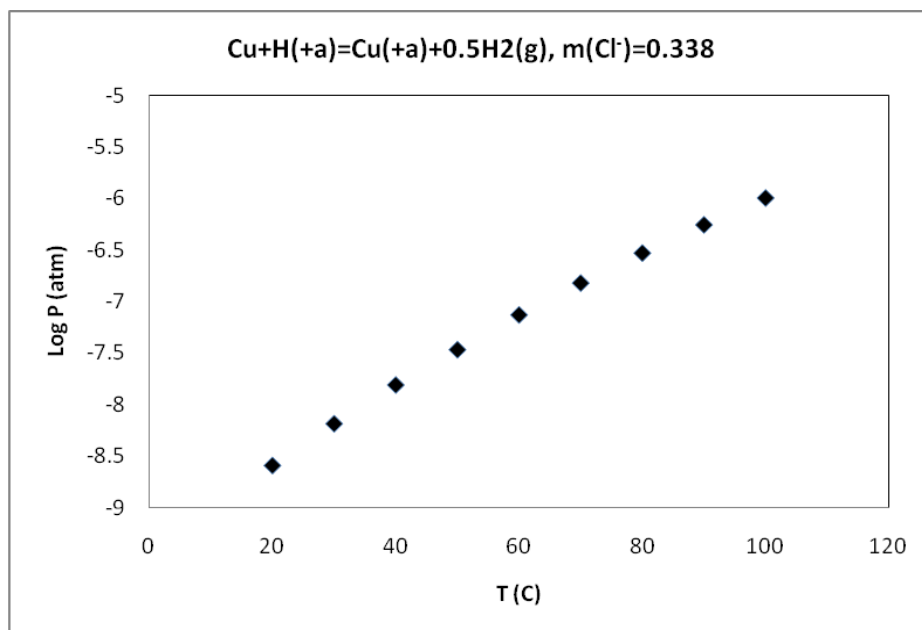


Figure 12: Calculated hydrogen pressure from the reaction, $Cu + H(+) = Cu(+) + 0.5H_2(g)$, in *pH*-neutral *NaCl* solution. $[Cl^-] = 0.338$ m.

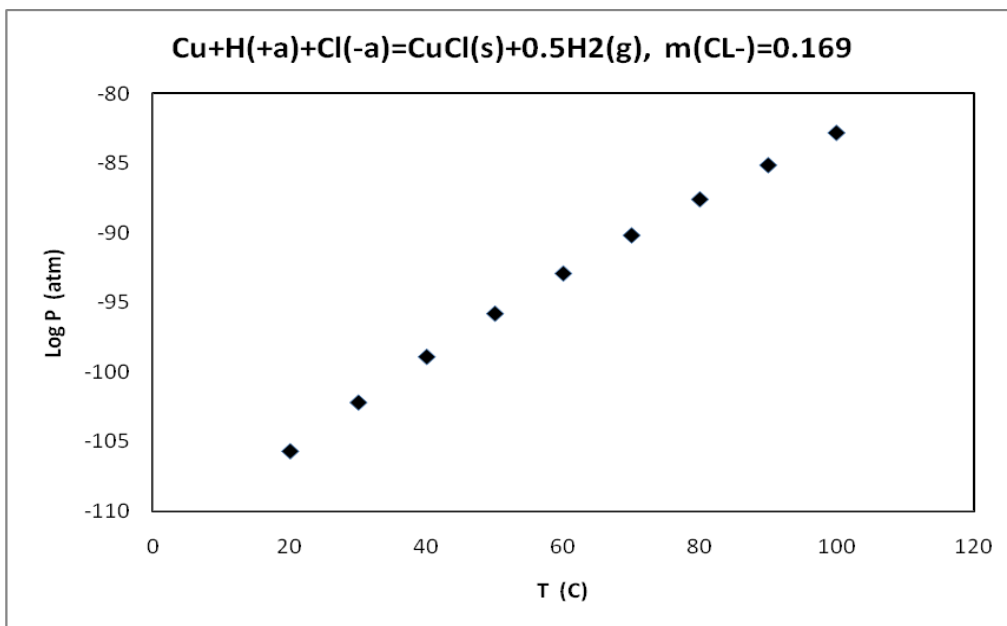


Figure 13: Calculated hydrogen pressure from the reaction, $Cu+H(+a)+Cl(-a) = CuCl(s) + 0.5H_2(g)$, in *pH*-neutral *NaCl* solution. $[Cl^-] = 0.169$ m.

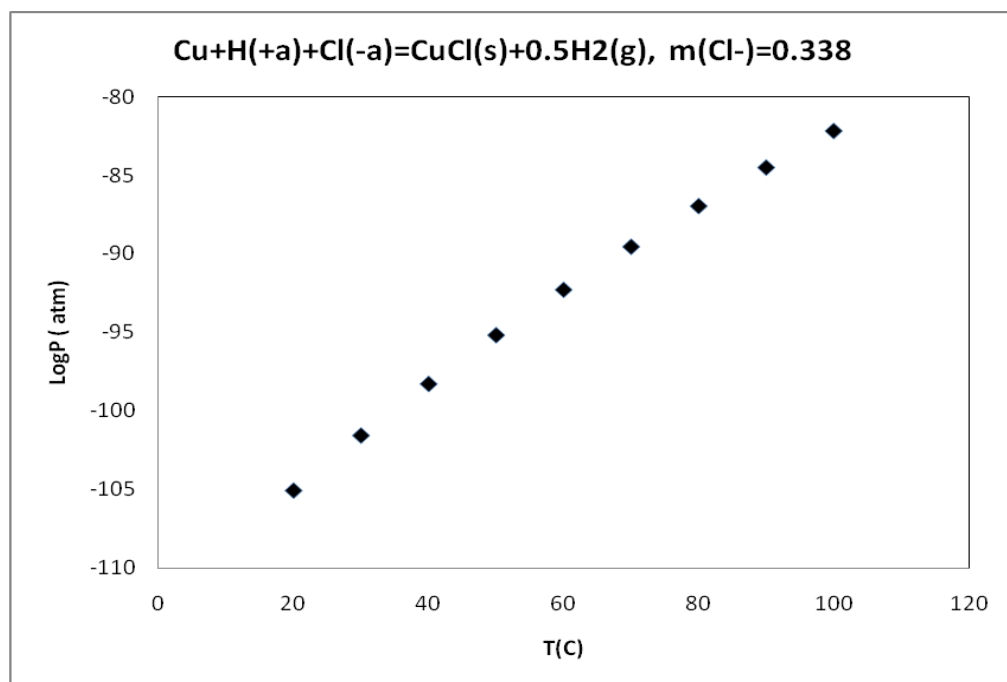


Figure 14: Calculated hydrogen pressure from the reaction, $Cu+H(+a)+Cl(-a) = CuCl(s) + 0.5H_2(g)$, in *pH*-neutral *NaCl* solution. $[Cl^-] = 0.338$ m.

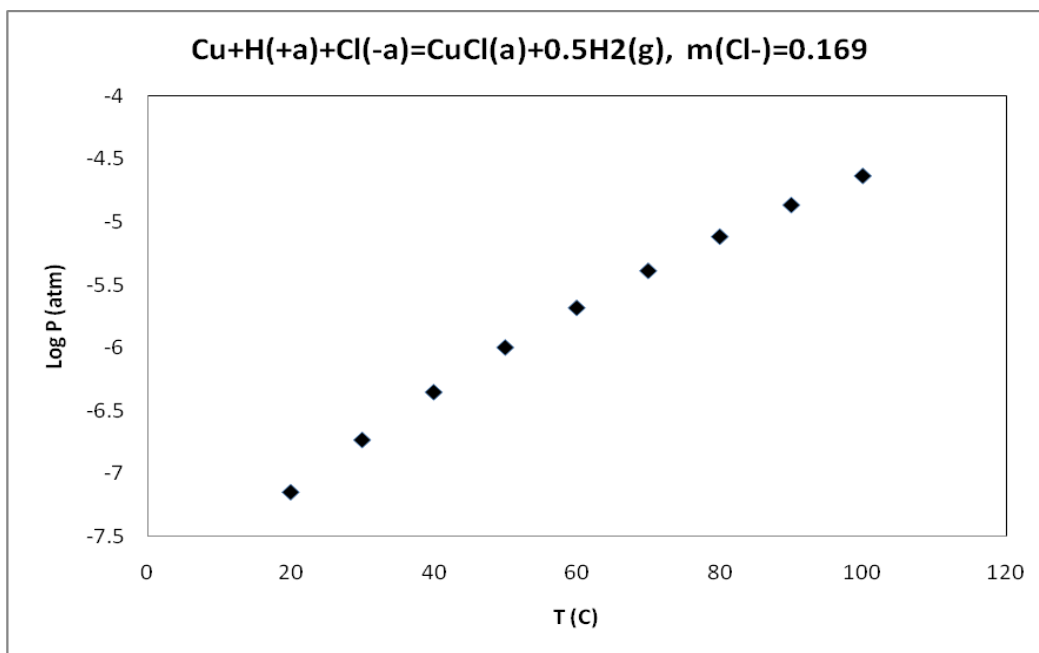


Figure 15: Calculated hydrogen pressure from the reaction, $Cu+H(+a)+Cl(-a) = CuCl(a) + 0.5H_2(g)$, in *pH*-neutral *NaCl* solution. $[Cl^-] = 0.169$ m.

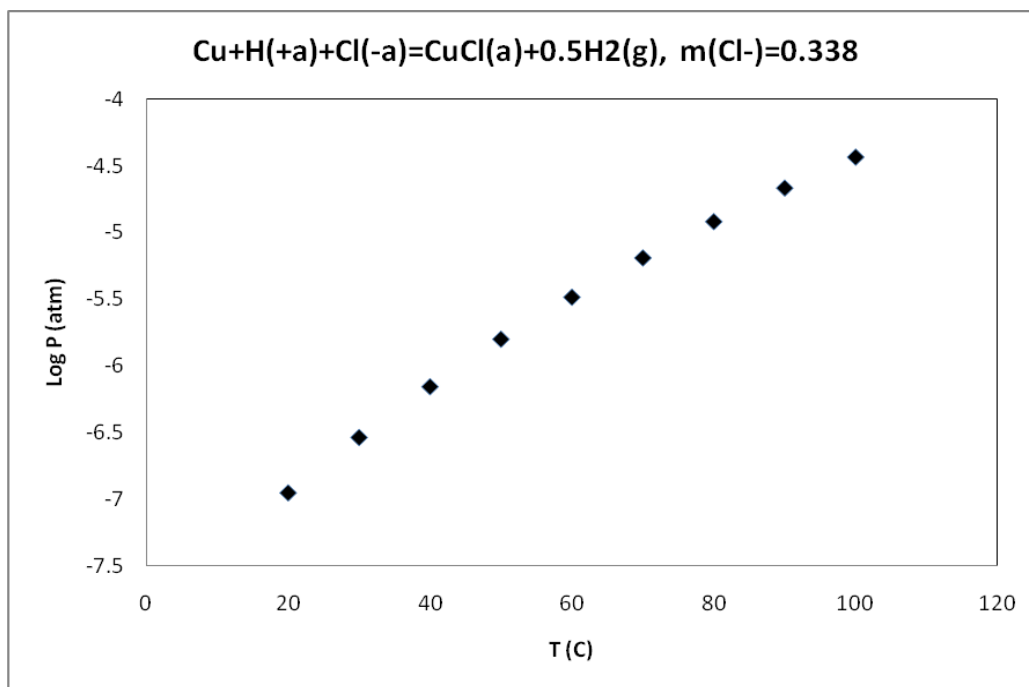


Figure 16: Calculated hydrogen pressure from the reaction, $Cu+H(+a)+Cl(-a) = CuCl(a) + 0.5H_2(g)$, in *pH*-neutral *NaCl* solution. $[Cl^-] = 0.338$ m.

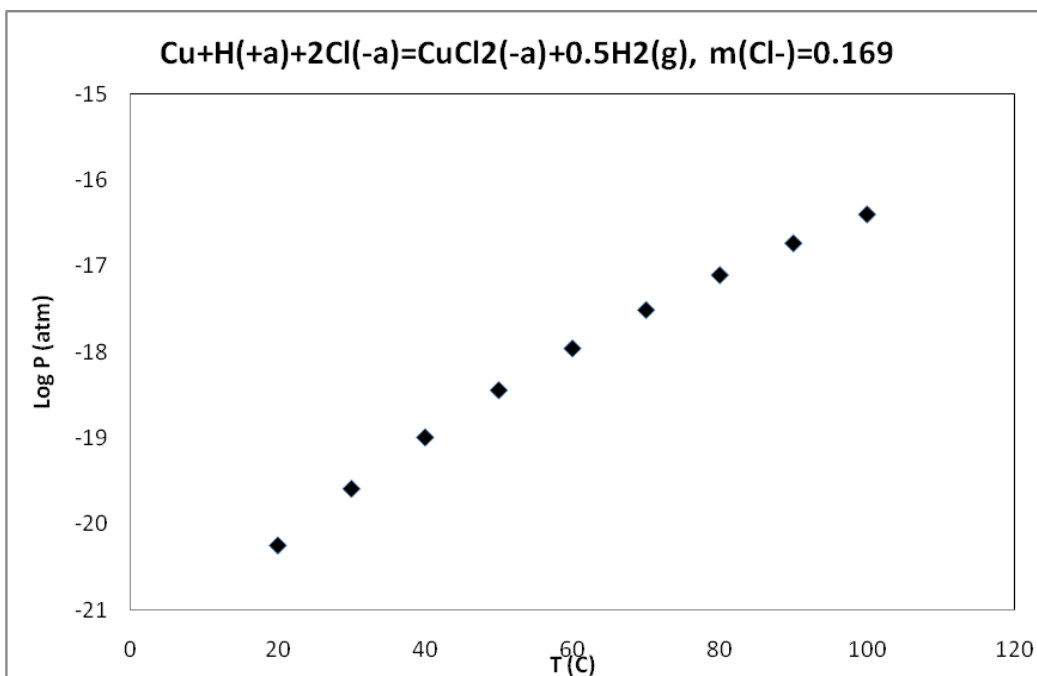


Figure 17: Calculated hydrogen pressure from the reaction, $Cu+H(+a)+2Cl(-a) = CuCl_2(-a) + 0.5H_2(g)$, in *pH*-neutral *NaCl* solution. $[Cl] = 0.169$ m.

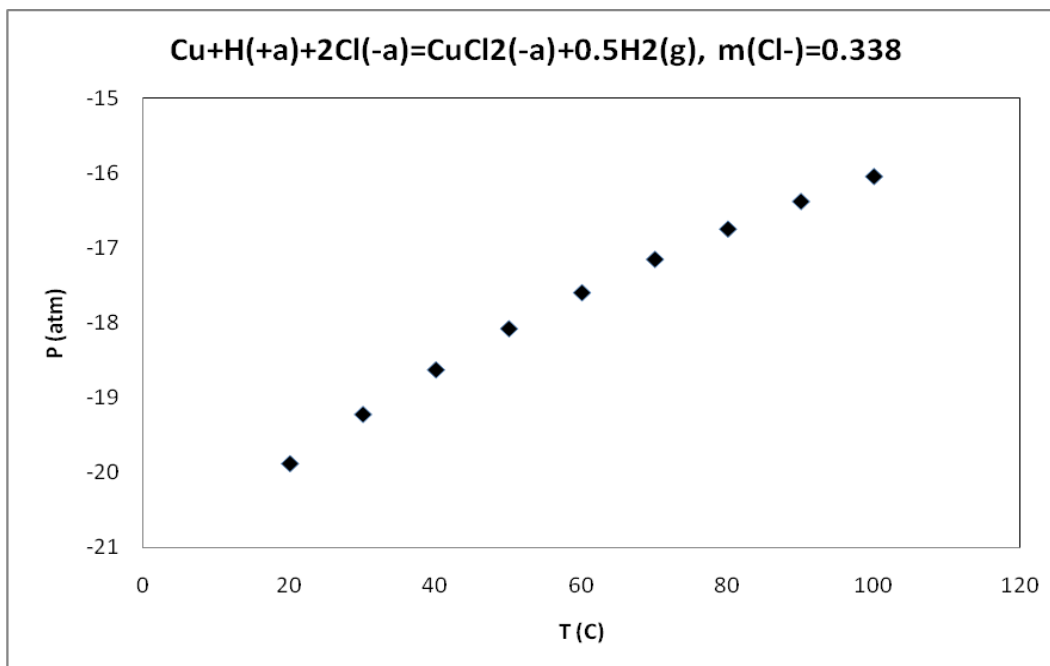


Figure 18: Calculated hydrogen pressure from the reaction, $Cu+H(+a)+2Cl(-a) = CuCl_2(-a) + 0.5H_2(g)$, in *pH*-neutral *NaCl* solution. $[Cl] = 0.338$ m.

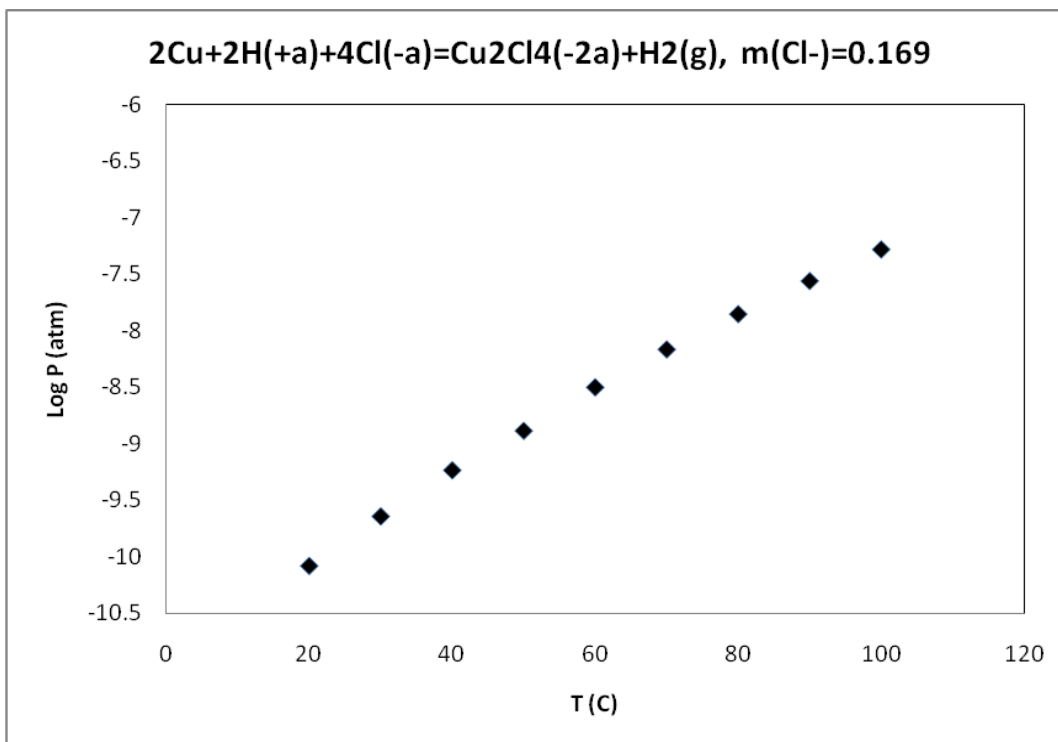


Figure 19: Calculated hydrogen pressure from the reaction, $2\text{Cu}+2\text{H}(+a)+4\text{Cl}(-a) = \text{Cu}_2\text{Cl}_4(-2a)+\text{H}_2(\text{g})$, in *pH*-neutral *NaCl* solution. $[\text{Cl}^-] = 0.169$ m.

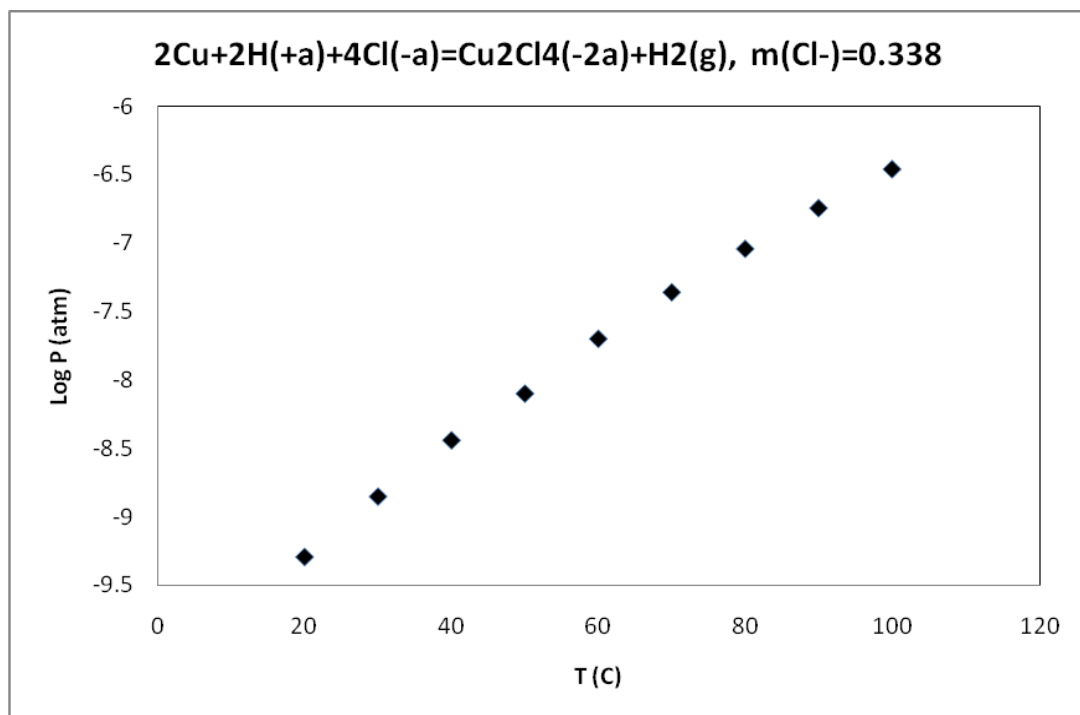


Figure 20: Calculated hydrogen pressure from the reaction, $2\text{Cu}+2\text{H}(+a)+4\text{Cl}(-a) = \text{Cu}_2\text{Cl}_4(-2a)+\text{H}_2(\text{g})$, in *pH*-neutral *NaCl* solution. $[\text{Cl}^-] = 0.338$ m.

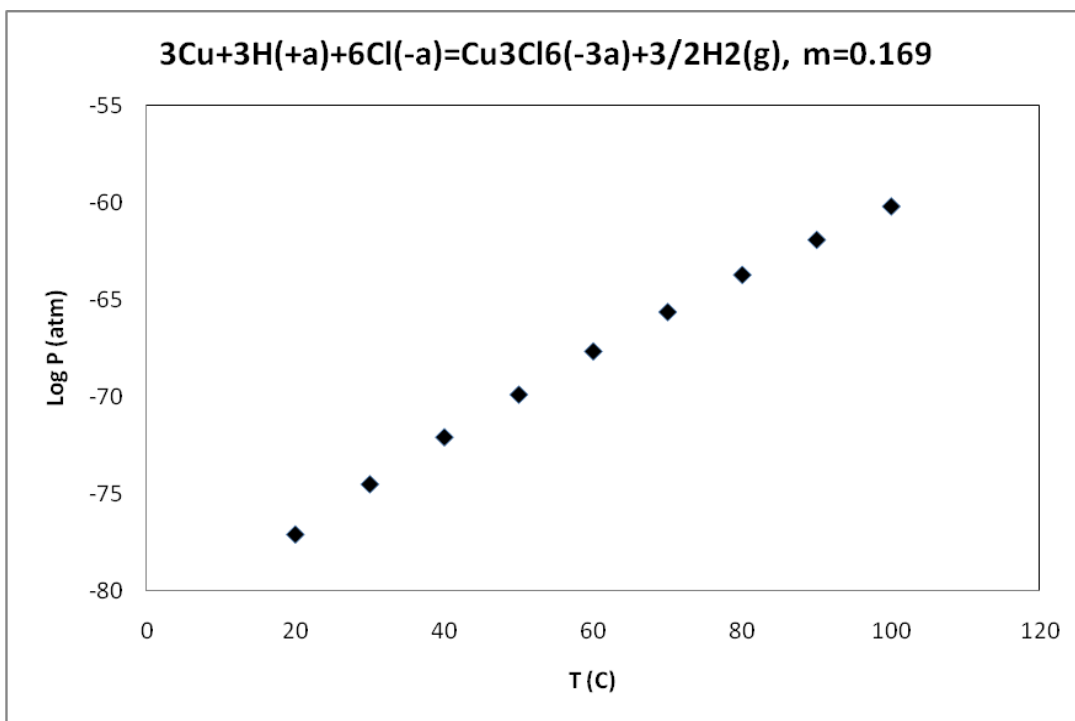


Figure 21: Calculated hydrogen pressure from the reaction, $3\text{Cu}+3\text{H}(+a)+6\text{Cl}(-a) = \text{Cu}_3\text{Cl}_6(-3a)+3/2\text{H}_2(\text{g})$, in *pH*-neutral *NaCl* solution. $[\text{Cl}^-] = 0.169 \text{ m}$.

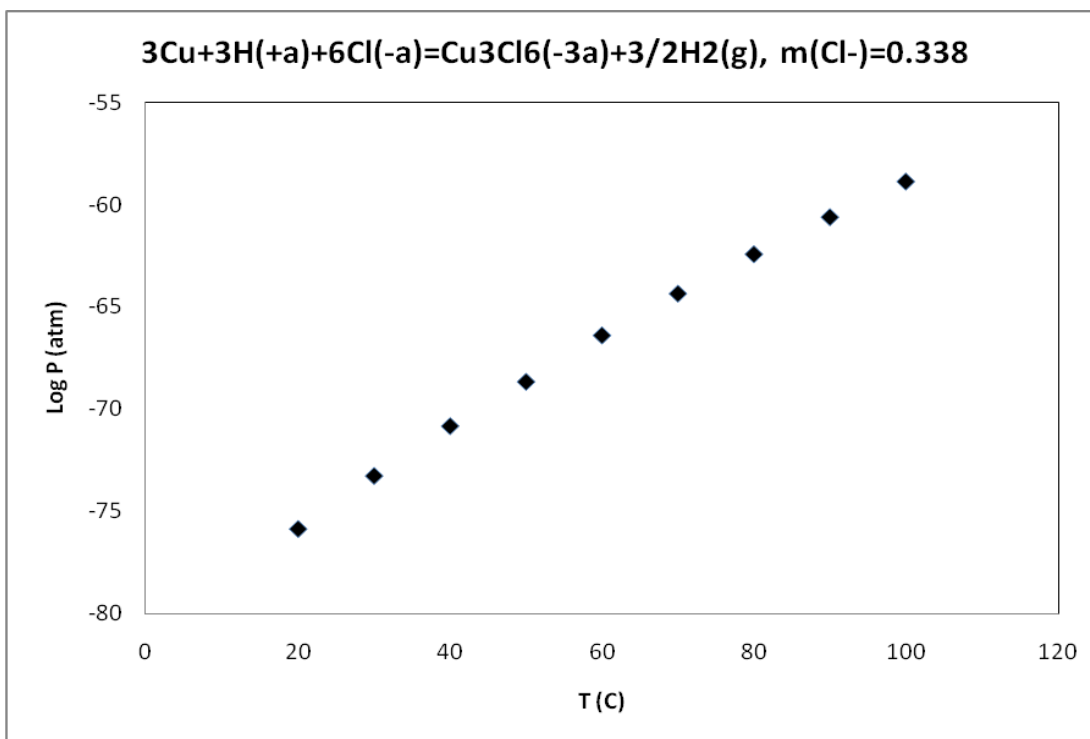


Figure 22: Calculated hydrogen pressure from the reaction, $3\text{Cu}+3\text{H}(+a)+6\text{Cl}(-a) = \text{Cu}_3\text{Cl}_6(-3a)+3/2\text{H}_2(\text{g})$, in *pH*-neutral *NaCl* solution. $[\text{Cl}^-] = 0.338 \text{ m}$.

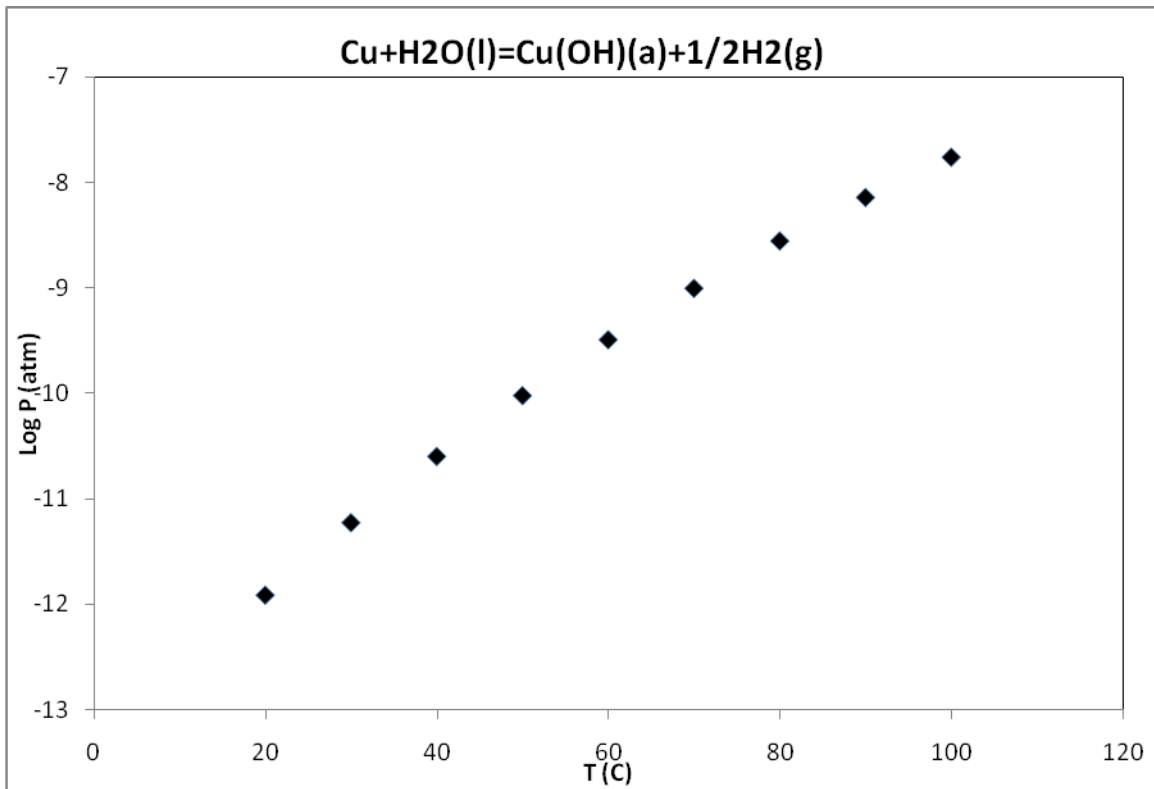


Figure 23: Calculated hydrogen pressure from the reaction, $\text{Cu} + \text{H}_2\text{O}(l) = \text{Cu}(\text{OH})(a) + 1/2\text{H}_2(g)$, in *pH*-neutral, *NaCl* solution. Note that, because *Cl* is not involved in the reaction, and since the activity of water is assumed to be unity, it is not necessary to explicitly state the chloride concentration.

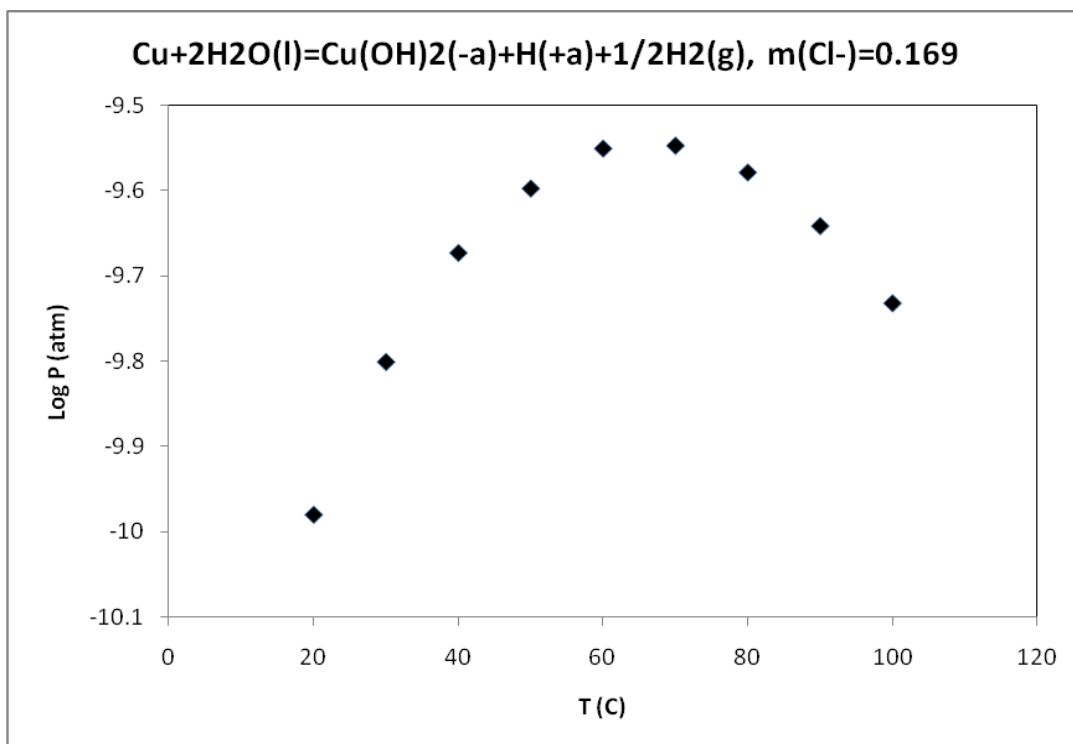


Figure 24: Calculated hydrogen pressure from the reaction, $Cu+2H_2O(l) = Cu(OH)_2(-3a)+H(+a)+1/2H_2(g)$, in *pH*-neutral *NaCl* solution. $[Cl^-] = 0.169$ m.

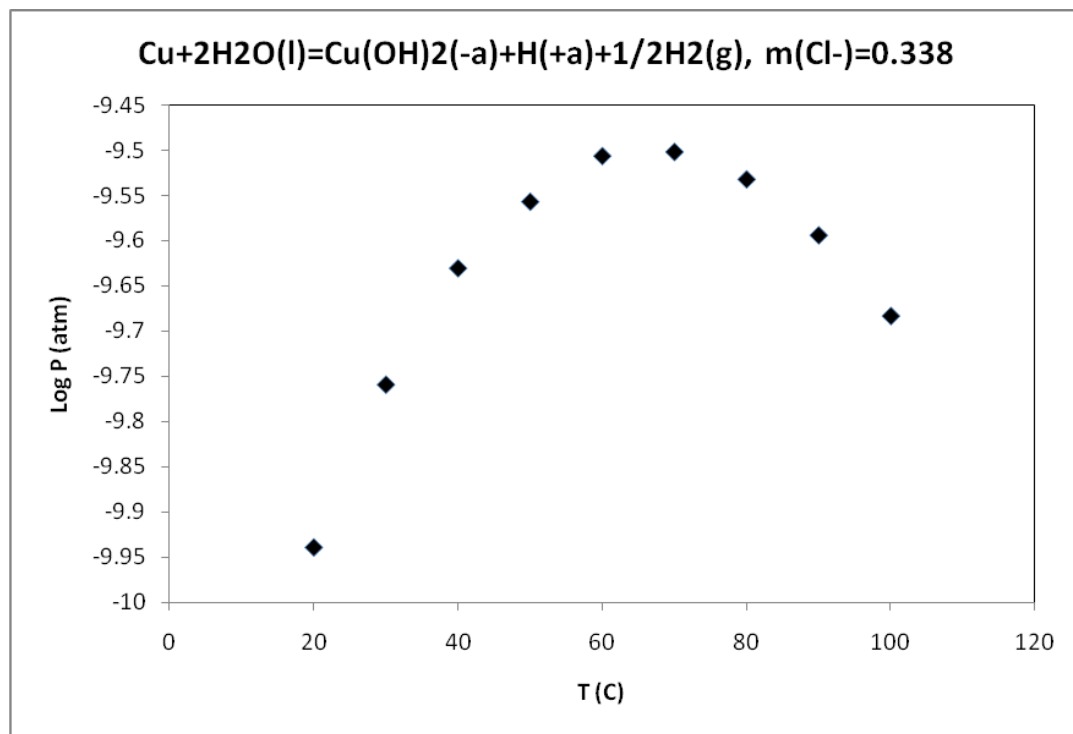


Figure 25: Calculated hydrogen pressure from the reaction, $Cu+2H_2O(l) = Cu(OH)_2(-3a)+H(+a)+1/2H_2(g)$, in *pH*-neutral *NaCl* solution. $[Cl^-] = 0.338$ m.

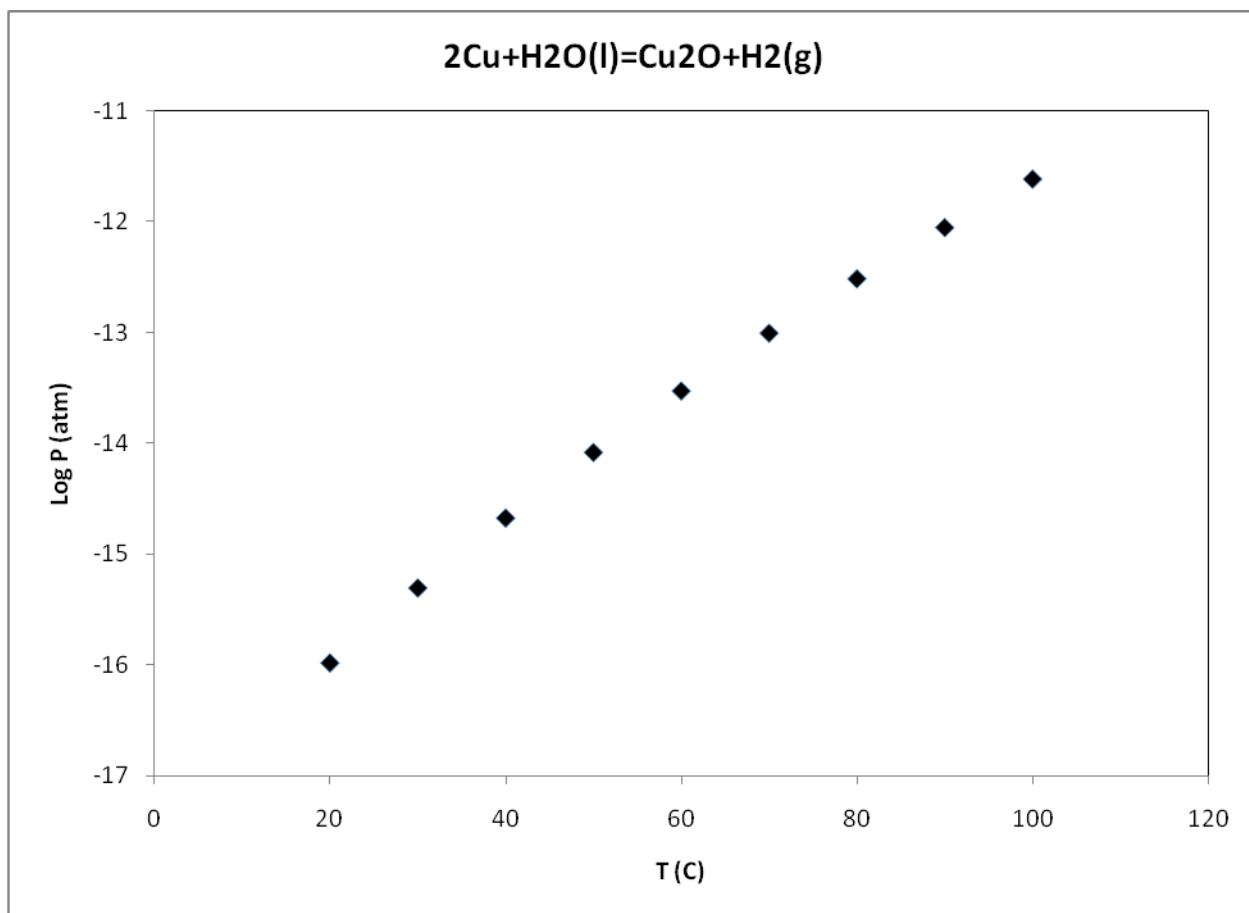


Figure 26: Calculated hydrogen pressure from the reaction, $2\text{Cu} + \text{H}_2\text{O}(l) = \text{Cu}_2\text{O} + \text{H}_2(g)$, in *pH*-neutral, *NaCl* solution.. Note that, because *Cl* is not involved in the reaction, and since the activity of water is assumed to be unity, it is not necessary to explicitly state the chloride concentration.

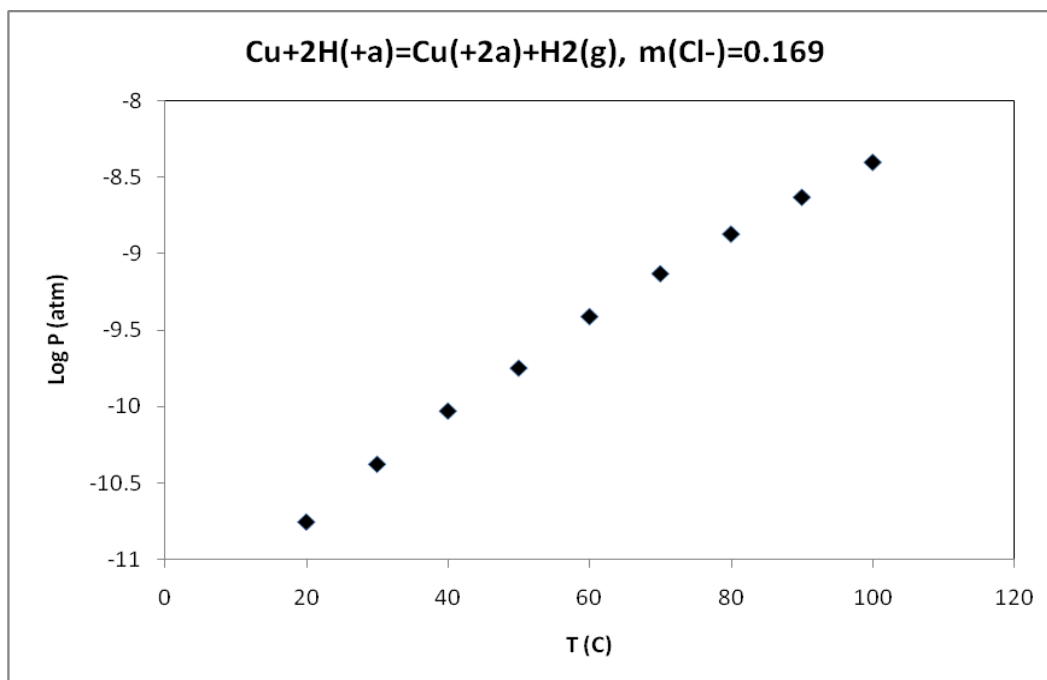


Figure 27: Calculated hydrogen pressure from the reaction, $Cu+2H(+a) = Cu(+2a)+H_2(g)$, in *pH*-neutral, *NaCl* solution. $[Cl^-] = 0.169$ m.

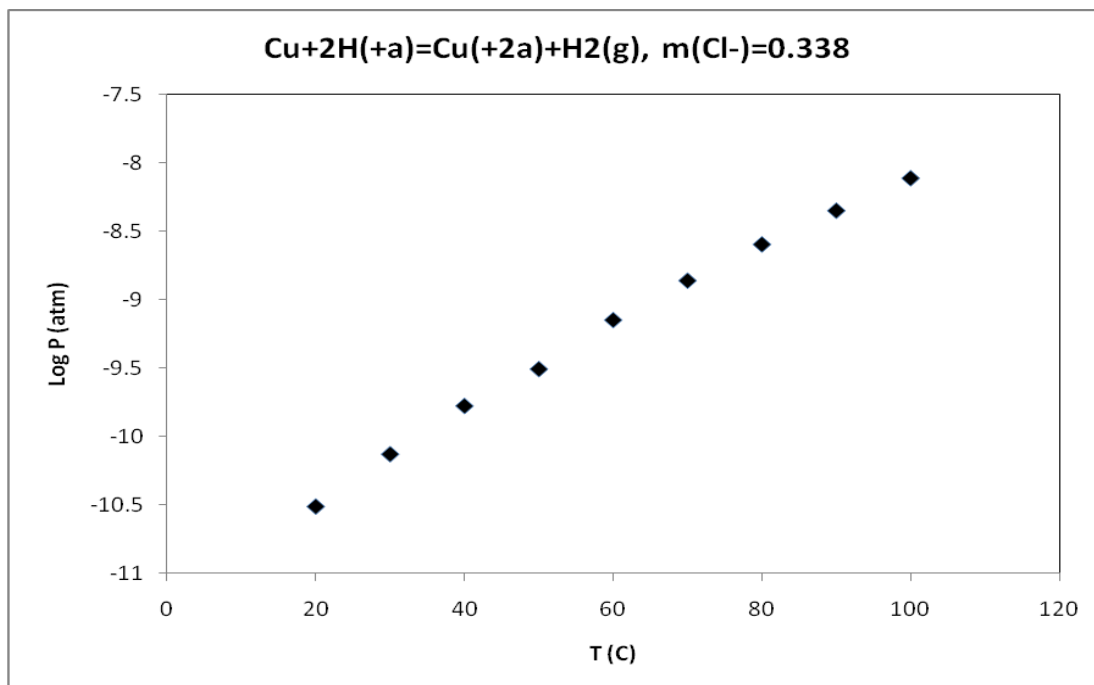


Figure 28: Calculated hydrogen pressure from the reaction, $Cu+2H(+a) = Cu(+2a)+H_2(g)$, in *pH*-neutral *NaCl* solution. $[Cl^-] = 0.338$ m.

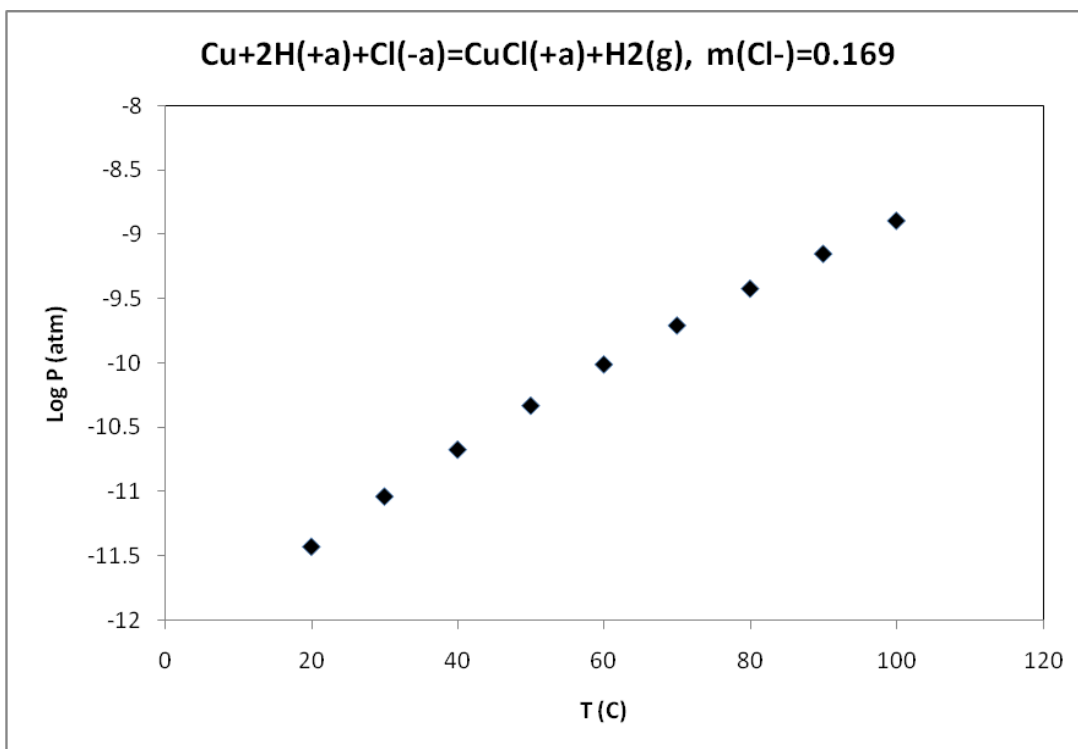


Figure 29: Calculated hydrogen pressure from the reaction, $Cu+2H(+a)+Cl(-a) = CuCl(+a)+H_2(g)$, in *pH*-neutral *NaCl* solution. $[Cl^-] = 0.169$ m.

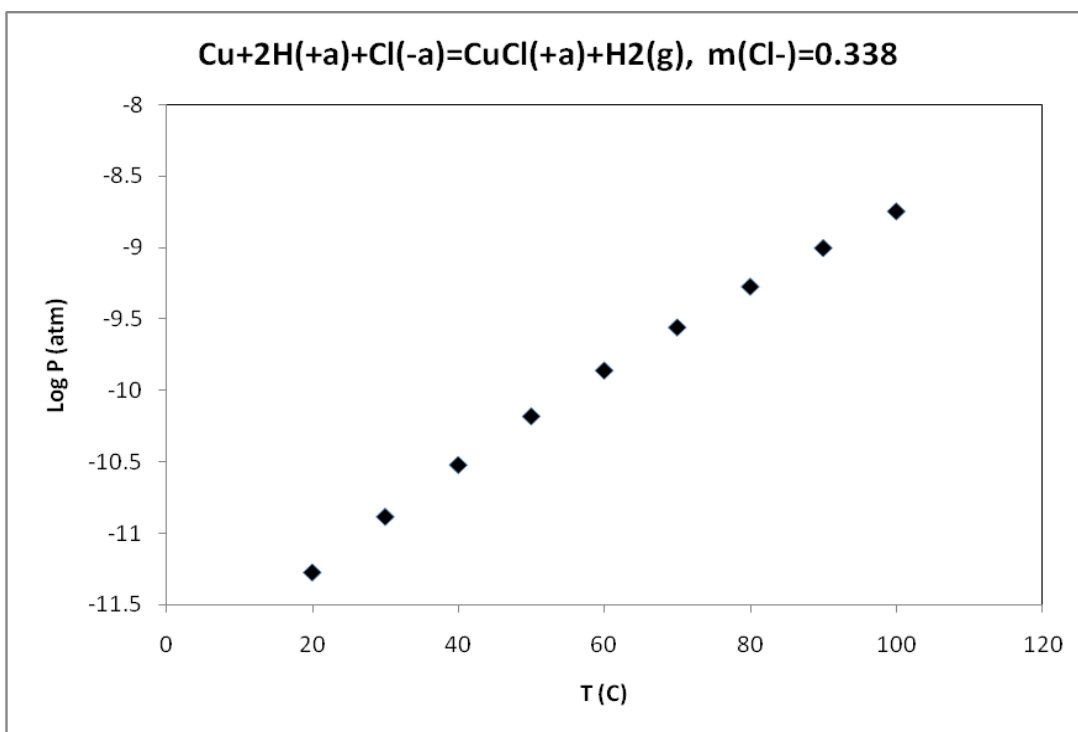


Figure 30: Calculated hydrogen pressure from the reaction, $Cu+2H(+a)+Cl(-a) = CuCl(+a)+H_2(g)$, in *pH*-neutral *NaCl* solution. $[Cl^-] = 0.338$ m.

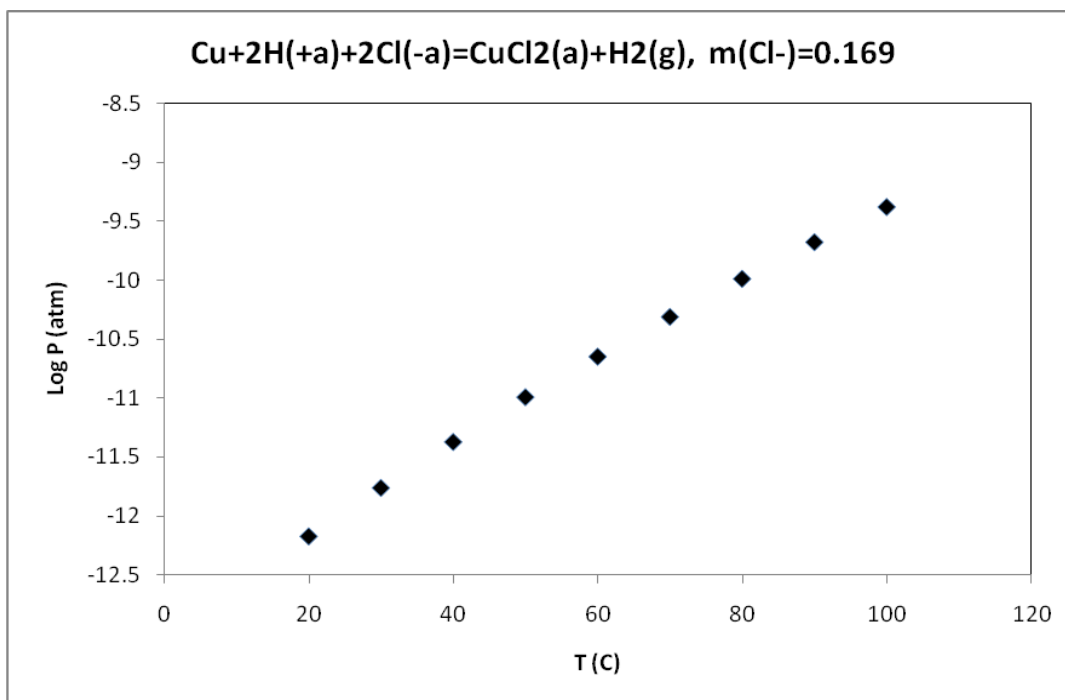


Figure 31: Calculated hydrogen pressure from the reaction, $Cu+2H(+a)+2Cl(-a) = CuCl_2(a)+H_2(g)$, in *pH*-neutral *NaCl* solution. $[Cl] = 0.169$ m.

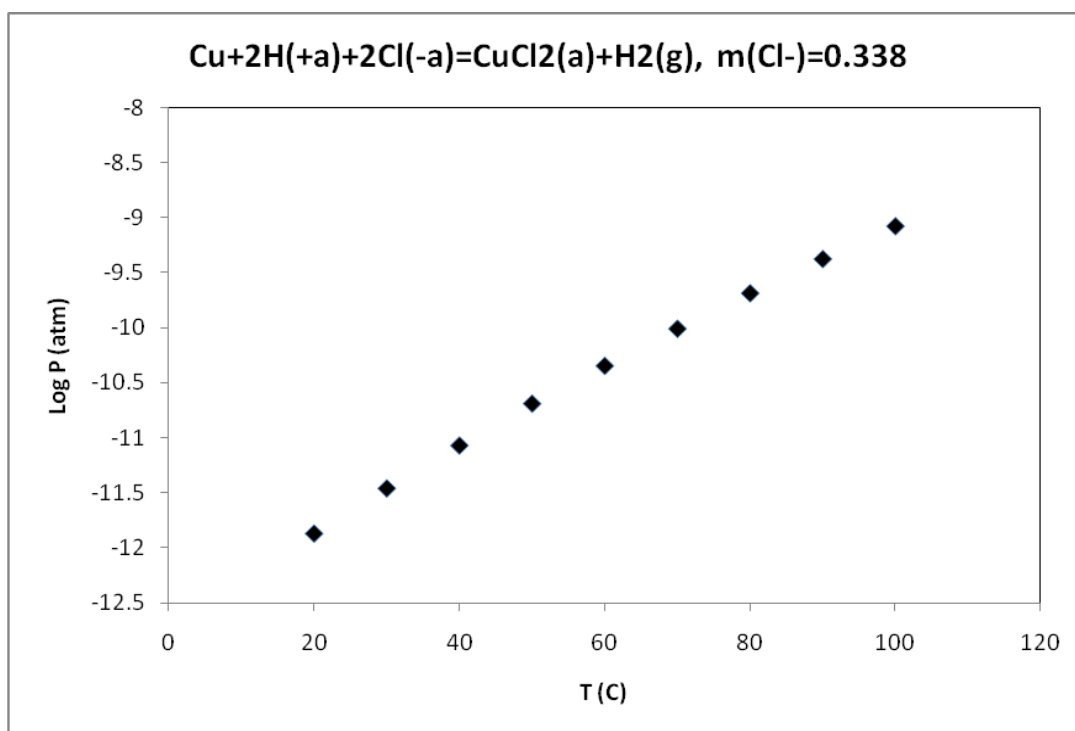


Figure 32: Calculated hydrogen pressure from the reaction, $Cu+2H(+a)+2Cl(-a) = CuCl_2(a)+H_2(g)$, in *pH*-neutral *NaCl* solution. $[Cl] = 0.338$ m.

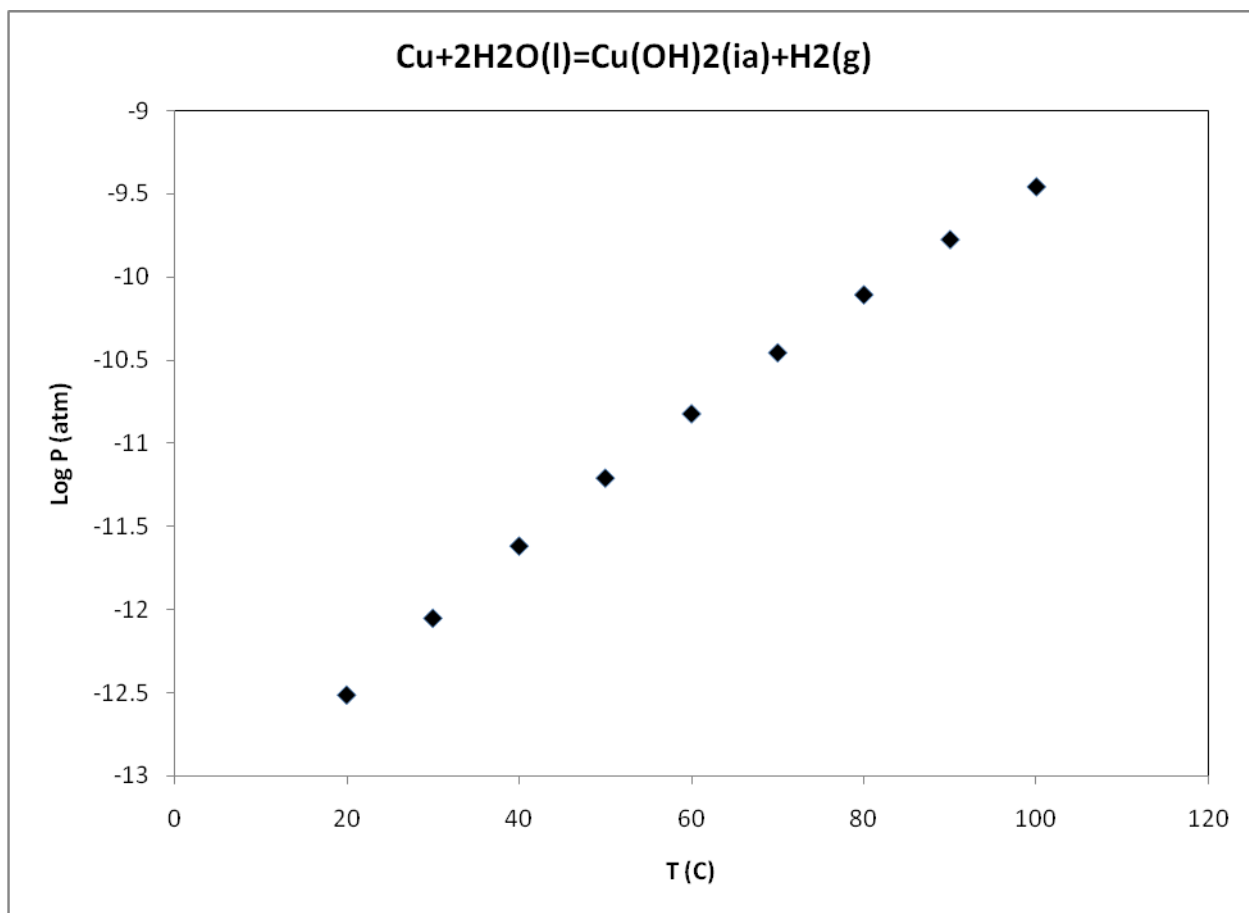


Figure 33: Calculated hydrogen pressure from the reaction, $\text{Cu} + 2\text{H}_2\text{O}(l) = \text{Cu}(\text{OH})_2(a) + \text{H}_2(g)$, in *pH*-neutral *NaCl* solution.. Note that, because *Cl*⁻ is not involved in the reaction, and since the activity of water is assumed to be unity, it is not necessary to explicitly state the chloride concentration.

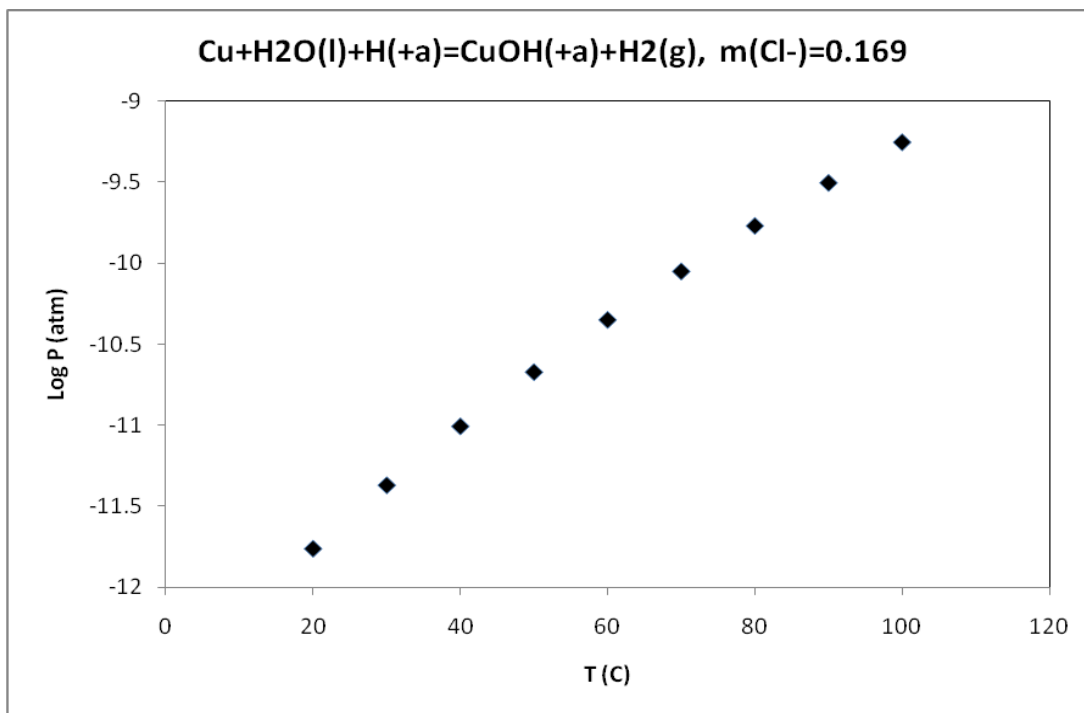


Figure 34: Calculated hydrogen pressure from the reaction, $Cu+H_2O(l)+H(+a) = CuOH(+a)+H_2(g)$, in *pH*-neutral *NaCl* solution. $[Cl^-] = 0.169$ m.

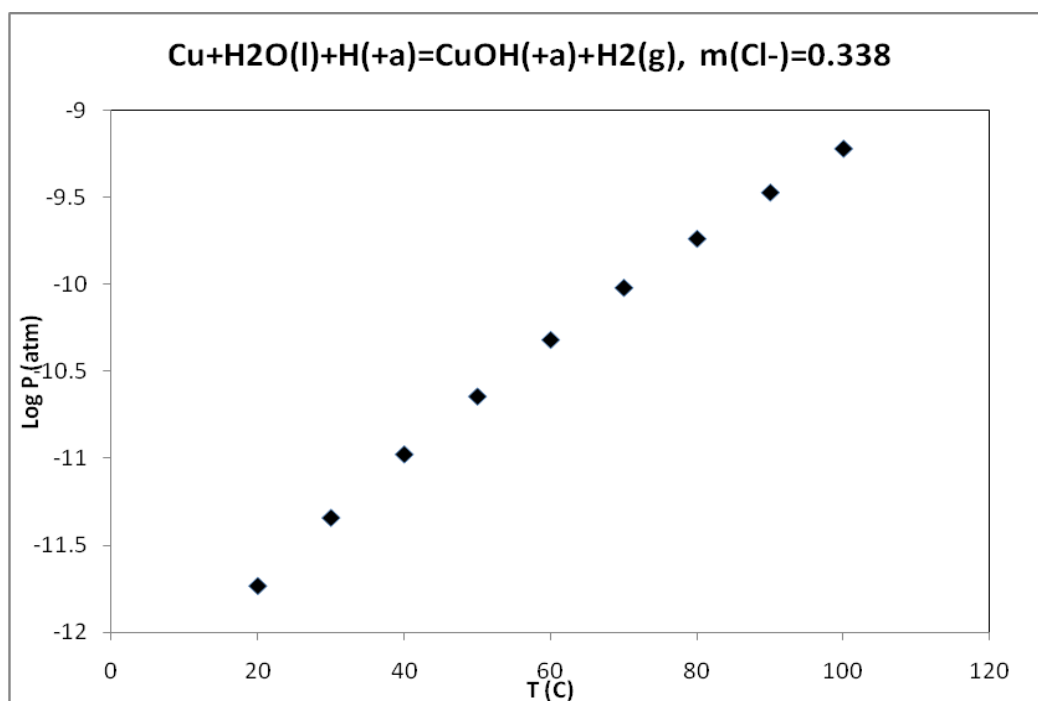


Figure 35: Calculated hydrogen pressure from the reaction, $Cu+H_2O(l)+H(+a) = CuOH(+a)+H_2(g)$, in *pH*-neutral *NaCl* solution. $[Cl^-] = 0.338$ m.

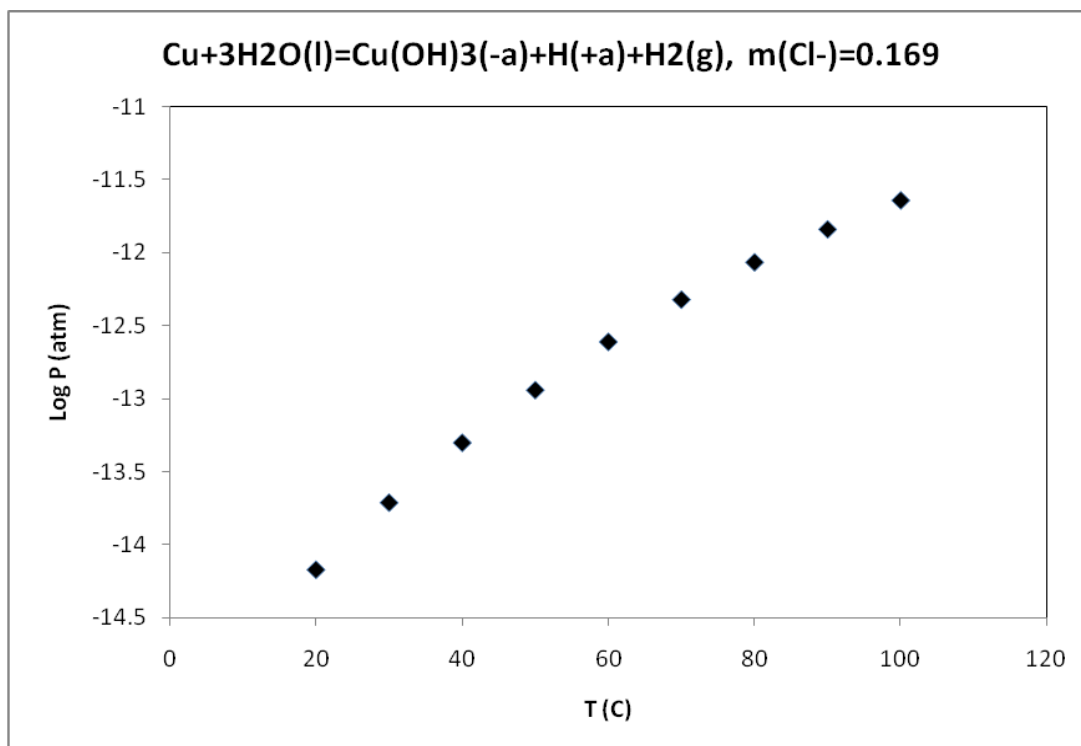


Figure 36: Calculated hydrogen pressure from the reaction, $Cu+3H_2O(l) = Cu(OH)_3(-a)+H(+a) +H_2(g)$, in *pH*-neutral *NaCl* solution. $[Cl^-] = 0.169$ m.

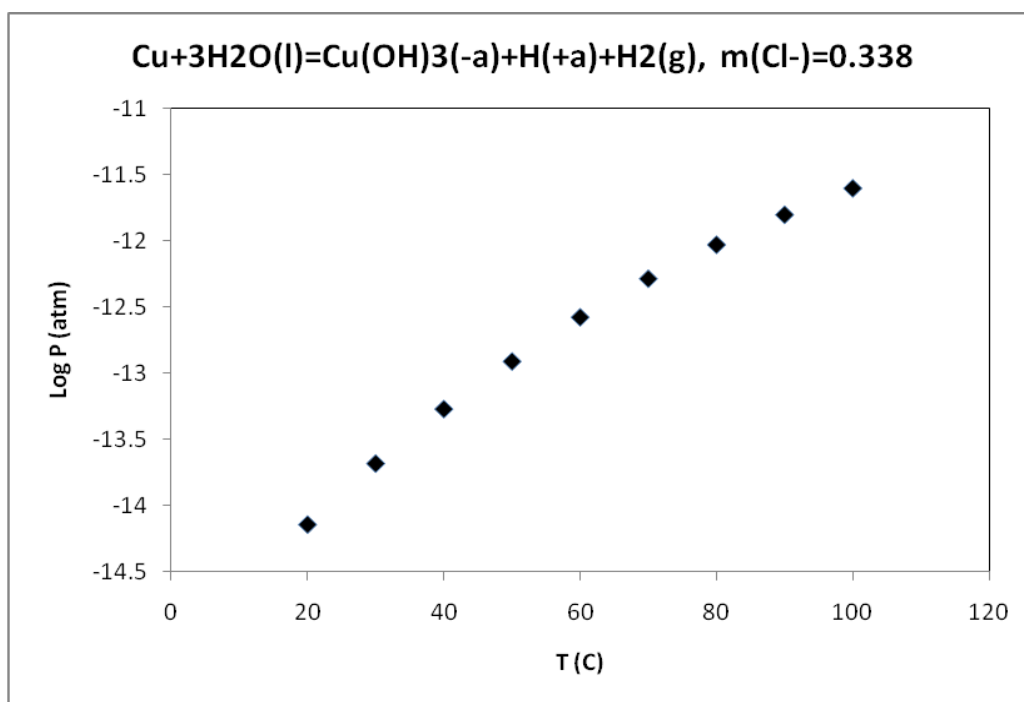


Figure 37: Calculated hydrogen pressure from the reaction, $Cu+3H_2O(l) = Cu(OH)_3(-a)+H(+a) +H_2(g)$, in *pH*-neutral *NaCl* solution. $[Cl^-] = 0.338$ m.

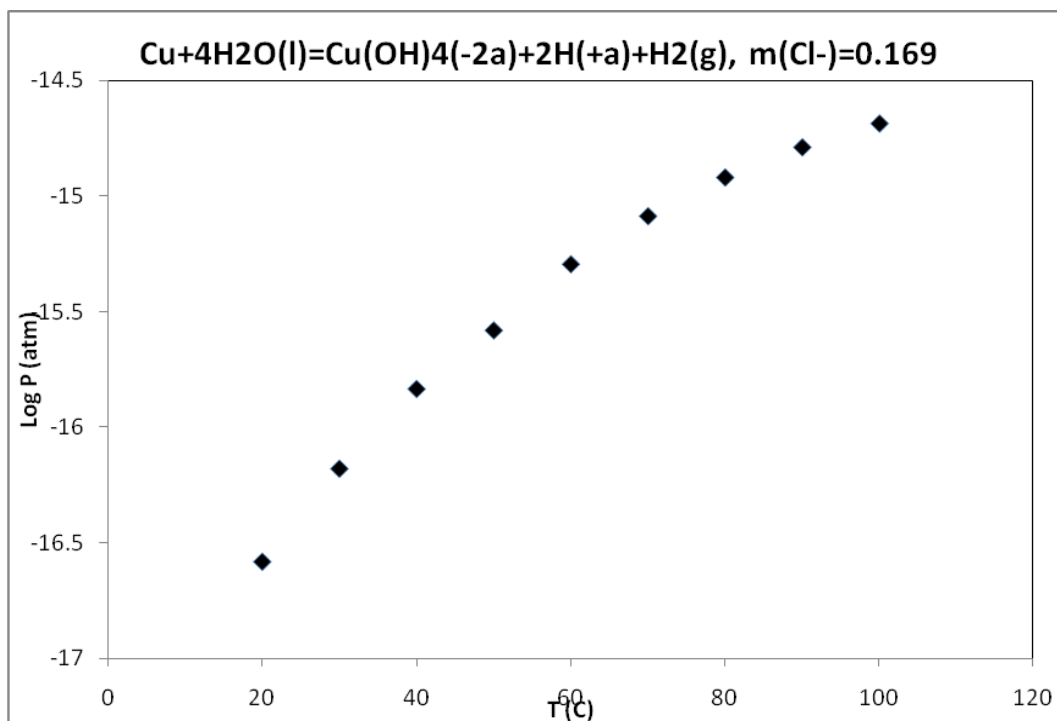


Figure 38: Calculated hydrogen pressure from the reaction, $Cu+4H_2O(l) = Cu(OH)_4(-2a)+2H(+a) +H_2(g)$, in *pH*-neutral *NaCl* solution. $[Cl^-] = 0.169$ m.

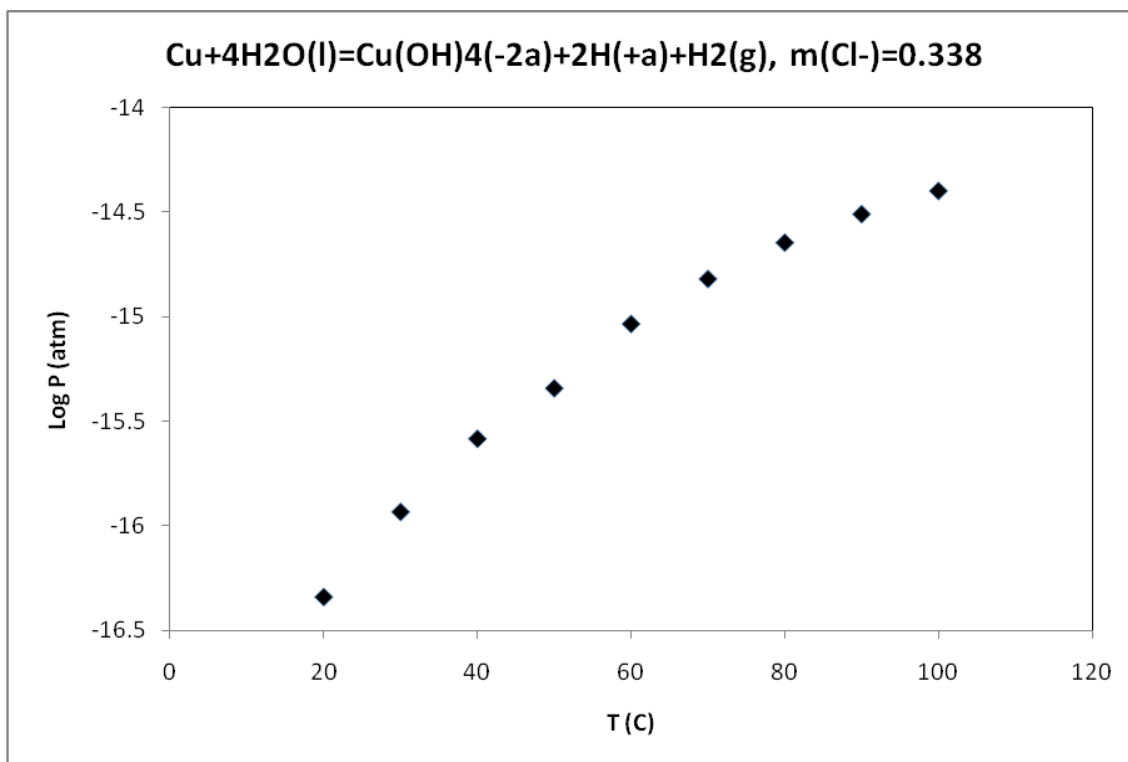


Figure 39: Calculated hydrogen pressure from the reaction, $Cu+4H_2O(l) = Cu(OH)_4(-2a)+2H(+a) +H_2(g)$, in *pH*-neutral *NaCl* solution. $[Cl^-] = 0.338$ m.

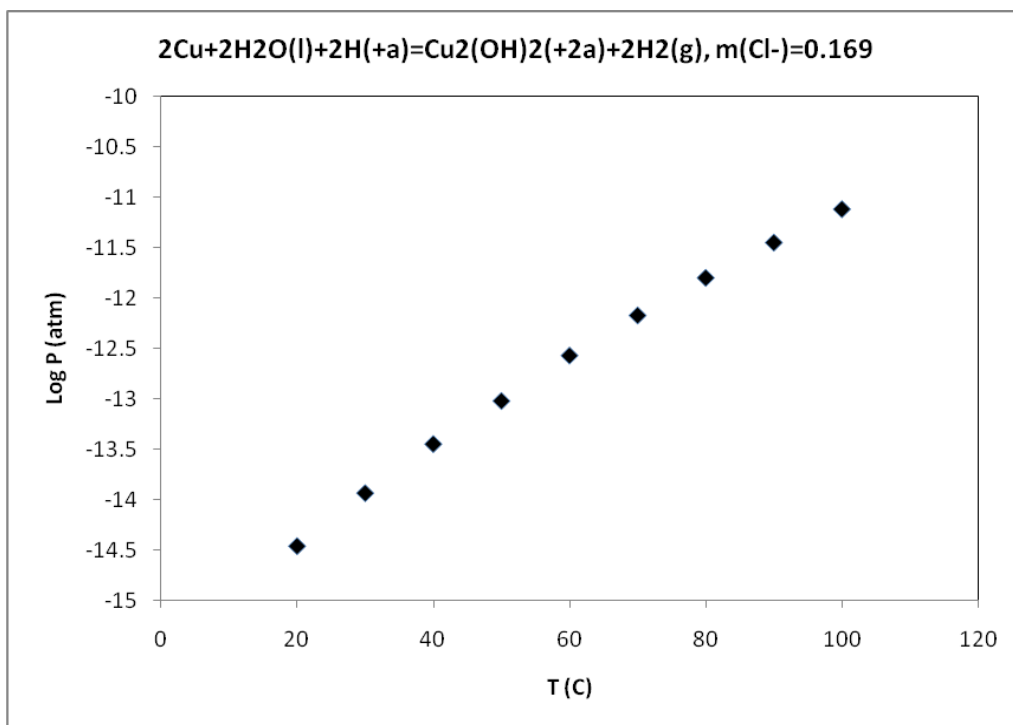


Figure 40: Calculated hydrogen pressure from the reaction, $2\text{Cu}+2\text{H}_2\text{O}(\text{l})+2\text{H}(\text{+a}) = \text{Cu}_2(\text{OH})_2(\text{+2a}) + 2\text{H}_2(\text{g})$, in *pH*-neutral *NaCl* solution. $[\text{Cl}^-] = 0.169$ m.

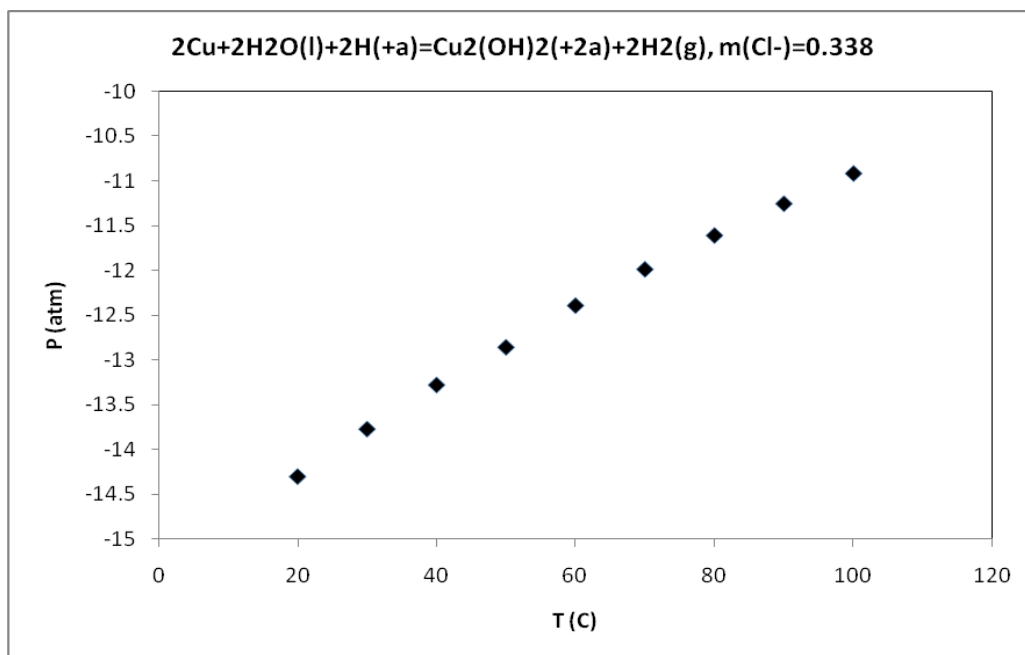


Figure 41: Calculated hydrogen pressure from the reaction, $2\text{Cu}+2\text{H}_2\text{O}(\text{l})+2\text{H}(\text{+a}) = \text{Cu}_2(\text{OH})_2(\text{+2a}) + 2\text{H}_2(\text{g})$, in *pH*-neutral *NaCl* solution. $[\text{Cl}^-] = 0.338$ m.

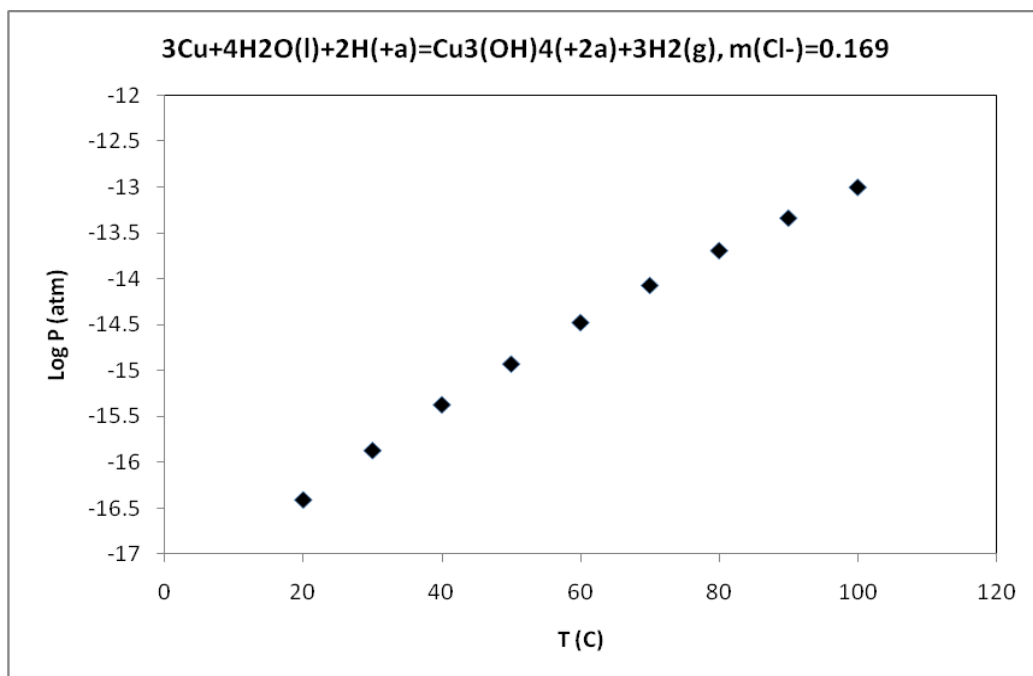


Figure 42: Calculated hydrogen pressure from the reaction, $3\text{Cu}+4\text{H}_2\text{O}(\text{l})+2\text{H}(\text{+a}) = \text{Cu}_3(\text{OH})_4(\text{+2a}) + 3\text{H}_2(\text{g})$ in *pH*-neutral *NaCl* solution, $[\text{Cl}^-] = 0.169$ m.

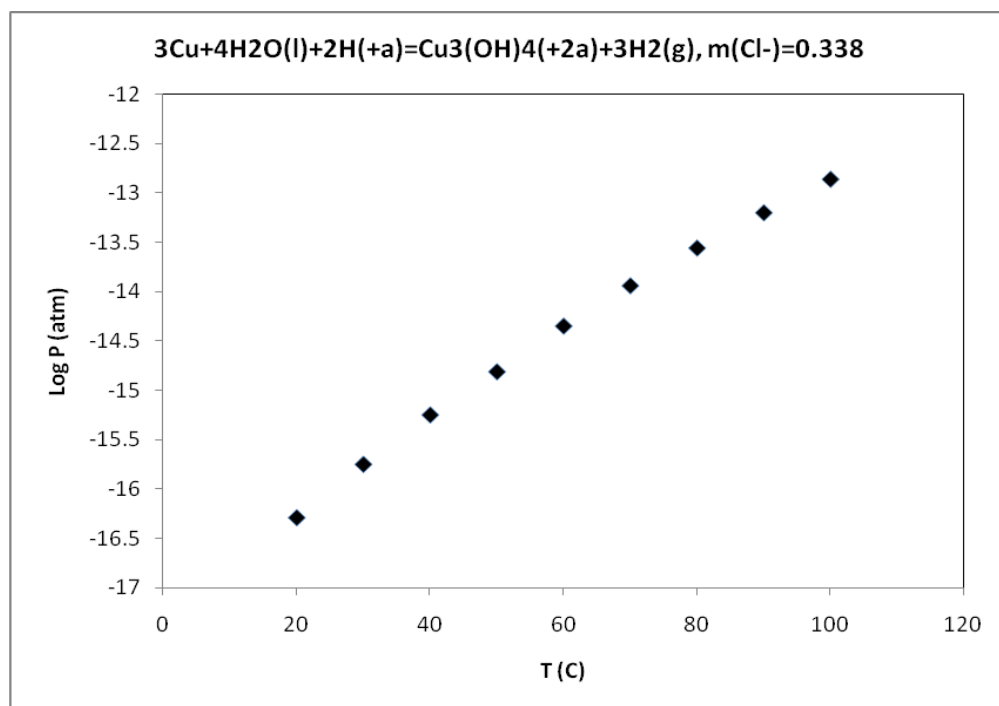


Figure 43: Calculated hydrogen pressure from the reaction, $3\text{Cu}+4\text{H}_2\text{O}(\text{l})+2\text{H}(\text{+a}) = \text{Cu}_3(\text{OH})_4(\text{+2a}) + 3\text{H}_2(\text{g})$, in *pH*-neutral *NaCl* solution, $[\text{Cl}^-] = 0.338$ m.

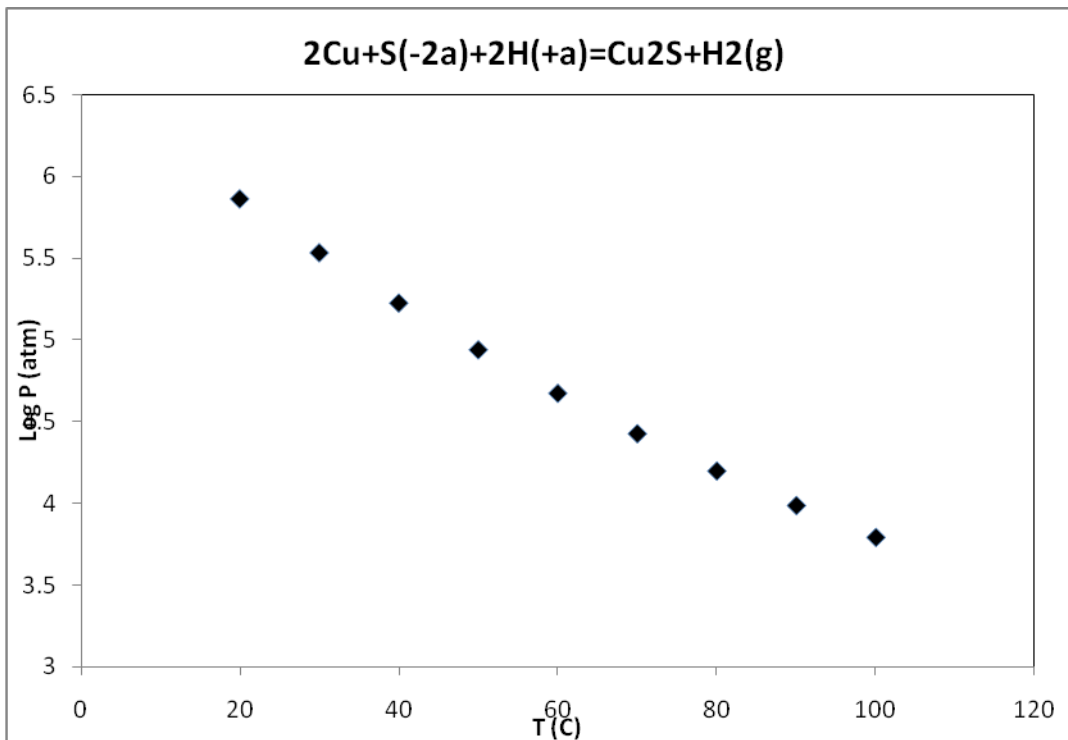


Figure 44: Calculated hydrogen pressure from the reaction, $2\text{Cu} + \text{S}(-2a) + 2\text{H}(+a) = \text{Cu}_2\text{S}(s) + \text{H}_2(g)$, in *pH*-neutral *NaCl* solution.

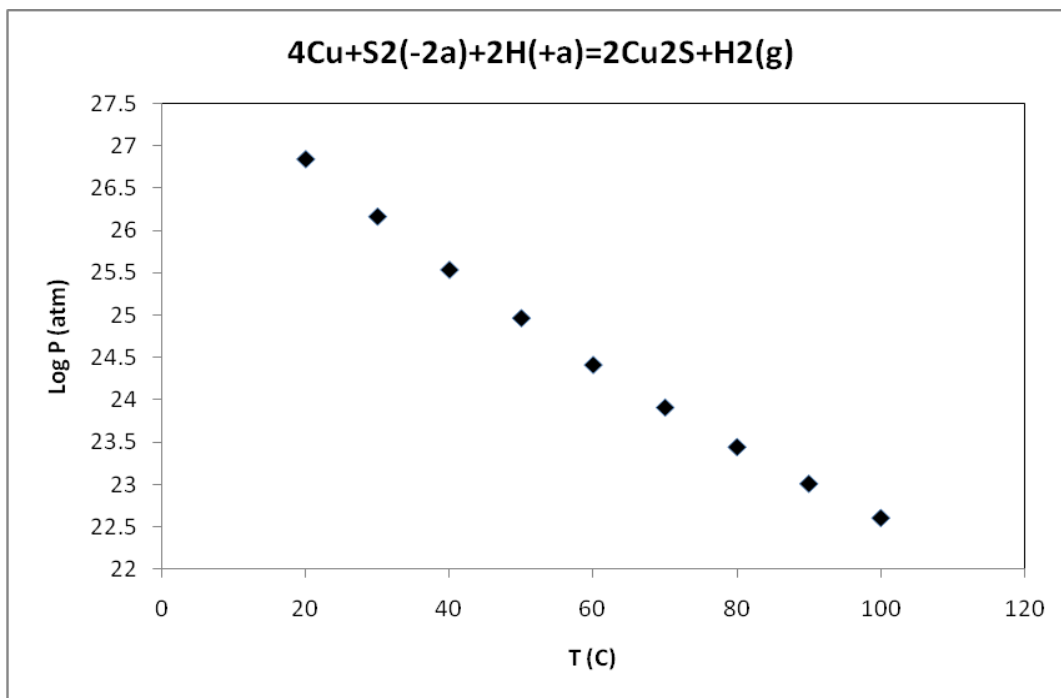


Figure 45: Calculated hydrogen pressure from the reaction, $4\text{Cu} + \text{S}_2(-2a) + 2\text{H}(+a) = 2\text{Cu}_2\text{S}(s) + \text{H}_2(g)$ in *pH*-neutral *NaCl* solution.

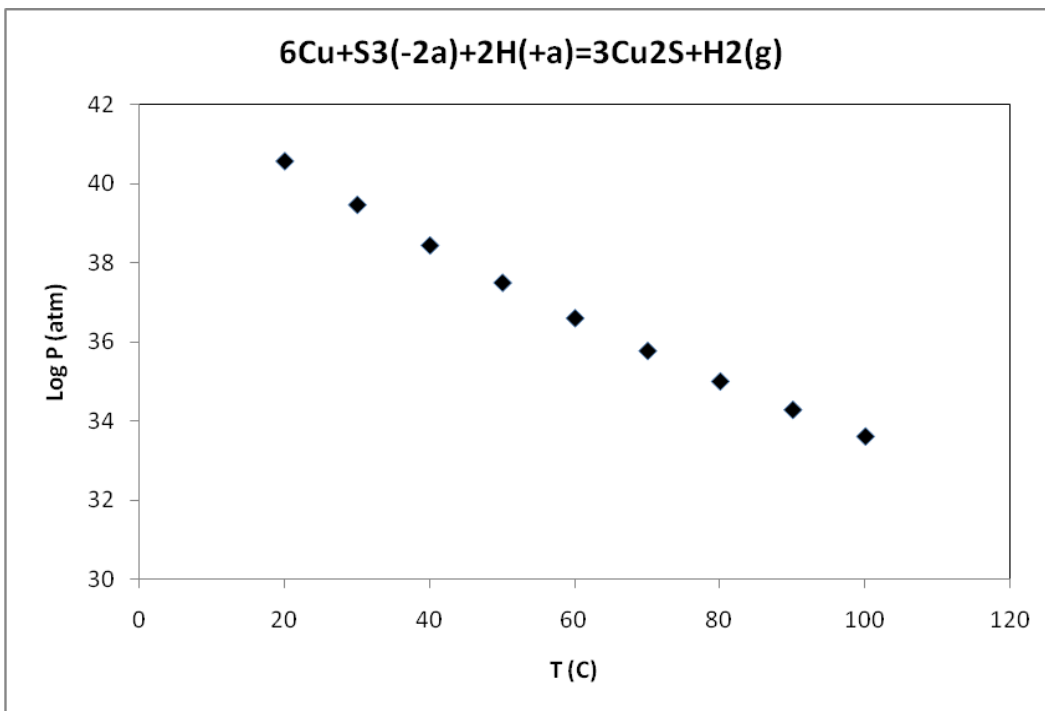


Figure 46: Calculated hydrogen pressure from the reaction, $6\text{Cu} + \text{S}_3(-2a) + 2\text{H}(+a) = 3\text{Cu}_2\text{S}(s) + \text{H}_2(g)$ in *pH*-neutral *NaCl* solution.

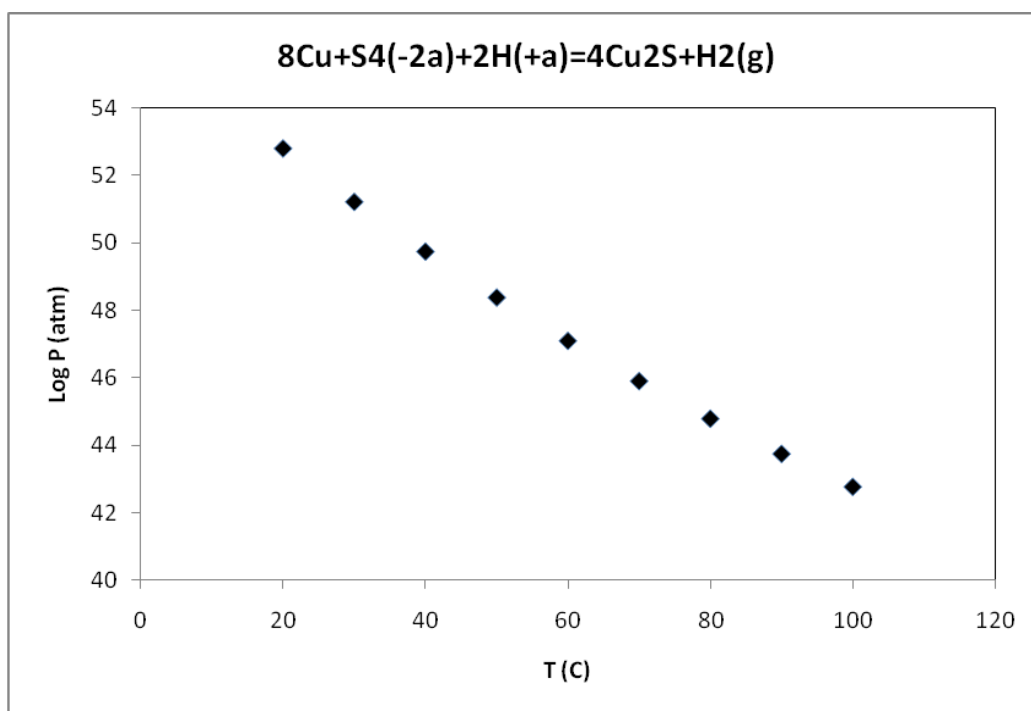


Figure 47: Calculated hydrogen pressure from the reaction, $8\text{Cu} + \text{S}_4(-2a) + 2\text{H}(+a) = 4\text{Cu}_2\text{S}(s) + \text{H}_2(g)$ in *pH*-neutral *NaCl* solution.

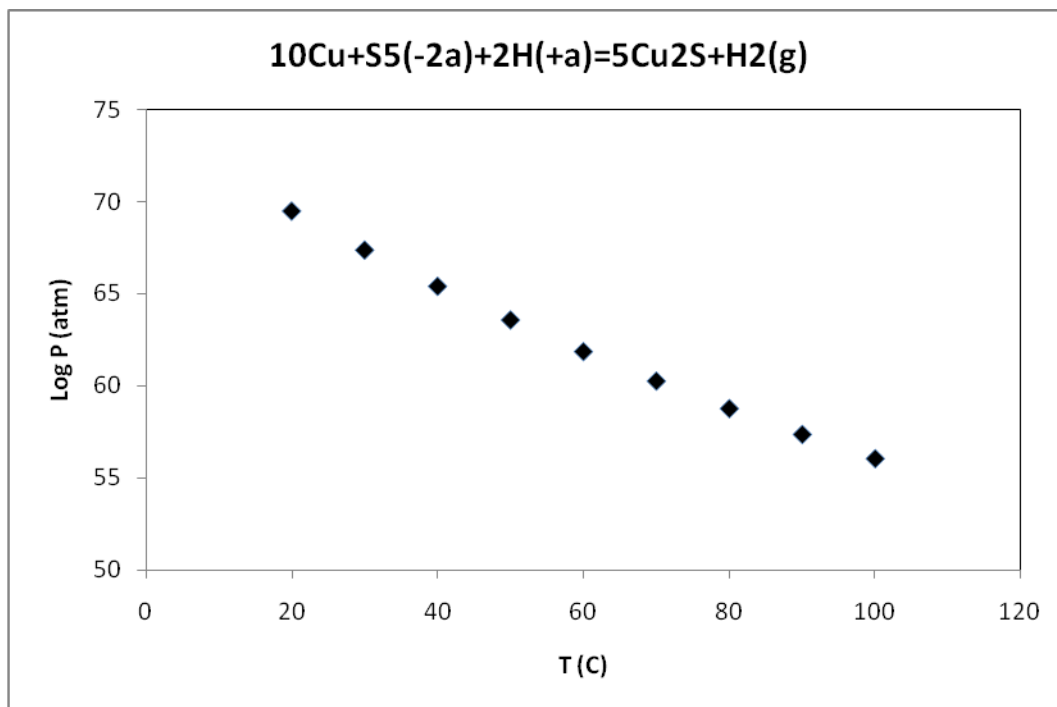


Figure 48: Calculated hydrogen pressure from the reaction, $10Cu+S_5(-2a)+2H(+a)=5Cu_2S(s)+H_2(g)$ in *pH*-neutral *NaCl* solution.

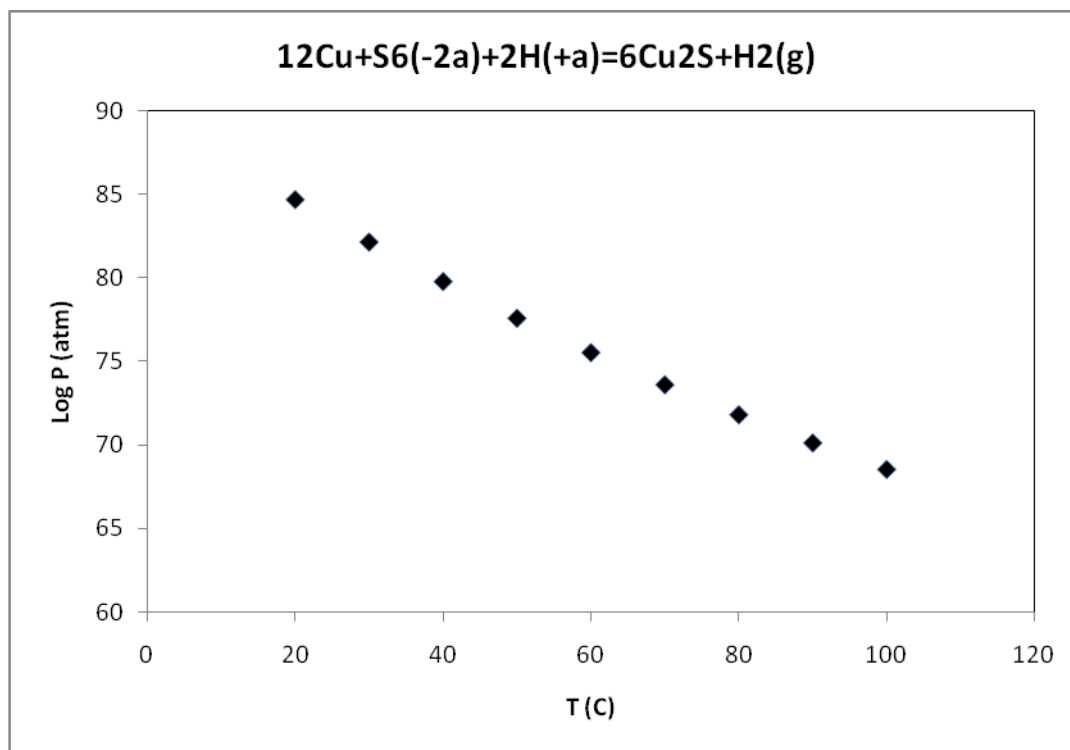


Figure 49: Calculated hydrogen pressure from the reaction, $12Cu+S_6(-2a)+2H(+a)=6Cu_2S(s)+H_2(g)$ in *pH*-neutral *NaCl* solution.

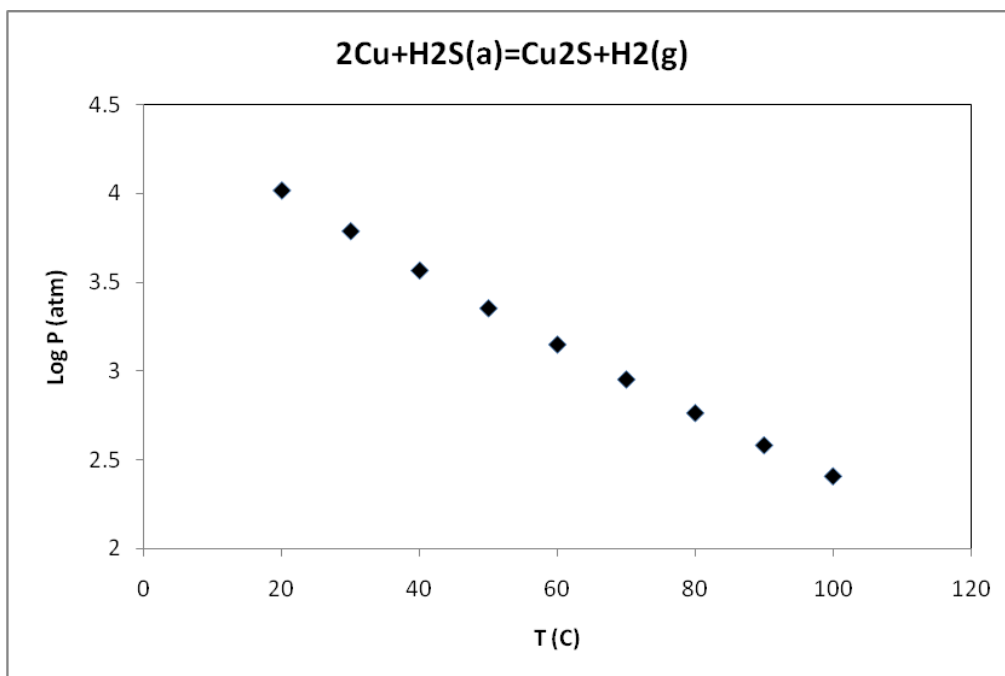


Figure 50: Calculated hydrogen pressure from the reaction, $2Cu + H_2S(a) = Cu_2S(s) + H_2(g)$ in *pH*-neutral *NaCl* solution.

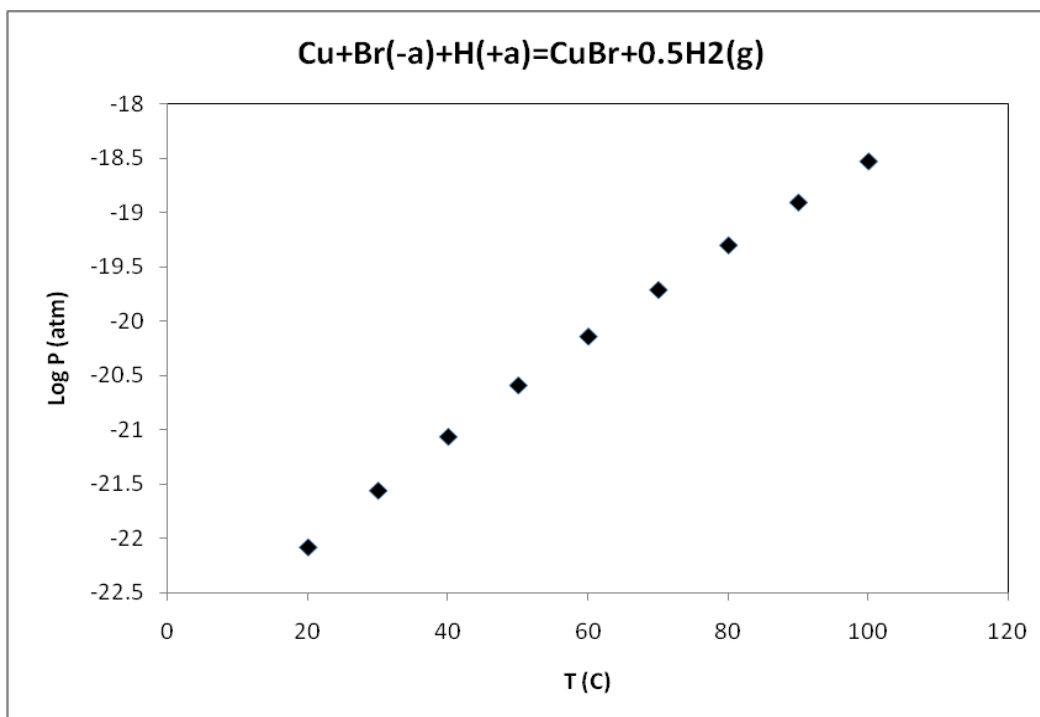


Figure 51: Calculated hydrogen pressure from the reaction, $Cu + Br(-a) + H(+a) = CuBr(s) + 0.5H_2(g)$ in *pH*-neutral *NaCl* solution

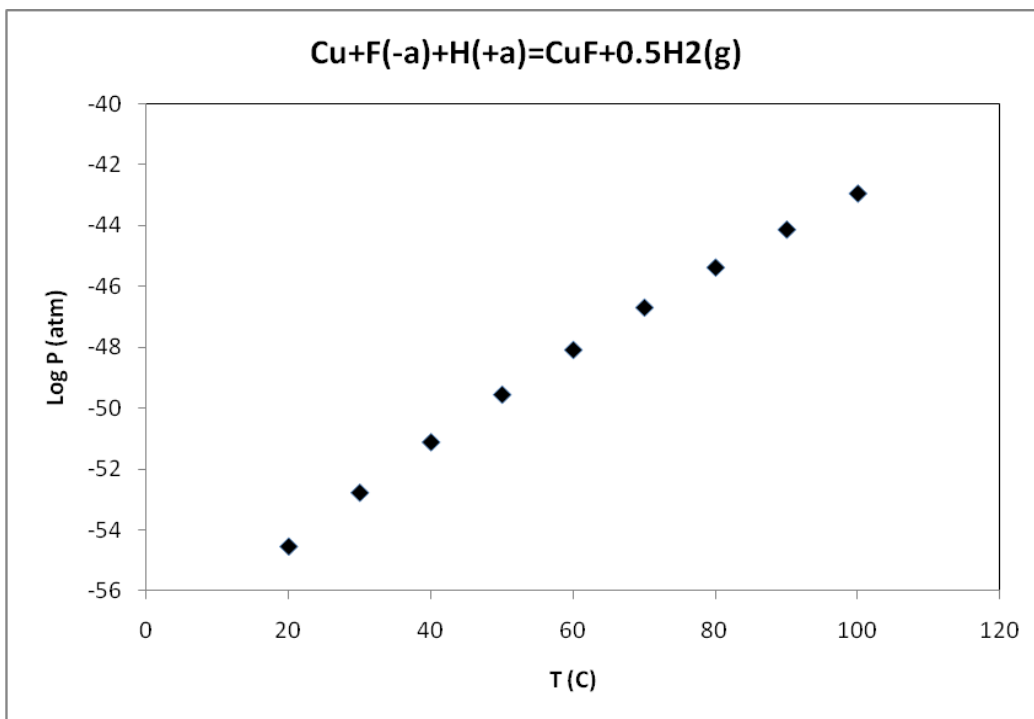


Figure 52: Calculated hydrogen pressure from the reaction, $Cu + F(-a) + H(+a) = CuF(s) + 0.5H_2(g)$ in *pH*-neutral *NaCl* solution.

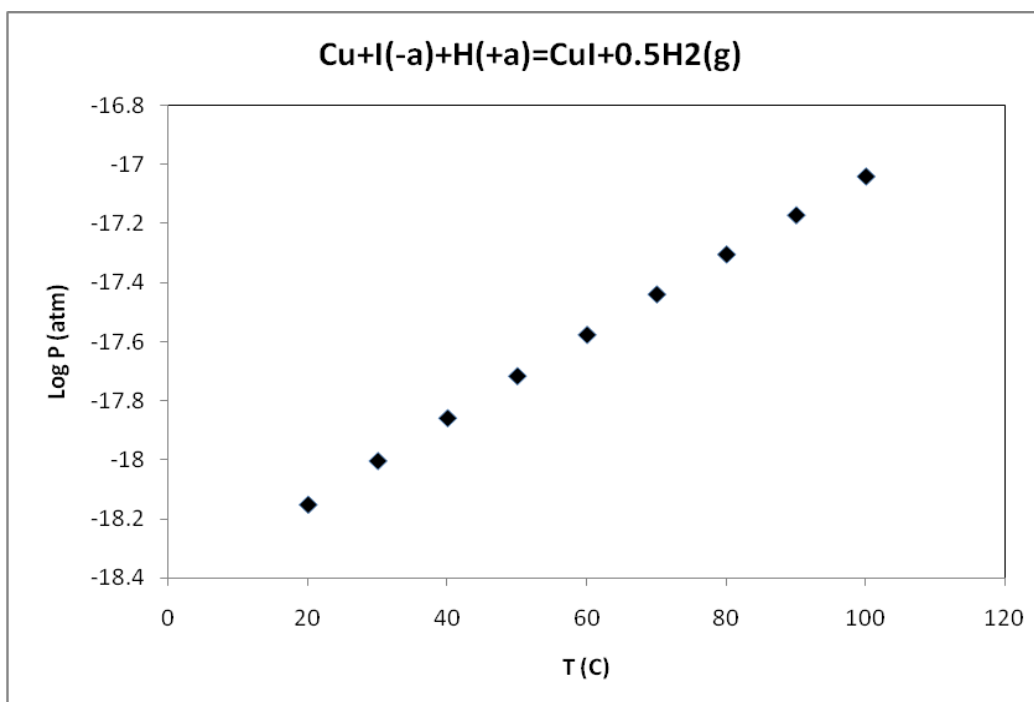


Figure 53: Calculated hydrogen pressure from the reaction, $Cu + I(-a) + H(+a) = CuI(s) + 0.5H_2(g)$ in *pH*-neutral *NaCl* solution.

VI. Simulation of the Repository – Gibbs Energy Minimization Studies

Gibbs Energy Minimization

The next objective of this project was speciation calculations to find out what species are likely to form in the repository in the vicinity of the canister. Several chemical equilibrium models/codes were evaluated for this task, utilizing the species in the thermodynamic database developed earlier in the project. Finally a comprehensive model, based on the Gibbs energy minimization method, has been developed for speciation of complex geochemical systems.

Theory

Although speciation calculations are well-known in the geochemical community, the codes that are used are often “canned” and downloaded from various sources, leaving the user with little appreciation of the nature of the calculation involved. It is for this reason that we present a brief description of the two principal methods for speciation; the equilibrium statement method and the Gibbs energy minimization technique.

The Gibbs energy (G), is defined as $G = H - TS$, where H and S are enthalpy and entropy, respectively, and T is absolute (Kelvin) temperature. The relationship between the Gibbs energy and the equilibrium constant can be found by considering chemical potentials. At constant temperature and pressure the Gibbs free energy (G) for a system, depends only on the composition of the system, as measured by some general composition variable, ξ , where $\xi = 0$ describes the reactants alone and $\xi = 1$ describes only the products. For a spontaneous change, G of the system can only decrease according to the Second Law of Thermodynamics. Consequently, the derivative of G with respect to the ξ must be negative for the reaction to occur spontaneously in the direction indicated (left to right). The Gibbs energy, G , in this case, refers to that of the system (solute + solvent, of the desired composition) and not to that for a particular species or reaction. At equilibrium, the Gibbs energy of the system must be at a minimum and, hence, the derivative is equal to zero:

$$\left(\frac{dG}{d\xi}\right)_{T,p} = 0 \quad \text{at equilibrium} \quad (20)$$

Thus, the problem in finding the equilibrium composition is to determine the number of moles of all components, as expressed by the vector ξ , at which the total Gibbs energy of the system is at a minimum. This method is termed “Gibbs energy minimization”. More is said about this technique below.

Alternatively, as originally developed by Lewis and Randall, the state of equilibrium can also be defined by writing the interchange and reaction of various components in terms of equilibrium equations of the form,



in which case the reaction is regarded as being the “system”. Again, the condition for equilibrium is that the Gibbs energy must be at a minimum, meaning that any arbitrarily small

change in the extent of the reaction, ξ , must result in the change in Gibbs energy being zero. However, in this method, the Gibbs energy change for the reaction is written in terms of the partial molal Gibbs energies or chemical potentials of the components in the reaction as [26]:

$$\Delta G = c\mu_C + d\mu_D - a\mu_A - B\mu_B \quad (22)$$

with $\Delta G = 0$ for the equilibrium state. This condition is demonstrated more rigorously below. In Equation (22), μ_X is the “chemical potential” or partial molar Gibbs energy, of component X in the system; that is, $\mu_X = (\partial G / \partial n_X)_{n_y, \dots}$ and the differential is evaluated with respect to component X, while holding the number of moles of all other components (including the solvent) constant. By appealing to the ideal, Henry’s Law, the chemical potential of a reagent A is a function of the activity (the “thermodynamic concentration”), a_A , of the component, and is written as.

$$\mu_A = \mu_A^0 + RT \ln(a_A) \quad (23)$$

where, μ_A^0 is the standard chemical potential (chemical potential when $a_A = 1$ (the “standard state”). In turn, the activity may be defined as $a_i = \gamma_i (m_i / m_i^0)$, where γ_i is the activity coefficient that corrects for the deviation of Equation (23) from ideality [to give a linear dependence of μ on $\ln(\gamma_i m)$] and m_i and m_i^0 are the actual molal concentration and the molal concentration in the standard state, respectively. For dissolved species, the Henry’s Law standard state is chosen to be the hypothetical 1 m solution that has the properties of an infinitely dilute solution, so that solute-solute interactions (the source of non-ideality) are absent. A similar expression to Equation (23) can be written for a gaseous species with the activity being expressed by the fugacity, $f_i = \hat{\gamma}_i (p_i / p_i^0)$, where $\hat{\gamma}_i$ is the fugacity coefficient, which corrects for deviations of the PVT properties of the gas from the ideal gas law, and p_i and p_i^0 are the actual partial pressure and the partial pressure in the standard state, respectively. The standard state is chosen to be the ideal gas at unit pressure. For solids, the composition is invariant, and the activity is defined as being equal to one.

For a closed system (i.e., one that can exchange energy but not matter with the surroundings) and for arbitrary small changes in composition, the change in Gibbs energy of the system, G , takes the form:

$$dG = VdP - SdT + \sum_{i=1}^K \mu_i dN_i \quad (24)$$

where K is the total number of components in the system. Now,

$$dN_i = \nu_i d\xi \quad (25)$$

where, ν_i corresponds to the stoichiometric coefficient and $d\xi$ is the differential of the extent of reaction. At constant pressure and temperature we obtain:

$$\left(\frac{dG}{d\xi}\right)_{T,p} = \sum_{i=1}^k \mu_i \nu_i = \Delta_r G_{T,p} \quad (26)$$

which corresponds to the Gibbs free energy change for the reaction. This results in:

$$\Delta_r G_{T,p} = c\mu_C + d\mu_D - \alpha\mu_A - \beta\mu_B \quad (27)$$

by substituting the chemical potentials and rearranging the equations:

$$\Delta_r G_{T,p} = (c\mu_C^0 + d\mu_D^0) - (\alpha\mu_A^0 + \beta\mu_B^0) + (cRT \ln\{C\} + dRT \ln\{D\}) - (\alpha RT \ln\{A\} + \beta RT \ln\{B\}) \quad (28)$$

the relationship becomes:

$$\Delta_r G_{T,p} = \sum_{i=1}^k \mu_i^0 \nu_i + RT \ln \frac{\{C\}^c \{D\}^d}{\{A\}^\alpha \{B\}^\beta} \quad (29)$$

which $\sum_{i=1}^k \mu_i^0 \nu_i = \Delta_r G^0$ is the standard Gibbs energy change for the reaction. It is a constant at a given temperature, which can be calculated, using thermodynamic data tables. [26]. We now define

$$RT \ln \frac{\{C\}^c \{D\}^d}{\{A\}^\alpha \{B\}^\beta} = RT \ln Q_r \quad (30)$$

where Q_r is the reaction proportion when the system is not at equilibrium (i.e., $\Delta_r G \neq 0$). Therefore,

$$\left(\frac{dG}{d\xi}\right)_{T,p} = \Delta_r G_{T,p} = \Delta_r G^0 + RT \ln Q_r \quad (31)$$

At equilibrium,

$$\begin{aligned} \left(\frac{dG}{d\xi}\right)_{T,p} &= \Delta_r G_{T,p} = 0 \\ Q_r &= K_{eq} \end{aligned} \quad (32)$$

the reaction quotient becomes equal to the equilibrium constant, leading to:

$$0 = \Delta_r G^0 + RT \ln K_{eq} \quad (33)$$

and

$$\Delta_r G^0 = -RT \ln K_{eq} \quad (34)$$

Obtaining the value of the standard Gibbs energy change, allows the calculation of the equilibrium constant and if all components in the system are related by reactions at equilibrium, the composition is readily calculated. Thus, for each equilibrium in the system, with all species being involved in at least one equilibrium, we develop a set of equations (“equilibrium statements”) of the type:

Equilibrium Statement Method

The equilibrium constant defined in Equation 34 may be expressed explicitly as:

$$K_i = \frac{a_C^c a_D^d}{a_A^a a_B^b} \quad i = 1, \dots, L$$

where the activities are the values at equilibrium and L is the number of equilibria. However the number of unknowns in the system is found to be greater than the number of equilibrium statements (L), so that the problem is mathematically under-determined. This issue is resolved by noting that the total amount of each element in the system must be conserve. This condition can be expressed as:

$$\sum_{j=1}^m a_{ij} N_j = b_i^0$$

where j is the number of the species (compound), a_{ij} is the amount of element i in j , N_j is the number of moles of each species in the system, and b_i^0 is to total amount of element i in the system (specified as an input). These equations act as constraints and hence impart determinism to the calculation. If the system contains B elements, then the total number of equations is $L + B$, and one finds that there are now as many equations as there are unknowns, so that the problem is mathematically determined.

This is the basis of the “equilibrium statement” method of speciation, which has its roots in the original work of Lewis and Randall at the University of California, Berkeley, in the early part of the twentieth century. Various commercial codes use this method for predicting speciation in complex chemical systems. However, the path-independence condition of the change in a state function (e.g., G) dictates that specifying reactions is superfluous and unnecessary and this has led to the development of Gibbs energy minimization codes beginning with SOLGASMIX that was developed in the 1960s to describe combustion in rocket motors.

Minimization of Gibbs Energy

AS noted above, at equilibrium, the Gibbs Energy of the system G is at a global minimum:

$$dG = \sum_{j=1}^m \mu_j dN_j = 0 \quad (35)$$

For a closed system, no particles may enter or leave, although they may combine in various ways. The total number of atoms of each element will remain constant. This means that the minimization above must be subjected to the constraints:

$$\sum_{j=1}^m a_{ij} N_j = b_i^0 \quad (36)$$

where a_{ij} is the number of atoms of element i in molecule j and b_i^0 is the total number of atoms of element i , which is a constant, since the system is closed. If there are a total of k types of atoms in the system, then there will be k such constraining equations.

This is a standard problem in optimization, known as constrained minimization. The most common method of solving for the composition is using the method of Lagrange undetermined multipliers; however other methods may be used. [27]

$$\zeta = G + \sum_{i=1}^k \lambda_i \left(\sum_{j=1}^m a_{ij} N_j - b_i^0 \right) = 0 \quad (37)$$

where λ_i are the Lagrange multipliers, one for each element. This allows each of the N_j to be treated independently, and it can be shown using the tools of multivariate calculus that the equilibrium condition is given by

$$\frac{d\zeta}{dN_j} = 0 \quad \text{and} \quad \frac{d\zeta}{d\lambda_i} = 0 \quad (38)$$

This is a set of $(m+k)$ equations in $(m+k)$ unknowns (the N_j and the λ_i) and may, therefore, be solved for the equilibrium concentrations N_j as long as the chemical potentials are known as functions of the concentrations at the given temperature and pressure. (See “Thermodynamic Databases for Pure Substances [27]).

This Gibbs energy minimization method of calculating equilibrium chemical concentrations is useful for systems with a large number of different molecules. The use of k atomic element conservation equations for the mass constraints is straightforward, and replaces the use of the stoichiometric coefficient equations. [27]. One great advantage over the equilibrium statement method outlined above, in concert with the path independence condition for the change is a state function (G), is that it does not require statement of equilibria and hence is the more fundamental of the two methods.

Modeling

The technique of Gibbs energy minimization to estimate the equilibrium composition for a given set of species is enabled by many process simulation packages, including *OLI Systems Stream Analyser* [28], *GEM-Selektor*[29], *FactSage*[30], *Aspen Plus*[31], *METSIM*[32] and *HSC Chemistry*[24] among many others. The software packages have varied levels of sophistication, with some being able to predict the behavior of non-ideal solutions at elevated temperatures and pressures. Gibbs energy minimization has been used to characterize different systems varying from extractive metallurgy, to corrosion engineering, geochemistry, and environmental chemistry, *etc.*

Amongst these simulation compilers, we found *GEM-Selektor* to be more appropriate for our modeling work. *GEM-Selektor* (GEMS) is a broad-purpose, geochemical modeling code. It uses an advanced convex programming method for Gibbs energy minimization (GEM), which is implemented in an efficient Interior Points Method (IPM), numerical module [29]. Using GEMS, one can compute an equilibrium phase assemblage and speciation in a complex chemical system from its total bulk elemental composition at a given temperature and pressure (optionally, with some metastability or kinetic constraints). Overall, when using the GEMS code, one has the power of advanced chemical thermodynamic modeling at one's fingertips, and one will eventually achieve an unmatched efficiency in interpreting even complex subsurface- or hydrothermal aquatic systems. Of course, GEMS solves traditional equilibrium aqueous speciation problems, perhaps, somewhat slower than the LMA code, but providing even more output parameters for less input data. The *pH*, E_h , ionic strength and fugacities of gases are always obtained as output (not input) parameters in GEMS calculations. This helps greatly, for instance, in investigating the behavior of redox-dependent systems. [29]

In order to describe an ionic system, the first step is to specify the various species and components present in solution. Our selection was based on the information provided by the KBS-3 [33] and commonly available compounds in the groundwater systems. To complete this step, several thermodynamic databases are available (*NBS 1982*; *Woley, 1992*; *HSC Chemistry* and *etc.*) For most of the components, we used the *HSC Chemistry* database or the data provided by the KBS-3 report [33], because our early analysis indicated that these were the most extensive for the compounds of interest. By “species” or “compound” we mean any chemical substance present in the solution (ion, complex or molecule); and any other type of component, such as solids and gases, respectively, to complete the system description. After collecting the necessary thermodynamic parameters of all species and compounds present in in the HSC database and in the KBS-3 report [33], we added thermodynamic data for additional species that we gleaned from the recent literature. These species were primarily the polysulfides and polysulfur oxyanions that are so important in the chemistry of copper.

The second step is to define the initial composition of the system, in order to satisfy the equilibrium relations. In other words, we should define the system in a way that the entire set of selected elements have some input value, in order to be taken into account by the specified species and compounds in the calculations. The selected temperature range (18-80°C) was based upon the temperature evolution in the repository, as reported in the KBS-3. [34]. Table 6 shows a typical set of input values in the global system calculations:

Table 6-Input material in Anoxic condition

	$H_2O(aq)$	$H_2(g)$	$O_2(g)$	$N_2(g)$	$CO_2(g)$	$H^3PO_4(aq)$	$FeS_2(s)$	$CuO(s)$	$NH_3(aq)$	$HCl(aq)$
input	1000g	1M	1e-77M	1e-10M	1e-10M	1e-10M	100g	100g	1e-10M	1e-10M

As can be seen, the selected system satisfies anoxic conditions, by specifying an extraordinarily low oxygen concentration and a high hydrogen concentration. The hydrogen gas input concentration is selected as a 1M in order to achieve an output concentration close to the 1e-11 M reported by Bath [21] once equilibrium is achieved. Note that the output hydrogen concentration is much less than that corresponding to the input concentration ($1.37\text{E}-11\text{M}$), because much of the hydrogen reacts with other components of the system in coming to equilibrium. Thus, what is important for the input is the amount specified and it is for this reason that the initial hydrogen content is specified as a concentration rather than as a pressure (recall that the system is assumed to be closed).

The last step of simulation is running the software and obtaining the results. We checked out the equilibrium results by comparing the calculated equilibrium constants against literature data for well-known reactions, such as the water dissociation reaction: $H_2O(l) = H^+(+a) + OH^-(a)$, $K_w = 1.02\text{E}-14$ (at $T = 25\text{ }^\circ\text{C}$). In our output results from GEMS: $[H^+] = 5.7848\text{E}-9\text{ M}$, $[OH^-] = 1.7923\text{E}-6\text{ M}$. Accordingly, the value of K_w calculated from the GEMS output is: $K_w = 1.03\text{E}-14$ (at $T = 25\text{ }^\circ\text{C}$), which is in very good agreement with the reported equilibrium constant for water in different databases. This same type of calculation was carried out for many other, well-known equilibria (e.g., HCO_3^-/CO_3^{2-} , HSO_4^-/SO_4^{2-}) and the calculated equilibrium constants were, again, found to be in good agreement with literature data, demonstrating the efficacy of GEMS for modeling complex geochemical systems.

Since we were had some doubts about the thermodynamic data of some compounds, such as $S_xO_3(-2a)^i$ ($x = 3 - 7$), we excluded them from the speciation calculation of the system.

The following tables summarize the results of the Gibbs energy minimization of the system under anoxic conditions. These calculations were carried out for several temperatures within the range ($18\text{ }^\circ\text{C}$ to $80\text{ }^\circ\text{C}$) that are predicted to exist within the anoxic storage period of 10 to more than 10,000 years (Figure 60). All simulations were carried out for anoxic conditions with the hydrogen concentration being adjusted to about 10^{-11} M by carefully specifying the input $[H_2]$. In Tables 7 – 13, any concentration that was predicted to be lower than $1\text{e}-20$ was set equal to zero, but this will be set to a much lower value (e.g., $1\text{e}-50$) in future work, because the CDDs predict that some sulfur-containing species may be activating at concentrations down to about $1\text{e}-44$. Note that, because the amount of water chosen as input was 1 kg, the “Quantity in the system” data in the tables correspond to the molal concentrations, m (mol/kg).

Global System-Anoxic Condition

1-18 °C

State variables:

P(bar)= 1 T= 18 (C) = 291.15 (K) V(cm3)= 1057.3875 Mass(kg)= 1.2,

Min-potential (moles): G(x)= -5614.45712

Aqueous phase:

ⁱ The designation $S_xO_3(-2a)$ comes from the HSC-5 database in which the “-2” indicates that the species is aqueous with a charge of -2.

$I(\text{molal})= 2.437\text{e-}006$ $pH= 8.451$ $pe= -6.076$ $E_h(\text{V})= -0.3503$

Table 7-Parameters of Dependent Components (DC, Species) at 18°C

Species name	Quantity in the system	Species name	Quantity in the system
Cu (NH3) +2	0	Cu+2	0
Cu (NH3) 2 (OH) 2@	0	Cu2 (OH) 2+2	0
Cu (NH3) 2+	1.80E-13	Cu3 (OH) 4+2	0
Cu (NH3) 2+2	0	CuCl+	0
Cu (NH3) 3 (OH) +	1.83E-18	CuCl2@	0
Cu (NH3) 3+2	1.94E-17	CuCl3-	0
Cu (NH3) 4+2	1.47E-10	CuCl4-2	0
Cu2Cl4-2	0	CuH2PO4+	0
Cu3Cl6-3	0	CuO2-2	0
Cu (HCO3) +	0	CuO2H-	0
Cu (HPO4) H2PO4-	0	CuO@	0
Cu (OH) 2-	1.19E-17	CuOH+	0
Cu (OH) @	0	Fe (CO3) @	2.75E-15
Cu+	2.36E-18	Fe (HCO3) +	1.18E-15
CuCl2-	0	Fe (HSO4) +	0
CuCl3-2	0	Fe (SO4) @	5.05E-20
CuCl@	0	Fe+2	8.11E-07
CuH2PO4@	0	FeCl+	1.09E-16
Cu (CO3) 2-2	0	FeCl2@	0
Cu (HPO4) (H2PO4	0	FeO2H-	3.37E-11
Cu (HPO4) 2-2	0	FeO@	9.28E-11
Cu (HPO4) @	0	FeOH+	4.33E-08
Cu (NO2) +	0	Fe (HSO4) +2	0
Cu (NO2) 2@	0	Fe (SO4) +	0
Cu (NO3) +	0	Fe (SO4) 2-	0
Cu (NO3) 2@	0	Fe+3	0
Cu (OH) 2@	0	Fe2 (OH) 2+4	0
Cu (OH) 3-	0	Fe3 (OH) 4+5	0
Cu (OH) 4-2	0	FeCl+2	0

Table 7-Parameters of Dependent Components (DC, Species)-Cont'd

Species name	Quantity in the system	Species name	Quantity in the system
FeCl2+	0	H3PO3@	0
FeCl3@	0	HPO3-2	0
FeO+	4.02E-15	H2P2O7-2	0
FeO2-	1.47E-14	H2PO4-	5.71E-12
FeO2H@	8.13E-14	H3P2O7-	0
FeOH+2	6.24E-20	H3PO4@	2.59E-18

CO@	0	H4P2O7@	0
CO2@	1.16E-13	HP2O7-3	0
CO3-2	1.49E-13	HPO4-2	9.43E-11
HCO3-	1.32E-11	P2O7-4	0
CH4@	8.65E-11	PO4-3	1.03E-14
CN-	0	HS7O3-	0
HCN@	0	HS6O3-	0
OCN-	0	HS5O3-	0
SCN-	0	HS4O3-	0
ClO-	0	HS3O3-	0
HClO@	0	S7O6-2	0
ClO2-	0	S6O6-2	0
HClO2@	0	H2S2O3@	0
ClO3-	0	HS2O3-	0
ClO4-	0	S2O3-2	0
Cl-	1.00E-10	S5O6-2	0
HCl@	7.58E-20	S4O6-2	0
H2@	1.03E-08	H2S2O4@	0
H2N2O2@	0	HS2O4-	0
HN2O2-	0	S2O4-2	0
N2O2-2	0	S3O6-2	0
HNO2@	0	HS2O5-	0
NO2-	0	HSO3-	0
HNO3@	0	S2O5-2	0
NO3-	0	SO2@	0
N2H5+	0	SO3-2	0
N2H6+2	0	HS2O6-	0
NH3@	1.05E-11	S2O6-2	0
NH4+	1.42E-10	HS2O7-	0
N2@	0	HSO4-	0
O2@	0	S2O7-2	0
H2O2@	0	SO3@	0
HO2-	0	SO4-2	3.84E-16
H2PO2-	0	HS2O8-	0
H3PO2@	0	S2O8-2	0
H2PO3-	0	HSO5-	0

Table 7-Parameters of Dependent Components (DC, Species)-Cont'd

Species name	Quantity in the system	Species name	Quantity in the system
S8-2	0	NH3 (g)	1.40E-19
S7-2	0	N2 (g)	0
HS6-	0	O2 (g)	0
S6-2	0	SO2 (g)	0
HS5-	0	H2S (g)	7.02E-16

HS4-	0	S2 (g)	0
HS3-	0	H2O(g)	1.13E-06
S2-2	0	Cu (s)	0
S3-2	0	Chalcopyrite (s)	0.485712
S4-2	0	Cuprite (s)	0
S5-2	0	Tenorite (s)	0
HS2-	4.80E-19	Chalcocite (s)	0.385716
H2S@	8.10E-11	Fe (s)	0
HS-	1.76E-09	FeCO3 (pr) (s)	0
S-2	1.65E-20	Fe2-Ox (s)	0
OH-	1.67E-06	Hematite (s)	0
H+	3.71E-09	Magnetite (s)	0.064286
H2O@	56.5084	Fe (OH) 3 (am) (s)	0
CO (g)	0	Fe (OH) 3 (mic) (s)	0
CO2 (g)	3.07E-18	Pyrite (s)	0.154909
CH4 (g)	6.02E-14	Pyrrhotite (s)	0
H2 (g)	1.37E-11	Sulfur (s)	0

*Concentration and activity are given for aqueous species in mol/(kgH2O), for other species - in the mole fraction scale.

2-42 °C

State variables:

P(bar)= 1 T= 42 (C) = 315.15 (K) V(cm3)= 1064.789 Mass(kg)= 1.2,

Min-potential (moles): G(x)= -5224.90413

Aqueous phase:

I(molal)= 2.994e-006 pH= 7.792 pe= -5.348 Eh(V)= -0.3338

Table 8-Parameters of Dependent Components (DC, Species) at 42°C

Species name	Quantity in the system	Species name	Quantity in the system
Cu (NH3) +2	0	Cu+2	0
Cu (NH3) 2 (OH) 2@	0	Cu2 (OH) 2+2	0
Cu (NH3) 2+	2.41E-13	Cu3 (OH) 4+2	0
Cu (NH3) 2+2	0	CuCl+	0
Cu (NH3) 3 (OH) +	3.07E-18	CuCl2@	0
Cu (NH3) 3+2	4.87E-17	CuCl3-	0
Cu (NH3) 4+2	2.61E-10	CuCl4-2	0
Cu2Cl4-2	0	CuH2PO4+	0
Cu3Cl6-3	0	CuO2-2	0
Cu (HCO3) +	0	CuO2H-	0

Cu (HPO4) H2PO4-	0	CuO@	0
Cu (OH) 2-	1.49E-17	CuOH+	0
Cu (OH) @	9.92E-20	Fe (CO3) @	7.00E-15
Cu+	6.84E-17	Fe (HCO3) +	5.49E-15
CuCl2-	0	Fe (HSO4) +	0
CuCl3-2	0	Fe (SO4) @	4.09E-18
CuCl@	0	Fe+2	9.90E-07
CuH2PO4@	0	FeCl+	1.44E-16
Cu (CO3) 2-2	0	FeCl2@	0
Cu (HPO4) (H2PO4	0	FeO2H-	2.94E-11
Cu (HPO4) 2-2	0	FeO@	1.81E-10
Cu (HPO4) @	0	FeOH+	6.09E-08
Cu (NO2) +	0	Fe (HSO4) +2	0
Cu (NO2) 2@	0	Fe (SO4) +	0
Cu (NO3) +	0	Fe (SO4) 2-	0
Cu (NO3) 2@	0	Fe+3	0
Cu (OH) 2@	0	Fe2 (OH) 2+4	0
Cu (OH) 3-	0	Fe3 (OH) 4+5	0
Cu (OH) 4-2	0	FeCl+2	0

Table 8-Parameters of Dependent Components (DC, Species)-Cont'd

Species name	Quantity in the system	Species name	Quantity in the system
FeCl2+	0	H3PO3@	0
FeCl3@	0	HPO3-2	0
FeO+	3.17E-14	H2P2O7-2	0
FeO2-	1.16E-13	H2PO4-	1.72E-11
FeO2H@	9.05E-13	H3P2O7-	0
FeOH+2	7.01E-19	H3PO4@	5.45E-17
CO@	0	H4P2O7@	0
CO2@	2.17E-12	HP2O7-3	0
CO3-2	2.66E-13	HPO4-2	8.28E-11
HCO3-	7.09E-11	P2O7-4	0
CH4@	2.66E-11	PO4-3	2.89E-15
CN-	0	HS7O3-	0
HCN@	0	HS6O3-	0
OCN-	0	HS5O3-	0
SCN-	0	HS4O3-	0
ClO-	0	HS3O3-	0
HClO@	0	S7O6-2	0
ClO2-	0	S6O6-2	0
HClO2@	0	H2S2O3@	0
ClO3-	0	HS2O3-	0
ClO4-	0	S2O3-2	0
Cl-	1.00E-10	S5O6-2	0

HCl@	2.71E-19	S4O6-2	0
H2@	2.28E-08	H2S2O4@	0
H2N2O2@	0	HS2O4-	0
HN2O2-	0	S2O4-2	0
N2O2-2	0	S3O6-2	0
HNO2@	0	HS2O5-	0
NO2-	0	HSO3-	0
HNO3@	0	S2O5-2	0
NO3-	0	SO2@	0
N2H5+	0	SO3-2	0
N2H6+2	0	HS2O6-	0
NH3@	2.61E-12	S2O6-2	0
NH4+	3.66E-11	HS2O7-	0
N2@	0	HSO4-	4.94E-20
O2@	0	S2O7-2	0
H2O2@	0	SO3@	0
HO2-	0	SO4-2	1.92E-14
H2PO2-	0	HS2O8-	0
H3PO2@	0	S2O8-2	0
H2PO3-	0	HSO5-	0

Table 8-Parameters of Dependent Components (DC, Species)-Cont'd

Species name	Quantity in the system	Species name	Quantity in the system
S8-2	0	NH3 (g)	1.02E-19
S7-2	0	N2 (g)	0
HS6-	0	O2 (g)	0
S6-2	0	SO2 (g)	0
HS5-	0	H2S (g)	1.03E-14
HS4-	0	S2 (g)	0
HS3-	0	H2O (g)	1.14E-06
S2-2	0	Cu (s)	0
S3-2	0	Chalcopyrite (s)	0.485711
S4-2	0	Cuprite (s)	0
S5-2	0	Tenorite (s)	0
HS2-	0.00E+00	Chalcocite (s)	0.385716
H2S@	6.06E-10	Fe (s)	0
HS-	6.00E-09	FeCO3 (pr) (s)	0
S-2	3.93E-19	Fe2-Ox (s)	0
OH-	2.05E-06	Hematite (s)	0
H+	1.65E-08	Magnetite (s)	0.064286
H2O@	56.5084	Fe (OH) 3 (am) (s)	0
CO (g)	0	Fe (OH) 3 (mic) (s)	0
CO2 (g)	1.08E-16	Pyrite (s)	0.15491
CH4 (g)	2.89E-14	Pyrrhotite (s)	0

H2 (g)	3.51E-11	Sulfur (s)	0
--------	----------	------------	---

*Concentration and activity are given for aqueous species in mol/(kgH2O), for other species - in the mole fraction scale.

3-45 °C

State variables:

P(bar)= 1 T= 45 (C) = 318.15 (K) V(cm3)= 1066.0581 Mass(kg)= 1.2,

Min-potential (moles): G(x)= -5180.55892

Aqueous phase:

I(molal)= 3.047e-006 pH= 7.718 pe= -5.266 Eh(V)= -0.3317

Table 9-Parameters of Dependent Components (DC, Species) at 45°C

Species name	Quantity in the system	Species name	Quantity in the system
Cu (NH3) +2	0	Cu+2	0
Cu (NH3) 2 (OH) 2@	0	Cu2 (OH) 2+2	0
Cu (NH3) 2+	2.39E-13	Cu3 (OH) 4+2	0
Cu (NH3) 2+2	0	CuCl+	0
Cu (NH3) 3 (OH) +	3.10E-18	CuCl2@	0
Cu (NH3) 3+2	5.19E-17	CuCl3-	0
Cu (NH3) 4+2	2.80E-10	CuCl4-2	0
Cu2Cl4-2	0	CuH2PO4+	0
Cu3Cl6-3	0	CuO2-2	0
Cu (HCO3) +	0	CuO2H-	0
Cu (HPO4) H2PO4-	0	CuO@	0
Cu (OH) 2-	1.51E-17	CuOH+	0
Cu (OH) @	1.74E-19	Fe (CO3) @	7.00E-15
Cu+	1.00E-16	Fe (HCO3) +	5.96E-15
CuCl2-	0	Fe (HSO4) +	0
CuCl3-2	0	Fe (SO4) @	6.71E-18
CuCl@	0	Fe+2	1.01E-06
CuH2PO4@	0	FeCl+	1.49E-16
Cu (CO3) 2-2	0	FeCl2@	0
Cu (HPO4) (H2PO4)	0	FeO2H-	2.91E-11
Cu (HPO4) 2-2	0	FeO@	1.96E-10
Cu (HPO4) @	0	FeOH+	6.31E-08
Cu (NO2) +	0	Fe (HSO4) +2	0
Cu (NO2) 2@	0	Fe (SO4) +	0
Cu (NO3) +	0	Fe (SO4) 2-	0
Cu (NO3) 2@	0	Fe+3	0

Cu (OH) 2@	0	Fe2 (OH) 2+4	0
Cu (OH) 3-	0	Fe3 (OH) 4+5	0
Cu (OH) 4-2	0	FeCl+2	0

Table 9-Parameters of Dependent Components (DC, Species)-Cont'd

Species name	Quantity in the system	Species name	Quantity in the system
FeCl2+	0	H3PO3@	0
FeCl3@	0	HPO3-2	0
FeO+	3.97E-14	H2P2O7-2	0
FeO2-	1.45E-13	H2PO4-	1.86E-11
FeO2H@	1.17E-12	H3P2O7-	0
FeOH+2	9.16E-19	H3PO4@	7.94E-17
CO@	0	H4P2O7@	0
CO2@	2.78E-12	HP2O7-3	0
CO3-2	2.55E-13	HPO4-2	8.14E-11
HCO3-	7.68E-11	P2O7-4	0
CH4@	2.01E-11	PO4-3	2.53E-15
CN-	0	HS7O3-	0
HCN@	0	HS6O3-	0
OCN-	0	HS5O3-	0
SCN-	0	HS4O3-	0
ClO-	0	HS3O3-	0
HClO@	0	S7O6-2	0
ClO2-	0	S6O6-2	0
HClO2@	0	H2S2O3@	0
ClO3-	0	HS2O3-	0
ClO4-	0	S2O3-2	0
Cl-	1.00E-10	S5O6-2	0
HCl@	3.16E-19	S4O6-2	0
H2@	2.51E-08	H2S2O4@	0
H2N2O2@	0	HS2O4-	0
HN2O2-	0	S2O4-2	0
N2O2-2	0	S3O6-2	0
HNO2@	0	HS2O5-	0
NO2-	0	HSO3-	0
HNO3@	0	S2O5-2	0
NO3-	0	SO2@	0
N2H5+	0	SO3-2	0
N2H6+2	0	HS2O6-	0
NH3@	2.11E-12	S2O6-2	0
NH4+	1.76E-11	HS2O7-	0
N2@	0	HSO4-	9.94E-20
O2@	0	S2O7-2	0
H2O2@	0	SO3@	0

HO2-	0	SO4-2	2.97E-14
H2PO2-	0	HS2O8-	0
H3PO2@	0	S2O8-2	0
H2PO3-	0	HSO5-	0

Table 9-Parameters of Dependent Components (DC, Species)-Cont'd

Species name	Quantity in the system	Species name	Quantity in the system
S8-2	0	NH3 (g)	9.38E-20
S7-2	0	N2 (g)	0
HS6-	0	O2 (g)	0
S6-2	0	SO2 (g)	0
HS5-	0	H2S (g)	1.39E-14
HS4-	0	S2 (g)	0
HS3-	0	H2O (g)	1.15E-06
S2-2	0	Cu (s)	0
S3-2	0	Chalcopyrite (s)	0.485711
S4-2	0	Cuprite (s)	0
S5-2	0	Tenorite (s)	0
HS2-	0.00E+00	Chalcocite (s)	0.385716
H2S@	7.72E-10	Fe (s)	0
HS-	6.90E-09	FeCO3 (pr) (s)	0
S-2	5.64E-19	Fe2-Ox (s)	0
OH-	2.09E-06	Hematite (s)	0
H+	1.95E-08	Magnetite (s)	0.064286
H2O@	56.5084	Fe(OH)3 (am) (s)	0
CO (g)	0	Fe(OH)3 (mic) (s)	0
CO2 (g)	1.46E-16	Pyrite (s)	0.15491
CH4 (g)	2.40E-14	Pyrrhotite (s)	0
H2 (g)	3.86E-11	Sulfur (s)	0

*Concentration and activity are given for aqueous species in mol/(kgH2O), for other species - in the mole fraction scale.

4-58 °C

State variables:

P(bar)= 1 T= 58 (C) = 331.15 (K) V(cm3)= 1072.3167 Mass(kg)= 1.2,

Min-potential (moles): G(x)= -4998.1927

Aqueous phase:

I(molal)= 3.234e-006 pH= 7.417 pe= -4.927 Eh(V)= -0.3231

Table 10-Parameters of Dependent Components (DC, Species) at 58°C

Species name	Quantity in the system	Species name	Quantity in the system
Cu (NH3) +2	0	Cu+2	0
Cu (NH3) 2 (OH) 2@	0	Cu2 (OH) 2+2	0
Cu (NH3) 2+	2.32E-13	Cu3 (OH) 4+2	0
Cu (NH3) 2+2	0	CuCl+	0
Cu (NH3) 3 (OH) +	3.21E-18	CuCl2@	0
Cu (NH3) 3+2	6.76E-17	CuCl3-	0
Cu (NH3) 4+2	2.92E-10	CuCl4-2	0
Cu2Cl4-2	0	CuH2PO4+	0
Cu3Cl6-3	0	CuO2-2	0
Cu (HCO3) +	0	CuO2H-	0
Cu (HPO4) H2PO4-	0	CuO@	0
Cu (OH) 2-	1.54E-17	CuOH+	0
Cu (OH) @	1.75E-18	Fe (CO3) @	5.42E-15
Cu+	4.90E-16	Fe (HCO3) +	6.62E-15
CuCl2-	0	Fe (HSO4) +	0
CuCl3-2	0	Fe (SO4) @	5.08E-17
CuCl@	0	Fe+2	1.06E-06
CuH2PO4@	0	FeCl+	1.74E-16
Cu (CO3) 2-2	0	FeCl2@	0
Cu (HPO4) (H2PO4	0	FeO2H-	2.95E-11
Cu (HPO4) 2-2	0	FeO@	2.80E-10
Cu (HPO4) @	0	FeOH+	7.27E-08
Cu (NO2) +	0	Fe (HSO4) +2	0
Cu (NO2) 2@	0	Fe (SO4) +	0
Cu (NO3) +	0	Fe (SO4) 2-	0
Cu (NO3) 2@	0	Fe+3	0
Cu (OH) 2@	0	Fe2 (OH) 2+4	0
Cu (OH) 3-	0	Fe3 (OH) 4+5	0
Cu (OH) 4-2	0	FeCl+2	0

Table 10-Parameters of Dependent Components (DC, Species)-Cont'd

Species name	Quantity in the system	Species name	Quantity in the system
FeCl2+	0	H3PO3@	0
FeCl3@	0	HPO3-2	0
FeO+	9.68E-14	H2P2O7-2	0
FeO2-	3.59E-13	H2PO4-	8.15E-11
FeO2H@	3.25E-12	H3P2O7-	0
FeOH+2	2.71E-18	H3PO4@	3.10E-16
CO@	0	H4P2O7@	0
CO2@	6.22E-12	HP2O7-3	0
CO3-2	1.64E-13	HPO4-2	1.85E-11

HCO3-	8.64E-11	P2O7-4	0
CH4@	7.19E-12	PO4-3	1.15E-15
CN-	0	HS7O3-	0
HCN@	0	HS6O3-	0
OCN-	0	HS5O3-	0
SCN-	0	HS4O3-	0
ClO-	0	HS3O3-	0
HClO@	0	S7O6-2	0
ClO2-	0	S6O6-2	0
HClO2@	0	H2S2O3@	0
ClO3-	0	HS2O3-	0
ClO4-	0	S2O3-2	0
Cl-	1.00E-10	S5O6-2	0
HCl@	6.06E-19	S4O6-2	0
H2@	3.78E-08	H2S2O4@	0
H2N2O2@	0	HS2O4-	0
HN2O2-	0	S2O4-2	0
N2O2-2	0	S3O6-2	0
HNO2@	0	HS2O5-	0
NO2-	0	HSO3-	0
HNO3@	0	S2O5-2	0
NO3-	0	SO2@	0
N2H5+	0	SO3-2	0
N2H6+2	0	HS2O6-	0
NH3@	8.87E-13	S2O6-2	0
NH4+	7.28E-12	HS2O7-	0
N2@	0	HSO4-	1.78E-18
O2@	0	S2O7-2	0
H2O2@	0	SO3@	0
HO2-	0	SO4-2	1.77E-13
H2PO2-	0	HS2O8-	0
H3PO2@	0	S2O8-2	0
H2PO3-	0	HSO5-	0

Table 10-Parameters of Dependent Components (DC, Species)-Cont'd

Species name	Quantity in the system	Species name	Quantity in the system
S8-2	0	NH3 (g)	6.60E-20
S7-2	0	N2 (g)	0
HS6-	0	O2 (g)	0
S6-2	0	SO2 (g)	0
HS5-	0	H2S (g)	4.86E-14
HS4-	0	S2 (g)	0
HS3-	0	H2O (g)	1.16E-06
S2-2	0	Cu (s)	0

S3-2	0	Chalcopyrite (s)	0.485711
S4-2	0	Cuprite (s)	0
S5-2	0	Tenorite (s)	0
HS2-	0.00E+00	Chalcocite (s)	0.385716
H2S@	2.17E-09	Fe (s)	0
HS-	1.23E-08	FeCO3 (pr) (s)	0
S-2	2.50E-18	Fe2-Ox (s)	0
OH-	2.22E-06	Hematite (s)	0
H+	3.91E-08	Magnetite (s)	0.064286
H2O@	56.5084	Fe(OH)3 (am) (s)	0
CO (g)	0	Fe(OH)3 (mic) (s)	0
CO2 (g)	4.15E-16	Pyrite (s)	0.15491
CH4 (g)	8.60E-15	Pyrrhotite (s)	0
H2 (g)	5.99E-11	Sulfur (s)	0

*Concentration and activity are given for aqueous species in mol/(kgH2O), for other species - in the mole fraction scale.

5-65 °C

State variables:

P(bar)= 1 T= 65 (C) = 338.15 (K) V(cm3)= 1076.1712 Mass(kg)= 1.2,

Min-potential (moles): G(x)= -4906.13299

Aqueous phase:

I(molal)= 3.314e-006 pH= 7.266 pe= -4.757 Eh(V)= -0.3185

Table 11-Parameters of Dependent Components (DC, Species) at 65°C

Species name	Quantity in the system	Species name	Quantity in the system
Cu (NH3) +2	0	Cu+2	0
Cu (NH3) 2 (OH) 2@	0	Cu2 (OH) 2+2	0
Cu (NH3) 2+	2.25E-13	Cu3 (OH) 4+2	0
Cu (NH3) 2+2	0	CuCl+	0
Cu (NH3) 3 (OH) +	3.18E-18	CuCl2@	0
Cu (NH3) 3+2	7.61E-17	CuCl3-	0
Cu (NH3) 4+2	2.95E-10	CuCl4-2	0
Cu2Cl4-2	0	CuH2PO4+	0
Cu3Cl6-3	0	CuO2-2	0
Cu (HCO3) +	0	CuO2H-	0
Cu (HPO4) H2PO4-	0	CuO@	0
Cu (OH) 2-	1.54E-17	CuOH+	0
Cu (OH) @	5.58E-18	Fe (CO3) @	4.46E-15

Cu+	1.09E-15	Fe (HCO3) +	6.65E-15
CuCl2-	0	Fe (HSO4) +	0
CuCl3-2	0	Fe (SO4) @	1.40E-16
CuCl@	0	Fe+2	1.08E-06
CuH2PO4@	0	FeCl+	1.90E-16
Cu (CO3) 2-2	0	FeCl2@	0
Cu (HPO4) (H2PO4	0	FeO2H-	2.96E-11
Cu (HPO4) 2-2	0	FeO@	3.36E-10
Cu (HPO4) @	0	FeOH+	7.79E-08
Cu (NO2) +	0	Fe (HSO4) +2	0
Cu (NO2) 2@	0	Fe (SO4) +	0
Cu (NO3) +	0	Fe (SO4) 2-	0
Cu (NO3) 2@	0	Fe+3	0
Cu (OH) 2@	0	Fe2 (OH) 2+4	0
Cu (OH) 3-	0	Fe3 (OH) 4+5	0
Cu (OH) 4-2	0	FeCl+2	0

Table 11-Parameters of Dependent Components (DC, Species)-Cont'd

Species name	Quantity in the system	Species name	Quantity in the system
FeCl2+	0	H3PO3@	0
FeCl3@	0	HPO3-2	0
FeO+	1.49E-13	H2P2O7-2	0
FeO2-	5.60E-13	H2PO4-	4.95E-11
FeO2H@	5.32E-12	H3P2O7-	0
FeOH+2	4.63E-18	H3PO4@	5.72E-16
CO@	0	H4P2O7@	0
CO2@	8.98E-12	HP2O7-3	0
CO3-2	1.23E-13	HPO4-2	5.05E-11
HCO3-	8.70E-11	P2O7-4	0
CH4@	3.84E-12	PO4-3	7.01E-16
CN-	0	HS7O3-	0
HCN@	0	HS6O3-	0
OCN-	0	HS5O3-	0
SCN-	0	HS4O3-	0
ClO-	0	HS3O3-	0
HClO@	0	S7O6-2	0
ClO2-	0	S6O6-2	0
HClO2@	0	H2S2O3@	0
ClO3-	0	HS2O3-	0
ClO4-	0	S2O3-2	0
Cl-	1.00E-10	S5O6-2	0
HCl@	8.52E-19	S4O6-2	0
H2@	4.71E-08	H2S2O4@	0
H2N2O2@	0	HS2O4-	0

HN2O2-	0	S2O4-2	0
N2O2-2	0	S3O6-2	0
HNO2@	0	HS2O5-	0
NO2-	0	HSO3-	0
HNO3@	0	S2O5-2	0
NO3-	0	SO2@	0
N2H5+	0	SO3-2	0
N2H6+2	0	HS2O6-	0
NH3@	5.59E-13	S2O6-2	0
NH4+	4.38E-12	HS2O7-	7.19E-20
N2@	0	HSO4-	7.65E-18
O2@	0	S2O7-2	0
H2O2@	0	SO3@	0
HO2-	0	SO4-2	4.33E-13
H2PO2-	0	HS2O8-	0
H3PO2@	0	S2O8-2	0
H2PO3-	0	HSO5-	0

Table 11-Parameters of Dependent Components (DC, Species)-Cont'd

Species name	Quantity in the system	Species name	Quantity in the system
S8-2	0	NH3 (g)	5.41E-20
S7-2	0	N2 (g)	0
HS6-	0	O2 (g)	0
S6-2	0	SO2 (g)	0
HS5-	0	H2S (g)	9.17E-14
HS4-	0	S2 (g)	0
HS3-	0	H2O (g)	1.16E-06
S2-2	1.43E-20	Cu (s)	0
S3-2	0	Chalcopyrite (s)	0.485711
S4-2	0	Cuprite (s)	0
S5-2	0	Tenorite (s)	0
HS2-	0.00E+00	Chalcocite (s)	0.385716
H2S@	3.71E-09	Fe (s)	0
HS-	1.65E-08	FeCO3 (pr) (s)	0
S-2	5.31E-18	Fe2-Ox (s)	0
OH-	2.28E-06	Hematite (s)	0
H+	5.55E-08	Magnetite (s)	0.064286
H2O@	56.5084	Fe (OH) 3 (am) (s)	0
CO (g)	0	Fe (OH) 3 (mic) (s)	0
CO2 (g)	6.71E-16	Pyrite (s)	0.15491
CH4 (g)	4.82E-15	Pyrrhotite (s)	0
H2 (g)	7.46E-11	Sulfur (s)	0

*Concentration and activity are given for aqueous species in mol/(kgH2O), for other species - in the mole fraction scale.

6-70°C

State variables:

P(bar)= 1 T= 70 (C) = 343.15 (K) V(cm3)= 1079.123 Mass(kg)= 1.2,

Min-potential (moles): G(x)= -4842.8114

Aqueous phase:

I(molal)= 3.341e-006 pH= 7.164 pe= -4.64 E_h (V)= -0.3153

Table 12-Parameters of Dependent Components (DC, Species) at 70°C

Species name	Quantity in the system	Species name	Quantity in the system
Cu (NH3) +2	0	Cu+2	0
Cu (NH3) 2 (OH) 2@	0	Cu2 (OH) 2+2	0
Cu (NH3) 2+	2.19E-13	Cu3 (OH) 4+2	0
Cu (NH3) 2+2	0	CuCl+	0
Cu (NH3) 3 (OH) +	3.14E-18	CuCl2@	0
Cu (NH3) 3+2	8.21E-17	CuCl3-	0
Cu (NH3) 4+2	2.96E-10	CuCl4-2	0
Cu2Cl4-2	0	CuH2PO4+	0
Cu3Cl6-3	0	CuO2-2	0
Cu (HCO3) +	0	CuO2H-	0
Cu (HPO4) H2PO4-	0	CuO@	0
Cu (OH) 2-	1.52E-17	CuOH+	0
Cu (OH) @	1.24E-17	Fe (CO3) @	3.81E-15
Cu+	1.90E-15	Fe (HCO3) +	6.57E-15
CuCl2-	0	Fe (HSO4) +	0
CuCl3-2	0	Fe (SO4) @	2.81E-16
CuCl@	0	Fe+2	1.08E-06
CuH2PO4@	0	FeCl+	2.01E-16
Cu (CO3) 2-2	0	FeCl2@	0
Cu (HPO4) (H2PO4	0	FeO2H-	2.92E-11
Cu (HPO4) 2-2	0	FeO@	3.72E-10
Cu (HPO4) @	0	FeOH+	8.11E-08
Cu (NO2) +	0	Fe (HSO4) +2	0
Cu (NO2) 2@	0	Fe (SO4) +	0
Cu (NO3) +	0	Fe (SO4) 2-	0
Cu (NO3) 2@	0	Fe+3	0
Cu (OH) 2@	0	Fe2 (OH) 2+4	0
Cu (OH) 3-	0	Fe3 (OH) 4+5	0
Cu (OH) 4-2	0	FeCl+2	0

Table 12-Parameters of Dependent Components (DC, Species)-Cont'd

Species name	Quantity in the system	Species name	Quantity in the system
FeCl ₂ ⁺	0	H ₃ PO ₃ @	0
FeCl ₃ @	0	HPO ₃ - ₂	0
FeO ⁺	2.00E-13	H ₂ P ₂ O ₇ - ₂	0
FeO ₂ ⁻	7.55E-13	H ₂ PO ₄ ⁻	5.10E-11
FeO ₂ H@	7.40E-12	H ₃ P ₂ O ₇ ⁻	0
FeOH ₂ ⁺	6.66E-18	H ₃ PO ₄ @	1.10E-15
CO@	0	H ₄ P ₂ O ₇ @	0
CO ₂ @	1.15E-11	HP ₂ O ₇ - ₃	0
CO ₃ - ₂	9.86E-14	HPO ₄ - ₂	4.90E-11
HCO ₃ ⁻	8.59E-11	P ₂ O ₇ - ₄	0
CH ₄ @	2.46E-12	PO ₄ - ₃	6.20E-16
CN ⁻	0	HS ₇ O ₃ ⁻	0
HCN@	0	HS ₆ O ₃ ⁻	0
OCN ⁻	0	HS ₅ O ₃ ⁻	0
SCN ⁻	0	HS ₄ O ₃ ⁻	0
ClO ⁻	0	HS ₃ O ₃ ⁻	0
HClO@	0	S ₇ O ₆ - ₂	0
ClO ₂ ⁻	0	S ₆ O ₆ - ₂	0
HClO ₂ @	0	H ₂ S ₂ O ₃ @	0
ClO ₃ ⁻	0	HS ₂ O ₃ ⁻	0
ClO ₄ ⁻	0	S ₂ O ₃ - ₂	0
Cl ⁻	1.00E-10	S ₅ O ₆ - ₂	0
HCl@	1.08E-18	S ₄ O ₆ - ₂	0
H ₂ @	5.42E-08	H ₂ S ₂ O ₄ @	0
H ₂ N ₂ O ₂ @	0	HS ₂ O ₄ ⁻	0
HN ₂ O ₂ ⁻	0	S ₂ O ₄ - ₂	0
N ₂ O ₂ - ₂	0	S ₃ O ₆ - ₂	0
HNO ₂ @	0	HS ₂ O ₅ ⁻	0
NO ₂ ⁻	0	HSO ₃ ⁻	2.95E-20
HNO ₃ @	0	S ₂ O ₅ - ₂	0
NO ₃ ⁻	0	SO ₂ @	0
N ₂ H ₅ ⁺	0	SO ₃ - ₂	1.20E-20
N ₂ H ₆ ⁺	0	HS ₂ O ₆ ⁻	0
NH ₃ @	4.04E-13	S ₂ O ₆ - ₂	0
NH ₄ ⁺	3.05E-12	HS ₂ O ₇ ⁻	2.47E-18
N ₂ @	0	HSO ₄ ⁻	2.09E-17
O ₂ @	0	S ₂ O ₇ - ₂	0
H ₂ O ₂ @	0	SO ₃ @	0
HO ₂ ⁻	0	SO ₄ - ₂	7.96E-13
H ₂ PO ₂ ⁻	0	HS ₂ O ₈ ⁻	0
H ₃ PO ₂ @	0	S ₂ O ₈ - ₂	0
H ₂ PO ₃ ⁻	0	HSO ₅ ⁻	0

Table 12-Parameters of Dependent Components (DC, Species)-Cont'd

Species name	Quantity in the system	Species name	Quantity in the system
S8-2	0	NH3 (g)	4.65E-20
S7-2	0	N2 (g)	0
HS6-	0	O2 (g)	0
S6-2	0	SO2 (g)	0
HS5-	0	H2S (g)	1.41E-13
HS4-	0	S2 (g)	0
HS3-	0	H2O (g)	1.16E-06
S2-2	2.49E-20	Cu (s)	0
S3-2	0	Chalcopyrite (s)	0.485711
S4-2	0	Cuprite (s)	0
S5-2	0	Tenorite (s)	0
HS2-	0.00E+00	Chalcocite (s)	0.385716
H2S@	5.25E-09	Fe (s)	0
HS-	1.97E-08	FeCO3 (pr) (s)	0
S-2	8.92E-18	Fe2-Ox (s)	0
OH-	2.30E-06	Hematite (s)	0
H+	6.99E-08	Magnetite (s)	0.064286
H2O@	56.5084	Fe (OH) 3 (am) (s)	0
CO (g)	0	Fe (OH) 3 (mic) (s)	0
CO2 (g)	9.14E-16	Pyrite (s)	0.15491
CH4 (g)	3.16E-15	Pyrrhotite (s)	0
H2 (g)	8.48E-11	Sulfur (s)	0

*Concentration and activity are given for aqueous species in mol/(kgH2O), for other species - in the mole fraction scale.

7-80 °C

State variables:

P(bar)= 1 T= 80 (C) = 353.15 (K) V(cm3)= 1085.5108 Mass(kg)= 1.2,

Min-potential (moles): G(x)= -4721.87066

Aqueous phase:

I(molal)= 3.389e-006 pH= 6.969 pe= -4.417 Eh(V)= -0.3089

Table 13-Parameters of Dependent Components (DC, Species) at 80°C

Species name	Quantity in the system	Species name	Quantity in the system
Cu (NH3) +2	0	Cu+2	0
Cu (NH3) 2 (OH) 2@	0	Cu2 (OH) 2+2	0

Cu (NH3) 2+	2.07E-13	Cu3 (OH) 4+2	0
Cu (NH3) 2+2	0	CuCl+	0
Cu (NH3) 3 (OH) +	3.01E-18	CuCl2@	0
Cu (NH3) 3+2	9.39E-17	CuCl3-	0
Cu (NH3) 4+2	2.98E-10	CuCl4-2	0
Cu2Cl4-2	0	CuH2PO4+	0
Cu3Cl6-3	0	CuO2-2	0
Cu (HCO3) +	0	CuO2H-	0
Cu (HPO4) H2PO4-	0	CuO@	0
Cu (OH) 2-	1.47E-17	CuOH+	0
Cu (OH) @	5.63E-17	Fe (CO3) @	2.71E-15
Cu+	5.47E-15	Fe (HCO3) +	6.22E-15
CuCl2-	0	Fe (HSO4) +	0
CuCl3-2	0	Fe (SO4) @	1.05E-15
CuCl@	0	Fe+2	1.08E-06
CuH2PO4@	0	FeCl+	2.27E-16
Cu (CO3) 2-2	0	FeCl2@	0
Cu (HPO4) (H2PO4	0	FeO2H-	2.95E-11
Cu (HPO4) 2-2	0	FeO@	4.67E-10
Cu (HPO4) @	0	FeOH+	8.77E-08
Cu (NO2) +	0	Fe (HSO4) +2	0
Cu (NO2) 2@	0	Fe (SO4) +	0
Cu (NO3) +	0	Fe (SO4) 2-	0
Cu (NO3) 2@	0	Fe+3	0
Cu (OH) 2@	0	Fe2 (OH) 2+4	0
Cu (OH) 3-	0	Fe3 (OH) 4+5	0
Cu (OH) 4-2	0	FeCl+2	0

Table 13-Parameters of Dependent Components (DC, Species)-Cont'd

Species name	Quantity in the system	Species name	Quantity in the system
FeCl2+	0	H3PO3@	0
FeCl3@	0	HPO3-2	0
FeO+	3.44E-13	H2P2O7-2	0
FeO2-	1.32E-12	H2PO4-	6.55E-11
FeO2H@	1.37E-11	H3P2O7-	0
FeOH+2	1.32E-17	H3PO4@	1.94E-15
CO@	2.52E-20	H4P2O7@	0
CO2@	1.81E-11	HP2O7-3	0
CO3-2	6.16E-14	HPO4-2	3.45E-11
HCO3-	8.08E-11	P2O7-4	0
CH4@	1.02E-12	PO4-3	2.43E-16
CN-	0	HS7O3-	0
HCN@	0	HS6O3-	0
OCN-	0	HS5O3-	0

SCN-	0	HS403-	0
ClO-	0	HS303-	0
HClO@	0	S7O6-2	0
ClO2-	0	S6O6-2	0
HClO2@	0	H2S2O3@	0
ClO3-	0	HS203-	0
ClO4-	0	S2O3-2	0
Cl-	1.00E-10	S5O6-2	0
HCl@	1.73E-18	S4O6-2	0
H2@	7.25E-08	H2S2O4@	0
H2N2O2@	0	HS204-	0
HN2O2-	0	S2O4-2	0
N2O2-2	0	S3O6-2	0
HNO2@	0	HS205-	2.83E-20
NO2-	0	HSO3-	2.11E-19
HNO3@	0	S2O5-2	0
NO3-	0	SO2@	0
N2H5+	0	SO3-2	4.46E-20
N2H6+2	0	HS206-	0
NH3@	2.14E-13	S2O6-2	0
NH4+	1.50E-12	HS207-	2.17E-15
N2@	0	HSO4-	1.44E-16
O2@	0	S2O7-2	0
H2O2@	0	SO3@	0
HO2-	0	SO4-2	2.53E-12
H2PO2-	0	HS208-	0
H3PO2@	0	S2O8-2	0
H2PO3-	0	HSO5-	0

Table 13-Parameters of Dependent Components (DC, Species)-Cont'd

Species name	Quantity in the system	Species name	Quantity in the system
S8-2	0	NH3 (g)	3.45E-20
S7-2	0	N2 (g)	0
HS6-	0	O2 (g)	0
S6-2	0	SO2 (g)	0
HS5-	0	H2S (g)	3.23E-13
HS4-	0	S2 (g)	0
HS3-	0	H2O (g)	1.17E-06
S2-2	7.17E-20	Cu (s)	0
S3-2	0	Chalcopyrite (s)	0.485711
S4-2	0	Cuprite (s)	0
S5-2	0	Tenorite (s)	0
HS2-	0.00E+00	Chalcocite (s)	0.385716
H2S@	1.06E-08	Fe (s)	0

HS-	2.84E-08	FeCO3(pr) (s)	0
S-2	2.41E-17	Fe2-Ox(s)	0
OH-	2.34E-06	Hematite(s)	0
H+	1.09E-07	Magnetite(s)	0.064286
H2O@	56.5084	Fe(OH)3(am) (s)	0
CO(g)	0	Fe(OH)3(mic) (s)	0
CO2(g)	1.61E-15	Pyrite(s)	0.15491
CH4(g)	1.36E-15	Pyrrhotite(s)	0
H2(g)	1.12E-10	Sulfur(s)	0

*Concentration and activity are given for aqueous species in mol/(kgH2O), for other species - in the mole fraction scale.

Currently, there exist data on the chemical composition of the ground water that is the result of analyzing “grab” samples from bore holes. While this procedure is notoriously unreliable, particularly when volatile gases are involved, it does provide good measures of dissolved components provided that precipitation does not occur during the sampling process. Frequently, solid phases will precipitate in response to the loss of volatile gases, and unless the sampling capsule is tightly sealed considerable error may ensue. Given these caveats, as well as the fact that various techniques measure the total concentration of a element (e.g., sulfur as sulfate [21] by oxidizing all sulfur species in the system to SO_4^{2-} with a strong oxidizing agent, such as H_2O_2), we accept the analysis of the concentrations of the ionic species, because they are measured using the normally reliable method of ion chromatography. However, these anions (e.g., Cl^- , Br^- , CO_3^{2-} , etc) are generally not particularly strong activators and hence are of only secondary interest in determining the corrosion behavior of copper. Accordingly, we decided to employ a modern, sophisticated Gibbs Energy Minimization algorithm to predict the composition of the repository environment as a function of temperature and redox condition, with the latter being adjusted by changing the relative concentrations of hydrogen and oxygen in the system. As noted above, after evaluating several codes, we chose GEMS, which was developed in Switzerland by Prof. Dmitrii Kulik. This code is designed specifically to model geochemical systems, contains a large database of compounds, and is in general use in the geochemical community. Prior to using the code to model the repository, we upgraded the database by adding thermodynamic data for various polysulfur species (polysulfides, poly thiosulfates, and polythionates) that had been developed earlier in this program. However, the code became ill-behaved when the data for $S_xO_3^{2-}$, $x = 3 - 7$ was added. Consultation with the code developer, Prof. Dmitrii Kulik at Paul Scherer Institute in Switzerland failed to identify and isolate the problem and, accordingly, it was necessary to remove those species from the database. The reader will recall that these are the very species that, anomalously, do not activate copper. With the code in its present form, we have modeled the repository under both oxic and anoxic conditions with the greatest emphasis being placed on the latter, because the great fraction of the storage time is under anoxic conditions. The most important finding to date is that the concentrations of the polysulfur species (polysulfides, poly thiosulfates, and polythionates) under anoxic conditions are predicted to be very low, but it is still not possible, because of the uncertainty in the calculations, to ascertain with certainty whether these species will activate copper in the repository. However, the point may be moot, because sulfide species (S^{2-} , HS^- , and

H_2S) are predicted to be present in sufficient concentration to activate copper and cause the metal to corrode under simulated repository conditions.

To give reader a better view of the concentrations of species predicted to be present in the global system, we derived the concentration (logarithmic scale) vs. temperature curves (Figure 55). As can be seen, the temperature does not have a major effect on the concentrations of the stable species in the system. Since we are primarily interested in studying the behavior of sulfur-containing compounds in this project, we selected the sulfur-containing species for which we have thermodynamic data and derived concentration versus temperature curves for them.(Figure 56). As one can see, increasing temperature is predicted to have more or less the same effect on all of the species present in the system. In other words, the concentrations of sulfur-containing species increase with increasing temperature with some of species being present at significant concentration only at higher temperatures.($>42^\circ\text{C}$) Figure 57 shows the relative concentration of sulfur containing species in the system. It is clear that HS^- and $H_2S(\text{aq})$ are present at the highest concentrations in the system and the previous calculation of $\log P$ for the $H_2S(\text{aq})$ and S^{2-} revealed that these species can activate copper. Even though the polysulfur species are predicted to be present at very low concentrations (e.g., 10^{-20} M, Tables 7 to 13), S_2^{2-} is predicted to activate copper [$\log(P) = 3-6$ for the prevailing hydrogen pressure (10^{-14} atm) in the repository, as shown in Figure 54. The reader will note that GEMS predicts that the concentrations of the great majority of the polysulfur species are “0”, but given that only minute amounts of these species are required to activate copper in is necessary to explore what “0” actually means. We suspect that it means that the concentration is less than some arbitrarily-chosen value (e.g., 10^{-20} M). Since we do not have access to the source code for GEMS, we are unable to ascertain the exact value of the cut-off or calculated concentrations. Theoretically, since P must be greater than about 10^{30} (Figure 54), and recognizing that the partial pressure of hydrogen is 10^{-14} atm, a concentration of S_2^{2-} , for example, only needs to exceed 10^{-44} M to activate copper. At these extremely low concentrations, however, it is expected that activation will be kinetically limited.

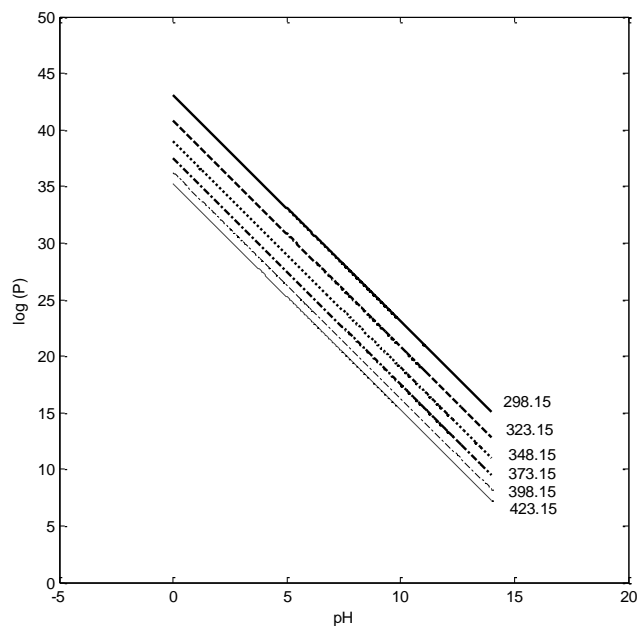


Figure 54: CDD for the reaction of Cu with S_2^{2-} as a function of temperature for conditions that are predicted to exist in the Forsmark repository.

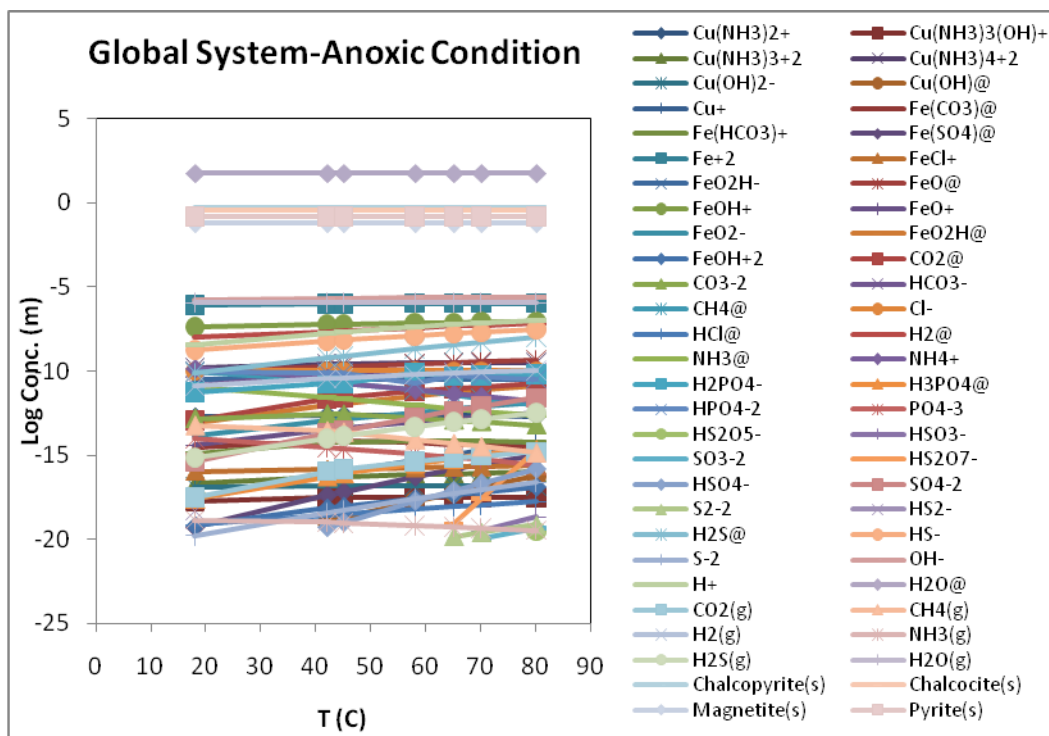


Figure-55: Concentrations of species versus temperature as predicted by GEMS.

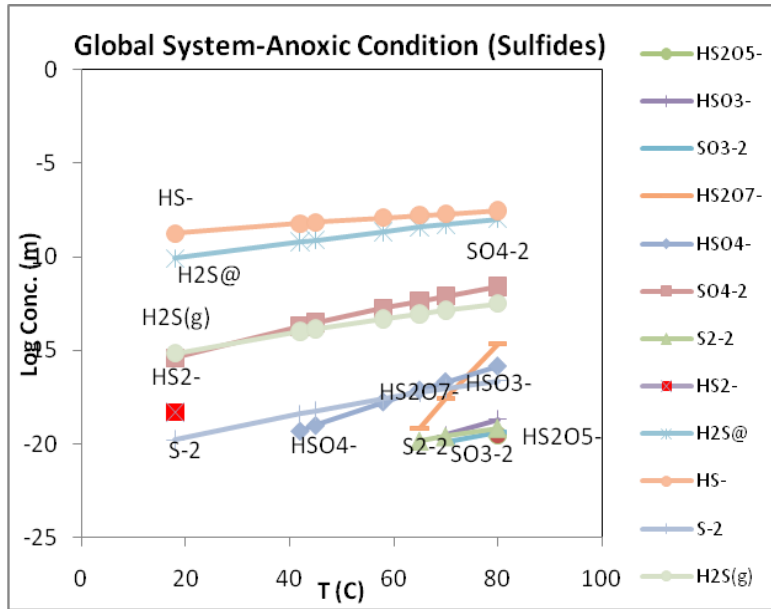


Figure-56: Concentrations of sulfur-containing species as a function of temperature as predicted by GEMS

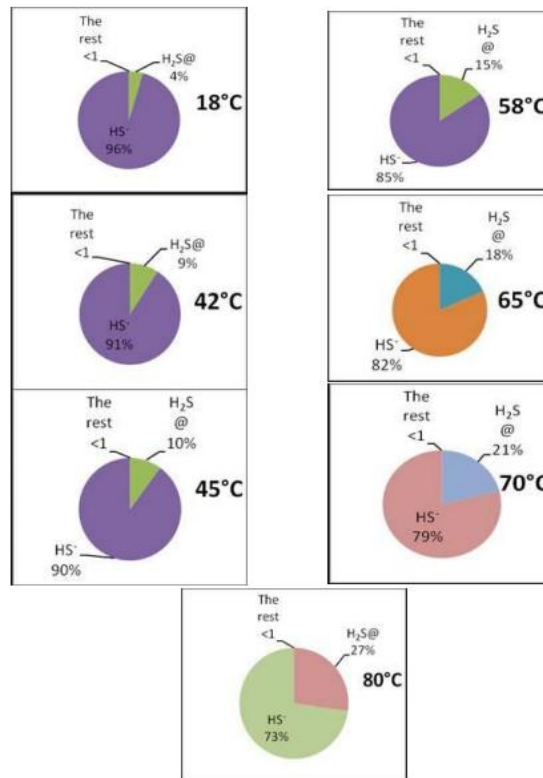


Figure-57: Relative concentrations of sulfur-containing species as predicted by GEMS.

VII. Definition of the Corrosion Evolutionary Path

The ultimate objective of this first-year program was to explore various corrosion issues related to the viability of copper for fabricating canisters for the disposal of High Level Nuclear Waste (HLNW) in a granitic repository of the type envisioned in Sweden. As shown above, copper is not thermodynamically immune in contact with granitic groundwater, primarily because of the presence of strongly activating species, such as sulfide (H_2S , HS^- , and S^{2-}) and possibly other sulfur species, even though the concentrations for many are predicted to be very low. These species activate copper by giving rise to the formation of a reaction product, Cu_2S , at a potential that is significantly more negative than that for the formation of Cu^+ or Cu_2O and also sufficiently negative that hydrogen evolution becomes a viable cathodic reaction in the overall corrosion process. Thus, corrosion is predicted to proceed spontaneously in the anoxic environments that will dominate the storage period. In order to define the corrosive environment more accurately, and to assess how it might change with time, we have performed Gibbs energy minimization speciation calculations at various times during the envisioned storage period (i.e., along the corrosion Evolutionary Path, CEP).

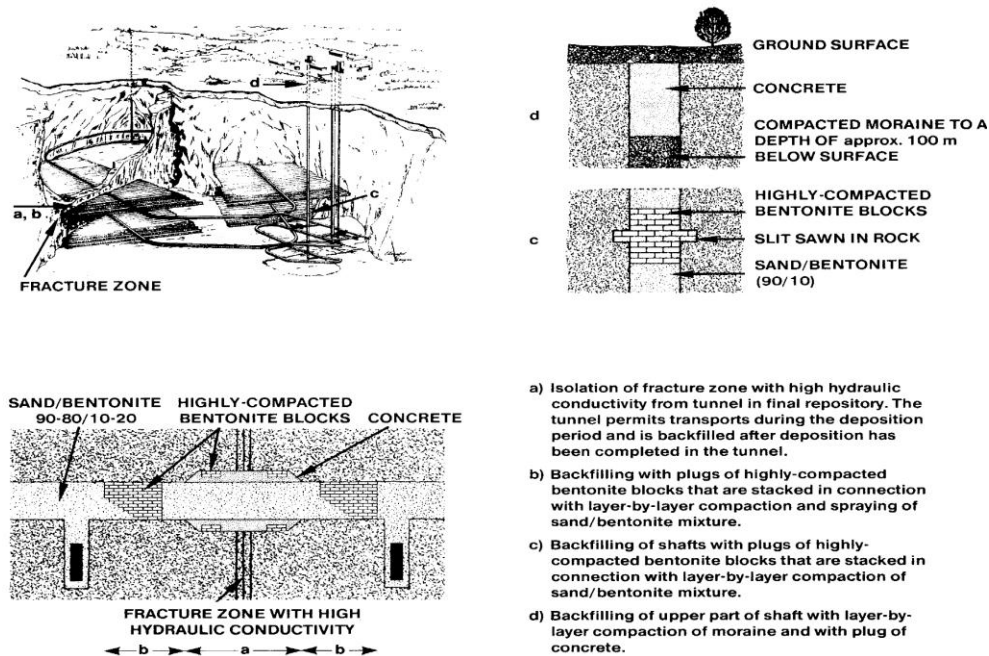


Figure 58: Schematic of the envisioned granitic rock repository for the final storage of spent nuclear fuel in Sweden.[35]

Although a detailed discussion of the KBS-3 plan is beyond the scope of this study, it is advantageous to briefly mention some aspects of the plan to help place the present study in perspective. The KBS-3 plan calls for the emplacement of the copper HLNW canisters in the granitic repository as shown schematically in Figure 58. The canisters, which are 4.8 m long with a diameter of 1.05 m, are located in boreholes in the floors of the disposal tunnels, some 500 m below the surface (Figure 59). The canisters are held in place by highly compacted bentonite, which, when fully hydrated, has an extremely low hydraulic conductivity (10^{-14} to 10^{-11} m/s) and imparts very low diffusivities to ionic species (10^{-11} to 10^{-12} m²/s). When fully

hydrated, the bentonite is expected to exert an external pressure on the canister of about 15 MPa. Thus the bentonite buffer represents a considerable barrier to the flow of groundwater and the transport of ions.

The granitic groundwater that is expected to inundate the repository and eventually contact the copper canisters has a typical composition as indicated in Table 14.

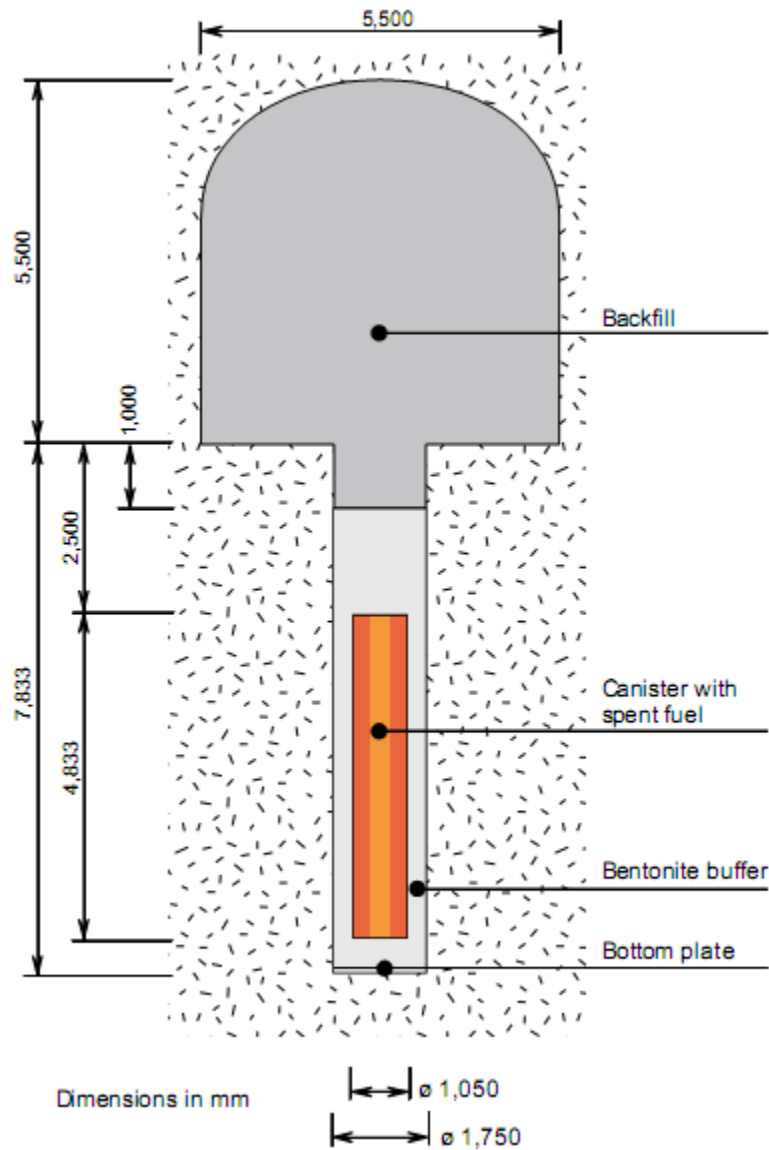


Figure 59: Schematic of an emplaced canister in the the Swedish envisioned granitic rock repository, according to the KBS-3 plan for the isolation of High Level Nuclear Waste. ([35]).

Table 14: Composition of deep granitic ground water. ([35])

	Forsmark	Laxemar	Äspö	Finnisjön	Gideå	Grimsel: inter-acted glacial meltwater	"Most saline" groundwater at Laxemar	"Most saline" groundwater at Olkiluoto	Cement pore water	Baltic seawater	Ocean water	Maximum salinity from glacial upconing
pH	7.2	7.9	7.7	7.9	9.3	9.6	7.9	7.0	12.5	7.9	8.15	7.9
Na	0.089	0.034	0.091	0.012	0.0046	0.00069	0.349	0.415	0.002	0.089	0.469	0.25
Ca	0.023	0.0058	0.047	0.0035	0.00052	0.00014	0.464	0.449	0.018	0.0024	0.0103	0.27
Mg	0.0093	0.00044	0.0017	0.0007	0.000045	0.0000006	0.0001	0.0053	< 0.0001	0.010	0.053	0.0001
K	0.0009	0.00014	0.0002	0.00005	0.00005	0.000005	0.0007	0.0007	0.0057	0.002	0.01	0.0005
Fe	33·10 ⁻⁶	8·10 ⁻⁶	4·10 ⁻⁶	32·10 ⁻⁶	0.9·10 ⁻⁶	0.003·10 ⁻⁶	8·10 ⁻⁶	60·10 ⁻⁶	≤10·10 ⁻⁶	0.3·10 ⁻⁶	0.04·10 ⁻⁶	2·10 ⁻⁶
HCO ₃ ⁻	0.0022	0.0031	0.00016	0.0046	0.00023	0.00045	0.00010	0.00014	≈ 0	0.0016	0.0021	0.00015
Cl ⁻	0.153	0.039	0.181	0.0157	0.0050	0.00016	1.283	1.275	≈ 0	0.106	0.546	0.82
SO ₄ ²⁻	0.0052	0.0013	0.0058	0.00051	0.000001	0.00006	0.009	0.00009	≈ 0	0.0051	0.0282	0.01
HS ⁻	≈ 0	3·10 ⁻⁷	5·10 ⁻⁶	-	< 3·10 ⁻⁷	-	< 3·10 ⁻⁷	< 1.6·10 ⁻⁷	≈ 0	-	-	< 3·10 ⁻⁷
O ₂ fugacity (bar)	<< 10 ⁻²⁰	<< 10 ⁻²⁰	<< 10 ⁻²⁰	<< 10 ⁻²⁰	<< 10 ⁻²⁰	< 10 ^{-0.17} 4)	<< 10 ⁻²⁰	<< 10 ⁻²⁰	≈ 10 ⁻²⁰	10 ^{-0.7}	10 ^{-0.7}	<< 10 ⁻²⁰
Ionic strength (kmol/m ³)	0.19	0.053	0.24	0.025	0.006	0.0013	1.75	1.76	0.057	0.13	0.65	1.09
TDS (g/L)	9.32	2.78	11.1	1.33	0.33	0.08	73.7	73.4	1.63	6.81	35.1	47.2
Reference	1	2	3	3	3	4	5	6	7	2	8	2
Notes	Borehole KFM02A; 512 m depth	Borehole KLX03; 380 m depth	Repository depth	Repository depth	Repository depth	O ₂ fugacity only to illustrate effect	Depth ≈ 1,500 m	See also /Pitkänen 1999; depth = 863 m; sample 42		Sampled at Simpevarp		Laxemar water at 1,350 m

4) Oxygen fugacity for glacial conditions: The maximum content is 1.4·10⁻³ M for glacial meltwater at 0°C. The corresponding maximum fugacity at 0°C is 0.67 bar /Ahonen and Vieno 1994/. In Grimself the O₂ content is less than 3·10⁻⁸ M.

References: 1 = /SKB 2005e/, 2 = /SKB 2006g/, 3 = /Laaksoharju et al. 1998/, 4 = /Hoehn et al. 1998/, 5 = /Laaksoharju et al. 1995/, 6 = /Pitkänen et al. 2004/, 7 = /Engkvist et al. 1996, Berner 1987/, 8 = /Stumm and Morgan 1996/.

The temperature is predicted to evolve over 10,000 years as indicated in Figure 60. Of particular interest, in this analysis, is the temperature at the buffer inner surface, representing the interface between the copper and the environment. The temperature is predicted to increase over the first ten to twenty years of storage, corresponding to the placement of more canisters and the loss of convective air cooling as the tunnels are backfilled with a sand/bentonite mixture. At longer times, the temperature decreases as the various radioactive isotopes in the waste decay, such that after 10,000 years the temperature is predicted to be near ambient. In performing the GEMS calculations, we assume that the bentonite buffer is fully saturated with groundwater and that the conditions are anoxic. Attempts to perform Gibbs energy minimization for oxic conditions, where a significant concentration of oxygen was present, were unsuccessful as all of the pyrite was predicted to be consumed and the predicted pH was excessively low, corresponding to the oxidation of sulfur to sulfuric acid.

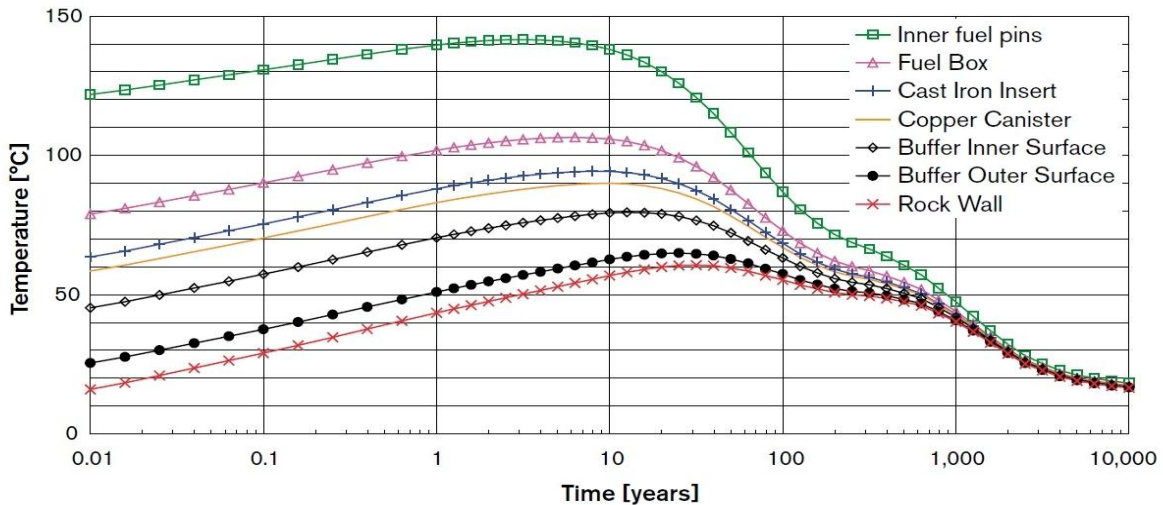


Figure 60: The thermal evolution for a number of locations in a canister at mid-height in a granitic repository. ([34]).

The composition of the granitic groundwater shown in Table 14 is predicted to be slightly alkaline pH ($pH = 7 - 9$) and to result in a redox potential (E_h) of 0 to $-0.45 V_{she}$, indicating a moderately reducing environment. Consequently, iron species in solution are mostly in the form of Fe^{2+} . Other major species are bicarbonate ion and Ca^{2+} . Sodium ion (not listed) and chloride ion are also present at significant concentrations.

The GEMS output for the four times probed along the CEP are presented in Tables 15, 16, 17, and 18 for temperatures of 80 °C, 64 °C, 42 °C, and 18 °C, respectively. Again, the predicted concentrations of the polysulfur species are very low or non-existent (the exception being HS_2^-), so that these species can probably be discounted as representing a threat to the

integrity of the copper canisters. Comparison with previously published data for the Forsmark repository shows good agreement.

1-80 °C (10 years after placement)

State variables:

$P(\text{bar})= 1$ $T= 80$ (C) = 353.15 (K) $V(\text{cm}^3)= 1085.5108$ $\text{Mass}(\text{kg})= 1.2,$

Min-potential (moles): $G(x)= -4721.87066$

Aqueous phase:

$I(\text{molal})= 3.389\text{e-}006$ $pH= 6.969$ $pe= -4.417$ $E_h(\text{V})= -0.3089$

Table 15-Parameters of Dependent Components (DC, Species) at 80°C

Species name	Quantity in the system	Species name	Quantity in the system
Cu (NH3) +2	0	Cu+2	0
Cu (NH3) 2 (OH) 2@	0	Cu2 (OH) 2+2	0
Cu (NH3) 2+	2.07E-13	Cu3 (OH) 4+2	0
Cu (NH3) 2+2	0	CuCl+	0
Cu (NH3) 3 (OH) +	3.01E-18	CuCl2@	0
Cu (NH3) 3+2	9.39E-17	CuCl3-	0
Cu (NH3) 4+2	2.98E-10	CuCl4-2	0
Cu2Cl4-2	0	CuH2PO4+	0
Cu3Cl6-3	0	CuO2-2	0
Cu (HCO3) +	0	CuO2H-	0
Cu (HPO4) H2PO4-	0	CuO@	0
Cu (OH) 2-	1.47E-17	CuOH+	0
Cu (OH) @	5.63E-17	Fe (CO3) @	2.71E-15
Cu+	5.47E-15	Fe (HCO3) +	6.22E-15
CuCl2-	0	Fe (HSO4) +	0
CuCl3-2	0	Fe (SO4) @	1.05E-15
CuCl@	0	Fe+2	1.08E-06
CuH2PO4@	0	FeCl+	2.27E-16
Cu (CO3) 2-2	0	FeCl2@	0
Cu (HPO4) (H2PO4	0	FeO2H-	2.95E-11
Cu (HPO4) 2-2	0	FeO@	4.67E-10
Cu (HPO4) @	0	FeOH+	8.77E-08
Cu (NO2) +	0	Fe (HSO4) +2	0
Cu (NO2) 2@	0	Fe (SO4) +	0
Cu (NO3) +	0	Fe (SO4) 2-	0
Cu (NO3) 2@	0	Fe+3	0
Cu (OH) 2@	0	Fe2 (OH) 2+4	0
Cu (OH) 3-	0	Fe3 (OH) 4+5	0
Cu (OH) 4-2	0	FeCl+2	0

Table 15-Parameters of Dependent Components (DC, Species)-Cont'd

Species name	Quantity in the system	Species name	Quantity in the system
FeCl ₂ ⁺	0	H ₃ PO ₃ @	0
FeCl ₃ @	0	HPO ₃ - ₂	0
FeO ⁺	3.44E-13	H ₂ P ₂ O ₇ - ₂	0
FeO ₂ ⁻	1.32E-12	H ₂ PO ₄ ⁻	6.55E-11
FeO ₂ H@	1.37E-11	H ₃ P ₂ O ₇ -	0
FeOH ₂ ⁺	1.32E-17	H ₃ PO ₄ @	1.94E-15
CO@	2.52E-20	H ₄ P ₂ O ₇ @	0
CO ₂ @	1.81E-11	HP ₂ O ₇ - ₃	0
CO ₃ - ₂	6.16E-14	HPO ₄ - ₂	3.45E-11
HCO ₃ ⁻	8.08E-11	P ₂ O ₇ - ₄	0
CH ₄ @	1.02E-12	PO ₄ - ₃	2.43E-16
CN ⁻	0	HS ₇ O ₃ -	0
HCN@	0	HS ₆ O ₃ -	0
OCN ⁻	0	HS ₅ O ₃ -	0
SCN ⁻	0	HS ₄ O ₃ -	0
ClO ⁻	0	HS ₃ O ₃ -	0
HClO@	0	S ₇ O ₆ - ₂	0
ClO ₂ ⁻	0	S ₆ O ₆ - ₂	0
HClO ₂ @	0	H ₂ S ₂ O ₃ @	0
ClO ₃ ⁻	0	HS ₂ O ₃ -	0
ClO ₄ ⁻	0	S ₂ O ₃ - ₂	0
Cl ⁻	1.00E-10	S ₅ O ₆ - ₂	0
HCl@	1.73E-18	S ₄ O ₆ - ₂	0
H ₂ @	7.25E-08	H ₂ S ₂ O ₄ @	0
H ₂ N ₂ O ₂ @	0	HS ₂ O ₄ -	0
HN ₂ O ₂ ⁻	0	S ₂ O ₄ - ₂	0
N ₂ O ₂ - ₂	0	S ₃ O ₆ - ₂	0
HNO ₂ @	0	HS ₂ O ₅ -	2.83E-20
NO ₂ ⁻	0	HSO ₃ -	2.11E-19
HNO ₃ @	0	S ₂ O ₅ - ₂	0
NO ₃ ⁻	0	SO ₂ @	0
N ₂ H ₅ ⁺	0	SO ₃ - ₂	4.46E-20
N ₂ H ₆ ⁺ ₂	0	HS ₂ O ₆ -	0
NH ₃ @	2.14E-13	S ₂ O ₆ - ₂	0
NH ₄ ⁺	1.50E-12	HS ₂ O ₇ -	2.17E-15
N ₂ @	0	HSO ₄ -	1.44E-16
O ₂ @	0	S ₂ O ₇ - ₂	0
H ₂ O ₂ @	0	SO ₃ @	0
HO ₂ ⁻	0	SO ₄ - ₂	2.53E-12
H ₂ PO ₂ ⁻	0	HS ₂ O ₈ -	0
H ₃ PO ₂ @	0	S ₂ O ₈ - ₂	0
H ₂ PO ₃ ⁻	0	HSO ₅ -	0

Table 15-Parameters of Dependent Components (DC, Species)-Cont'd

Species name	Quantity in the system	Species name	Quantity in the system
S8-2	0	NH3 (g)	3.45E-20
S7-2	0	N2 (g)	0
HS6-	0	O2 (g)	0
S6-2	0	SO2 (g)	0
HS5-	0	H2S (g)	3.23E-13
HS4-	0	S2 (g)	0
HS3-	0	H2O (g)	1.17E-06
S2-2	7.17E-20	Cu (s)	0
S3-2	0	Chalcopyrite (s)	0.485711
S4-2	0	Cuprite (s)	0
S5-2	0	Tenorite (s)	0
HS2-	0	Chalcocite (s)	0.385716
H2S@	1.06E-08	Fe (s)	0
HS-	2.84E-08	FeCO3 (pr) (s)	0
S-2	2.41E-17	Fe2-Ox (s)	0
OH-	2.34E-06	Hematite (s)	0
H+	1.09E-07	Magnetite (s)	0.064286
H2O@	56.5084	Fe(OH)3 (am) (s)	0
CO (g)	0	Fe(OH)3 (mic) (s)	0
CO2 (g)	1.61E-15	Pyrite (s)	0.15491
CH4 (g)	1.36E-15	Pyrrhotite (s)	0
H2 (g)	1.12E-10	Sulfur (s)	0

*Concentration and activity are given for aqueous species in mol/(kgH2O), for other species - in the mole fraction scale.

2-65 °C (100 years after placement)

State variables:

P(bar)= 1 T= 65 (C) = 338.15 (K) V(cm3)= 1076.1712 Mass(kg)= 1.2,

Min-potential (moles): G(x)= -4906.13299

Aqueous phase:

I(molal)= 3.314e-006 pH= 7.266 pe= -4.757 Eh(V)= -0.3185

Table 16-Parameters of Dependent Components (DC, Species) at 65°C

Species name	Quantity in the system	Species name	Quantity in the system
Cu (NH3) +2	0	Cu+2	0
Cu (NH3) 2 (OH) 2@	0	Cu2 (OH) 2+2	0
Cu (NH3) 2+	2.25E-13	Cu3 (OH) 4+2	0
Cu (NH3) 2+2	0	CuCl+	0
Cu (NH3) 3 (OH) +	3.18E-18	CuCl2@	0

Cu (NH3) 3+2	7.61E-17	CuCl3-	0
Cu (NH3) 4+2	2.95E-10	CuCl4-2	0
Cu2Cl4-2	0	CuH2PO4+	0
Cu3Cl6-3	0	CuO2-2	0
Cu (HCO3) +	0	CuO2H-	0
Cu (HPO4) H2PO4-	0	CuO@	0
Cu (OH) 2-	1.54E-17	CuOH+	0
Cu (OH) @	5.58E-18	Fe (CO3) @	4.46E-15
Cu+	1.09E-15	Fe (HCO3) +	6.65E-15
CuCl2-	0	Fe (HSO4) +	0
CuCl3-2	0	Fe (SO4) @	1.40E-16
CuCl@	0	Fe+2	1.08E-06
CuH2PO4@	0	FeCl+	1.90E-16
Cu (CO3) 2-2	0	FeCl2@	0
Cu (HPO4) (H2PO4	0	FeO2H-	2.96E-11
Cu (HPO4) 2-2	0	FeO@	3.36E-10
Cu (HPO4) @	0	FeOH+	7.79E-08
Cu (NO2) +	0	Fe (HSO4) +2	0
Cu (NO2) 2@	0	Fe (SO4) +	0
Cu (NO3) +	0	Fe (SO4) 2-	0
Cu (NO3) 2@	0	Fe+3	0
Cu (OH) 2@	0	Fe2 (OH) 2+4	0
Cu (OH) 3-	0	Fe3 (OH) 4+5	0
Cu (OH) 4-2	0	FeCl+2	0

Table 16-Parameters of Dependent Components (DC, Species)-Cont'd

Species name	Quantity in the system	Species name	Quantity in the system
FeCl2+	0	H3PO3@	0
FeCl3@	0	HPO3-2	0
FeO+	1.49E-13	H2P2O7-2	0
FeO2-	5.60E-13	H2PO4-	4.95E-11
FeO2H@	5.32E-12	H3P2O7-	0
FeOH+2	4.63E-18	H3PO4@	5.72E-16
CO@	0	H4P2O7@	0
CO2@	8.98E-12	HP2O7-3	0
CO3-2	1.23E-13	HPO4-2	5.05E-11
HCO3-	8.70E-11	P2O7-4	0
CH4@	3.84E-12	PO4-3	7.01E-16
CN-	0	HS7O3-	0
HCN@	0	HS6O3-	0
OCN-	0	HS5O3-	0
SCN-	0	HS4O3-	0
ClO-	0	HS3O3-	0
HClO@	0	S7O6-2	0

C1O2-	0	S6O6-2	0
HC1O2@	0	H2S2O3@	0
C1O3-	0	HS2O3-	0
C1O4-	0	S2O3-2	0
C1-	1.00E-10	S5O6-2	0
HCl@	8.52E-19	S4O6-2	0
H2@	4.71E-08	H2S2O4@	0
H2N2O2@	0	HS2O4-	0
HN2O2-	0	S2O4-2	0
N2O2-2	0	S3O6-2	0
HNO2@	0	HS2O5-	0
NO2-	0	HSO3-	0
HNO3@	0	S2O5-2	0
NO3-	0	SO2@	0
N2H5+	0	SO3-2	0
N2H6+2	0	HS2O6-	0
NH3@	5.59E-13	S2O6-2	0
NH4+	4.38E-12	HS2O7-	7.19E-20
N2@	0	HSO4-	7.65E-18
O2@	0	S2O7-2	0
H2O2@	0	SO3@	0
HO2-	0	SO4-2	4.33E-13
H2PO2-	0	HS2O8-	0
H3PO2@	0	S2O8-2	0
H2PO3-	0	HSO5-	0

Table 16-Parameters of Dependent Components (DC, Species)-Cont'd

Species name	Quantity in the system	Species name	Quantity in the system
S8-2	0	NH3 (g)	5.41E-20
S7-2	0	N2 (g)	0
HS6-	0	O2 (g)	0
S6-2	0	SO2 (g)	0
HS5-	0	H2S (g)	9.17E-14
HS4-	0	S2 (g)	0
HS3-	0	H2O (g)	1.16E-06
S2-2	1.43E-20	Cu (s)	0
S3-2	0	Chalcopyrite (s)	0.485711
S4-2	0	Cuprite (s)	0
S5-2	0	Tenorite (s)	0
HS2-	0	Chalcocite (s)	0.385716
H2S@	3.71E-09	Fe (s)	0
HS-	1.65E-08	FeCO3 (pr) (s)	0
S-2	5.31E-18	Fe2-Ox (s)	0
OH-	2.28E-06	Hematite (s)	0

H+	5.55E-08	Magnetite (s)	0.064286
H2O@	56.5084	Fe (OH) 3 (am) (s)	0
CO (g)	0	Fe (OH) 3 (mic) (s)	0
CO2 (g)	6.71E-16	Pyrite (s)	0.15491
CH4 (g)	4.82E-15	Pyrrhotite (s)	0
H2 (g)	7.46E-11	Sulfur (s)	0

*Concentration and activity are given for aqueous species in mol/(kgH2O), for other species - in the mole fraction scale.

3-42C (1,000 years after placement)

State variables:

P(bar)= 1 T= 42 (C) = 315.15 (K) V(cm3)= 1064.789 Mass(kg)= 1.2,

Min-potential (moles): G(x)= -5224.90413

Aqueous phase:

I(molal)= 2.994e-006 pH= 7.792 pe= -5.348 Eh(V)= -0.3338

Table 17-Parameters of Dependent Components (DC, Species) at 42°C

Species name	Quantity in the system	Species name	Quantity in the system
Cu (NH3) +2	0	Cu+2	0
Cu (NH3) 2 (OH) 2@	0	Cu2 (OH) 2+2	0
Cu (NH3) 2+	2.41E-13	Cu3 (OH) 4+2	0
Cu (NH3) 2+2	0	CuCl+	0
Cu (NH3) 3 (OH) +	3.07E-18	CuCl2@	0
Cu (NH3) 3+2	4.87E-17	CuCl3-	0
Cu (NH3) 4+2	2.61E-10	CuCl4-2	0
Cu2Cl4-2	0	CuH2PO4+	0
Cu3Cl6-3	0	CuO2-2	0
Cu (HCO3) +	0	CuO2H-	0
Cu (HPO4) H2PO4-	0	CuO@	0
Cu (OH) 2-	1.49E-17	CuOH+	0
Cu (OH) @	9.92E-20	Fe (CO3) @	7.00E-15
Cu+	6.84E-17	Fe (HCO3) +	5.49E-15
CuCl2-	0	Fe (HSO4) +	0
CuCl3-2	0	Fe (SO4) @	4.09E-18
CuCl@	0	Fe+2	9.90E-07
CuH2PO4@	0	FeCl+	1.44E-16
Cu (CO3) 2-2	0	FeCl2@	0
Cu (HPO4) (H2PO4	0	FeO2H-	2.94E-11
Cu (HPO4) 2-2	0	FeO@	1.81E-10

Cu (HPO4) @	0	FeOH+	6.09E-08
Cu (NO2) +	0	Fe (HSO4) +2	0
Cu (NO2) 2@	0	Fe (SO4) +	0
Cu (NO3) +	0	Fe (SO4) 2-	0
Cu (NO3) 2@	0	Fe+3	0
Cu (OH) 2@	0	Fe2 (OH) 2+4	0
Cu (OH) 3-	0	Fe3 (OH) 4+5	0
Cu (OH) 4-2	0	FeCl+2	0

Table 17-Parameters of Dependent Components (DC, Species)-Cont'd

Species name	Quantity in the system	Species name	Quantity in the system
FeCl2+	0	H3PO3@	0
FeCl3@	0	HPO3-2	0
FeO+	3.17E-14	H2P2O7-2	0
FeO2-	1.16E-13	H2PO4-	1.72E-11
FeO2H@	9.05E-13	H3P2O7-	0
FeOH+2	7.01E-19	H3PO4@	5.45E-17
CO@	0	H4P2O7@	0
CO2@	2.17E-12	HP2O7-3	0
CO3-2	2.66E-13	HPO4-2	8.28E-11
HCO3-	7.09E-11	P2O7-4	0
CH4@	2.66E-11	PO4-3	2.89E-15
CN-	0	HS7O3-	0
HCN@	0	HS6O3-	0
OCN-	0	HS5O3-	0
SCN-	0	HS4O3-	0
ClO-	0	HS3O3-	0
HClO@	0	S7O6-2	0
ClO2-	0	S6O6-2	0
HClO2@	0	H2S2O3@	0
ClO3-	0	HS2O3-	0
ClO4-	0	S2O3-2	0
Cl-	1.00E-10	S5O6-2	0
HCl@	2.71E-19	S4O6-2	0
H2@	2.28E-08	H2S2O4@	0
H2N2O2@	0	HS2O4-	0
HN2O2-	0	S2O4-2	0
N2O2-2	0	S3O6-2	0
HNO2@	0	HS2O5-	0
NO2-	0	HSO3-	0
HNO3@	0	S2O5-2	0
NO3-	0	SO2@	0
N2H5+	0	SO3-2	0
N2H6+2	0	HS2O6-	0

NH3@	2.61E-12	S2O6-2	0
NH4+	3.66E-11	HS2O7-	0
N2@	0	HSO4-	4.94E-20
O2@	0	S2O7-2	0
H2O2@	0	SO3@	0
HO2-	0	SO4-2	1.92E-14
H2PO2-	0	HS2O8-	0
H3PO2@	0	S2O8-2	0
H2PO3-	0	HSO5-	0

Table 17-Parameters of Dependent Components (DC, Species)-Cont'd

Species name	Quantity in the system	Species name	Quantity in the system
S8-2	0	NH3 (g)	1.02E-19
S7-2	0	N2 (g)	0
HS6-	0	O2 (g)	0
S6-2	0	SO2 (g)	0
HS5-	0	H2S (g)	1.03E-14
HS4-	0	S2 (g)	0
HS3-	0	H2O (g)	1.14E-06
S2-2	0	Cu (s)	0
S3-2	0	Chalcopyrite (s)	0.485711
S4-2	0	Cuprite (s)	0
S5-2	0	Tenorite (s)	0
HS2-	0	Chalcocite (s)	0.385716
H2S@	6.06E-10	Fe (s)	0
HS-	6.00E-09	FeCO3 (pr) (s)	0
S-2	3.93E-19	Fe2-Ox (s)	0
OH-	2.05E-06	Hematite (s)	0
H+	1.65E-08	Magnetite (s)	0.064286
H2O@	56.5084	Fe(OH)3 (am) (s)	0
CO (g)	0	Fe(OH)3 (mic) (s)	0
CO2 (g)	1.08E-16	Pyrite (s)	0.15491
CH4 (g)	2.89E-14	Pyrrhotite (s)	0
H2 (g)	3.51E-11	Sulfur (s)	0

*Concentration and activity are given for aqueous species in mol/(kgH2O), for other species - in the mole fraction scale.

5-18C (10,000 years after placement)

State variables:

P(bar)= 1 T= 18 (C) = 291.15 (K) V(cm3)= 1057.3875 Mass(kg)= 1.2,

Min-potential (moles): G(x)= -5614.45712

Aqueous phase:

$I(\text{molal})= 2.437\text{e-}006$ $pH= 8.451$ $pe= -6.076$ $E_h(\text{V})= -0.3503$

Table 18-Parameters of Dependent Components (DC, Species) at 18°C

Species name	Quantity in the system	Species name	Quantity in the system
Cu (NH3) +2	0	Cu+2	0
Cu (NH3) 2 (OH) 2@	0	Cu2 (OH) 2+2	0
Cu (NH3) 2+	1.80E-13	Cu3 (OH) 4+2	0
Cu (NH3) 2+2	0	CuCl+	0
Cu (NH3) 3 (OH) +	1.83E-18	CuCl2@	0
Cu (NH3) 3+2	1.94E-17	CuCl3-	0
Cu (NH3) 4+2	1.47E-10	CuCl4-2	0
Cu2Cl4-2	0	CuH2PO4+	0
Cu3Cl6-3	0	CuO2-2	0
Cu (HCO3) +	0	CuO2H-	0
Cu (HPO4) H2PO4-	0	CuO@	0
Cu (OH) 2-	1.19E-17	CuOH+	0
Cu (OH) @	0	Fe (CO3) @	2.75E-15
Cu+	2.36E-18	Fe (HCO3) +	1.18E-15
CuCl2-	0	Fe (HSO4) +	0
CuCl3-2	0	Fe (SO4) @	5.05E-20
CuCl@	0	Fe+2	8.11E-07
CuH2PO4@	0	FeCl+	1.09E-16
Cu (CO3) 2-2	0	FeCl2@	0
Cu (HPO4) (H2PO4	0	FeO2H-	3.37E-11
Cu (HPO4) 2-2	0	FeO@	9.28E-11
Cu (HPO4) @	0	FeOH+	4.33E-08
Cu (NO2) +	0	Fe (HSO4) +2	0
Cu (NO2) 2@	0	Fe (SO4) +	0
Cu (NO3) +	0	Fe (SO4) 2-	0
Cu (NO3) 2@	0	Fe+3	0
Cu (OH) 2@	0	Fe2 (OH) 2+4	0
Cu (OH) 3-	0	Fe3 (OH) 4+5	0
Cu (OH) 4-2	0	FeCl+2	0

Table 18-Parameters of Dependent Components (DC, Species)-Cont'd

Species name	Quantity in the system	Species name	Quantity in the system
FeCl2+	0	H3PO3@	0
FeCl3@	0	HPO3-2	0
FeO+	4.02E-15	H2P2O7-2	0
FeO2-	1.47E-14	H2PO4-	5.71E-12
FeO2H@	8.13E-14	H3P2O7-	0
FeOH+2	6.24E-20	H3PO4@	2.59E-18

CO@	0	H4P2O7@	0
CO2@	1.16E-13	HP2O7-3	0
CO3-2	1.49E-13	HPO4-2	9.43E-11
HCO3-	1.32E-11	P2O7-4	0
CH4@	8.65E-11	PO4-3	1.03E-14
CN-	0	HS7O3-	0
HCN@	0	HS6O3-	0
OCN-	0	HS5O3-	0
SCN-	0	HS4O3-	0
ClO-	0	HS3O3-	0
HClO@	0	S7O6-2	0
ClO2-	0	S6O6-2	0
HClO2@	0	H2S2O3@	0
ClO3-	0	HS2O3-	0
ClO4-	0	S2O3-2	0
Cl-	1.00E-10	S5O6-2	0
HCl@	7.58E-20	S4O6-2	0
H2@	1.03E-08	H2S2O4@	0
H2N2O2@	0	HS2O4-	0
HN2O2-	0	S2O4-2	0
N2O2-2	0	S3O6-2	0
HNO2@	0	HS2O5-	0
NO2-	0	HSO3-	0
HNO3@	0	S2O5-2	0
NO3-	0	SO2@	0
N2H5+	0	SO3-2	0
N2H6+2	0	HS2O6-	0
NH3@	1.05E-11	S2O6-2	0
NH4+	1.42E-10	HS2O7-	0
N2@	0	HSO4-	0
O2@	0	S2O7-2	0
H2O2@	0	SO3@	0
HO2-	0	SO4-2	3.84E-16
H2PO2-	0	HS2O8-	0
H3PO2@	0	S2O8-2	0
H2PO3-	0	HSO5-	0

Table 18-Parameters of Dependent Components (DC, Species)-Cont'd

Species name	Quantity in the system	Species name	Quantity in the system
S8-2	0	NH3 (g)	1.40E-19
S7-2	0	N2 (g)	0
HS6-	0	O2 (g)	0
S6-2	0	SO2 (g)	0
HS5-	0	H2S (g)	7.02E-16

HS4-	0	S2 (g)	0
HS3-	0	H2O (g)	1.13E-06
S2-2	0	Cu (s)	0
S3-2	0	Chalcopyrite (s)	0.485712
S4-2	0	Cuprite (s)	0
S5-2	0	Tenorite (s)	0
HS2-	4.80E-19	Chalcocite (s)	0.385716
H2S@	8.10E-11	Fe (s)	0
HS-	1.76E-09	FeCO3 (pr) (s)	0
S-2	1.65E-20	Fe2-Ox (s)	0
OH-	1.67E-06	Hematite (s)	0
H+	3.71E-09	Magnetite (s)	0.064286
H2O@	56.5084	Fe (OH) 3 (am) (s)	0
CO (g)	0	Fe (OH) 3 (mic) (s)	0
CO2 (g)	3.07E-18	Pyrite (s)	0.154909
CH4 (g)	6.02E-14	Pyrrhotite (s)	0
H2 (g)	1.37E-11	Sulfur (s)	0

*Concentration and activity are given for aqueous species in mol/(kgH2O), for other species - in the mole fraction scale.

Considerable work has been carried out to characterize the chemical and to a lesser extent, the electrochemical, environments that are likely to exist in a granitic rock, HLNW repository. The measurements of specie concentrations, pH , and E_h have been carried out on samples collected from boreholes at the Forsmark site and the data are summarized in Table 19. The pH is found to vary from about 7.4 to 8; within the range specified in KBS-3 (Table 19), but most of the numbers do fall within the KBS-3 range. The E_h data fall mostly within the range specified by KBS-3 but are slightly more positive than those estimated in this work using GEMS. We point out, however, that the temperatures at which the Forsmark samples were taken (6 °C – 17 °C) are significantly lower than those assumed in our calculations (25 °C - 80 °C).

Table19: Experimentally-determined composition, E_h , and pH data for the Forsmark repository [21].Part 1

Borehole/depth	$T^{\circ}C$	pH -note 1	E_h (mV)-note 2	pe -note 2	Na^+	K^+	Ca^{2+}
KFM01A/115	6.91	7.65	-194	-3.48	1740	25.6	874
KFM01A/180	7.6	7.41	-187	-3.36	2000	29.2	934
KFM01D/432	9.65	8.1	-264	-4.7	1550	9	1430
KFM01D/572	10.75	8.25	-262	-4.64	1770	7.7	1830
KFM02A/512	11.4	6.88	-144	-2.55	2040	34.2	934
KFM03A/452	10.7	7.28	-177	-3.14	2180	27.5	1070
KFM03A/642	13.1	7.43	-199	-3.5	1660	14.3	1440
KFM03A/943	17.2	7.42	-231	-4	1890	10.4	3100
KFM06A/357	8.94	7.12	-168	-3	1470	13.4	1280
KFM07A/925	14.2	8.04	10	0.17	2850	13.7	5840

KFM08A/687	11.9	8	-211	-3.73	1560	10.6	2090
KFM08D/673	11.7	8.35	-262	-4.64	1900	5.4	2740
KFM10A/302	8.56	8	-281	-5.02	1350	6.6	1130
KFM10A/483	9.46	7.7	-259	-4.61	1410	29.1	731
KFM11A/451	9.71	7.53	-204	-3.63	1250	5.9	1280

Note 1: *pH* is average of downhole and surface measurements with Chemmac tool (see Table 1 in SSM Research Report 2009:28)

Note 2: E_h & pe are as measured by downhole and/or surface Chemmac E_h probes (see table 2 in SSM Research Report 2009:28)

Table19:Part 2

Borehole/depth	Mg^{2+}	HCO_3^-	Cl^-	$S_{total}SO_4^{2-}$	Fe^{2+}	NO_3^-	NH_4^+	F^-	Br^-	I^-
KFM01A/115	142	61	4563	315.7	0.953	nm*	1.07	1.36	18.4	nm
KFM01A/180	204	99	5330	547	0.475	<0.01	1.01	<1	20.1	0.035
KFM01D/432	20	36	4940	125	2.04	<0.0003	0.2	1.22	34	0.163
KFM01D/572	15	20	5800	38.3	1.23	0.0003	0.12	1.2	46.2	0.328
KFM02A/512	226	125	5410	498	1.84	nm	2.3	<1	23.8	nm
KFM03A/452	216	93	5330	511	1.11	nm	nm	1.6	20.9	0.041
KFM03A/642	53	22	5430	197	0.233	nm	0.16	<1	38.2	nm
KFM03A/943	18	9	8560	73.9	0.208	nm	nm	nm	72.3	0.241
KFM06A/357	74	48	4850	157	nm	nm	nm	1.26	29.5	0.104
KFM07A/925	20	6	14800	99.3	0.162	nm	0.02	1.34	nm	0.721
KFM08A/687	14	10	6100	91.5	0.726	<0.0003	0.09	1.25	44.9	0.235
KFM08D/673	5	7	7460	101	0.006	0.0003	0.04	1.48	57.1	0.228
KFM10A/302	30	21	4050	215	1.43	0.0004	nm	1.47	18.8	0.074
KFM10A/483	151	169	3690	400	15.4	0.0003	nm	1.38	14	0.028
KFM11A/451	38	24	4210	264	0.24	0.0009	0.05	1.06	19.7	0.059

*nm: not measured

Table19:Part 3

	<i>Ionic strength</i>	<i>Fe(II)</i>	<i>Fe(III)</i>	<i>S(VI)</i>	<i>Cu</i>
Borehole/depth	M	Totals, molar			
KFM01A/115	1.58E-01	1.72E-05	7.76E-07	3.31E-03	1.59E-08
KFM01A/180	1.80E-01	8.58E-06	1.12E-06	5.75E-03	1.59E-08
KFM01D/432	1.76E-01	3.68E-05		1.24E-03	6.03E-08
KFM01D/572	2.16E-01	2.22E-05		4.02E-04	7.94E-09
KFM02A/512	1.85E-01	3.33E-05	1.81E-07	5.23E-03	7.94E-09
KFM03A/452	1.99E-01	2.01E-05	1.81E-07	5.37E-03	1.59E-08
KFM03A/642	1.86E-01	4.21E-06	1.81E-08	2.07E-03	1.59E-08
KFM03A/943	3.16E-01	3.78E-06	1.45E-07	7.37E-04	2.39E-08

KFM06A/357	1.68E-01			1.65E-03	3.17E-09
KFM07A/925	5.65E-01	2.97E-06		1.06E-03	1.93E-08
KFM08A/687	2.26E-01	1.31E-05		9.62E-04	1.59E-08
KFM08D/673	2.88E-01	1.09E-07		1.06E-03	1.59E-08
KFM10A/302	1.46E-01	2.58E-05		5.18E-05	7.92E-09
KFM10A/483	1.34E-01	2.78E-04			7.92E-09
KFM11A/451	1.54E-01	4.33E-06			7.92E-09

Table19:Part 4

	$\log P_{CO_2}$	$\log O_2$	$\log H_2$	$Eh(Fe^{3+}/Fe^{2+})$	$Eh(SO_4/HS)$	$Eh(Fe^{2+}/Fe(OH)_3)$
Borehole/depth	P in bars	calculated, molar		Calculated Eh for redox couples, mV		
KFM01A/115	-3.15	-74.78	-11.84	94	-182	-272
KFM01A/180	-2.70	-75.04	-11.59	161	-176	-214
KFM01D/432	-3.86	-76.99	-10.24		-254	-377
KFM01D/572	-4.31	-75.81	-10.64		-252	-394
KFM02A/512	-2.04	-72.73	-12.07	165	-135	-170
KFM03A/452	-2.59	-73.71	-11.70	114	-168	-224
KFM03A/642	-3.35	-73.80	-11.23	64	-191	-224
KFM03A/943	-3.77	-74.62	-10.14	118	-226	-231
KFM06A/357	-2.71	-74.33	-11.70		-158	
KFM07A/925	-4.74	-56.39	-19.80			-317
KFM08A/687	-4.33	-72.82	-11.94		-203	-344
KFM08D/673	-4.94	-75.13	-10.83		-254	-283
KFM10A/302	-3.97	-79.01	-9.42		-270	-349
KFM10A/483	-2.74	-78.29	-9.62			-352
KFM11A/451	-3.42	-74.97	-11.24			-231

Table19:Part 5

	Fe^{2+}	Cl	HCO_3^-	CO_3^{2-}	HS^-	H_2S	S^{2-}	$S_2O_3^{2-}$
Borehole/depth	Modeled (PHREEQC-LLNL) molar concentration of species							
KFM01A/115	1.37E-05	1.24E-01	8.12E-04	2.52E-06	5.64E-10	1.78E-10	1.82E-15	1.75E-15
KFM01A/180	6.32E-06	1.38E-01	1.32E-03	2.48E-06	1.31E-08	6.92E-09	2.65E-14	1.16E-13
KFM01D/432	3.12E-05	1.37E-01	4.33E-04	4.18E-06	6.68E-05	6.67E-06	7.68E-10	2.50E-11
KFM01D/572	1.97E-05	1.69E-01	2.18E-04	3.24E-06	2.47E-07	1.65E-08	4.57E-12	1.97E-14
KFM02A/512	2.38E-05	1.42E-01	1.68E-03	1.04E-06	1.27E-10	1.97E-10	1.02E-16	3.17E-15
KFM03A/452	1.52E-05	1.54E-01	1.23E-03	1.90E-06	1.85E-09	1.16E-09	3.59E-15	1.89E-14
KFM03A/642	3.78E-06	1.44E-01	2.89E-04	6.61E-07	1.74E-08	7.12E-09	5.59E-14	4.68E-14
KFM03A/943	3.52E-06	2.37E-01	1.05E-04	3.00E-07	3.23E-05	1.11E-05	1.55E-10	2.49E-11
KFM06A/357	1.00E-09	1.30E-01	6.47E-04	6.34E-07	1.66E-09	1.64E-09	1.88E-15	8.04E-15
KFM07A/925	2.71E-06	4.17E-01	5.05E-05	6.59E-07				
KFM08A/687	1.21E-05	1.72E-01	1.15E-04	1.00E-06	4.48E-12	5.06E-13	5.12E-17	1.45E-18
KFM08D/673	9.89E-08	2.18E-01	6.55E-05	1.36E-06	6.17E-08	3.07E-09	1.65E-12	9.31E-15

KFM10A/302	ALKALINITY DID NOT CONVERGE							
KFM10A/483	ALKALINITY DID NOT CONVERGE							
KFM11A/451	3.82E-06	1.16E-01	3.21E-04	8.06E-07	5.77E-08	2.16E-08	1.74E-13	1.84E-13

Table19:Part 6

	SO_3^{2-}	HSO_3^-	SO_4^{2-}	$CaSO_4^0$	$NaSO_4^-$	$MgSO_4^0$	KSO_4^-	$FeSO_4^0$	HSO_4^-
Borehole/depth	Modeled (PHREEQC-LLNL) molar concentration of species								
KFM01A/115	1.10E-15	1.45E-16	2.13E-03	6.12E-04	3.23E-04	2.41E-04	3.12E-06	5.13E-07	1.18E-09
KFM01A/180	3.32E-15	7.40E-16	3.61E-03	1.00E-03	5.94E-04	5.35E-04	5.71E-06	3.66E-07	3.40E-09
KFM01D/432	1.54E-14	7.20E-16	7.74E-04	3.52E-04	9.97E-05	1.26E-05	3.84E-07	3.96E-07	1.58E-10
KFM01D/572	1.90E-15	6.02E-17	2.42E-04	1.25E-04	3.28E-05	2.71E-06	9.48E-08	6.73E-08	3.38E-11
KFM02A/512	9.50E-16	7.38E-16	3.22E-03	9.07E-04	5.32E-04	5.71E-04	5.94E-06	1.20E-06	1.13E-08
KFM03A/452	2.25E-15	6.78E-16	3.28E-03	1.00E-03	5.62E-04	5.24E-04	4.71E-06	7.41E-07	4.38E-09
KFM03A/642	2.53E-15	5.62E-16	1.27E-03	5.72E-04	1.71E-04	5.72E-05	9.84E-07	7.42E-08	1.31E-09
KFM03A/943	9.62E-15	1.97E-15	4.00E-04	2.83E-04	4.92E-05	4.95E-06	1.83E-07	1.51E-08	3.98E-10
KFM06A/357	7.25E-16	3.25E-16	1.03E-03	4.28E-04	1.28E-04	6.25E-05	7.73E-07	1.00E-09	2.00E-09
KFM07A/925	2.84E-24	1.15E-25	5.16E-04	4.62E-04	7.62E-05	4.65E-06	2.42E-07	1.03E-08	9.38E-11
KFM08A/687	2.23E-16	1.25E-17	5.65E-04	3.25E-04	6.63E-05	5.89E-06	2.99E-07	9.31E-08	1.43E-10
KFM08D/673	3.07E-15	7.18E-17	6.00E-04	3.85E-04	7.78E-05	1.91E-06	1.47E-07	6.88E-10	6.25E-11
KFM10A/302	ALKALINITY DID NOT CONVERGE								
KFM10A/483	ALKALINITY DID NOT CONVERGE								
KFM11A/451	3.51E-15	6.32E-16	1.75E-03	7.69E-04	1.91E-04	5.79E-05	5.99E-07	1.18E-07	1.39E-09

Table19:Part 7

	NH_4^+	NH_3	Cu^+	$CuCl_3^{2-}$	$CuCl_2^-$	Cu^{2+}
Borehole/depth	Modeled (PHREEQC-LLNL) molar concentration of species					
KFM01A/115	5.95E-05	2.85E-07	1.20E-11	9.33E-09	6.52E-09	2.91E-17
KFM01A/180	5.63E-05	1.62E-07	9.23E-12	9.85E-09	6.02E-09	2.94E-17
KFM01D/432	1.10E-05	1.82E-07	3.52E-11	3.73E-08	2.29E-08	4.73E-18
KFM01D/572	6.55E-06	1.63E-07	2.75E-12	5.36E-09	2.58E-09	4.24E-19
KFM02A/512	1.29E-04	1.46E-07	4.27E-12	5.00E-09	2.94E-09	7.67E-17
KFM03A/452			6.95E-12	1.03E-08	5.53E-09	3.34E-17
KFM03A/642	8.91E-06	4.07E-08	8.23E-12	1.01E-08	5.82E-09	1.56E-17
KFM03A/943			3.36E-12	1.82E-08	5.71E-09	1.92E-18
KFM06A/357			2.13E-12	1.91E-09	1.26E-09	1.46E-17
KFM07A/925	1.12E-06	1.97E-08	5.59E-13	1.67E-08	2.62E-09	5.86E-15
KFM08A/687	4.96E-06	7.52E-08	5.28E-12	1.08E-08	5.07E-09	6.39E-18
KFM08D/673	2.17E-06	7.05E-08	2.81E-12	1.18E-08	4.13E-09	4.42E-19
KFM10A/302	ALKALINITY DID NOT CONVERGE					
KFM10A/483	ALKALINITY DID NOT CONVERGE					
KFM11A/451	2.78E-06	1.26E-08	7.18E-12	4.52E-09	3.40E-09	1.10E-17

Table19:Part 8

	$CuCO_3^0$	$CuOH^+$	$CuCl^+$	$CuSO_4^0$	$Cu(CO_3)_2^{2-}$
Borehole/depth	Modeled (PHREEQC-LLNL) molar concentration of species				
KFM01A/115	1.22E-16	3.23E-17	3.48E-18	1.57E-18	8.62E-19
KFM01A/180	1.09E-16	1.83E-17	3.76E-18	2.46E-18	7.51E-19
KFM01D/432	2.53E-17	1.45E-17	6.06E-19	8.56E-20	2.47E-19
KFM01D/572	1.69E-18	1.76E-18	6.27E-20	2.09E-21	1.41E-20
KFM02A/512	1.06E-16	1.40E-17	1.00E-17	5.57E-18	2.78E-19
KFM03A/452	8.23E-17	1.51E-17	4.62E-18	2.35E-18	4.04E-19
KFM03A/642	1.31E-17	1.01E-17	2.06E-18	4.43E-19	2.10E-20
KFM03A/943	3.73E-19	1.09E-18	3.54E-19	1.19E-20	2.00E-22
KFM06A/357	1.40E-17	4.73E-18	1.80E-18	3.64E-19	2.38E-20
KFM07A/925	2.45E-15	1.24E-14	1.62E-15	3.23E-17	4.09E-18
KFM08A/687	7.41E-18	1.48E-17	9.46E-19	7.11E-20	1.86E-20
KFM08D/673	5.99E-19	2.18E-18	7.74E-20	4.44E-21	2.08E-21
KFM10A/302	ALKALINITY DID NOT CONVERGE				
KFM10A/483	ALKALINITY DID NOT CONVERGE				
KFM11A/451	1.39E-17	9.31E-18	1.24E-18	4.94E-19	2.93E-20

The GEMS code also predicts the E_h value and the pH as shown in Figures 61 and 62. The code predicts that the E_h shifts to more negative values under the unequivocal anoxic conditions that exist for times greater than about 50 years. This shift in the E_h value to more negative is primarily due to the fall in temperature and not due to the change in concentration of any electroactive species in the system. The calculated pH (7 – 8.5) falls within the range specified in the KBS-3 plan (7 – 9), with the pH steadily increasing as the canister cools over the 10,000 year storage period. Again, this change can be attributed to the fall in temperature and its impact upon acid/base equilibria in the system.

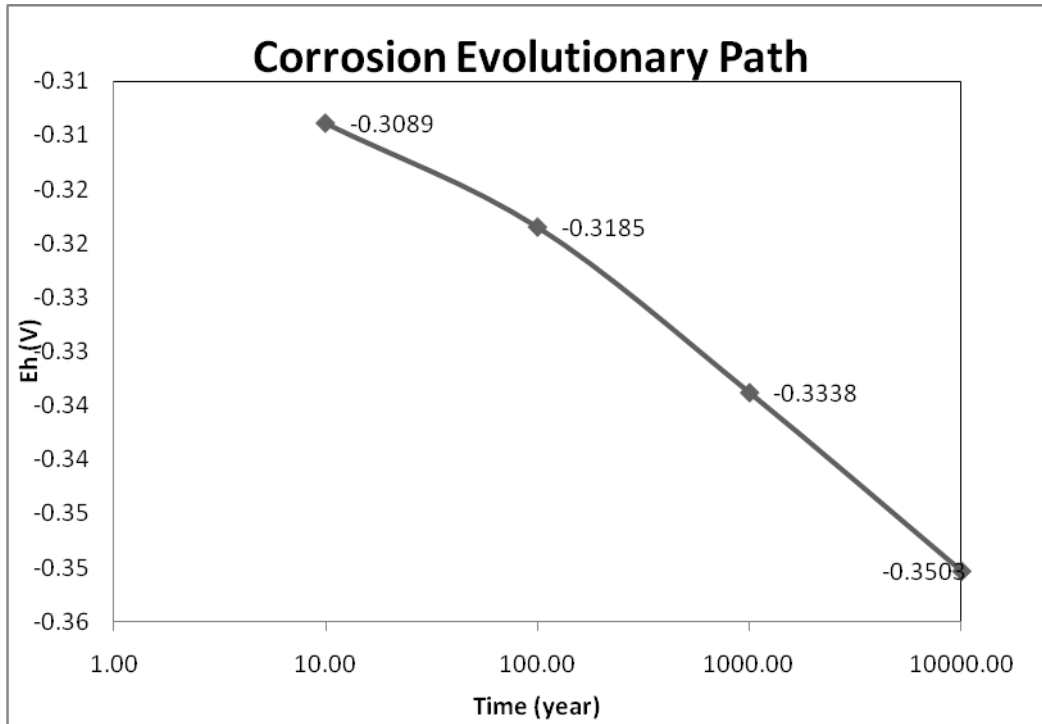


Figure 61: Predicted E_h versus time data along the Corrosion Evolutionary Path (CEP) defined by the temperature of the inner surface of the buffer versus time profile shown in Figure 59.

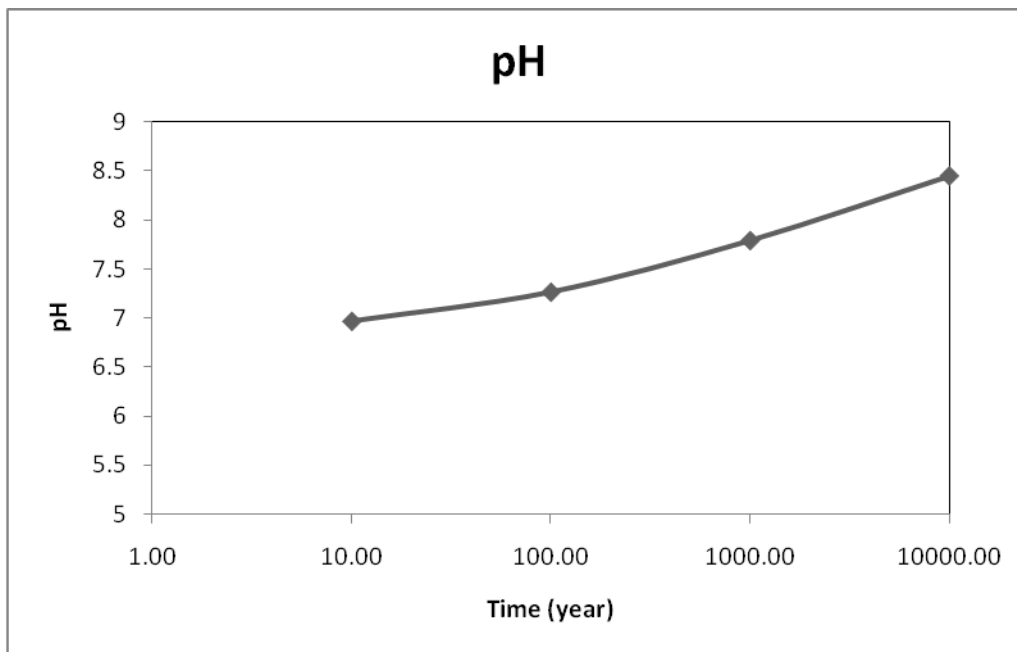


Figure 62: Variation of predicted pH versus time data along the Corrosion Evolutionary Path (CEP) defined by the temperature of the inner surface of the buffer versus time profile shown in Figure 59.

VIII. Summary and Conclusions

The work reported here has resulted in a number of important conclusions that have a bearing on the behavior of copper in a Forsmark type repository. These conclusions are as follows:

Corrosion Domain Diagrams

- The thermodynamic conditions for the corrosion of copper in water have been defined. For all practical purposes, copper is not a noble metal, except possibly in very pure water, with sufficient Cu^+ and H_2 being present that $P > P^e$. These conditions will not exist in a repository.
- The current controversy with respect to the nobility of copper can probably be attributed to variability in the initial conditions of the experiments.
- The thermodynamic properties of copper are expressed in corrosion domain diagrams as P^e versus pH , where P^e is the partial quotient of the reaction at equilibrium. For any other value of the reaction quotient, P , where $P \neq P^e$, the system is not at equilibrium and, provided that $P < P^e$, the composition (as described by P) will change such that $P \rightarrow P^e$.
- Corrosion is spontaneous only for $P < P^e$. Cu is immune for $P > P^e$.
- Certain species commonly found in ground water, e.g. HS^- , polysulfides, and certain polysulfur oxyanions are deleterious by (thermodynamically) activating copper and hence denying the metal thermodynamic immunity.
- Some polythiosulfates, notably, $S_xO_3^{2-}$, $x = 3 - 7$, are found not to activate copper, for reasons that are not yet completely understood. These species tend to possess very negative volt equivalencies and to have low, positive average sulfur oxidation states.
- All polysulfides are predicted to activate copper.
- The halides, F^- , Cl^- , Br^- , and I^- , except bromide and iodide, are weakly activating and hence do not pose a threat to immunity. Bromide and iodide appear to activate copper only at low pH.
- Complex formation, e.g. $CuCl_2^-$, induces activation in chloride-containing media.
- The possibility of doping the bentonite with a $Cu(I)$ salt, such as Cu_2SO_3 , should be explored to determine whether immunity might be maintained over extended periods. Thus, the “scoping” calculations reported here for a scenario where the bentonite buffer is “doped” with a $Cu(I)$ salt containing a strongly reducing anion (e.g., SO_3^{2-}), suggest that immunity might be maintained over periods of several hundreds of thousands of years. Given that the performance horizon of the repository is 100,000 years, it may well be possible to impose immunity on the system over the entire, planned storage period, even in the presence of sulfur-containing, activating species, provided that their concentrations are not too high. Practically, this issue could be explored by inserting source terms in the model outlined above for Cu^+ and SO_3^{2-} from the bentonite buffer.

Volt-Equivalent Diagrams

- Volt Equivalent Diagrams (VEDs) are enormously useful in interpreting and predicting the chemistry of complex systems, such as $S-H_2O$.

- VEDs derived for the expected repository conditions predict that for any given homologous series; e.g., S_x^{2-} , $S_xO_y^{2-}$, and their acid forms, equilibrium mixtures of all members of the series will form.
- The activating effect appears to be attributable to the ability of the species to donate atomic sulfur or sulfide to the metal surface to form Cu_2S , and hence depends upon the orientation of the ion adsorbed on the copper surface. However, resolution of the activating effect will probably require density functional theoretical estimates of the charge densities on the sulfur atoms in the molecule and on the configuration of the adsorbate.
- Only the thermodynamic conditions have been examined. The kinetics must also be explored, because, even though copper is active, the rate of corrosion may be sufficiently low to meet the engineering requirements of HLNW isolation.

Gibbs Energy Minimization

- In order to explore the composition of granitic groundwater, we decided to employ a modern, sophisticated Gibbs energy minimization algorithm to predict the composition of the repository environment as a function of temperature and redox condition, with the latter being adjusted by changing the relative concentrations of hydrogen and oxygen in the input to the code.
- After evaluating several codes, we chose GEMS, which was developed in Switzerland by Prof. Dmitri Kulik. This code is designed specifically to model geochemical systems, contains a large database of compounds, and is in general use in the geochemical community.
- Prior to using the code to model the repository, we upgraded the database by adding thermodynamic data for various polysulfur species (polysulfides, poly thiosulfates, and polythionates) that had been developed earlier in this program. However, the code became ill-behaved when the data for $S_xO_3^{2-}$, $x = 3 - 7$ was added. Consultation with the code developer, Prof. Dmitrii Kulik at Paul Scherer Institute in Switzerland, failed to identify and isolate the problem and, accordingly, it was necessary to remove those species from the database. The reader will recall that these are the very species that, anomalously, do not activate copper.
- With the code in its present form, we have modeled the repository under both oxic and anoxic conditions with the greatest emphasis being placed on the latter, because the great fraction of the storage time is under anoxic conditions. The most important finding to date is that the concentrations of many, but not all, polysulfur species (polysulfides, poly thiosulfates, and polythionates) under anoxic conditions are predicted to be very low, but it is still not possible, because of the uncertainty in the calculations, to ascertain with certainty whether these species will activate copper in the repository. However, the point may be moot, because sulfide species (S^{2-} , HS^- , H_2S , HS_2^{2-} , and S_2^{2-}) are predicted to be present in sufficient concentration to activate copper and cause the metal to corrode under simulated repository conditions.

Corrosion Evolutionary Path

- We have initiated work to define the corrosion evolutionary path (CEP) in preparation for modeling the corrosion of the canisters at some future date. This task essentially involves predicting the redox potential (E_h), pH , and granitic groundwater composition as defined

by the variation of temperature (note that the temperature decreases roughly exponentially due to radioactive decay of the short-lived isotopes), and then applying Gibbs energy minimization to predict speciation at selected times along the path.

- At each step, the CDD for copper is derived and the value of P is compared to P^e to ascertain whether copper is active or thermodynamically immune. Although the polysulfur species are predicted to be present at very low concentration (e.g., HS_2^- and S_2^{2-}) or are predicted to be absent altogether (e.g., polysulfur oxyanions), the CDDs indicate that certain species need be present at only miniscule concentrations (10^{-44} M) for activation to occur. However, an unequivocal resolution of this issue must await access to the GEMS source code, in order to understand what “0” concentration means in the output. In any event, sulfide (H_2S , HS^- , and/or S^{2-}) are predicted to be present during the entire anoxic period at sufficiently high concentrations that they will activate copper.
- Accordingly, the assumption that copper will be immune during the anoxic storage period is untenable, despite the fact that native deposits of copper do occur in granitic formations. The success of the KBS-3 program must rely upon the multiple barriers being sufficiently impervious that the corrosion rate be reduced to an acceptable level.

General

The findings of this Phase I work are generally in accord with the stated positions of SKB, with the following exceptions:

- Sulfide ion (S^{2-}) is not the only $S(-II)$ species present in the repository at concentrations that will activate copper, but H_2S and HS^- are also present at sufficient concentrations, as well. Furthermore, the lowest polysulfides, HS_2^{2-} and S_2^{2-} , and possibly other polysulfur species are predicted to be also present at activating concentrations. Thus, the focus on S^{2-} , alone, is unjustified
- If the proposed corrosion scenario posed by SKB is correct, that the rate of copper corrosion is determined by the rate of mass transport of sulfide ion through the bentonite buffer, the question must then be asked: “Why use copper?” “Would not a less expensive and hence more cost-effective alternative, such as steel, suffice?” Answers to these questions possibly lie outside of the realm of corrosion science.

References

- [1] Hultqvist, G., *Corros. Sci.*, **26**, 173 (1986).
- [2] Hultqvist, G., Chuah, G. K., and Tan, K. L., *Corros. Sci.*, **29**, 1371 (1989).
- [3] Szakalos, P., Hultqvist, G. and Wikmark, G., *Electrochem. Solid State Letters*, **10**, C63 (2007).
- [4] Mattsson, E., *Br. Corros. J.*, **15**, 6 (1980).
- [5] Eriksen, T. E., Ndalamba, P., and Grenthe, I., *Corros. Sci.*, **28**, 1231 (1989).
- [6] Berskog B. and Puigdomenech, I., *J. Electrochem. Soc.*, **144**, 3476 (1997).
- [7] Kamyshny, A., Jr.; Goifman, A.; Gun, J.; Rizkov, D. and Lev, O. “Equilibrium Distribution of

Polysulfide Ions in Aqueous Solutions at 25 °C: A New Approach for the Study of Polysulfides' equilibria.", *Environ. Sci. Technol.*, **38**, 6633-6644 (2004).

[8] Shock E., Helgeson H. C., Calculation of the thermodynamic and transport properties of aqueous species at high pressures and temperatures: Correlation algorithms for ionic species and..., *Geochim. Cosmochim. Acta*, **52**: 2009-36, (1988).

[9] Shock E., Sassani D.C., Willis M., Sverjensky D.A Inorganic species in geologic fluids: Correlations among standard molal properties of aqueous ions and hydroxide complexes. *Geochim. Cosmochim. Acta*, **61**, 907-51 (1997).

[10] Bailey S. M., Churney K. L., Nuttall R. L.: The NBS Tables of Chemical Thermodynamic Properties, Selected Values for Inorganic and C1 and C2 Organic Substances in SI Units, *J. of Phys. and Chem. Ref. Data*, **11**, Suppl. No. 2 (1982).

[11] Williamson, M., Rimstidt, D., Correlation between structure and thermodynamic properties of aqueous sulfur species, *Geochim. Cosmochim.*, **56**, 3867-3880 (1992).

[12] Thermodynamic Tables for Nuclear Waste Isolation. Prepared by S. L. Philips, F. V. Hale, L. F. Silvester, *Lawrence Berkely Laboratory M. D. Siegel, Sandia National Laboratories*, 182, 1988.

[13] Helgeson H. C., Thermodynamics of hydrothermal systems at elevated temperatures and pressures. *American Journal of Science*, **267**: 729-804 (1969).

[14] Plyasunov, A.V., Shock, E.L., Correlation strategy for determining the parameters of the revised Helgeson-Kirkham-Flowers model for aqueous nonelectrolytes, *Geochimica et Cosmochimica Acta*, **65**, 3879-3900 (2001).

[15] Kivalo P., Ekman A., Rastas J.: Eräiden aineiden termodynaamisia arvoja. Finska kemists medd. 66 No 3-4 (1957) Suomen kemistis. tied., *Teknillinen Korkeakoulu, Helsinki*, 1957.

[16] Rossini F. D., Wagman D. D., Ewans W. H., Levine S., Jaffe I.: *Selected values of chemical thermodynamic properties*, 1952.

[17] Hyne, J. B., University of Calgary, personal communication (1972)

[18] L. Hallbeck and K. Pedersen, "Explorative analysis of microbes, colloids and gases", Microbial Analytics Sweden AB, SDM-Site Forsmark, SKB Report R-08-85, Svensk Kärnbränslehantering AB, Swedish Nuclear Fuel, and Waste Management Co Box 250, SE-101 24 Stockholm, August 2008.

[19] L.-H. Lin, G. F. Slater, L. B. Sherwood, G. Lacrampe-Couloumbe, and T. C. Onstott, "The yield and isotopic composition of radiolytic H₂, a potential energy source for the deep subsurface biosphere. *Geochimica et Cosmochimica Acta*, **69**(4), 893–903 (2005).

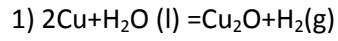
[20] J. A. Apps and P. C. van de Kamp, "Energy gases of abiogenic origin in the Earth's crust. The future of Energy gases". U.S. Geological Survey Professional Papers. United States Government Printing Office, Washington., pp. 81–132, 1993.

[21] Dr. Adrian Bath, private communication (2010).

- [22] L.Oritz, G. Volckaert, D. Mallants, “ Gas Generation and migration in Boom Clay, a potential host rock formation for nuclear waste storage”, *Eng. Geology* 64(2002) 287-296.
- [23] J. Faust Larsen, E. Knittle, Q. Williams, “ Constraints on the speciation of hydrogen in earth’s transition zone”, *Physics of the Earth Planetary Interiors* 136 (2003) 93-105.
- [24] <http://www.outotec.com/>
- [25] G.B. Naumov, “*Handbook of thermodynamic data*”, U.S. Geological Survey, Water Resources Division, 1974.
- [26] P.W. Atkins, “*Physical Chemistry*”, third edition, Oxford University Press, 1985.
- [27] Sanford Gordon and Bonnie J. Mcbrdie, “*Computer Program for Calculation of Complex Chemical Equilibrium Compositions and Applications*”, NASA Reference publication 1311, Oct. 1994.
- [28] <http://www.olisystems.com>
- [29] <http://gems.web.psi.ch/>
- [30] <http://www.factsage.com/>
- [31] <http://www.aspentech.com/>
- [32] <http://www.metsim.com/>
- [33] I Puigdomenech, C Taxén, “Thermodynamic data for copper: Implications for the corrosion of copper under repository conditions” *SKB TR-00-13, Svensk Kärnbränslehantering AB.Aug. 2000.*
- [34] Long-term safety for KBS-3 repositories at Forsmark and Laxemar – a first evaluation *SKB TR-06-09, Svensk Kärnbränslehantering AB.Oct. 2006.*
- [35] “Final Storage of spent Nuclear fuel-KBS-3, Part 3:Barriers”, *SKBF/KBS*, Stockholm, Sweden

Appendix I

Corrosion Domain Diagrams



$$\log(f_{\text{H}_2}) = \frac{-\Delta G^0}{2.303RT}$$

298.15: $\log(p) = -15.63$

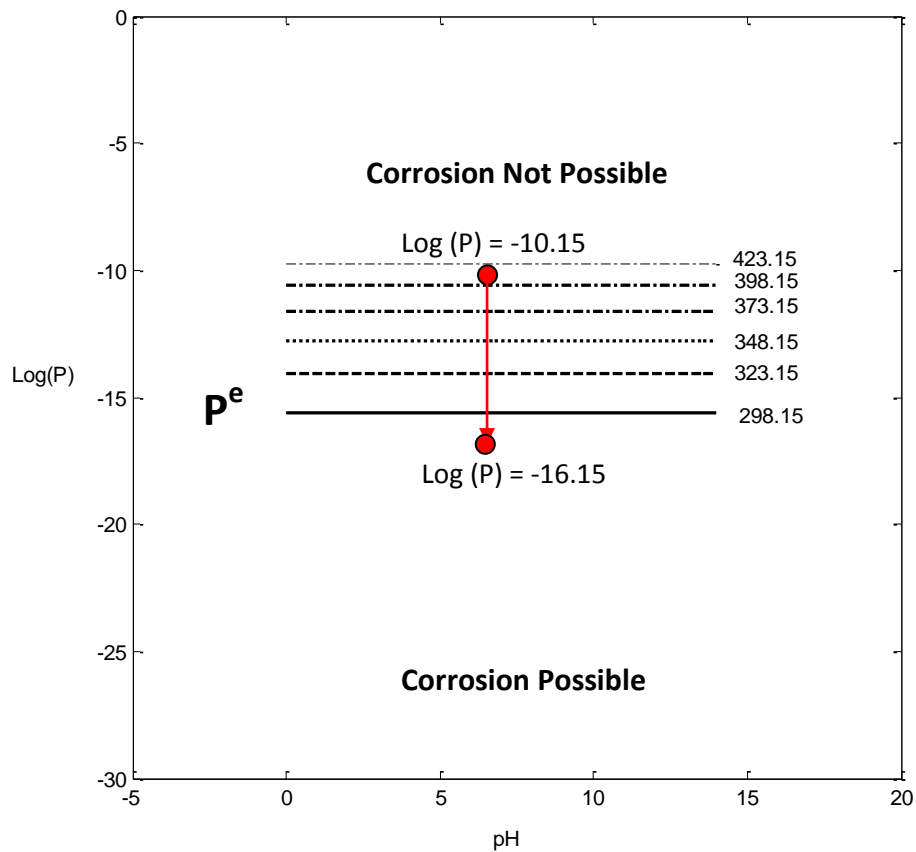
323.15: $\log(p) = -14.08$

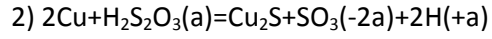
348.15: $\log(p) = -12.75$

373.15: $\log(p) = -11.61$

398.15: $\log(p) = -10.62$

423.15: $\log(p) = -9.75$





$$\log(a_{\text{SO}_3(2-)}) = \frac{-\Delta G^0}{2.303RT} + 2\text{pH}$$

298.15: $\log(p) = 6.14 + 2\text{pH}$

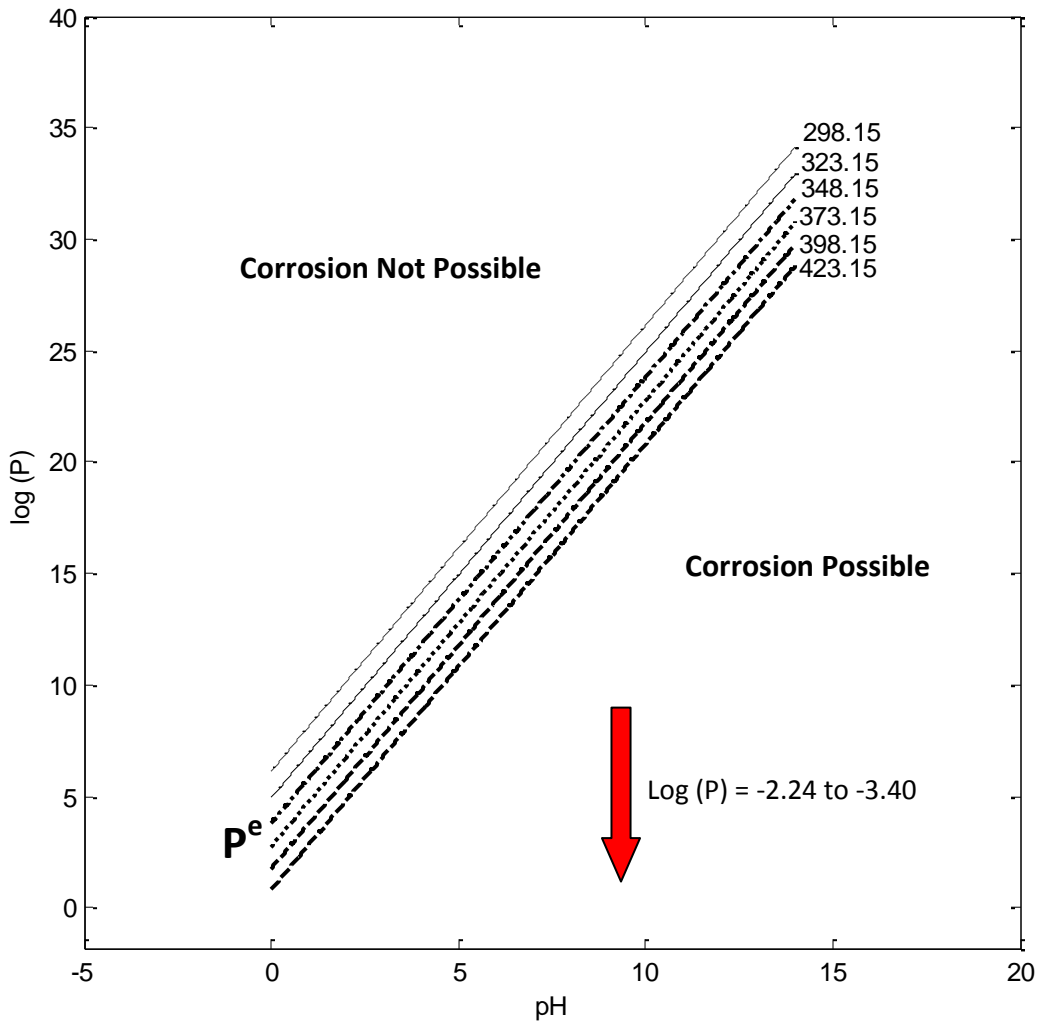
323.15: $\log(p) = 4.94 + 2\text{pH}$

348.15: $\log(p) = 3.81 + 2\text{pH}$

373.15: $\log(p) = 2.76 + 2\text{pH}$

398.15: $\log(p) = 1.77 + 2\text{pH}$

423.15: $\log(p) = 0.82 + 2\text{pH}$





$$\log(a_{\text{SO}_4^{2-}}) = \frac{-\Delta G^0}{2.303RT} + 2\text{pH}$$

298.15: $\log(p) = 37.10 + 2\text{pH}$

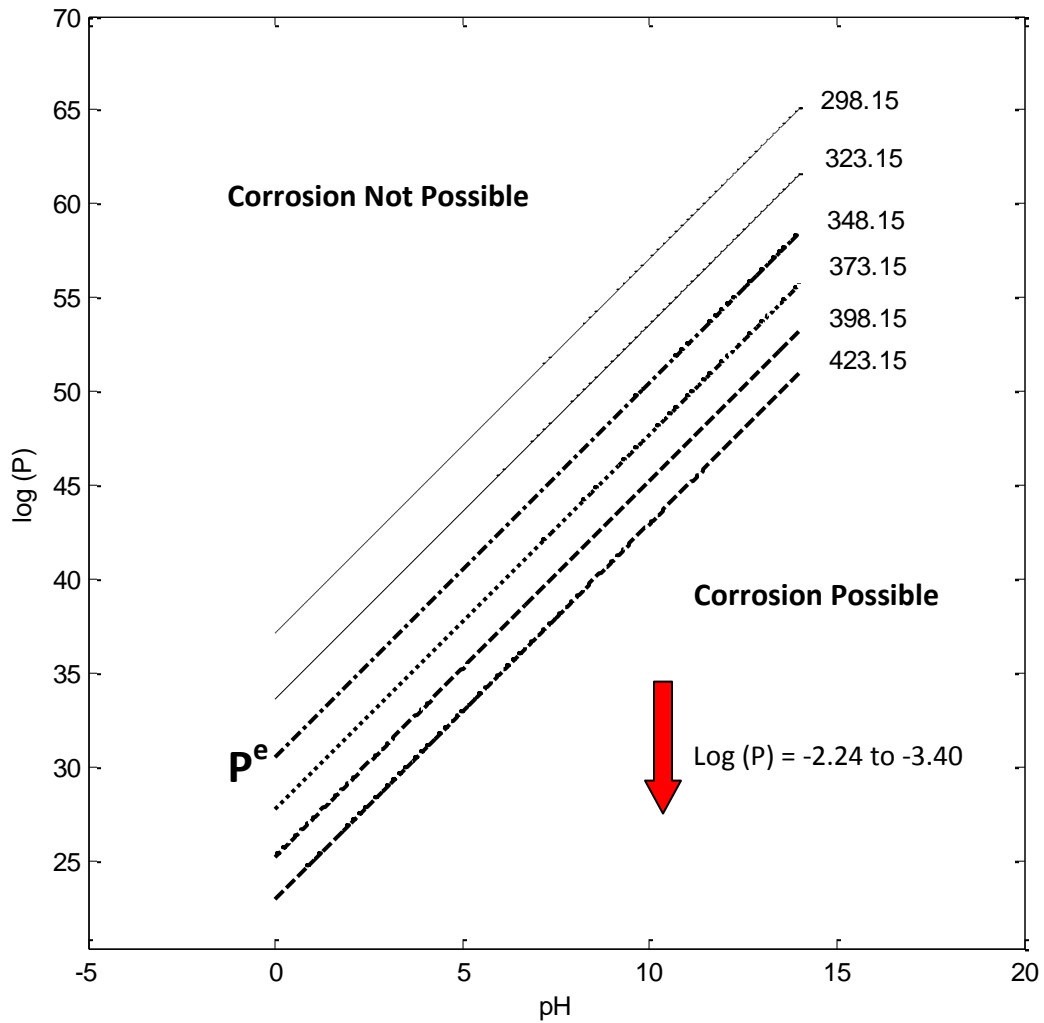
323.15: $\log(p) = 33.59 + 2\text{pH}$

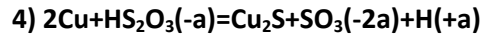
348.15: $\log(p) = 30.48 + 2\text{pH}$

373.15: $\log(p) = 27.72 + 2\text{pH}$

398.15: $\log(p) = 25.23 + 2\text{pH}$

423.15: $\log(p) = 22.96 + 2\text{pH}$





$$\log\left(\frac{a_{\text{SO}_3(2-)}}{a_{\text{HS}_2\text{O}_3(1-)}}\right) = \frac{-\Delta G^0}{2.303RT} + pH$$

298.15: $\log(p) = 6.75 + pH$

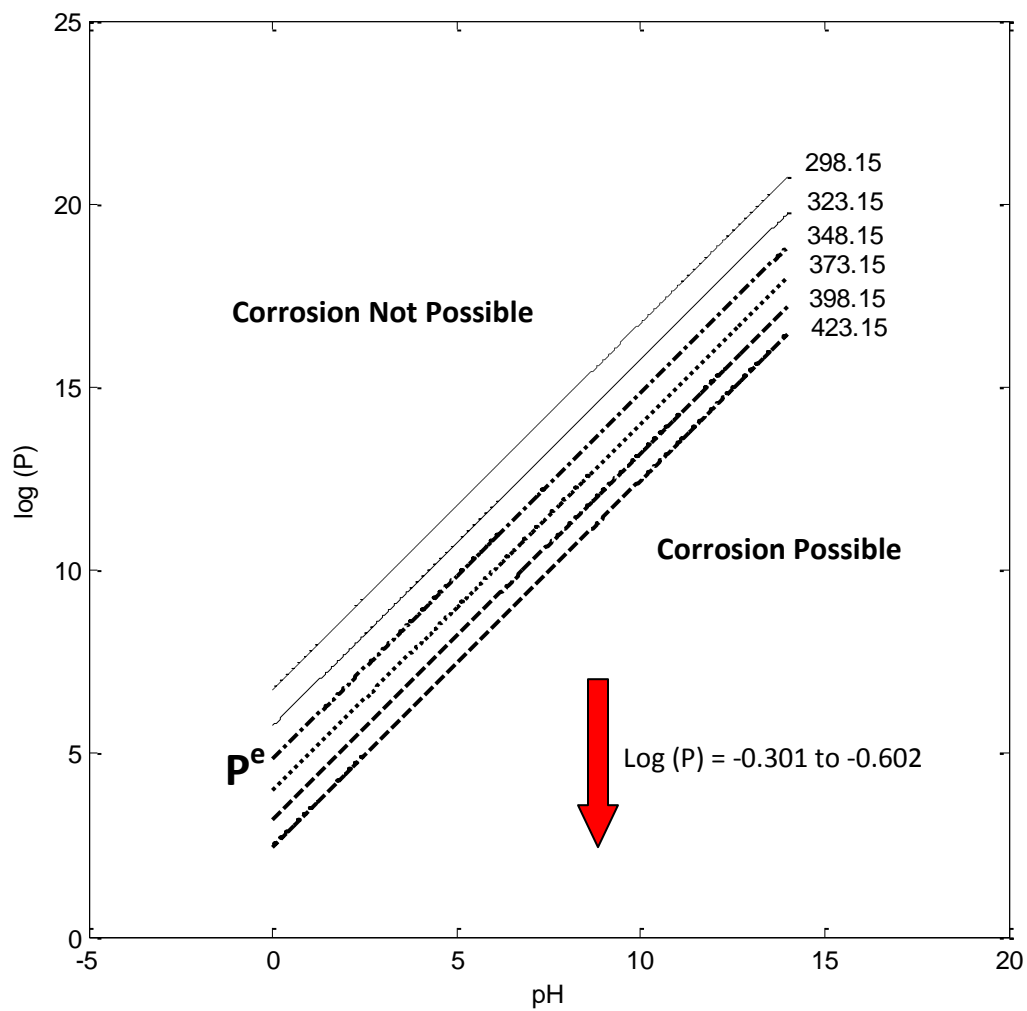
323.15: $\log(p) = 5.75 + pH$

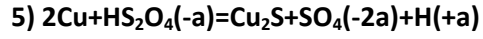
348.15: $\log(p) = 4.84 + pH$

373.15: $\log(p) = 3.99 + pH$

398.15: $\log(p) = 3.20 + pH$

423.15: $\log(p) = 2.46 + pH$





$$\log\left(\frac{a_{\text{SO}_4(2-)}}{a_{\text{HS}_2\text{O}_4(1-)}}\right) = \frac{-\Delta G^0}{2.303RT} + pH$$

298.15: $\log(p) = 37.49 + pH$

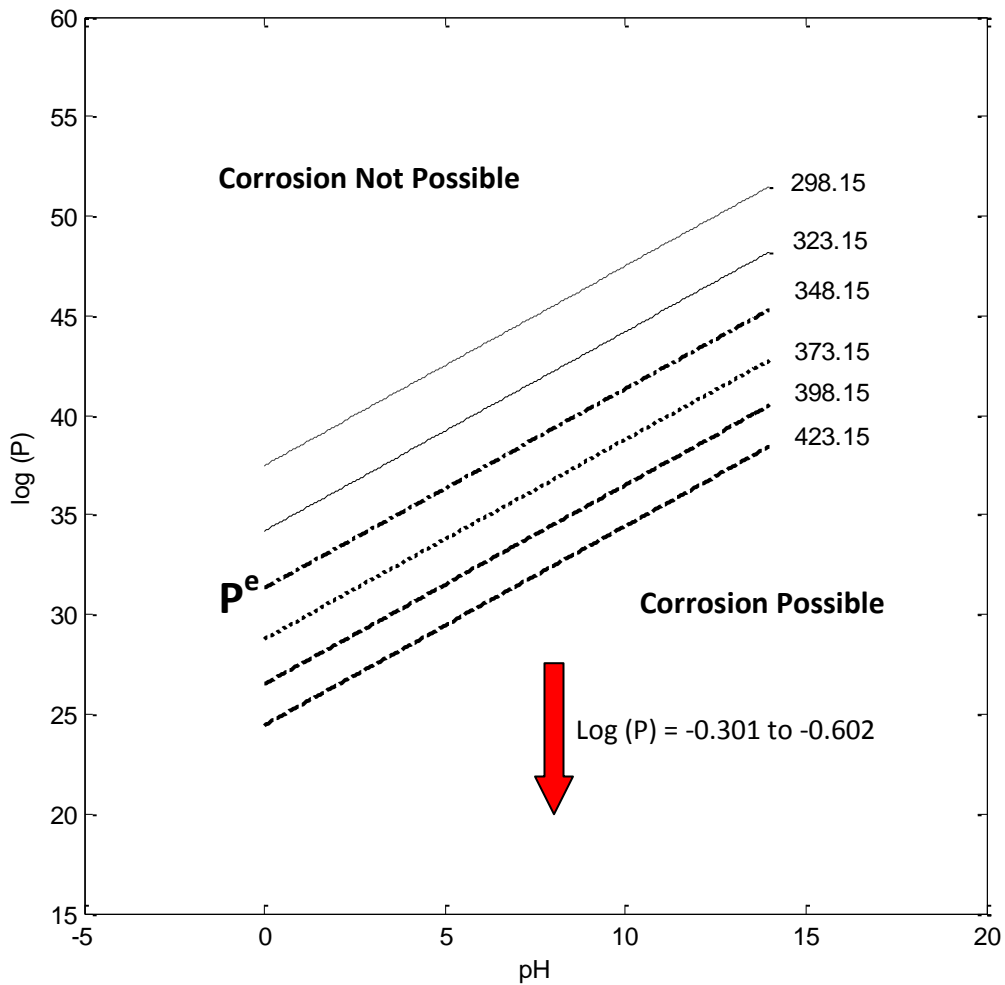
323.15: $\log(p) = 34.20 + pH$

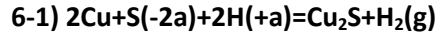
348.15: $\log(p) = 31.32 + pH$

373.15: $\log(p) = 28.77 + pH$

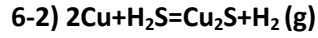
398.15: $\log(p) = 26.50 + pH$

423.15: $\log(p) = 24.44 + pH$



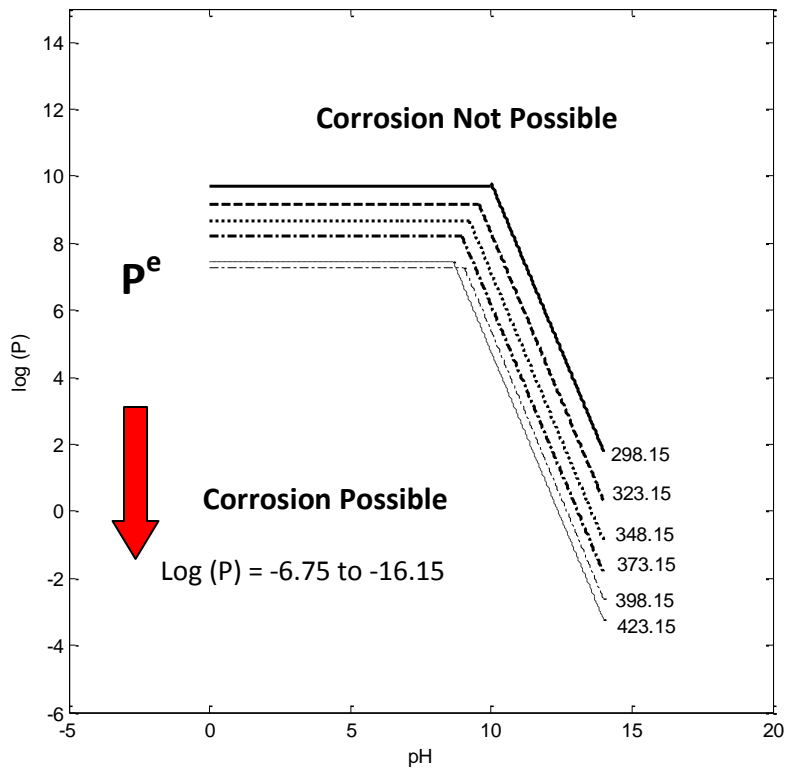


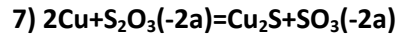
$$\log\left(\frac{P_{\text{H}_2(\text{g})}}{a_{\text{S}(-2)}}\right) = \frac{-\Delta G^0}{2.303RT} - 2\text{pH}$$



$$\log\left(\frac{P_{\text{H}_2(\text{g})}}{a_{\text{H}_2\text{S}}}\right) = \frac{-\Delta G^0}{2.303RT}$$

298.15: $\log(p) = 29.79 - 2\text{pH}$	298.15: $\log(p) = 9.72$ for $\text{pH} < 9.72$
323.15: $\log(p) = 28.31 - 2\text{pH}$	323.15: $\log(p) = 9.18$ for $\text{pH} < 9.18$
348.15: $\log(p) = 27.12 - 2\text{pH}$	348.15: $\log(p) = 8.68$ for $\text{pH} < 8.68$
373.15: $\log(p) = 26.15 - 2\text{pH}$	373.15: $\log(p) = 8.23$ for $\text{pH} < 8.23$
398.15: $\log(p) = 25.38 - 2\text{pH}$	398.15: $\log(p) = 7.28$ for $\text{pH} < 7.28$
423.15: $\log(p) = 24.76 - 2\text{pH}$	423.15: $\log(p) = 7.44$ for $\text{pH} < 7.44$





$$\log\left(\frac{a_{\text{SO}_3^{2-}}}{a_{\text{S}_2\text{O}_3^{2-}}}\right) = \frac{-\Delta G^0}{2.303RT}$$

298.15: $\log(p) = 9.11$

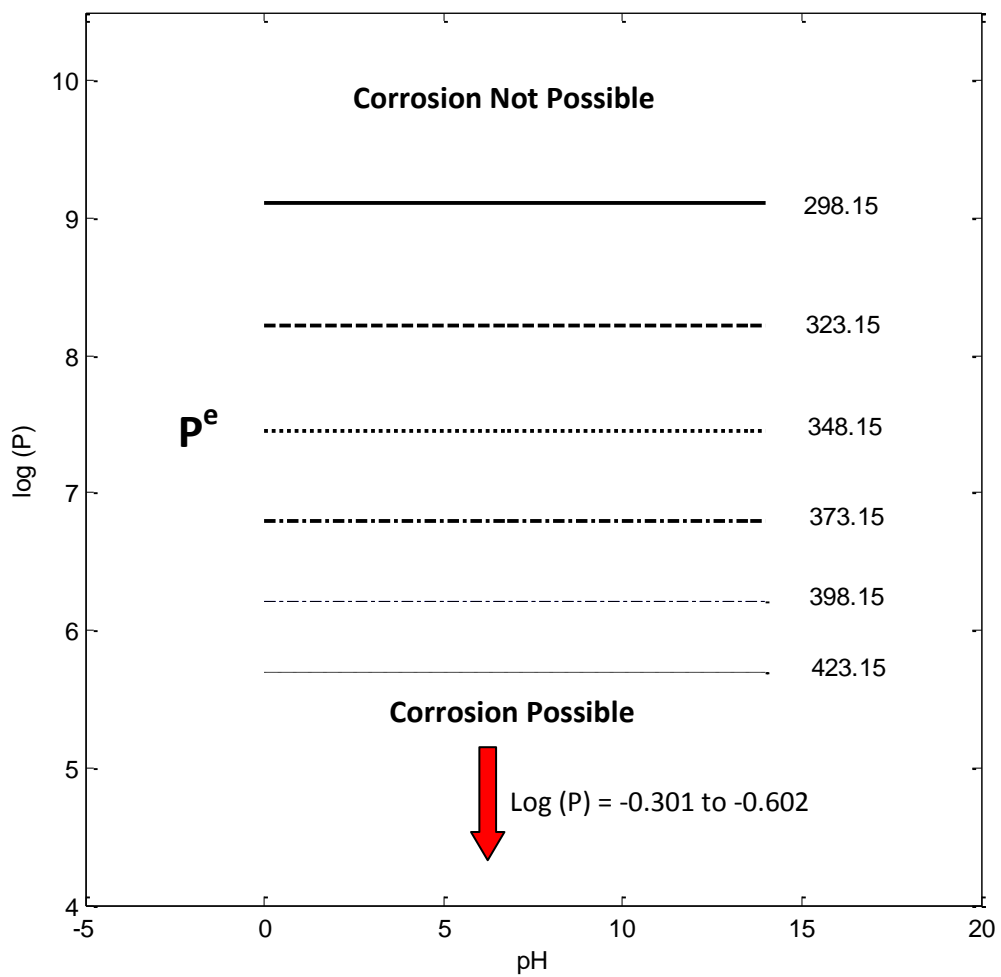
323.15: $\log(p) = 8.22$

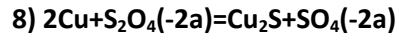
348.15: $\log(p) = 7.45$

373.15: $\log(p) = 6.79$

398.15: $\log(p) = 6.21$

423.15: $\log(p) = 5.70$





$$\log\left(\frac{a_{\text{SO}_4^{2-}}}{a_{\text{S}_2\text{O}_4^{2-}}}\right) = \frac{-\Delta G^0}{2.303RT}$$

298.15: $\log(p) = 39.92$

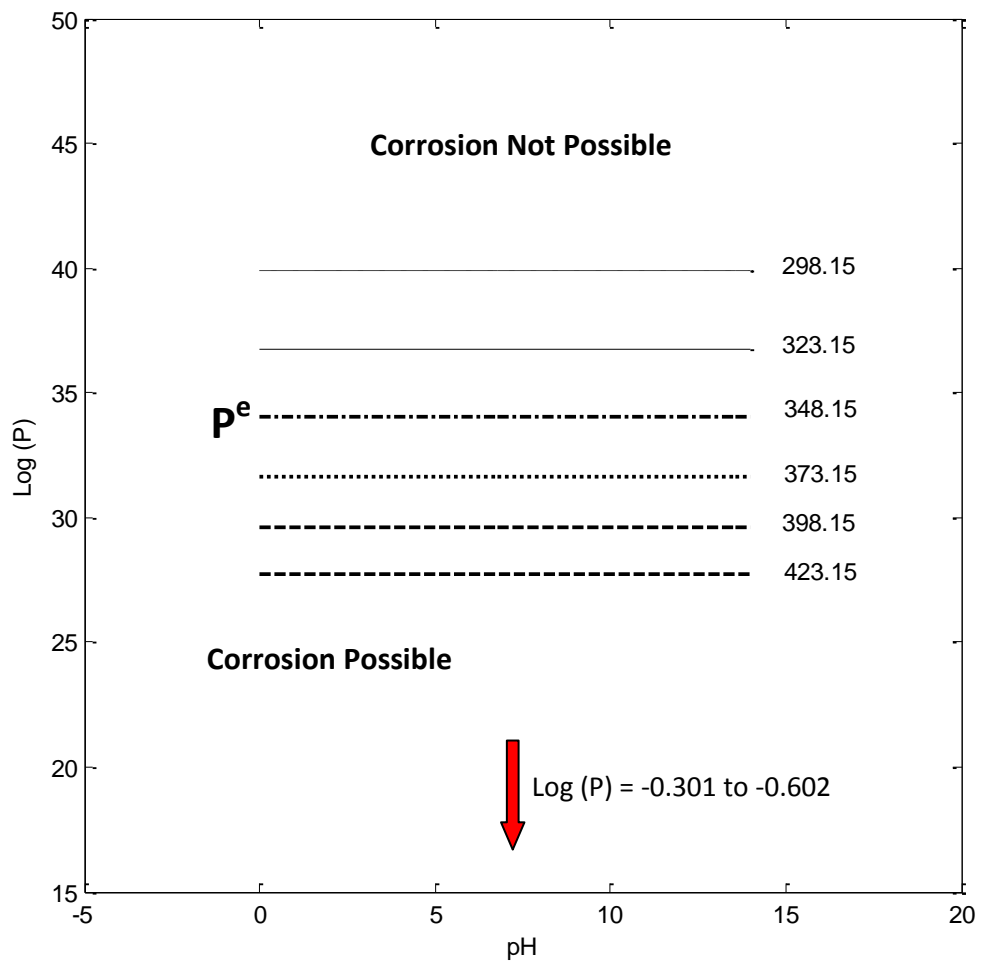
323.15: $\log(p) = 36.74$

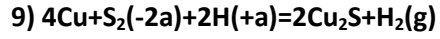
348.15: $\log(p) = 34.01$

373.15: $\log(p) = 31.64$

398.15: $\log(p) = 29.58$

423.15: $\log(p) = 27.75$





$$\log\left(\frac{P_{\text{H}_2(\text{g})}}{a_{\text{S}_2(-2)}}\right) = \frac{-\Delta G^0}{2.303RT} - 2\text{pH}$$

298.15: $\log(p) = 43.08 - 2\text{pH}$

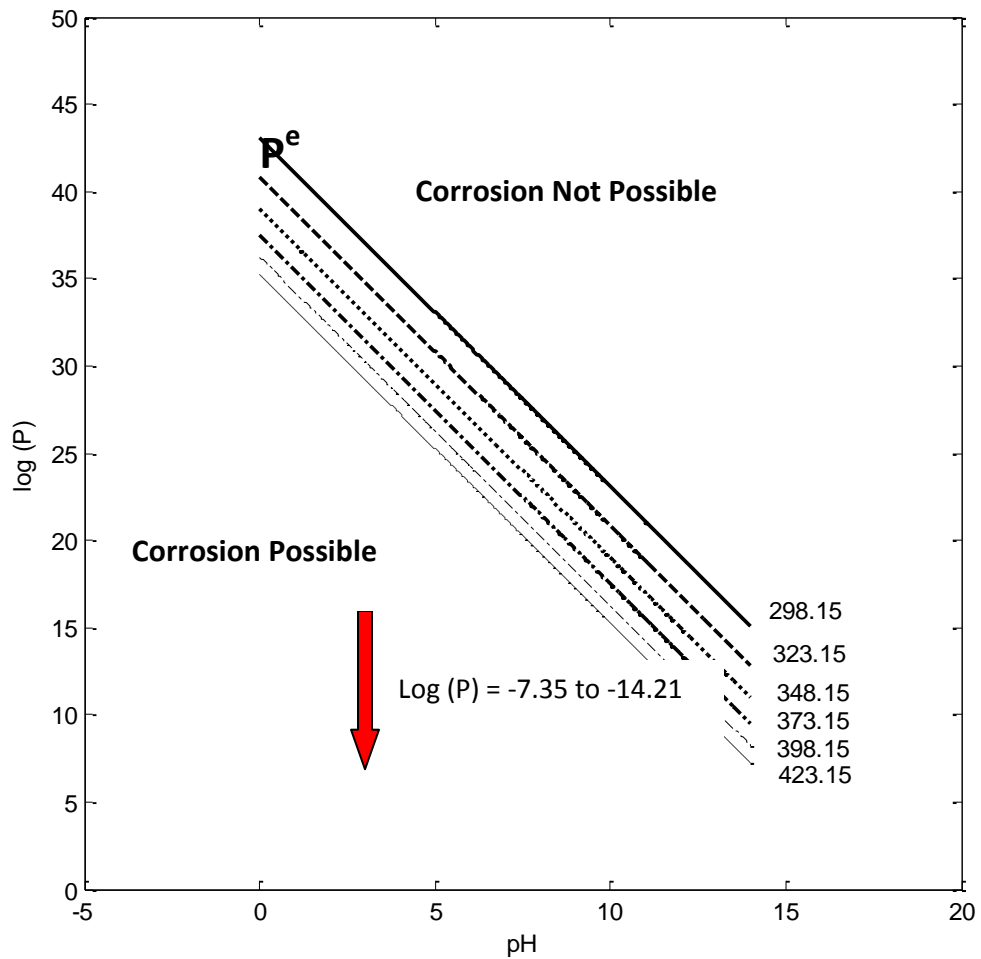
323.15: $\log(p) = 40.82 - 2\text{pH}$

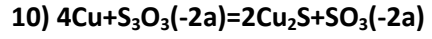
348.15: $\log(p) = 38.98 - 2\text{pH}$

373.15: $\log(p) = 37.48 - 2\text{pH}$

398.15: $\log(p) = 36.25 - 2\text{pH}$

423.15: $\log(p) = 35.25 - 2\text{pH}$





$$\log\left(\frac{a_{\text{SO}_3(-2)}}{a_{\text{S}_3\text{O}_3(-2)}}\right) = \frac{-\Delta G^0}{2.303RT}$$

298.15: $\log(p) = -30.20$

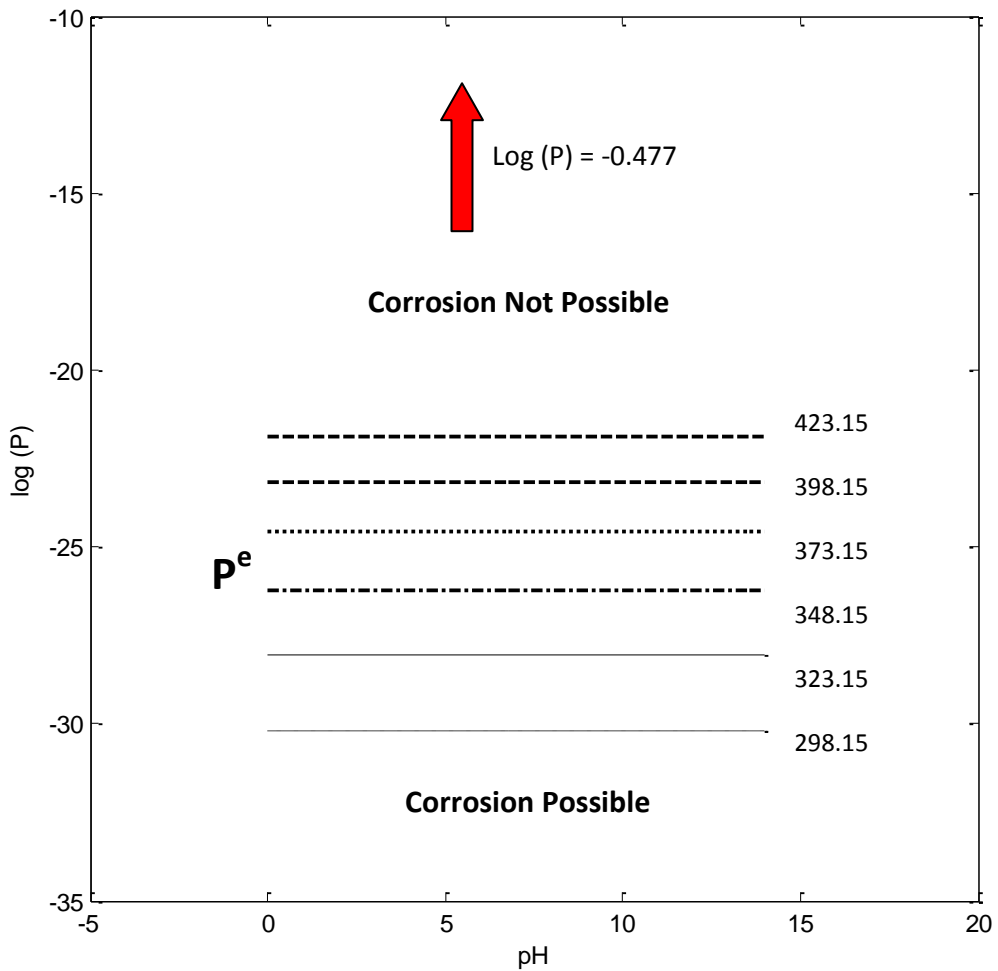
323.15: $\log(p) = -28.06$

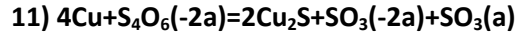
348.15: $\log(p) = -26.21$

373.15: $\log(p) = -24.59$

398.15: $\log(p) = -23.15$

423.15: $\log(p) = -21.88$





$$\log\left(\frac{a_{\text{SO}_3^{2-}}^2 \times a_{\text{SO}_3}}{a_{\text{S}_4\text{O}_6^{2-}}}\right) = \frac{-\Delta G^0}{2.303RT}$$

298.15: $\log(p) = 24.55$

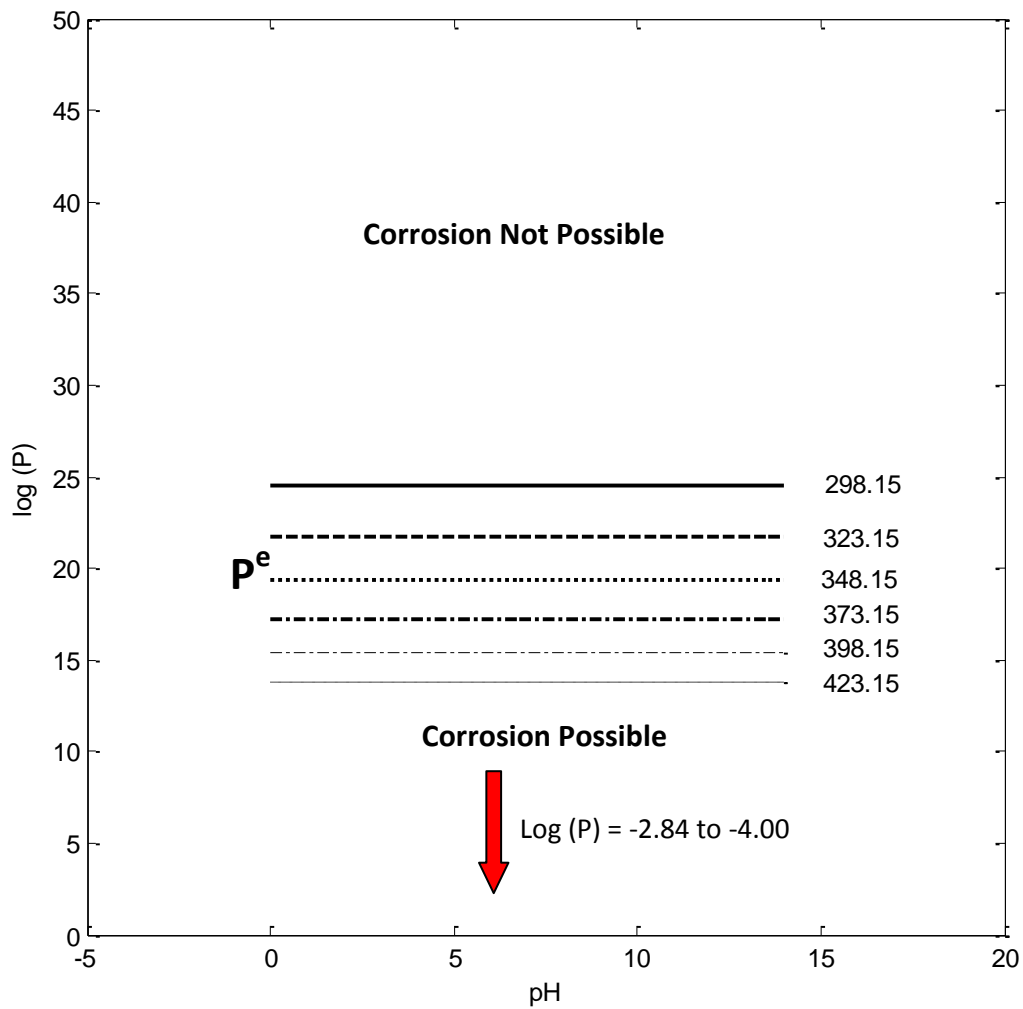
323.15: $\log(p) = 21.76$

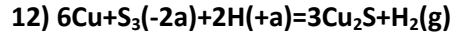
348.15: $\log(p) = 19.35$

373.15: $\log(p) = 17.25$

398.15: $\log(p) = 15.40$

423.15: $\log(p) = 13.75$





$$\log\left(\frac{P_{\text{H}_2(\text{g})}}{a_{\text{S}_3(-2)}}\right) = \frac{-\Delta G^0}{2.303RT} - 2\text{pH}$$

298.15: $\log(p) = 56.74 - 2\text{pH}$

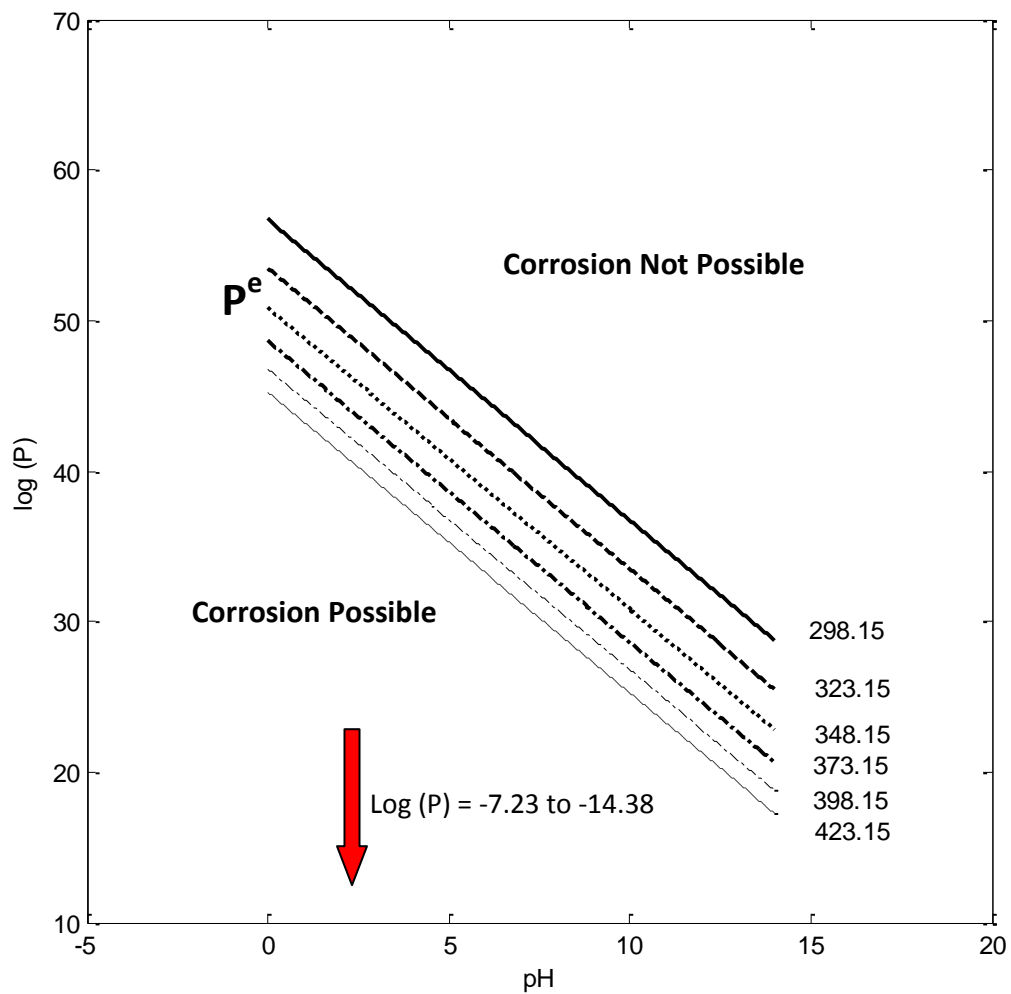
323.15: $\log(p) = 53.50 - 2\text{pH}$

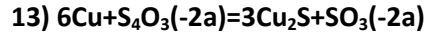
348.15: $\log(p) = 50.84 - 2\text{pH}$

373.15: $\log(p) = 48.64 - 2\text{pH}$

398.15: $\log(p) = 46.80 - 2\text{pH}$

423.15: $\log(p) = 45.27 - 2\text{pH}$





$$\log\left(\frac{a_{\text{SO}_3(-2)}}{a_{\text{S}_4\text{O}_3(-2)}}\right) = \frac{-\Delta G^0}{2.303RT}$$

298.15: $\log(p) = -38.28$

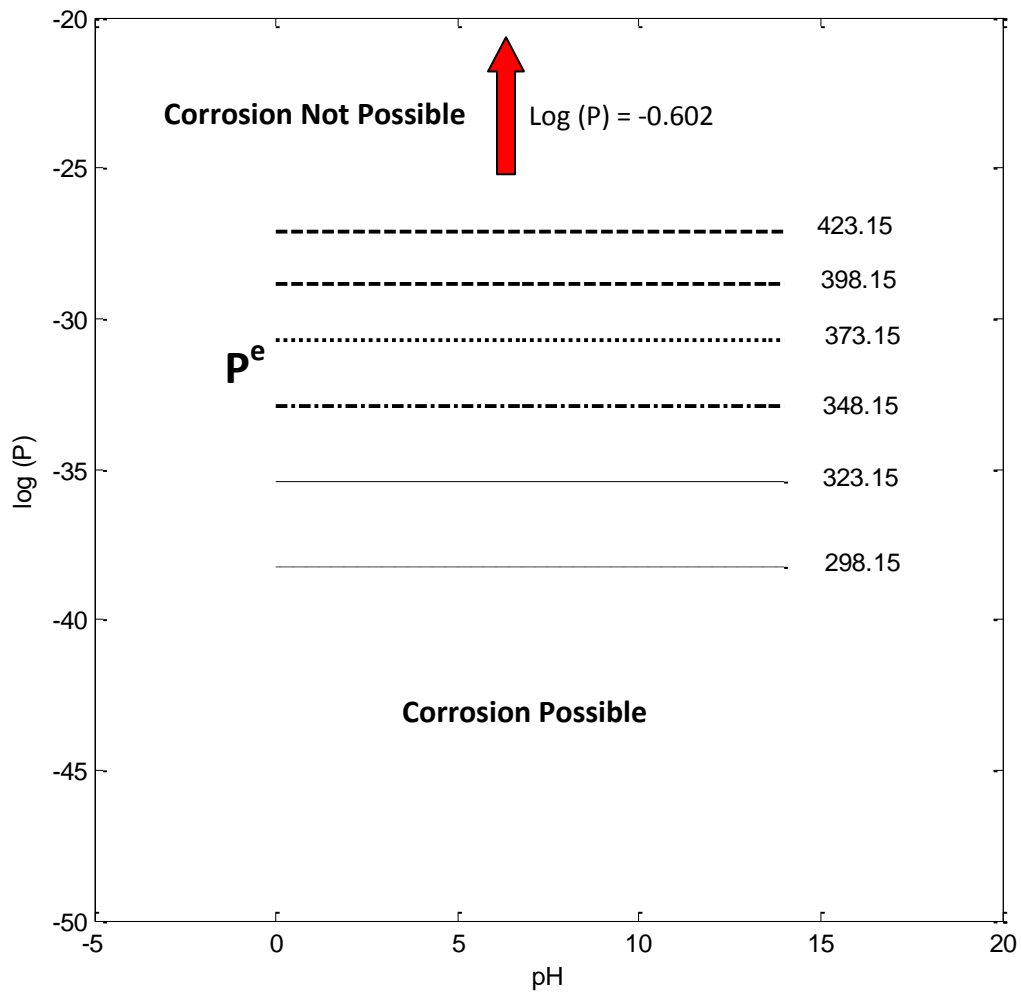
323.15: $\log(p) = -35.39$

348.15: $\log(p) = -32.90$

373.15: $\log(p) = -30.73$

398.15: $\log(p) = -28.82$

423.15: $\log(p) = -27.12$





$$\log\left(\frac{a_{\text{SO}_3(-2)} \times a_{\text{SO}_3}}{a_{\text{S}_5\text{O}_6(-2)}}\right) = \frac{-\Delta G^0}{2.303RT}$$

298.15: $\log(p) = 54.16$

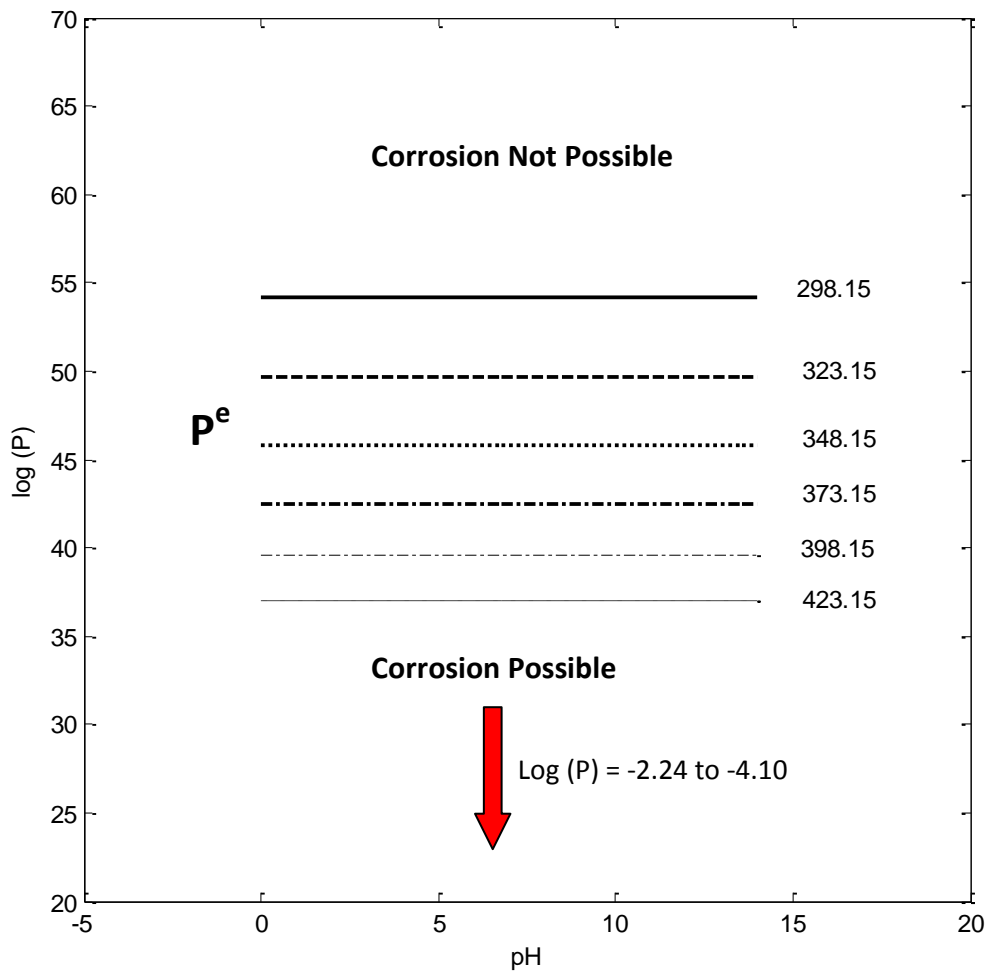
323.15: $\log(p) = 49.66$

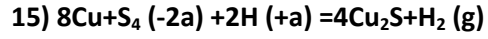
348.15: $\log(p) = 45.81$

373.15: $\log(p) = 42.48$

398.15: $\log(p) = 39.57$

423.15: $\log(p) = 37.00$





$$\log\left(\frac{P_{\text{H}_2(\text{g})}}{a_{\text{S}_4(-2)}}\right) = \frac{-\Delta G^0}{2.303RT} - 2pH$$

298.15: $\log(p) = 68.81 - 2pH$

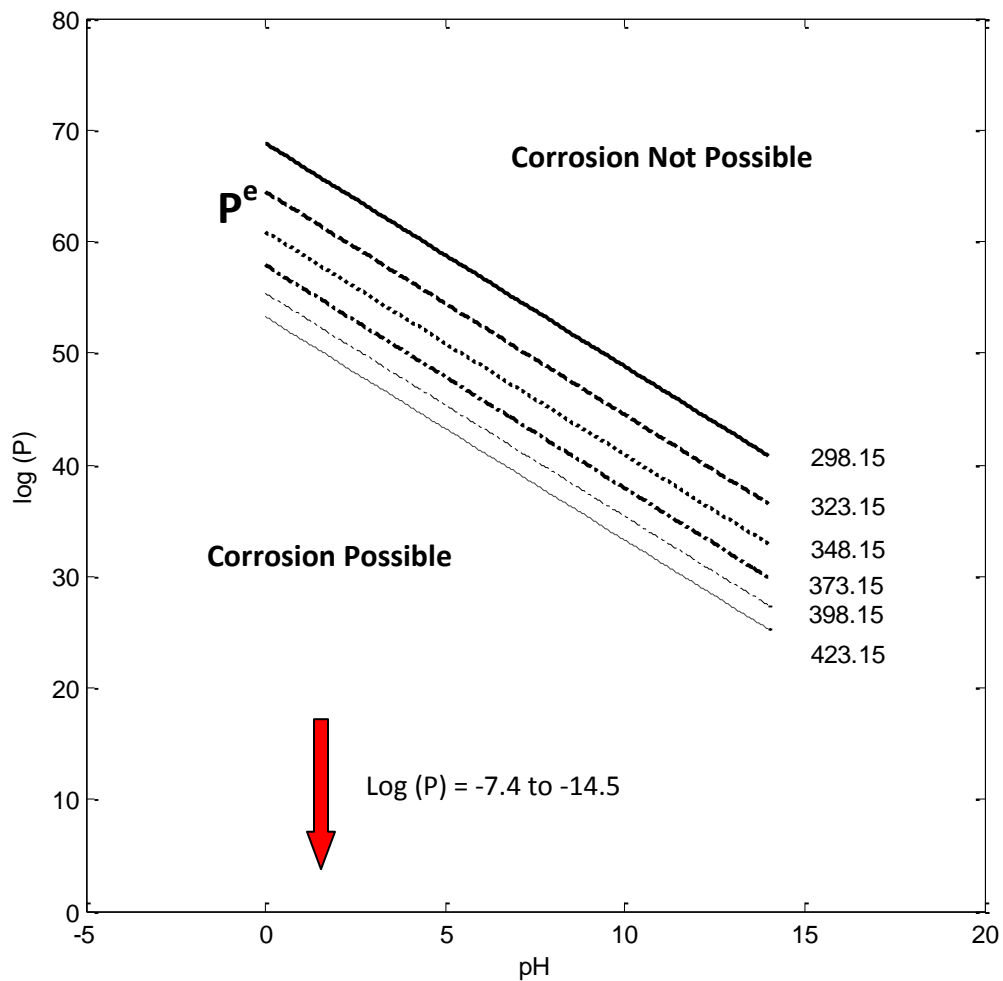
323.15: $\log(p) = 64.48 - 2pH$

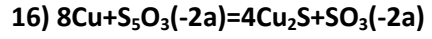
348.15: $\log(p) = 60.90 - 2pH$

373.15: $\log(p) = 57.90 - 2pH$

398.15: $\log(p) = 55.38 - 2pH$

423.15: $\log(p) = 53.26 - 2pH$





$$\log\left(\frac{a_{\text{SO}_3(-2)}}{a_{\text{S}_5\text{O}_3(-2)}}\right) = \frac{-\Delta G^0}{2.303RT}$$

298.15: $\log(p) = -36.28$

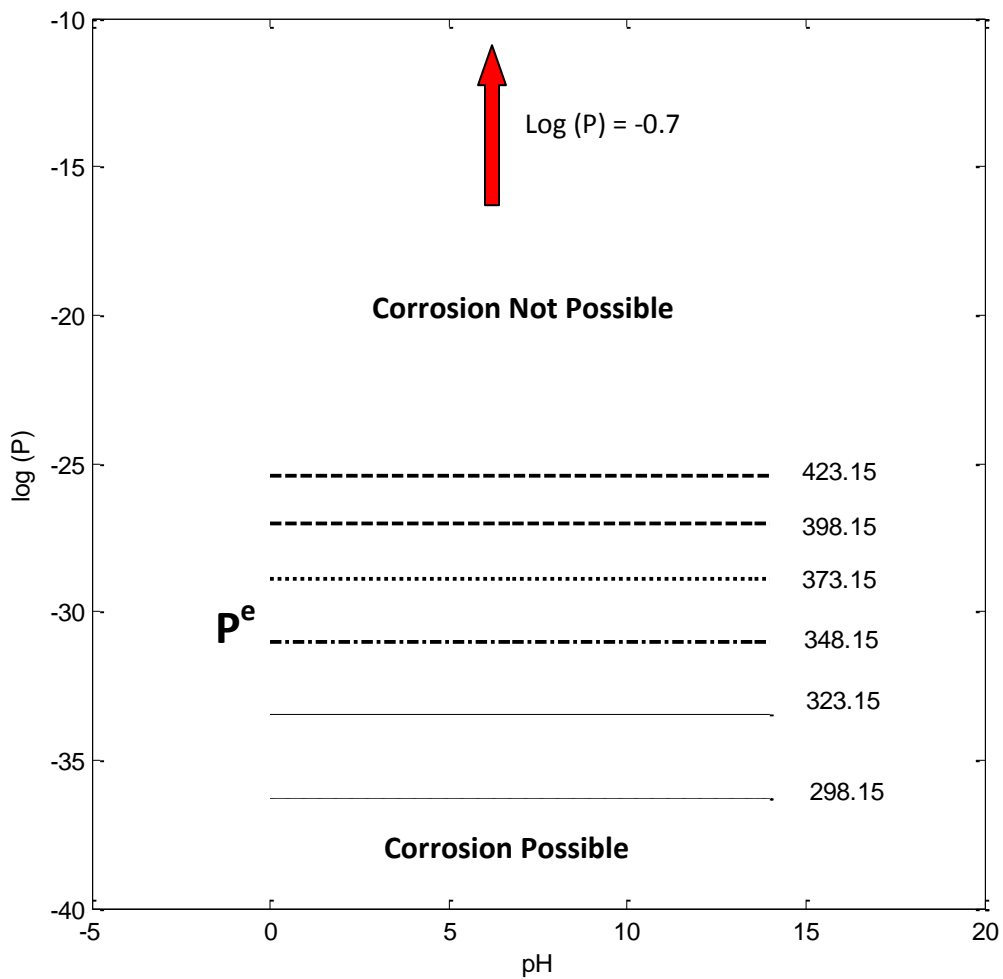
323.15: $\log(p) = -33.45$

348.15: $\log(p) = -31.01$

373.15: $\log(p) = -28.90$

398.15: $\log(p) = -27.03$

423.15: $\log(p) = -25.39$





$$\log\left(\frac{a_{\text{SO}_3^{(-2)}} \times a_{\text{SO}_3}}{a_{\text{S}_6\text{O}_6^{(-2)}}}\right) = \frac{-\Delta G^0}{2.303RT}$$

298.15: $\log(p) = 26.56$

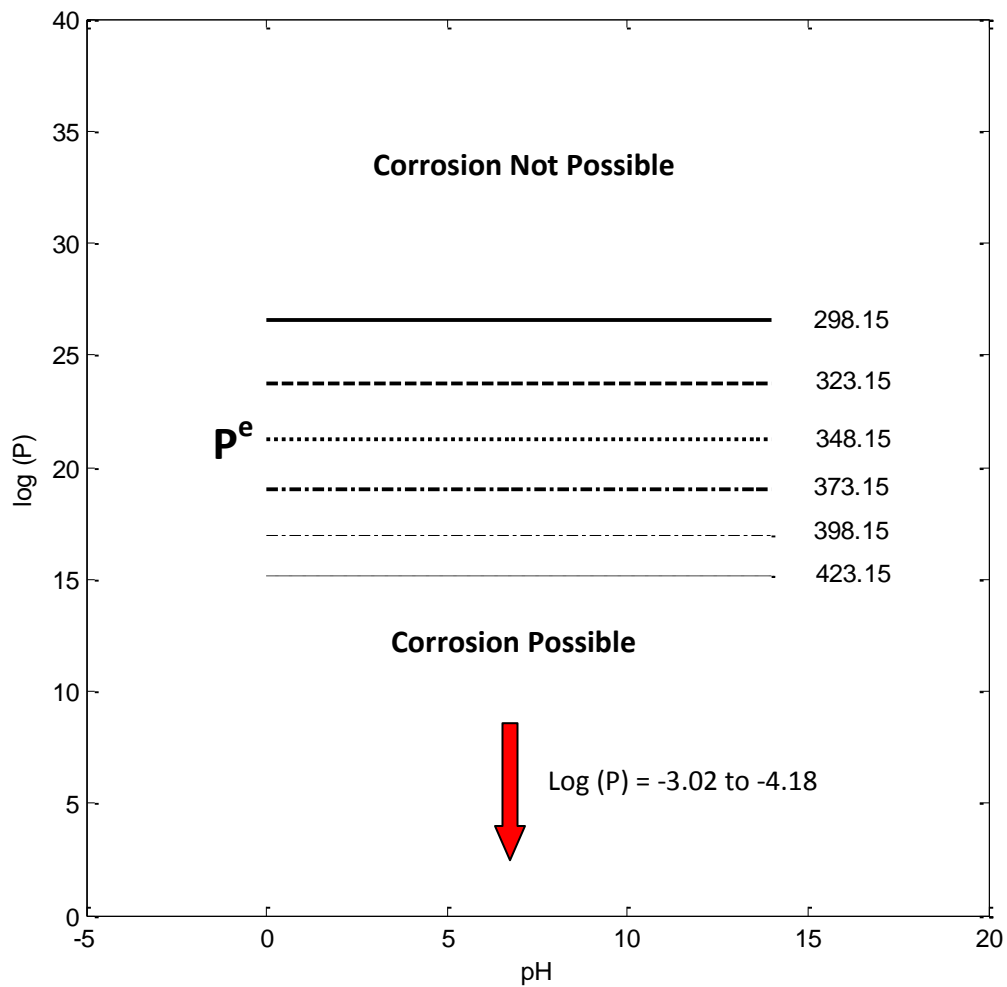
323.15: $\log(p) = 23.73$

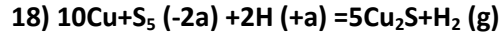
348.15: $\log(p) = 21.23$

373.15: $\log(p) = 19.00$

398.15: $\log(p) = 16.98$

423.15: $\log(p) = 15.13$





$$\log\left(\frac{P_{\text{H}_2(\text{g})}}{a_{\text{S}_5(-2)}}\right) = \frac{-\Delta G^0}{2.303RT} - 2\text{pH}$$

298.15: $\log (p) = 85.35 - 2\text{pH}$

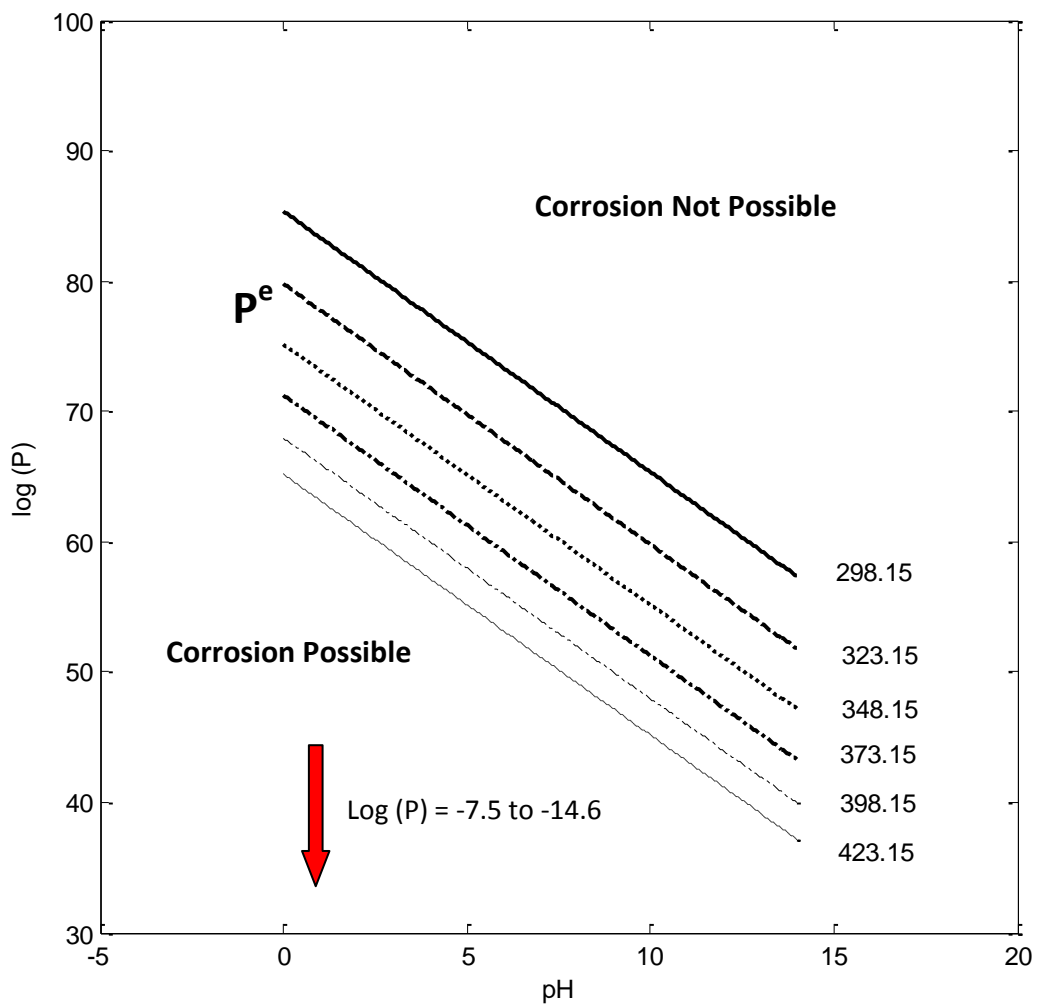
323.15: $\log (p) = 79.79 - 2\text{pH}$

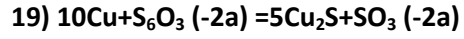
348.15: $\log (p) = 75.16 - 2\text{pH}$

373.15: $\log (p) = 71.27 - 2\text{pH}$

398.15: $\log (p) = 67.98 - 2\text{pH}$

423.15: $\log (p) = 65.18 - 2\text{pH}$





$$\log\left(\frac{a_{\text{SO}_3(-2)}}{a_{\text{S}_6\text{O}_3(-2)}}\right) = \frac{-\Delta G^0}{2.303RT}$$

298.15: $\log(p) = -29.30$

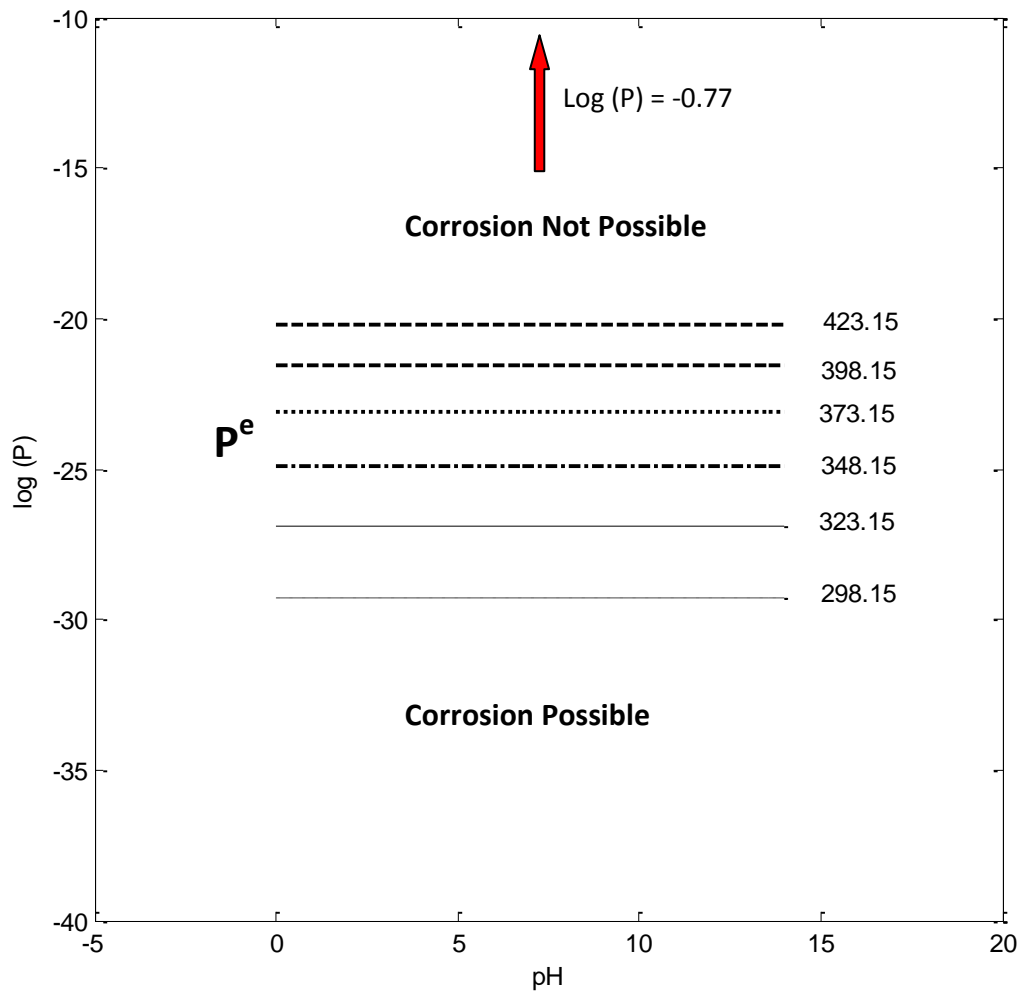
323.15: $\log(p) = -26.93$

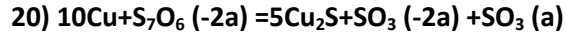
348.15: $\log(p) = -24.89$

373.15: $\log(p) = -23.12$

398.15: $\log(p) = -21.56$

423.15: $\log(p) = -20.19$





$$\log\left(\frac{a_{\text{SO}_3(-2)} \times a_{\text{SO}_3}}{a_{\text{S}_7\text{O}_6(-2)}}\right) = \frac{-\Delta G^0}{2.303RT}$$

298.15: $\log(p) = 34.57$

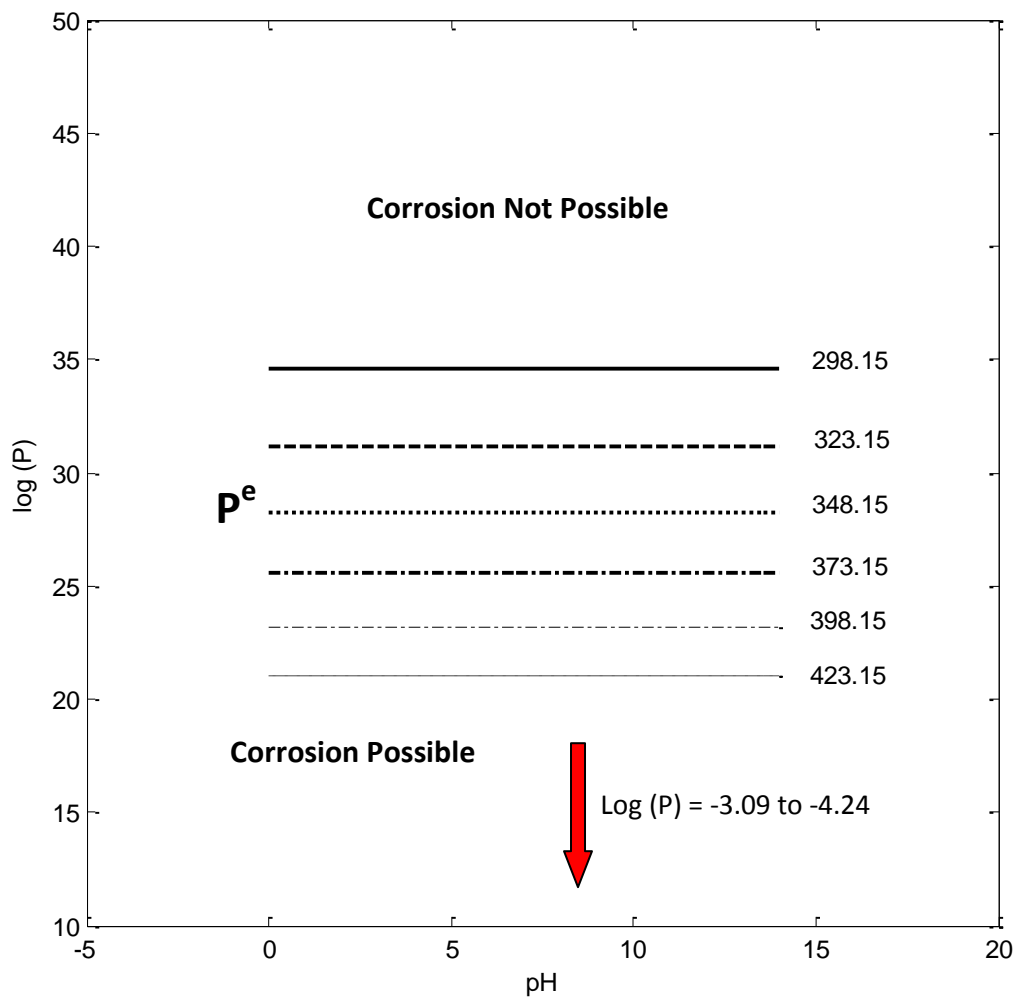
323.15: $\log(p) = 31.20$

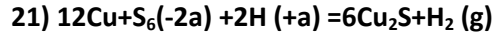
348.15: $\log(p) = 28.24$

373.15: $\log(p) = 25.59$

398.15: $\log(p) = 23.21$

423.15: $\log(p) = 21.04$





$$\log\left(\frac{P_{\text{H}_2(\text{g})}}{a_{\text{S}_6(-2)}}\right) = \frac{-\Delta G^0}{2.303RT} - 2\text{pH}$$

298.15: $\log(p) = 100.35 - 2\text{pH}$

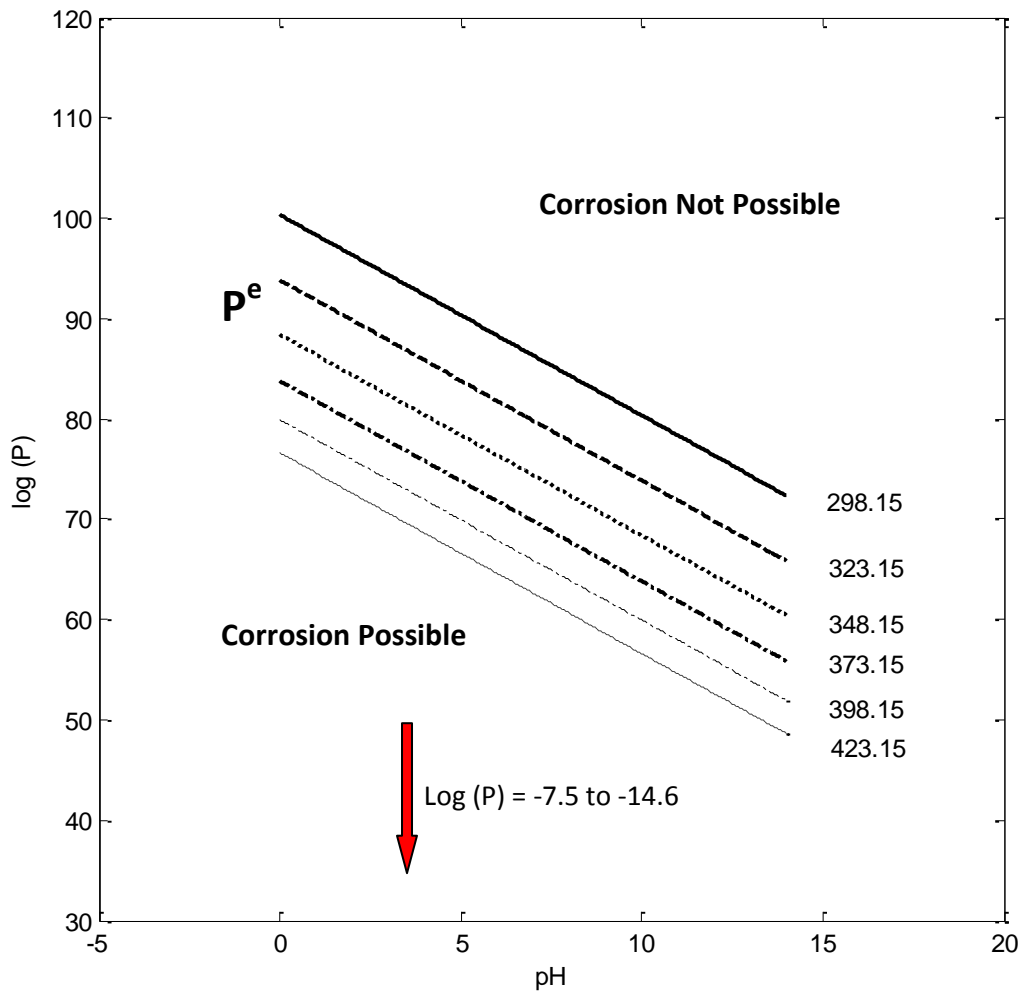
323.15: $\log(p) = 93.84 - 2\text{pH}$

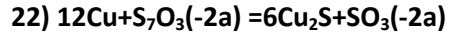
348.15: $\log(p) = 88.40 - 2\text{pH}$

373.15: $\log(p) = 83.82 - 2\text{pH}$

398.15: $\log(p) = 79.94 - 2\text{pH}$

423.15: $\log(p) = 76.62 - 2\text{pH}$





$$\log\left(\frac{a_{\text{SO}_3(-2)}}{a_{\text{S}_7\text{O}_3(-2)}}\right) = \frac{-\Delta G^0}{2.303RT}$$

298.15: $\log(p) = -19.89$

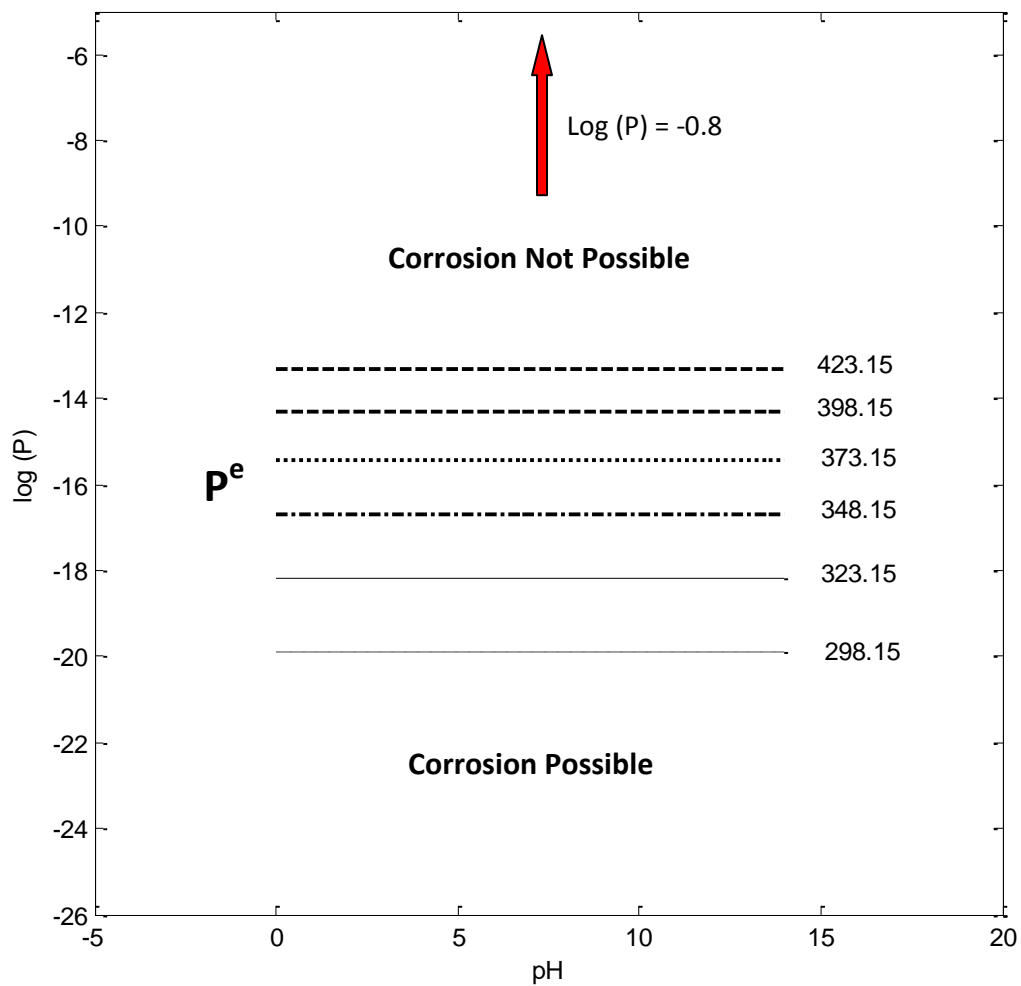
323.15: $\log(p) = -18.17$

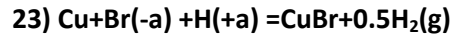
348.15: $\log(p) = -16.69$

373.15: $\log(p) = -15.41$

398.15: $\log(p) = -14.29$

423.15: $\log(p) = -13.31$





$$\log \left(\frac{P^{0.5}_{\text{H}_2(\text{g})}}{a_{\text{Br}(-1)}} \right) = \frac{-\Delta G^0}{2.303RT} - pH$$

298.15: $\log (p) = -0.52 - pH$

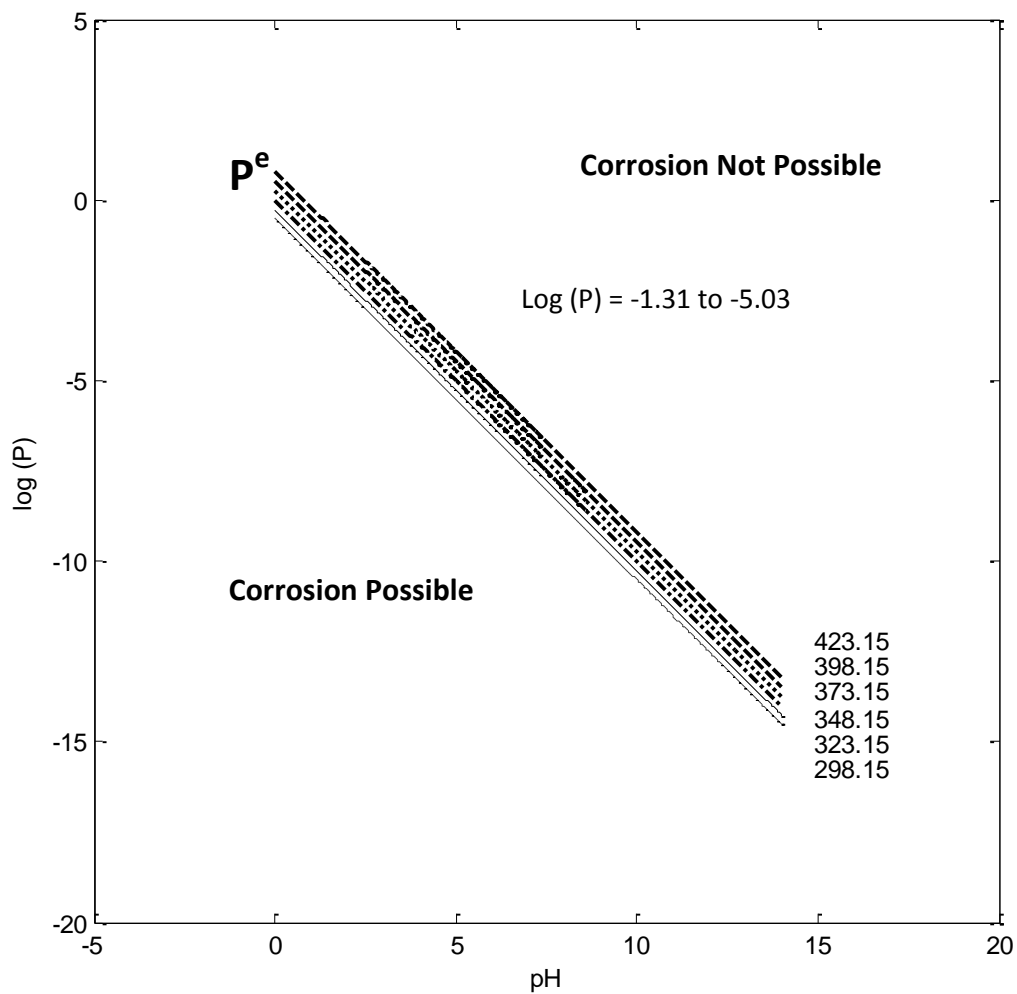
323.15: $\log (p) = -0.27 - pH$

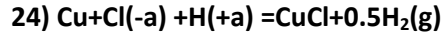
348.15: $\log (p) = -0.01 - pH$

373.15: $\log (p) = 0.26 - pH$

398.15: $\log (p) = 0.53 - pH$

423.15: $\log (p) = 0.80 - pH$





$$\log \left(\frac{P^{0.5}_{\text{H}_2(\text{g})}}{a_{\text{Cl}(-1)}} \right) = \frac{-\Delta G^0}{2.303RT} - pH$$

298.15: $\log (p) = -44.01 - pH$

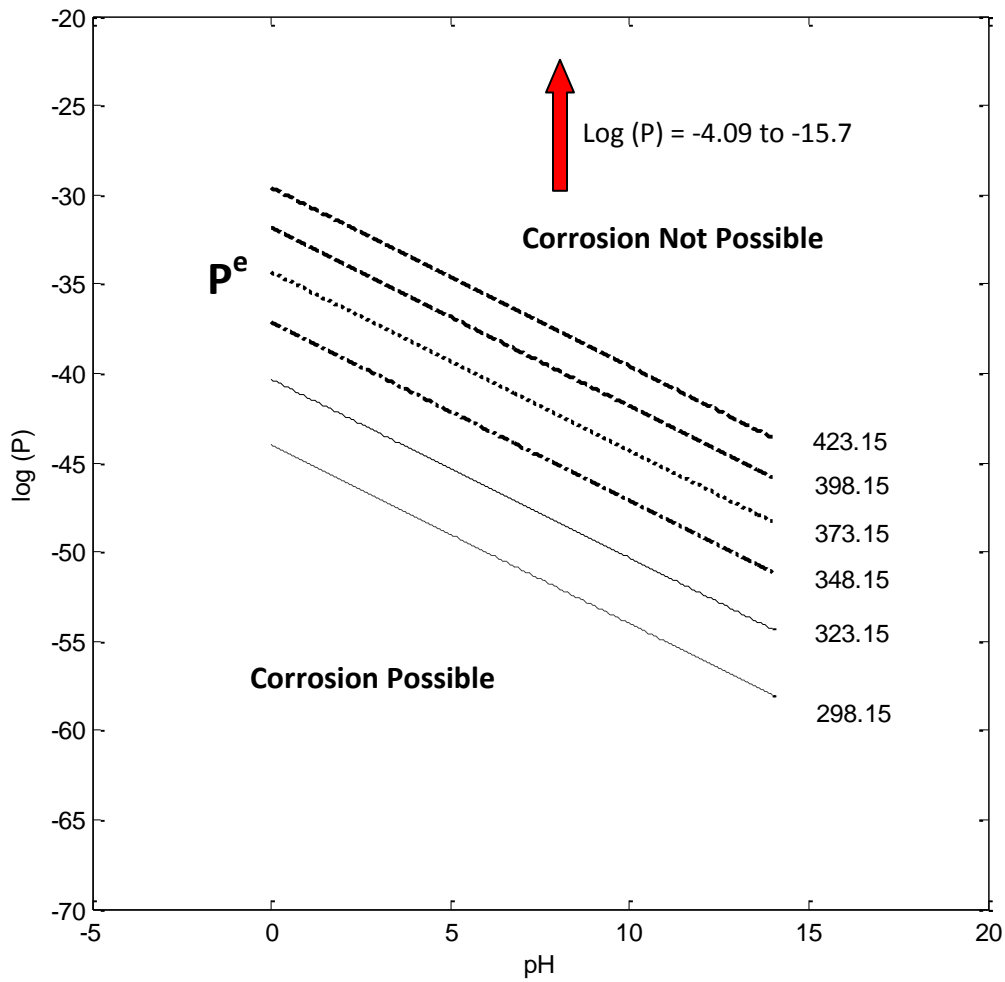
323.15: $\log (p) = -40.33 - pH$

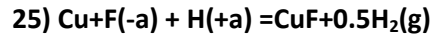
348.15: $\log (p) = -37.13 - pH$

373.15: $\log (p) = -34.32 - pH$

398.15: $\log (p) = -31.83 - pH$

423.15: $\log (p) = -29.60 - pH$





$$\log \left(\frac{P^{0.5} \text{H}_2(\text{g})}{a_{\text{F}(-1)}} \right) = \frac{-\Delta G^0}{2.303RT} - pH$$

298.15: $\log (p) = -15.68 - pH$

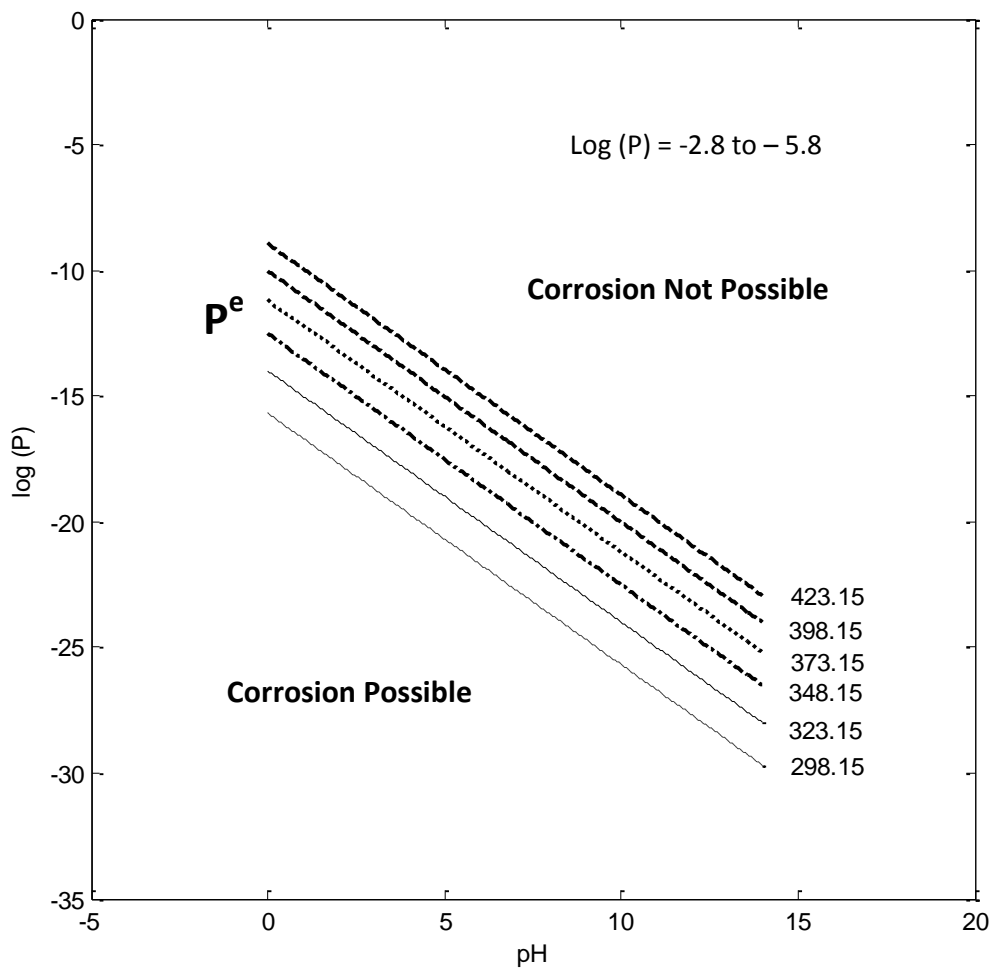
323.15: $\log (p) = -13.99 - pH$

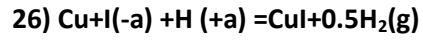
348.15: $\log (p) = -12.51 - pH$

373.15: $\log (p) = -11.19 - pH$

398.15: $\log (p) = -10.01 - pH$

423.15: $\log (p) = -8.93 - pH$





$$\log \left(\frac{P_{\text{H}_2(\text{g})}^{0.5}}{a_{\text{I}(-a)}} \right) = \frac{-\Delta G^0}{2.303RT} - pH$$

298.15: $\log (p) = 3.81 - pH$

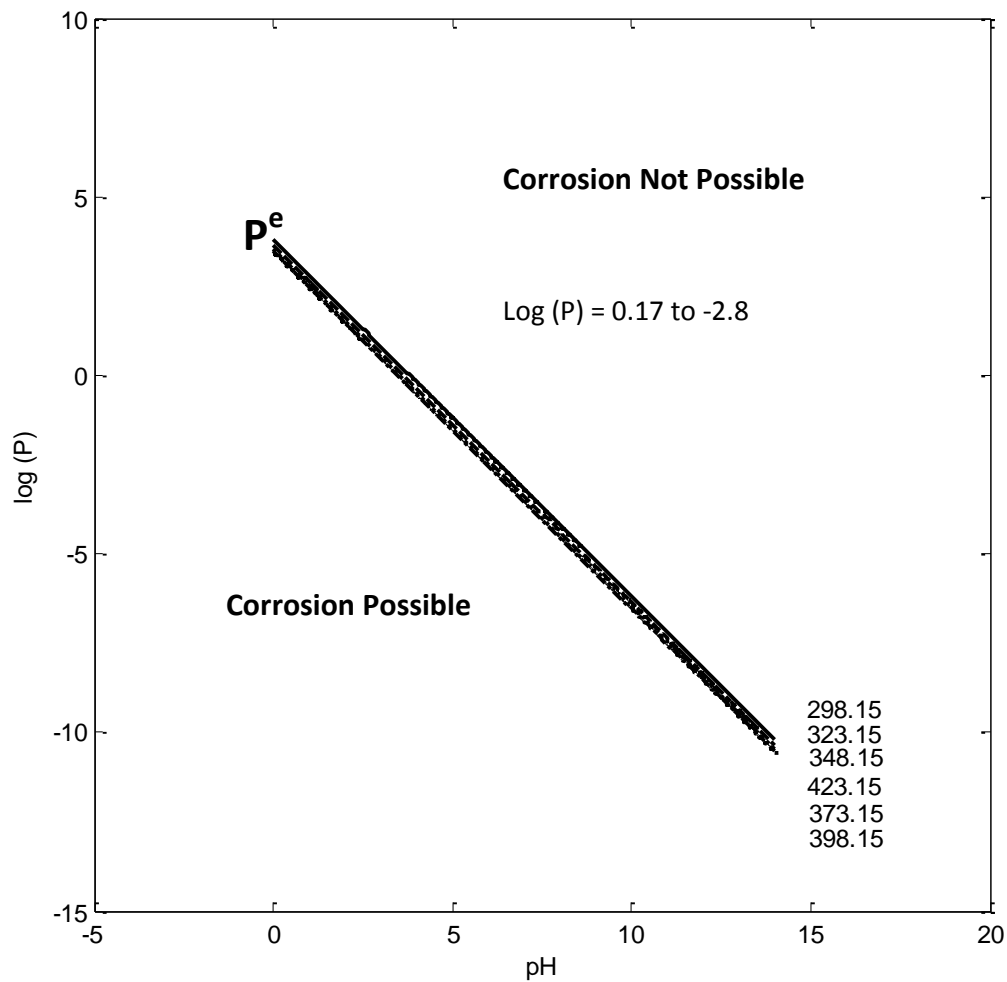
323.15: $\log (p) = 3.63 - pH$

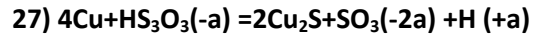
348.15: $\log (p) = 3.52 - pH$

373.15: $\log (p) = 3.46 - pH$

398.15: $\log (p) = 3.45 - pH$

423.15: $\log (p) = 3.47 - pH$





$$\log\left(\frac{a_{\text{SO}_3(2-)}}{a_{\text{HS}_3\text{O}_3(1-)}}\right) = \frac{-\Delta G^0}{2.303RT} + pH$$

298.15: $\log(p) = 32.12 + pH$

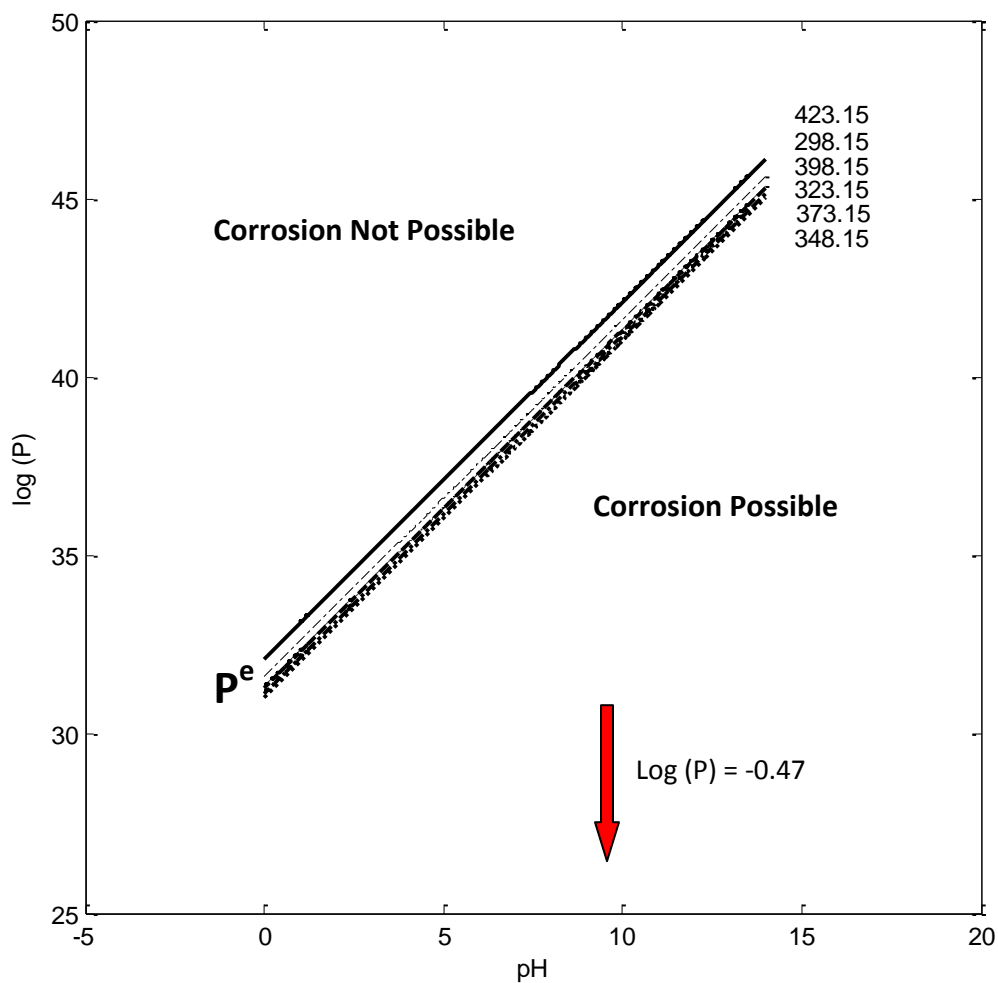
323.15: $\log(p) = 31.32 + pH$

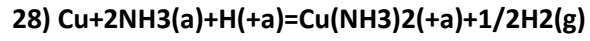
348.15: $\log(p) = 31.04 + pH$

373.15: $\log(p) = 31.16 + pH$

398.15: $\log(p) = 31.62 + pH$

423.15: $\log(p) = 32.35 + pH$





$$\log \left(\frac{a_{[\text{Cu}(\text{NH}_3)_2^+]} \times P_{\text{H}_2}^{0.5}}{a_{(\text{NH}_3)}^2} \right) = \frac{-\Delta G^0}{2.303RT} - pH$$

298.15: $\log (p) = 2.391 - pH$

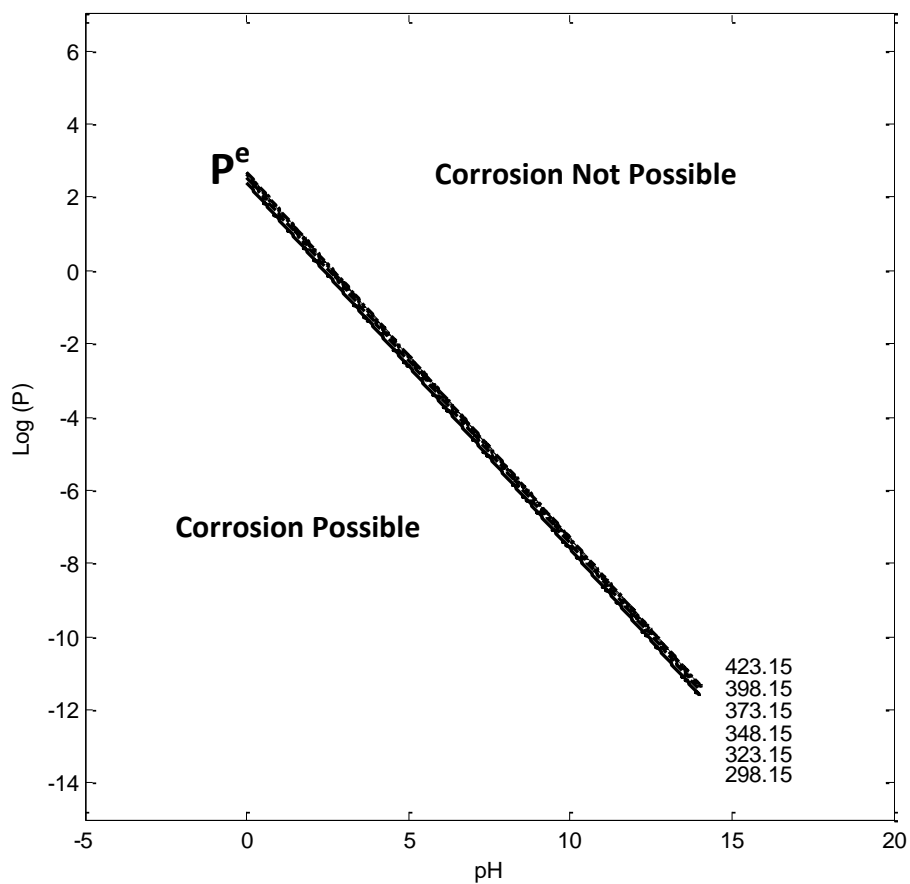
323.15: $\log (p) = 2.543 - pH$

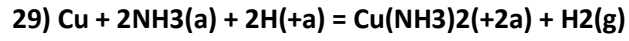
348.15: $\log (p) = 2.634 - pH$

373.15: $\log (p) = 2.678 - pH$

398.15: $\log (p) = 2.684 - pH$

423.15: $\log (p) = 2.661 - pH$





$$\log \left(\frac{a_{[\text{Cu}(\text{NH}_3)_2^{2+}] \times P_{\text{H}_2}}}{a_{(\text{NH}_3)}^2} \right) = \frac{-\Delta G^0}{2.303RT} - 2\text{pH}$$

298.15: $\log (p) = -3.442 - 2\text{pH}$

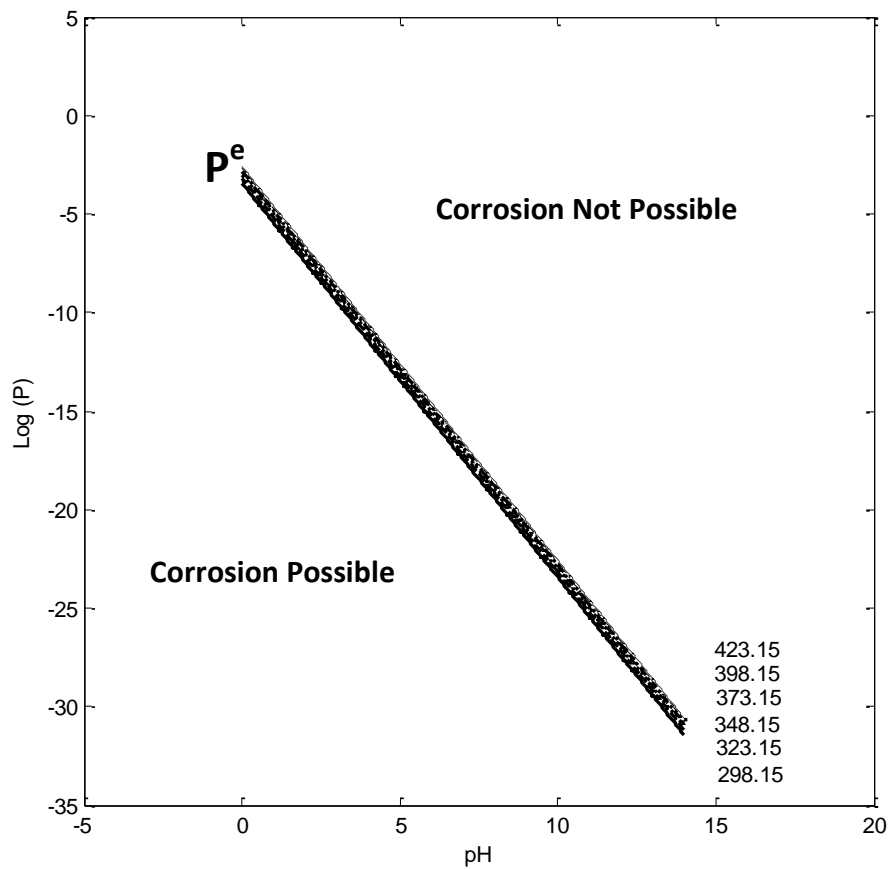
323.15: $\log (p) = -3.204 - 2\text{pH}$

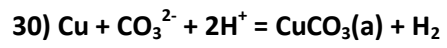
348.15: $\log (p) = -3.007 - 2\text{pH}$

373.15: $\log (p) = -2.842 - 2\text{pH}$

398.15: $\log (p) = -2.702 - 2\text{pH}$

423.15: $\log (p) = -2.581 - 2\text{pH}$





$$\log\left(\frac{p_{\text{H}_2} \times a_{\text{CuCO}_3}}{a_{\text{CO}_3^{2-}}}\right) = \frac{-\Delta G^0}{2.303RT} - 2\text{pH}$$

298.15: $\log(p) = -4.63 - 2\text{pH}$

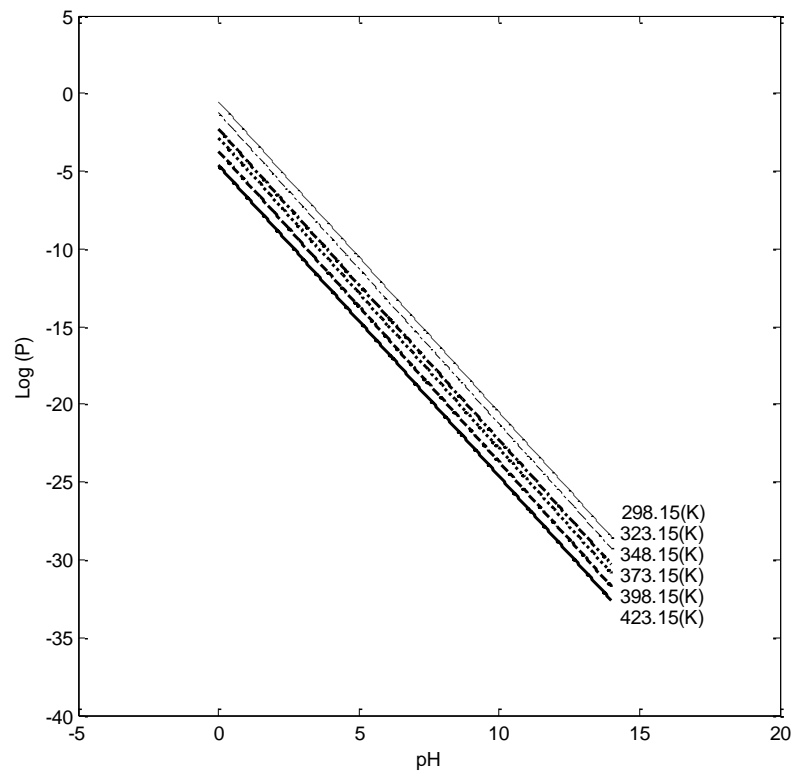
323.15: $\log(p) = -3.70 - 2\text{pH}$

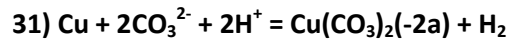
348.15: $\log(p) = -2.84 - 2\text{pH}$

373.15: $\log(p) = -2.30 - 2\text{pH}$

398.15: $\log(p) = -1.26 - 2\text{pH}$

423.15: $\log(p) = -0.52 - 2\text{pH}$





$$\log\left(\frac{p_{\text{H}_2} \times a_{\text{Cu}(\text{CO}_3)_2(-2)}}{a_{\text{CO}_3^{2-}}^2}\right) = \frac{-\Delta G^0}{2.303RT} - 2\text{pH}$$

$$298.15: \log(p) = -1.20 - 2\text{pH}$$

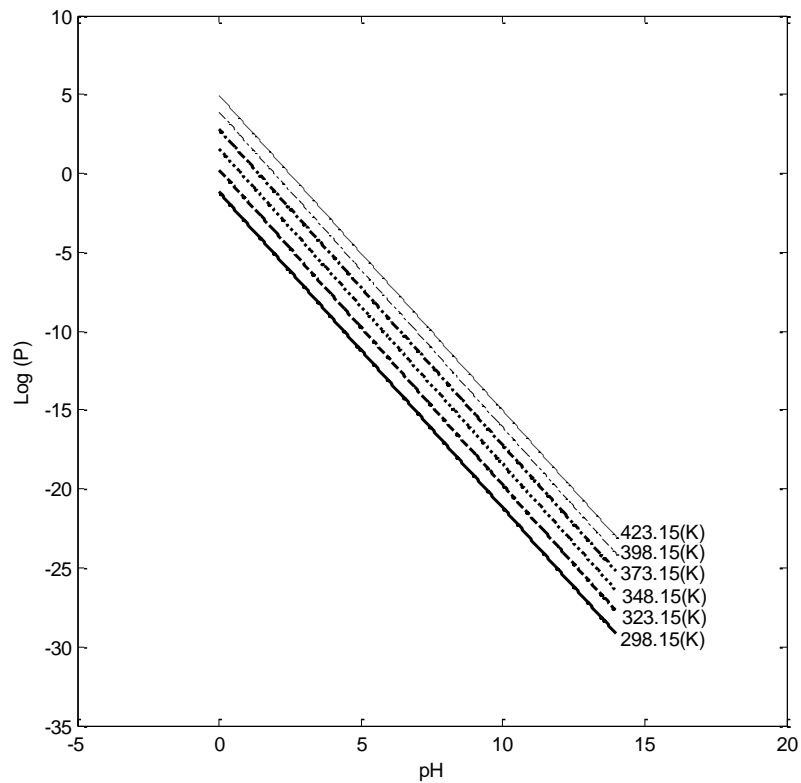
$$323.15: \log(p) = 0.24 - 2\text{pH}$$

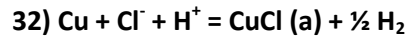
$$348.15: \log(p) = 1.56 - 2\text{pH}$$

$$373.15: \log(p) = 2.77 - 2\text{pH}$$

$$398.15: \log(p) = 3.89 - 2\text{pH}$$

$$423.15: \log(p) = 4.95 - 2\text{pH}$$





$$\log\left(\frac{p_{\text{H}_2}^{0.5} \times a_{\text{CuCl}}}{a_{\text{Cl}(-)}}\right) = \frac{-\Delta G^0}{2.303RT} - \text{pH}$$

298.15: $\log (p) = -5.27\text{-pH}$

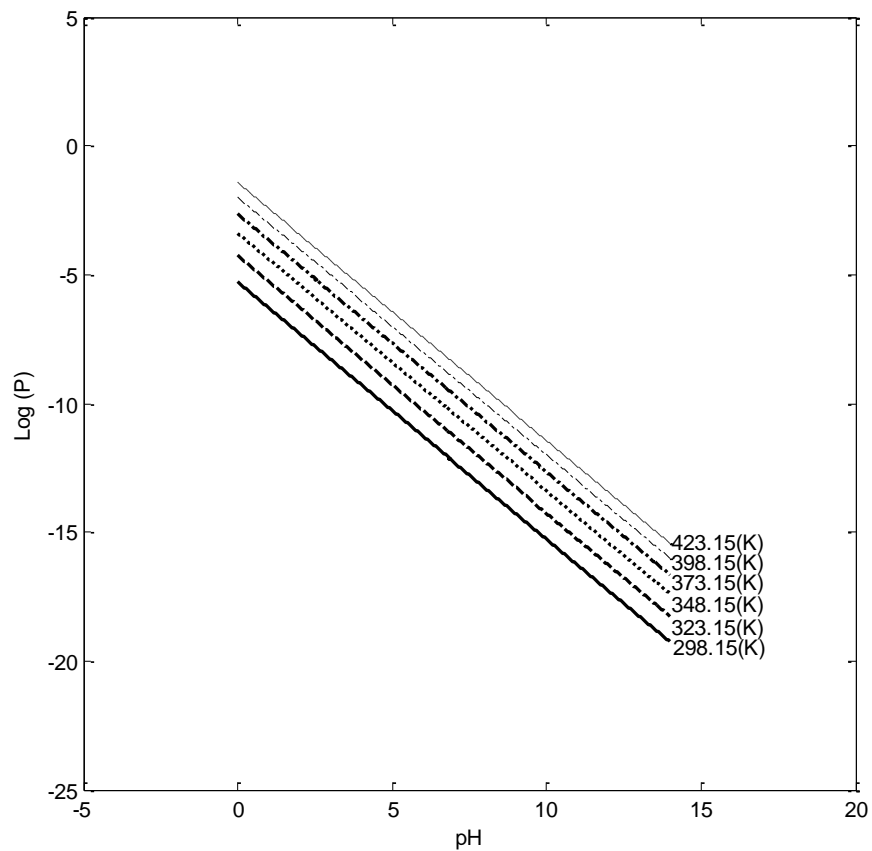
323.15: $\log (p) = -4.26\text{-pH}$

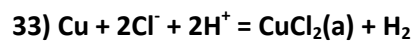
348.15: $\log (p) = -3.39\text{-pH}$

373.15: $\log (p) = -2.65\text{-pH}$

398.15: $\log (p) = -2.00\text{-pH}$

423.15: $\log (p) = -1.43\text{-pH}$





$$\log\left(\frac{p_{\text{H}_2} \times a_{\text{CuCl}_2}}{a_{\text{Cl}^-}^2}\right) = \frac{-\Delta G^0}{2.303RT} - 2\text{pH}$$

298.15: $\log(p) = -11.17 - 2\text{pH}$

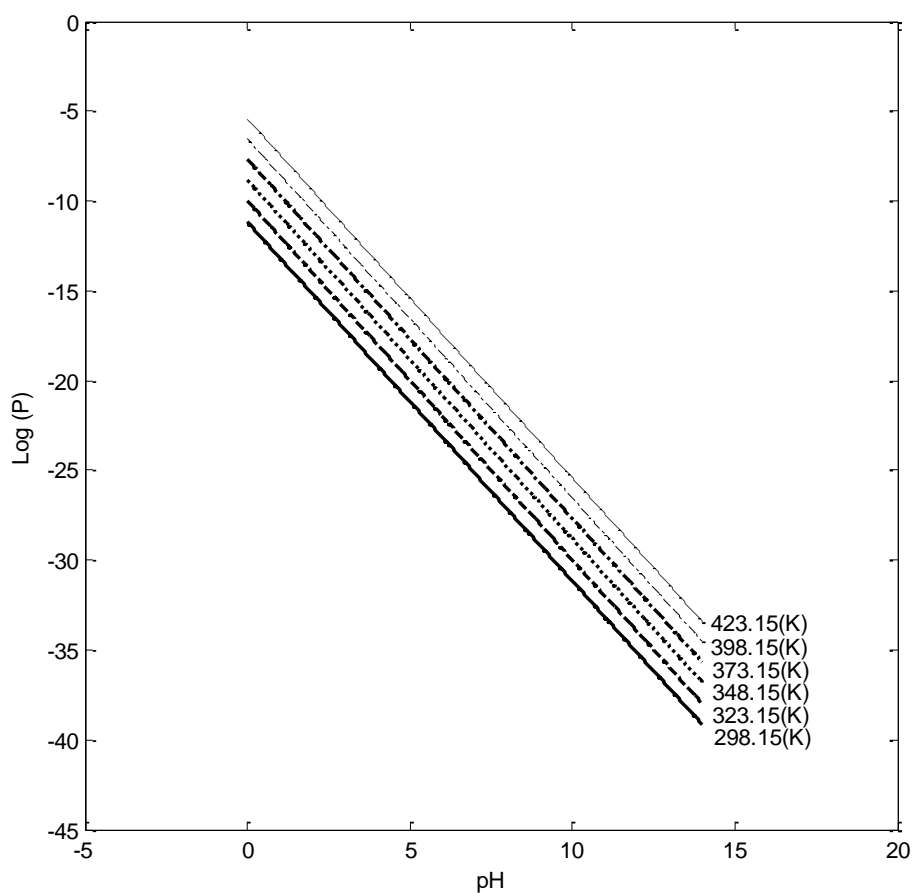
323.15: $\log(p) = -9.99 - 2\text{pH}$

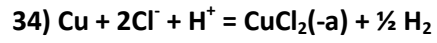
348.15: $\log(p) = -8.82 - 2\text{pH}$

373.15: $\log(p) = -7.68 - 2\text{pH}$

398.15: $\log(p) = -6.54 - 2\text{pH}$

423.15: $\log(p) = -5.42 - 2\text{pH}$





$$\log\left(\frac{p_{\text{H}_2}^{0.5} \times a_{\text{CuCl}_2(\text{-})}}{a_{\text{Cl}(\text{-})}^2}\right) = \frac{-\Delta G^0}{2.303RT} - \text{pH}$$

298.15: $\log(p) = -2.96\text{-pH}$

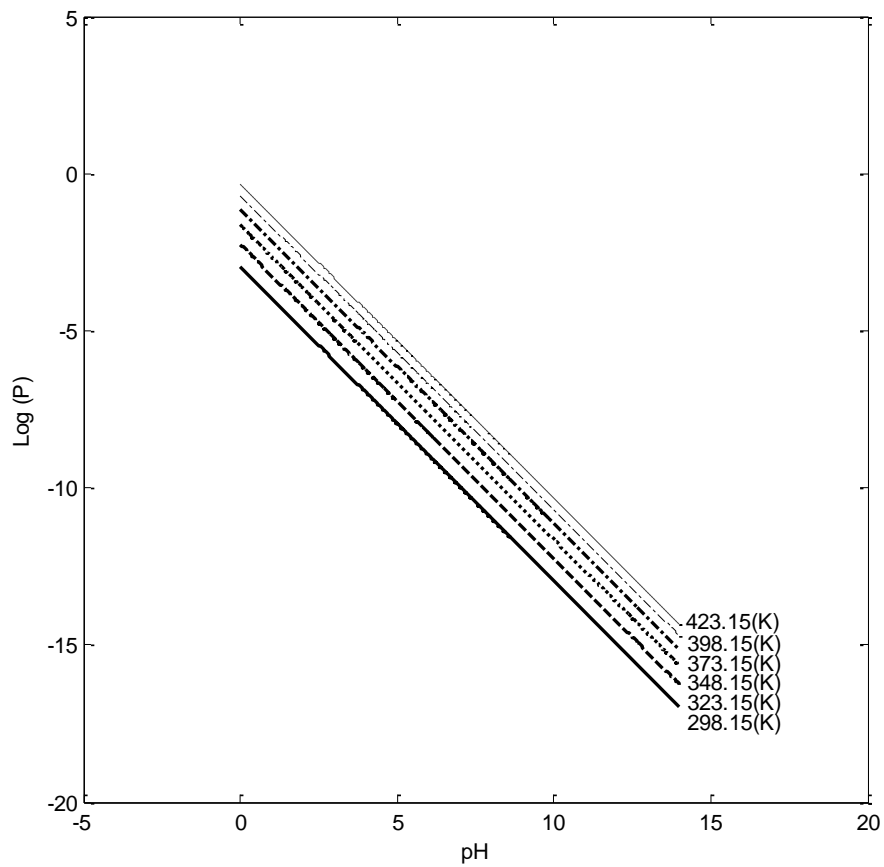
323.15: $\log(p) = -2.25\text{-pH}$

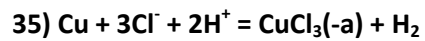
348.15: $\log(p) = -1.65\text{-pH}$

373.15: $\log(p) = -1.14\text{-pH}$

398.15: $\log(p) = -0.70\text{-pH}$

423.15: $\log(p) = -0.33\text{-pH}$





$$\log\left(\frac{p_{\text{H}_2} \times a_{\text{CuCl}_3(-)}}{a_{\text{Cl}(-)}^3}\right) = \frac{-\Delta G^0}{2.303RT} - 2\text{pH}$$

298.15: $\log(p) = -3.73 - 2\text{pH}$

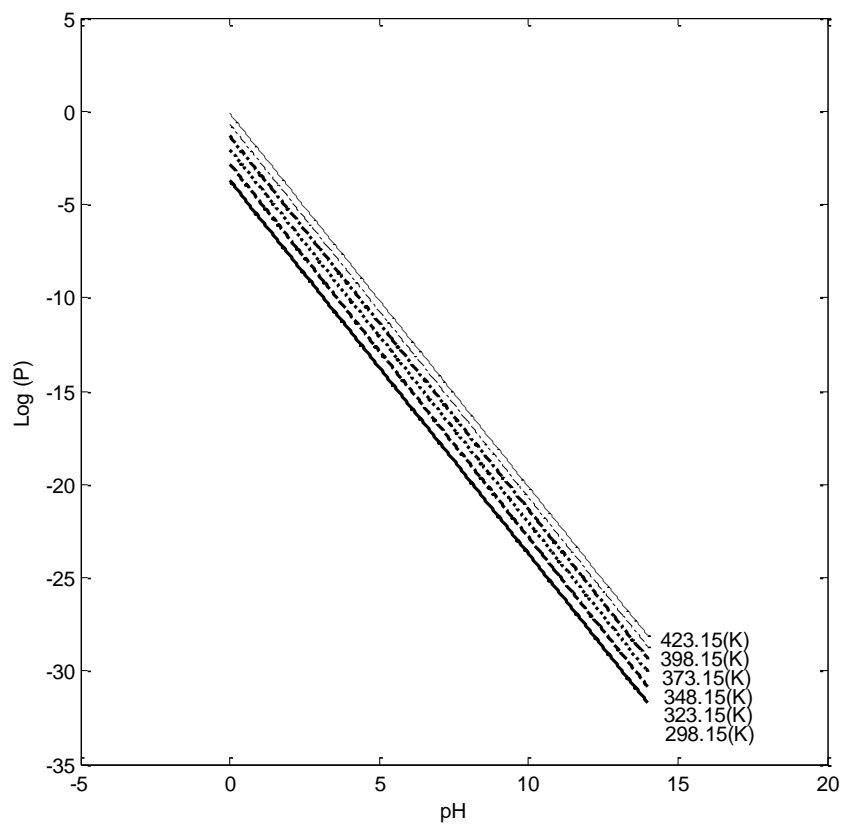
323.15: $\log(p) = -2.84 - 2\text{pH}$

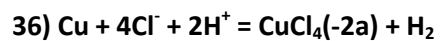
348.15: $\log(p) = -2.05 - 2\text{pH}$

373.15: $\log(p) = -1.35 - 2\text{pH}$

398.15: $\log(p) = -0.71 - 2\text{pH}$

423.15: $\log(p) = -0.13 - 2\text{pH}$





$$\log\left(\frac{p_{\text{H}_2} \times a_{\text{CuCl}_4^{2-}}}{a_{\text{Cl}^-}^4}\right) = \frac{-\Delta G^0}{2.303RT} - 2\text{pH}$$

$$298.15: \log(p) = -15.41 - 2\text{pH}$$

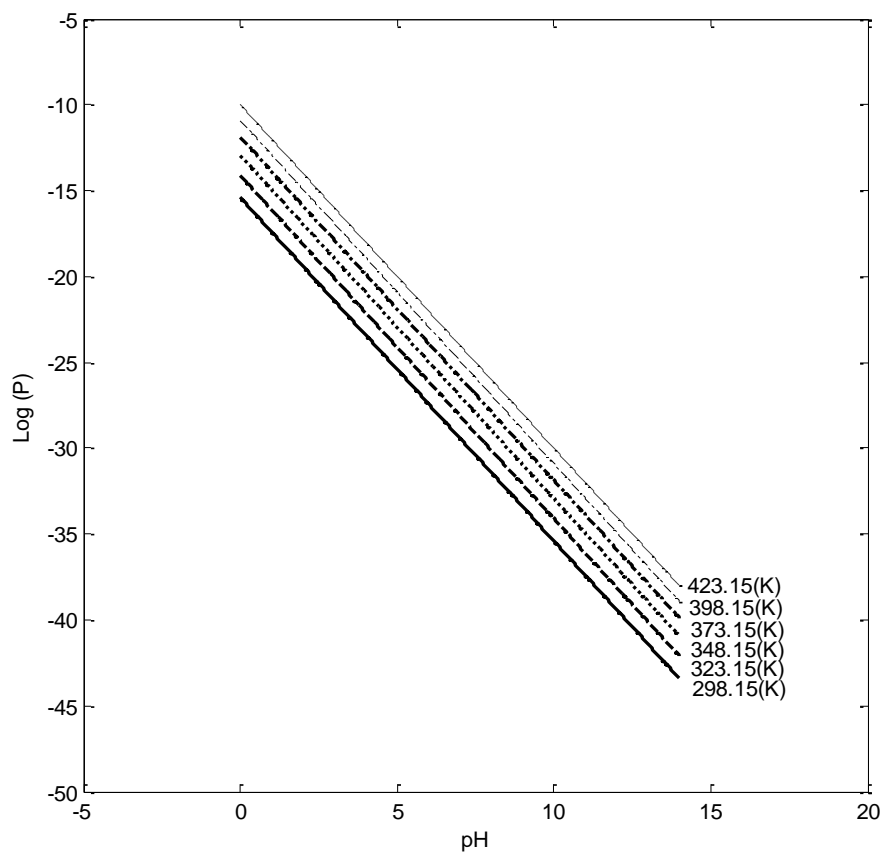
$$323.15: \log(p) = -14.11 - 2\text{pH}$$

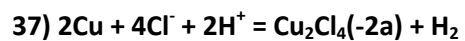
$$348.15: \log(p) = -12.94 - 2\text{pH}$$

$$373.15: \log(p) = -11.88 - 2\text{pH}$$

$$398.15: \log(p) = -10.91 - 2\text{pH}$$

$$423.15: \log(p) = -10.00 - 2\text{pH}$$





$$\log\left(\frac{p_{\text{H}_2} \times a_{\text{Cu}_2\text{Cl}_4(-2)}}{a_{\text{Cl}^-}^4}\right) = \frac{-\Delta G^0}{2.303RT} - 2\text{pH}$$

298.15: $\log(p) = -6.59 - 2\text{pH}$

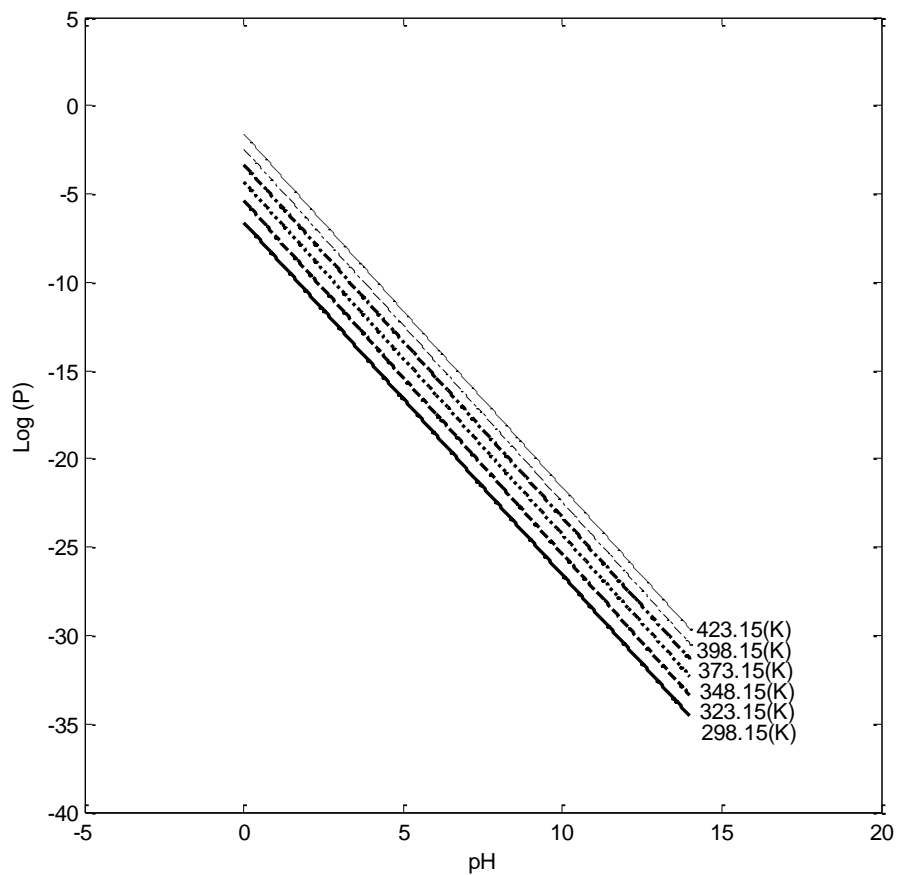
323.15: $\log(p) = -5.39 - 2\text{pH}$

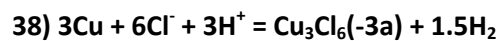
348.15: $\log(p) = -4.31 - 2\text{pH}$

373.15: $\log(p) = -3.34 - 2\text{pH}$

398.15: $\log(p) = -2.45 - 2\text{pH}$

423.15: $\log(p) = -1.62 - 2\text{pH}$





$$\log\left(\frac{p_{\text{H}_2}^{1.5} \times a_{\text{Cu}_3\text{Cl}_6(-3)}}{a_{\text{Cl}^-}^6}\right) = \frac{-\Delta G^0}{2.303RT} - 3\text{pH}$$

$$298.15: \log(p) = -170.11 - 3\text{pH}$$

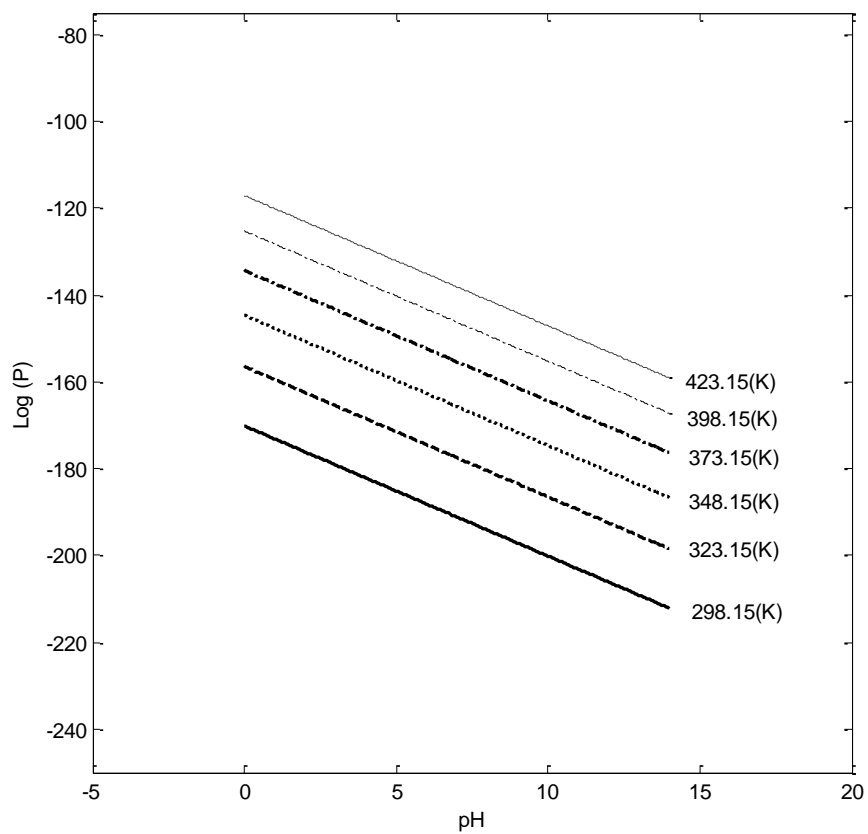
$$323.15: \log(p) = -156.46 - 3\text{pH}$$

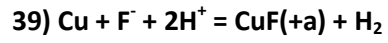
$$348.15: \log(p) = -144.65 - 3\text{pH}$$

$$373.15: \log(p) = -134.33 - 3\text{pH}$$

$$398.15: \log(p) = -125.22 - 3\text{pH}$$

$$423.15: \log(p) = -117.08 - 3\text{pH}$$





$$\log\left(\frac{p_{\text{H}_2} \times a_{\text{CuF}(+)}}{a_{\text{F}(-)}}\right) = \frac{-\Delta G^0}{2.303RT} - 2\text{pH}$$

298.15: $\log(p) = -9.85 - 2\text{pH}$

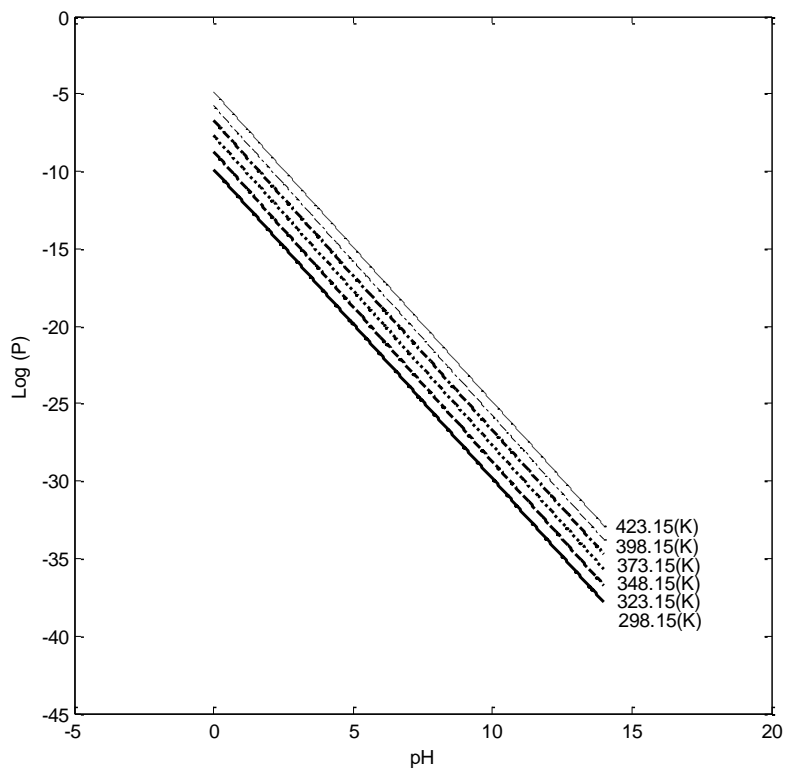
323.15: $\log(p) = -8.74 - 2\text{pH}$

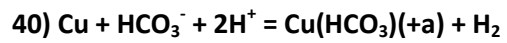
348.15: $\log(p) = -7.70 - 2\text{pH}$

373.15: $\log(p) = -6.72 - 2\text{pH}$

398.15: $\log(p) = -5.79 - 2\text{pH}$

423.15: $\log(p) = -4.88 - 2\text{pH}$





$$\log\left(\frac{p_{\text{H}_2} \times a_{\text{Cu}(\text{HCO}_3)(+)}}{a_{\text{HCO}_3(-)}}\right) = \frac{-\Delta G^0}{2.303RT} - 2\text{pH}$$

298.15: $\log(p) = -9.60 - 2\text{pH}$

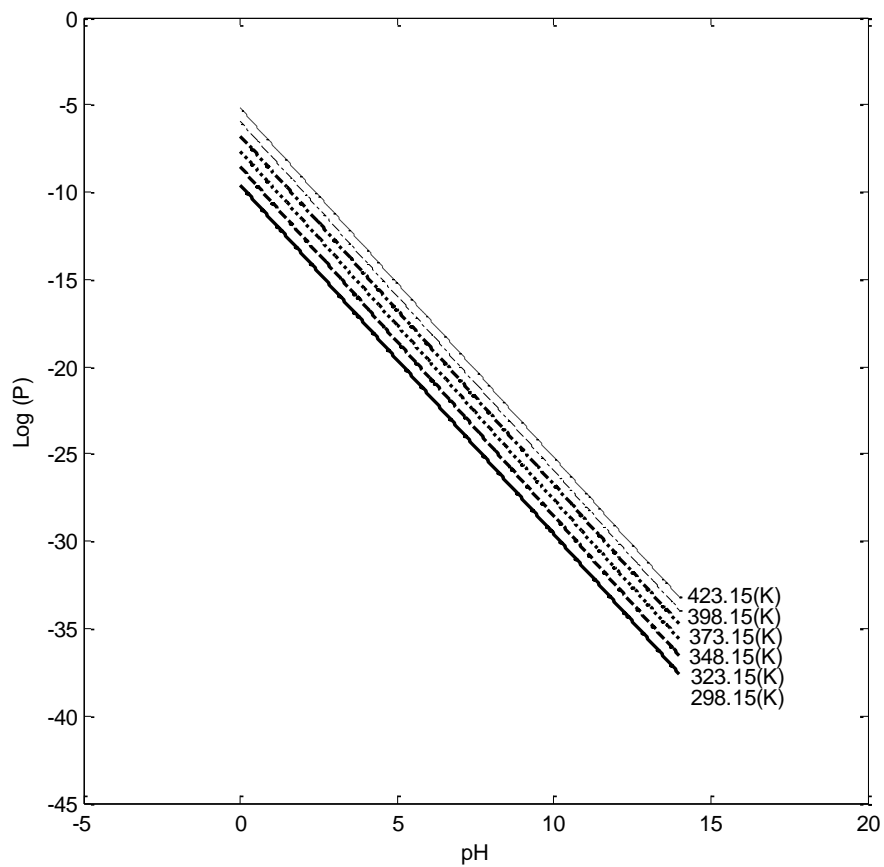
323.15: $\log(p) = -8.56 - 2\text{pH}$

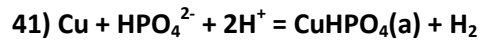
348.15: $\log(p) = -7.63 - 2\text{pH}$

373.15: $\log(p) = -6.76 - 2\text{pH}$

398.15: $\log(p) = -5.96 - 2\text{pH}$

423.15: $\log(p) = -5.21 - 2\text{pH}$





$$\log\left(\frac{p_{\text{H}_2} \times a_{\text{CuHPO}_4}}{a_{\text{HPO}_4^{(-2)}}}\right) = \frac{-\Delta G^0}{2.303RT} - 2\text{pH}$$

298.15: $\log(p) = -6.08 - 2\text{pH}$

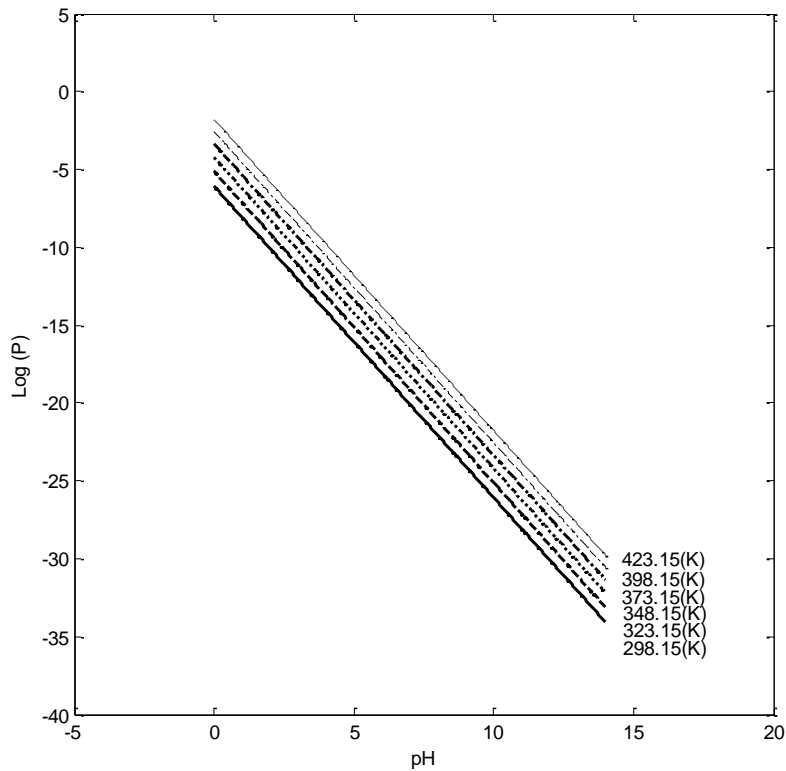
323.15: $\log(p) = -5.12 - 2\text{pH}$

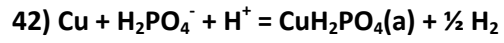
348.15: $\log(p) = -4.21 - 2\text{pH}$

373.15: $\log(p) = -3.36 - 2\text{pH}$

398.15: $\log(p) = -2.56 - 2\text{pH}$

423.15: $\log(p) = -1.78 - 2\text{pH}$





$$\log\left(\frac{p_{\text{H}_2}^{0.5} \times a_{\text{CuH}_2\text{PO}_4}}{a_{\text{H}_2\text{PO}_4(-)}}\right) = \frac{-\Delta G^0}{2.303RT} - \text{pH}$$

298.15: $\log(p) = -6.52 - \text{pH}$

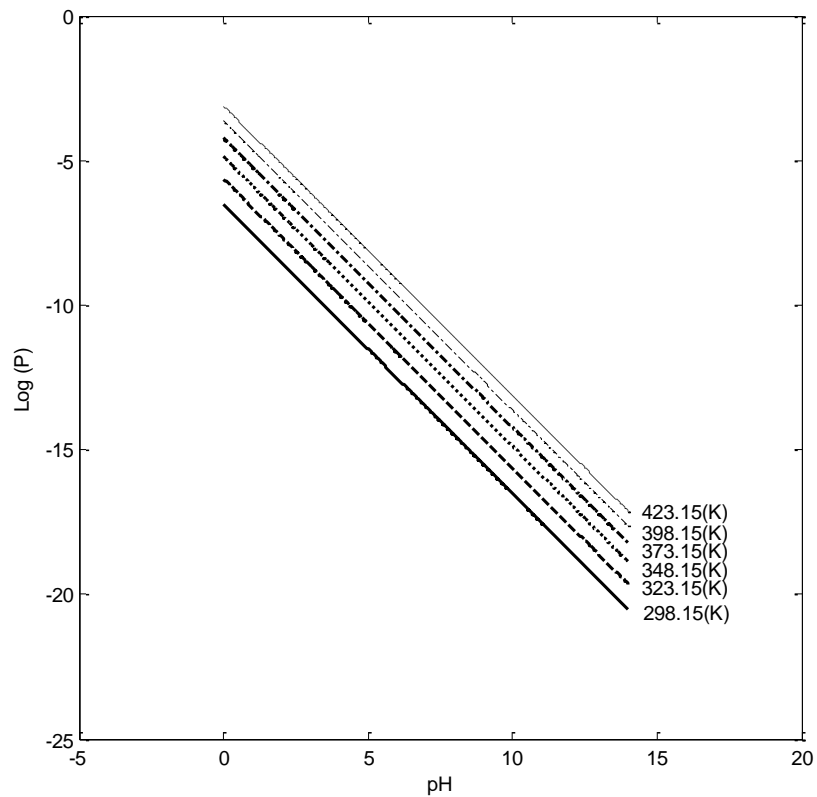
323.15: $\log(p) = -5.64 - \text{pH}$

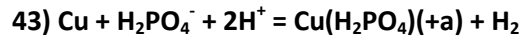
348.15: $\log(p) = -4.88 - \text{pH}$

373.15: $\log(p) = -4.23 - \text{pH}$

398.15: $\log(p) = -3.64 - \text{pH}$

423.15: $\log(p) = -3.12 - \text{pH}$





$$\log\left(\frac{p_{\text{H}_2} \times a_{\text{Cu}(\text{H}_2\text{PO}_4)(+)}}{a_{\text{H}_2\text{PO}_4(-)}}\right) = \frac{-\Delta G^0}{2.303RT} - 2\text{pH}$$

$$298.15: \log(p) = -9.04 - 2\text{pH}$$

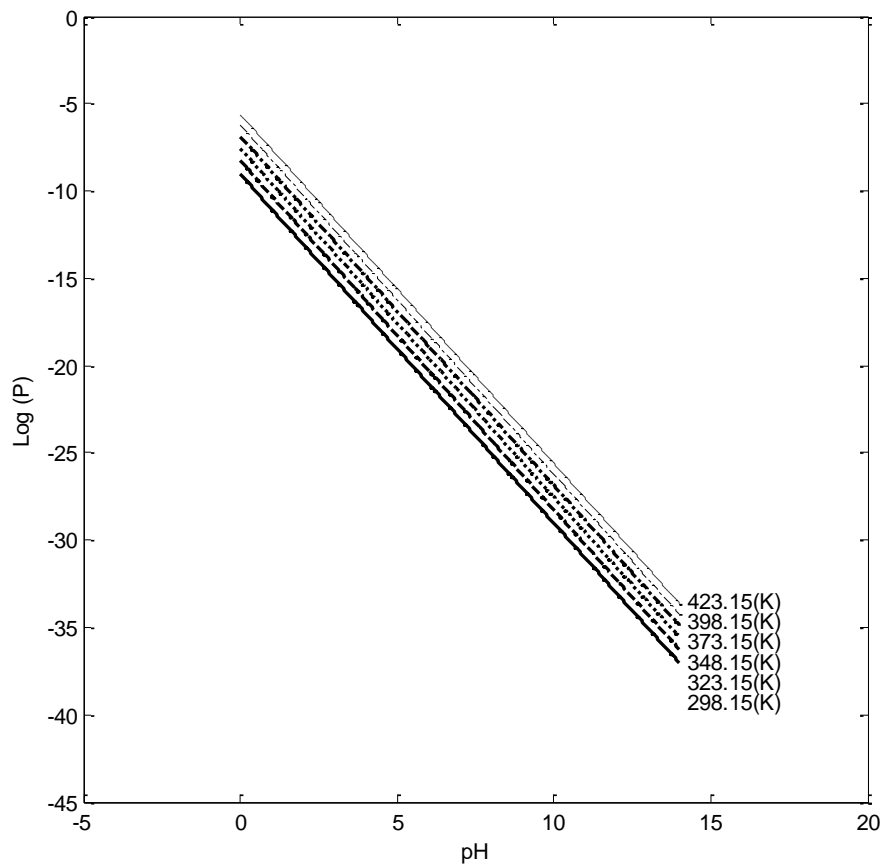
$$323.15: \log(p) = -8.27 - 2\text{pH}$$

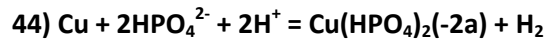
$$348.15: \log(p) = -7.56 - 2\text{pH}$$

$$373.15: \log(p) = -6.88 - 2\text{pH}$$

$$398.15: \log(p) = -6.23 - 2\text{pH}$$

$$423.15: \log(p) = -5.61 - 2\text{pH}$$





$$\log\left(\frac{p_{\text{H}_2} \times a_{\text{Cu}(\text{HPO}_4)_2(-2)}}{a_{\text{HPO}_4^{2-}}^2}\right) = \frac{-\Delta G^0}{2.303RT} - 2\text{pH}$$

298.15: $\log(p) = -1.61 - 2\text{pH}$

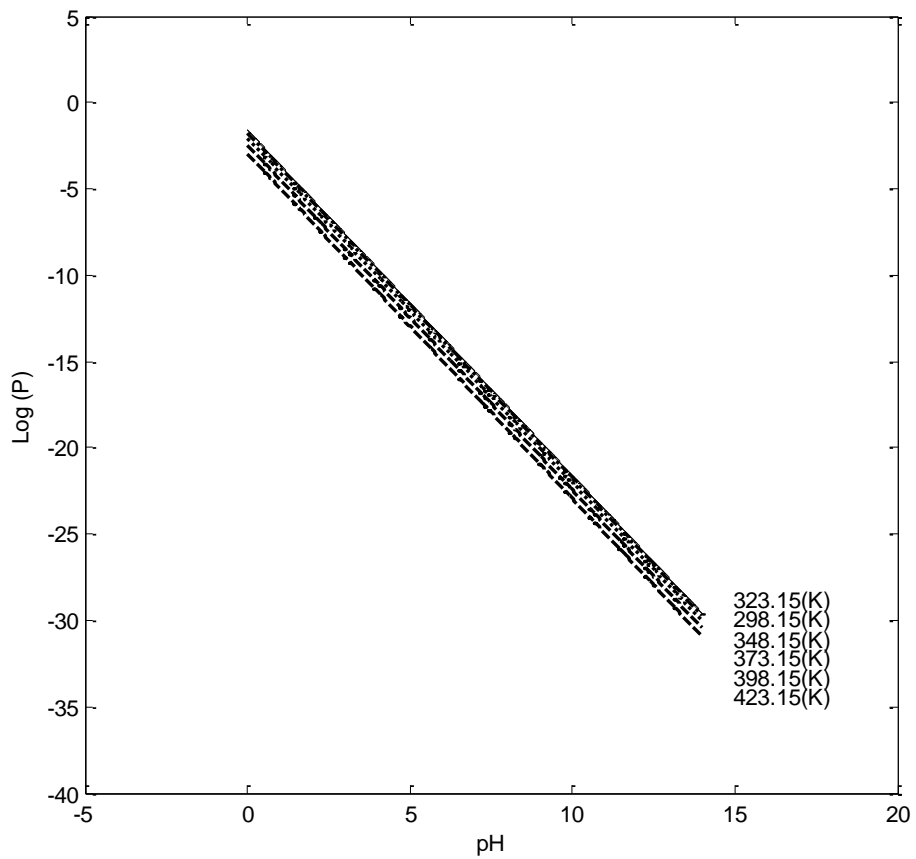
323.15: $\log(p) = -1.59 - 2\text{pH}$

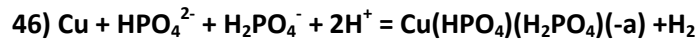
348.15: $\log(p) = -1.74 - 2\text{pH}$

373.15: $\log(p) = -2.04 - 2\text{pH}$

398.15: $\log(p) = -2.45 - 2\text{pH}$

423.15: $\log(p) = -2.95 - 2\text{pH}$





$$\log\left(\frac{p_{\text{H}_2} \times a_{\text{Cu}(\text{HPO}_4)(\text{H}_2\text{PO}_4)(-)}}{a_{\text{HPO}_4^{2-}} \times a_{\text{H}_2\text{PO}_4^-}}\right) = \frac{-\Delta G^0}{2.303RT} - 2\text{pH}$$

$$298.15: \log(p) = -3.62 - 2\text{pH}$$

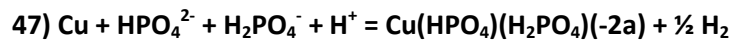
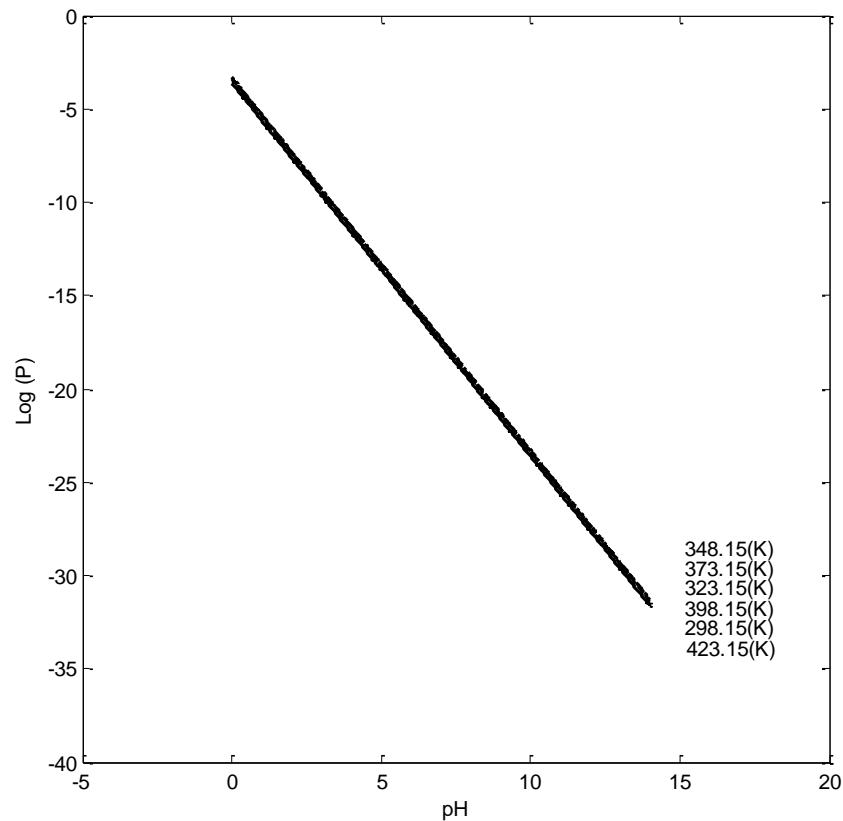
$$323.15: \log(p) = -3.39 - 2\text{pH}$$

$$348.15: \log(p) = -3.30 - 2\text{pH}$$

$$373.15: \log(p) = -3.33 - 2\text{pH}$$

$$398.15: \log(p) = -3.45 - 2\text{pH}$$

$$423.15: \log(p) = -3.64 - 2\text{pH}$$



$$\log\left(\frac{p_{H_2}^{0.5} \times a_{Cu(HPO_4)(H_2PO_4)(-2)}}{a_{HPO_4(-2)} \times a_{H_2PO_4(-)}}\right) = \frac{-\Delta G^0}{2.303RT} - pH$$

298.15: $\log(p) = -1.92 - pH$

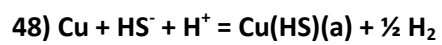
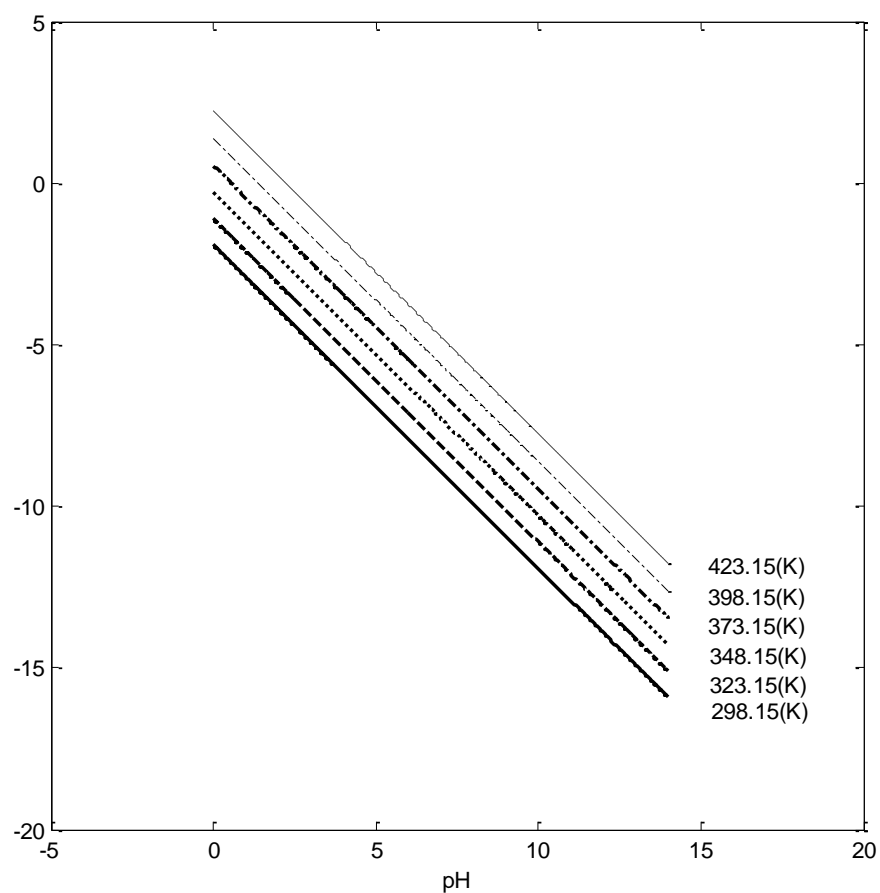
323.15: $\log(p) = -1.11 - pH$

348.15: $\log(p) = -0.29 - pH$

373.15: $\log(p) = 0.54 - pH$

398.15: $\log(p) = 1.38 - pH$

423.15: $\log(p) = 2.24 - pH$



$$\log\left(\frac{p_{H_2}^{0.5} \times a_{Cu(HS)}}{a_{HS(-)}}\right) = \frac{-\Delta G^0}{2.303RT} - pH$$

298.15: $\log(p) = 4.43 - pH$

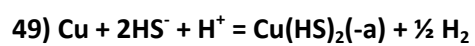
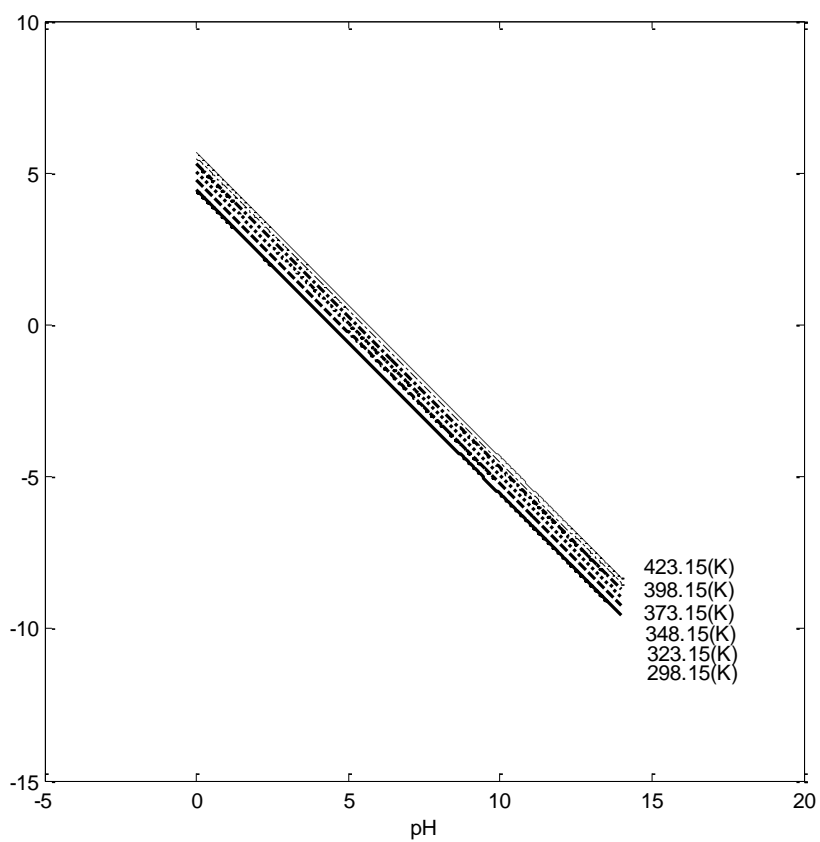
323.15: $\log(p) = 4.77 - pH$

348.15: $\log(p) = 5.05 - pH$

373.15: $\log(p) = 5.29 - pH$

398.15: $\log(p) = 5.49 - pH$

423.15: $\log(p) = 5.66 - pH$



$$\log\left(\frac{p_{H_2}^{0.5} \times a_{Cu(HS)_2(-)}}{a_{HS(-)}^2}\right) = \frac{-\Delta G^0}{2.303RT} - pH$$

298.15: $\log(p) = 8.26 - pH$

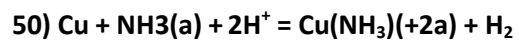
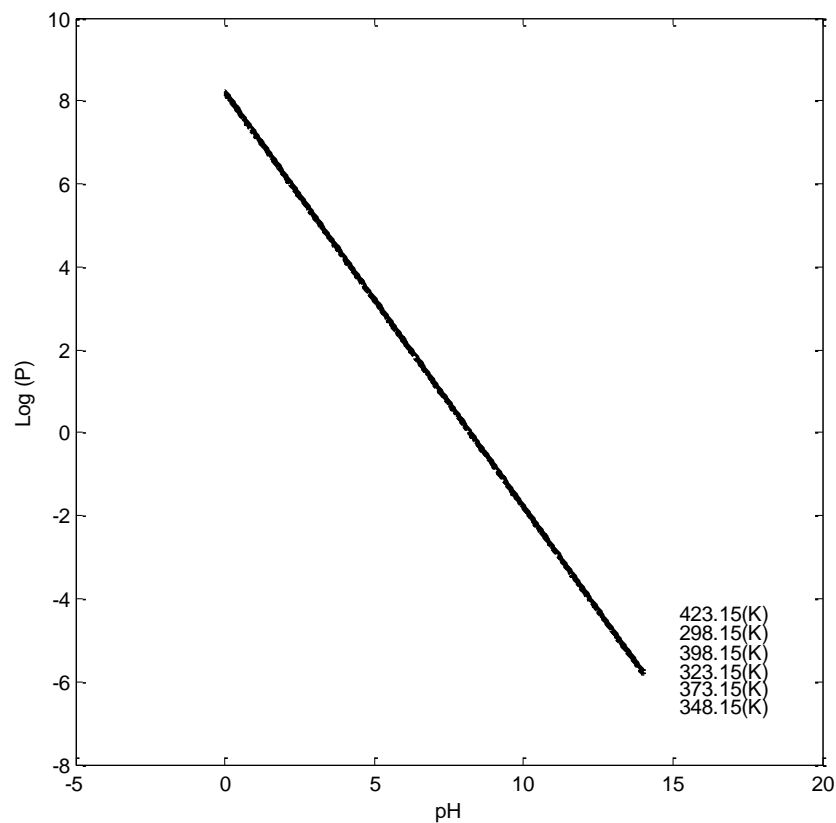
323.15: $\log(p) = 8.19 - pH$

348.15: $\log(p) = 8.16 - pH$

373.15: $\log(p) = 8.17 - pH$

398.15: $\log(p) = 8.21 - pH$

423.15: $\log(p) = 8.28 - pH$



$$\log\left(\frac{p_{H_2} \times a_{Cu(NH_3)(+2)}}{a_{NH_3}}\right) = \frac{-\Delta G^0}{2.303RT} - 2pH$$

298.15: $\log (p) = -7.08-2pH$

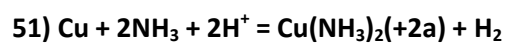
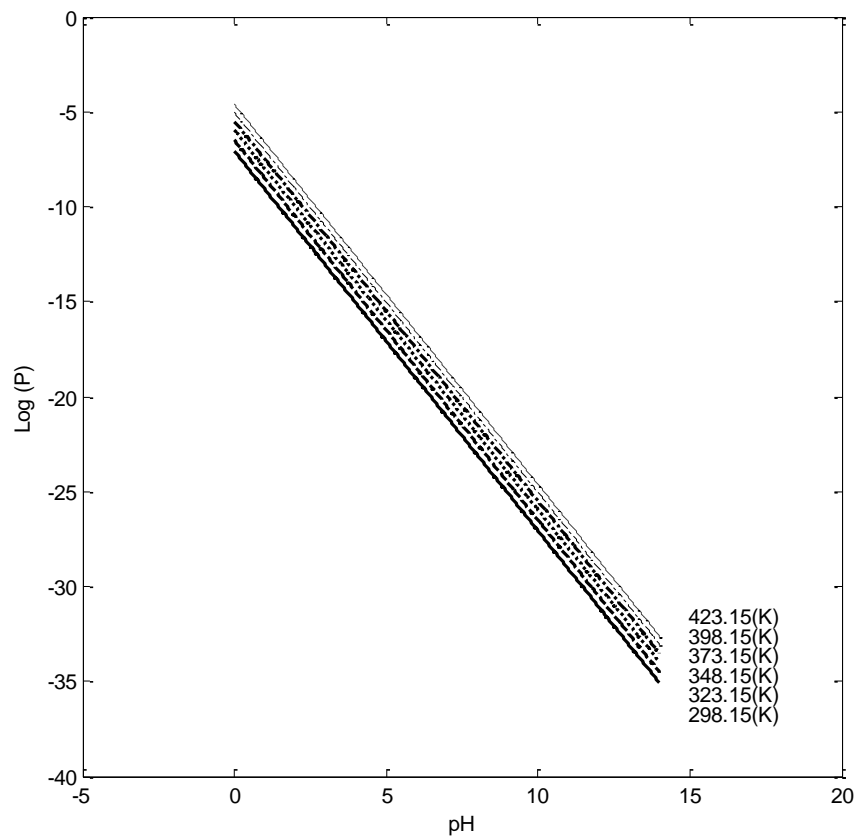
323.15: $\log (p) = -6.51-2pH$

348.15: $\log (p) = -5.98-2pH$

373.15: $\log (p) = -5.50-2pH$

398.15: $\log (p) = -5.05-2pH$

423.15: $\log (p) = -4.62-2pH$



$$\log\left(\frac{p_{H_2} \times a_{Cu(NH_3)_2(+2)}}{a_{NH_3}^2}\right) = \frac{-\Delta G^0}{2.303RT} - 2pH$$

298.15: $\log(p) = -3.44 - 2pH$

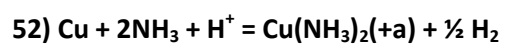
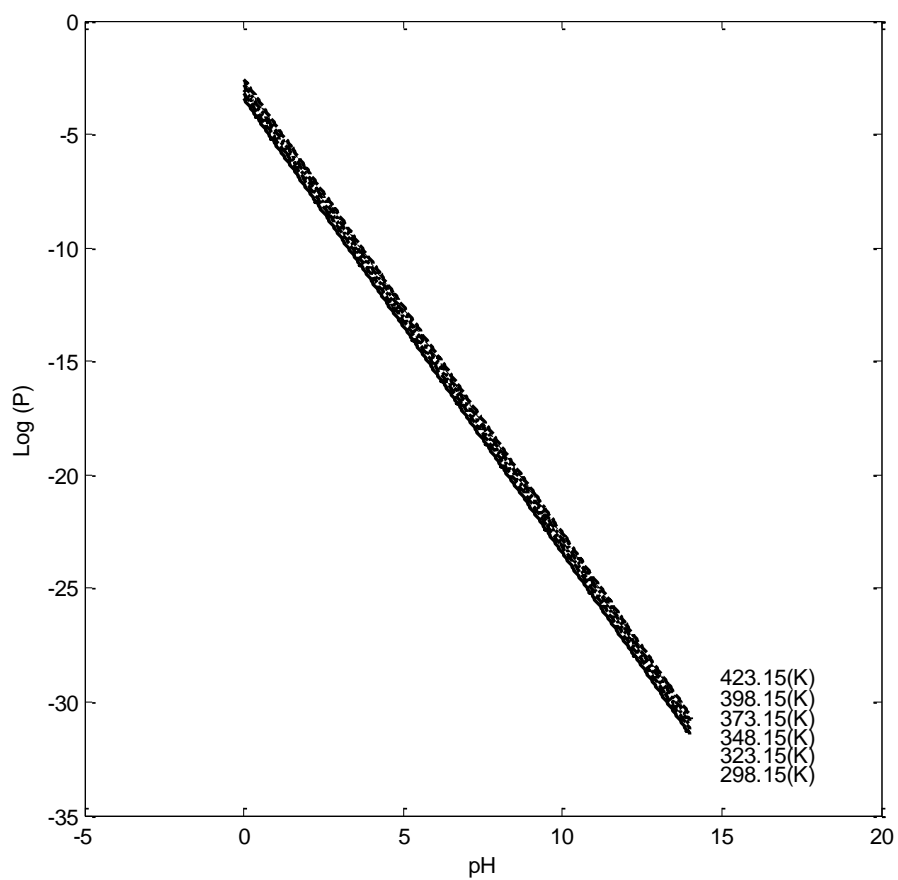
323.15: $\log(p) = -3.20 - 2pH$

348.15: $\log(p) = -3.01 - 2pH$

373.15: $\log(p) = -2.84 - 2pH$

398.15: $\log(p) = -2.70 - 2pH$

423.15: $\log(p) = -2.58 - 2pH$



$$\log\left(\frac{p_{H_2}^{0.5} \times a_{Cu(NH_3)_2(+)}}{a_{NH_3}^2}\right) = \frac{-\Delta G^0}{2.303RT} - pH$$

298.15: $\log(p) = 2.39 - pH$

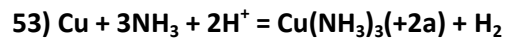
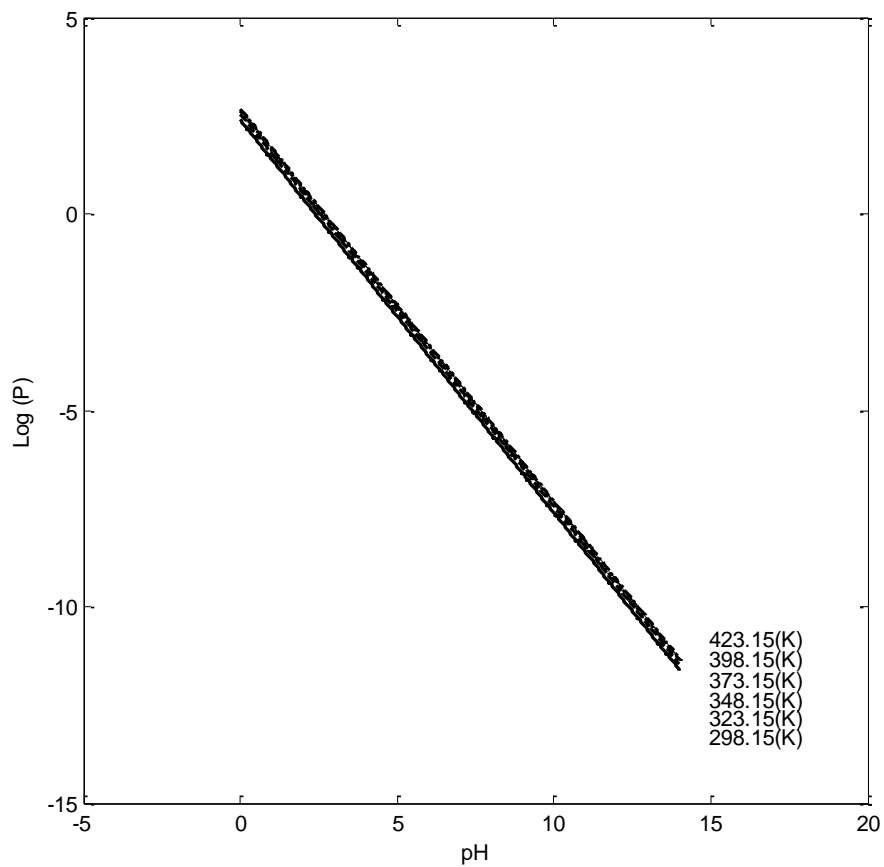
323.15: $\log(p) = 2.54 - pH$

348.15: $\log(p) = 2.63 - pH$

373.15: $\log(p) = 2.68 - pH$

398.15: $\log(p) = 2.67 - pH$

423.15: $\log(p) = 2.66 - pH$



$$\log\left(\frac{p_{H_2} \times a_{Cu(NH_3)_3(+2)}}{a_{NH_3}^3}\right) = \frac{-\Delta G^0}{2.303RT} - 2pH$$

298.15: $\log(p) = -0.42 - pH$

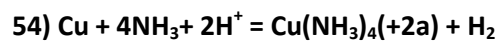
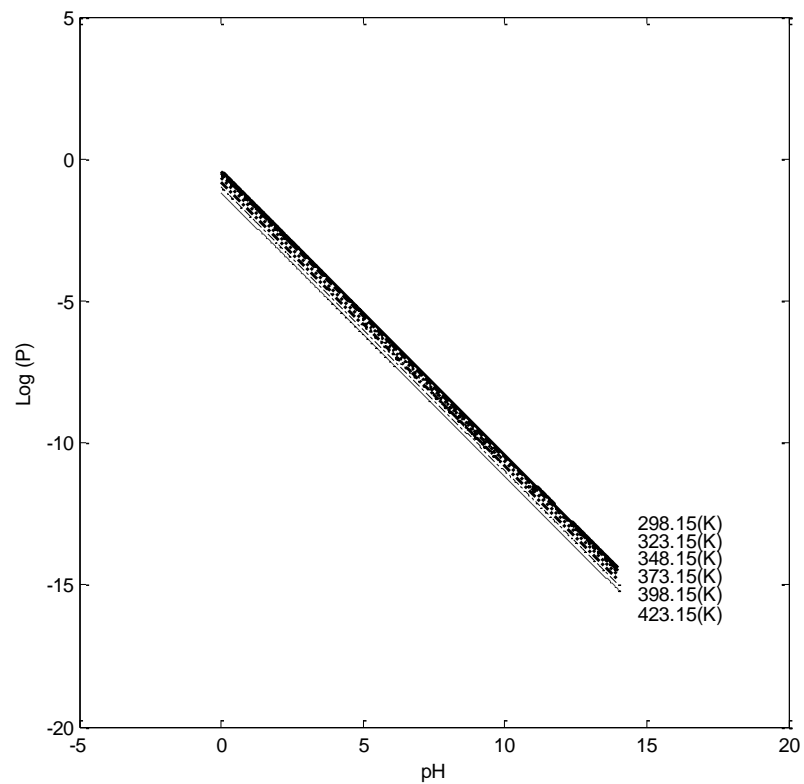
323.15: $\log(p) = -0.52 - pH$

348.15: $\log(p) = -0.66 - pH$

373.15: $\log(p) = -0.82 - pH$

398.15: $\log(p) = -1.00 - pH$

423.15: $\log(p) = -1.18 - pH$



$$\log\left(\frac{p_{H_2} \times a_{Cu(NH_3)_4^{+2}}}{a_{NH_3}^4}\right) = \frac{-\Delta G^0}{2.303RT} - 2pH$$

298.15: $\log(p) = 1.82 - 2pH$

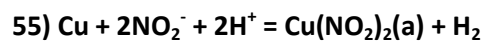
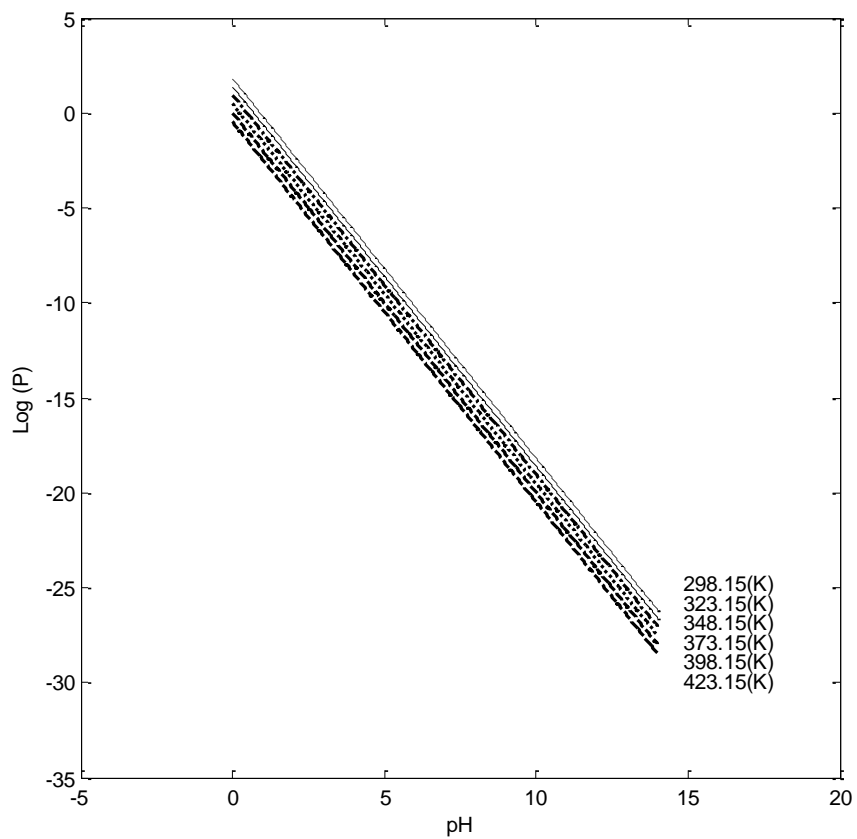
323.15: $\log(p) = 1.39 - 2pH$

348.15: $\log(p) = 0.94 - 2pH$

373.15: $\log(p) = 0.47 - 2pH$

398.15: $\log(p) = 0.00 - 2pH$

423.15: $\log(p) = -0.48 - 2pH$



$$\log\left(\frac{p_{H_2} \times a_{Cu(NO_2)_2}}{a_{NO_2(-)}^2}\right) = \frac{-\Delta G^0}{2.303RT} - 2pH$$

298.15: $\log(p) = -8.78 - 2pH$

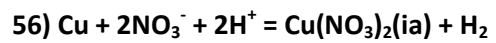
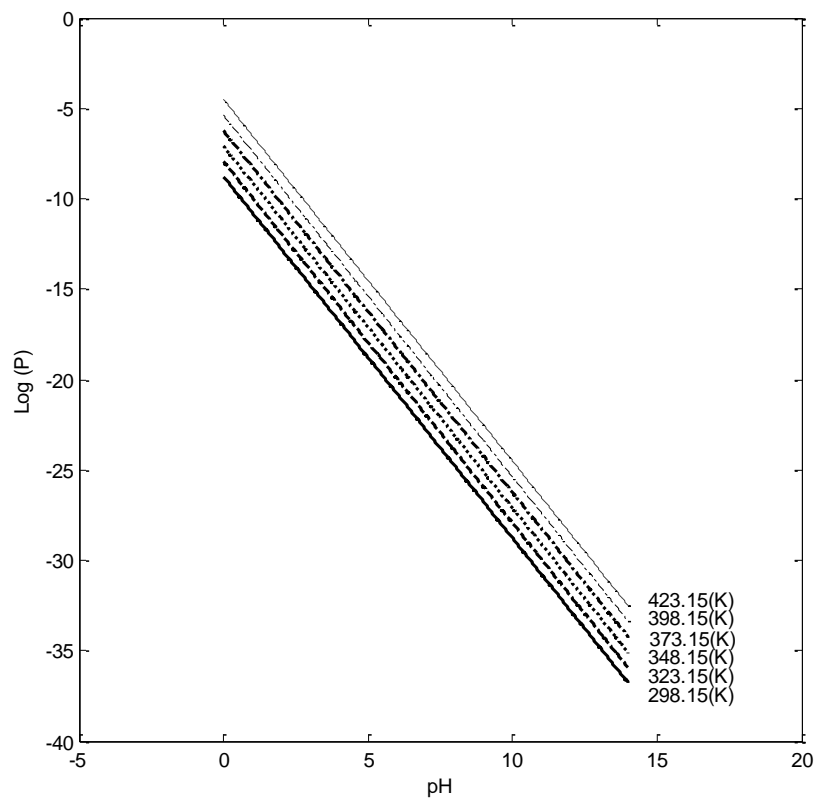
323.15: $\log(p) = -7.95 - 2pH$

348.15: $\log(p) = -7.11 - 2pH$

373.15: $\log(p) = -6.25 - 2pH$

398.15: $\log(p) = -5.39 - 2pH$

423.15: $\log(p) = -4.52 - 2pH$



$$\log\left(\frac{p_{H_2} \times a_{Cu(NO_3)_2}}{a_{NO_3^-}^2}\right) = \frac{-\Delta G^0}{2.303RT} - 2pH$$

298.15: $\log(p) = -11.81 - 2pH$

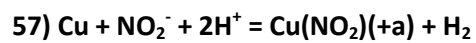
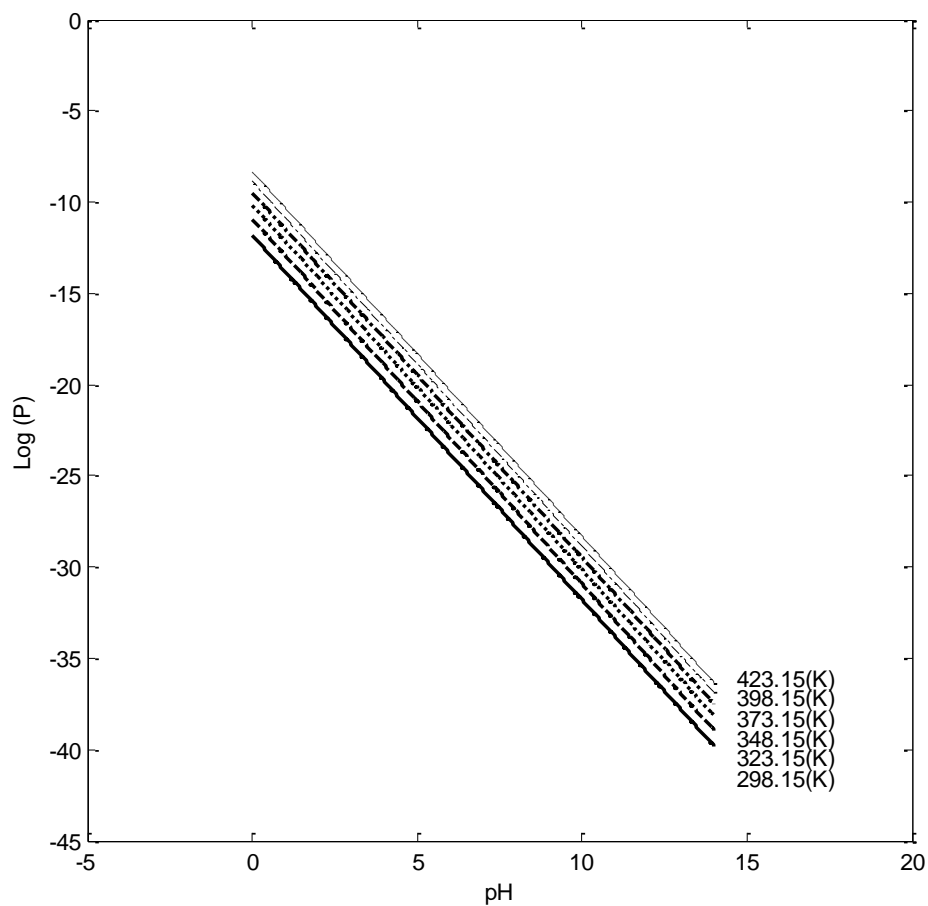
323.15: $\log(p) = -10.93 - 2pH$

348.15: $\log(p) = -10.15 - 2pH$

373.15: $\log(p) = -9.48 - 2pH$

398.15: $\log(p) = -8.87 - 2pH$

423.15: $\log(p) = -8.32 - 2pH$



$$\log\left(\frac{p_{H_2} \times a_{Cu(NO_2)(+)}}{a_{NO_2(-)}}\right) = \frac{-\Delta G^0}{2.303RT} - 2pH$$

298.15: $\log(p) = -9.41 - 2pH$

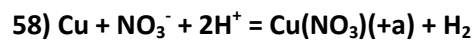
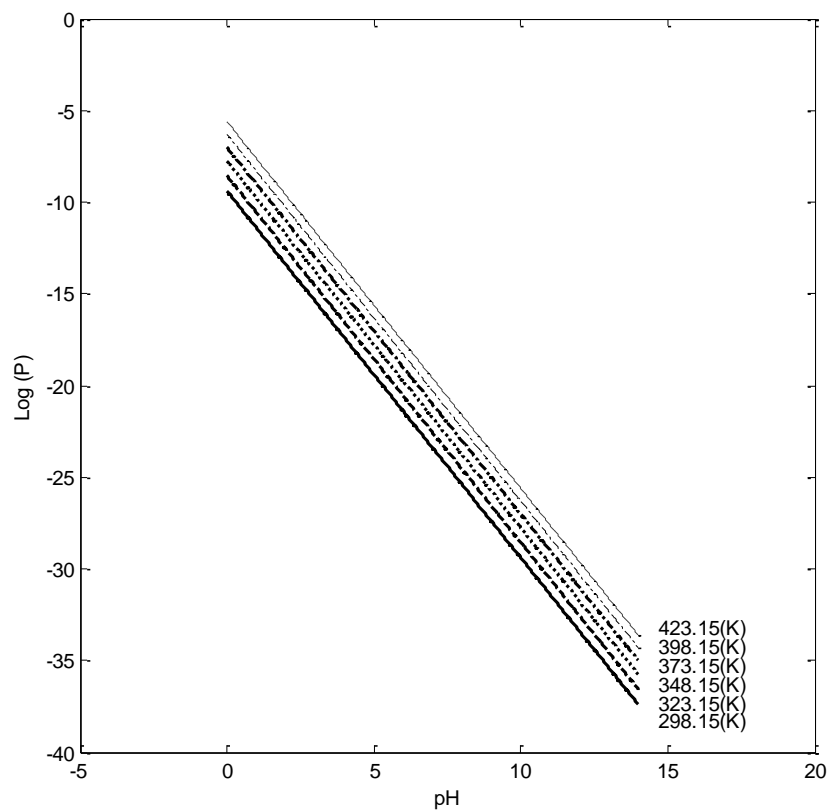
323.15: $\log(p) = -8.57 - 2pH$

348.15: $\log(p) = -7.77 - 2pH$

373.15: $\log(p) = -7.02 - 2pH$

398.15: $\log(p) = -6.31 - 2pH$

423.15: $\log(p) = -5.62 - 2pH$



$$\log\left(\frac{p_{H_2} \times a_{Cu(NO_3)_2(aq)}}{a_{NO_3^-}}\right) = \frac{-\Delta G^0}{2.303RT} - 2pH$$

298.15: $\log(p) = -10.90 - 2pH$

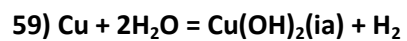
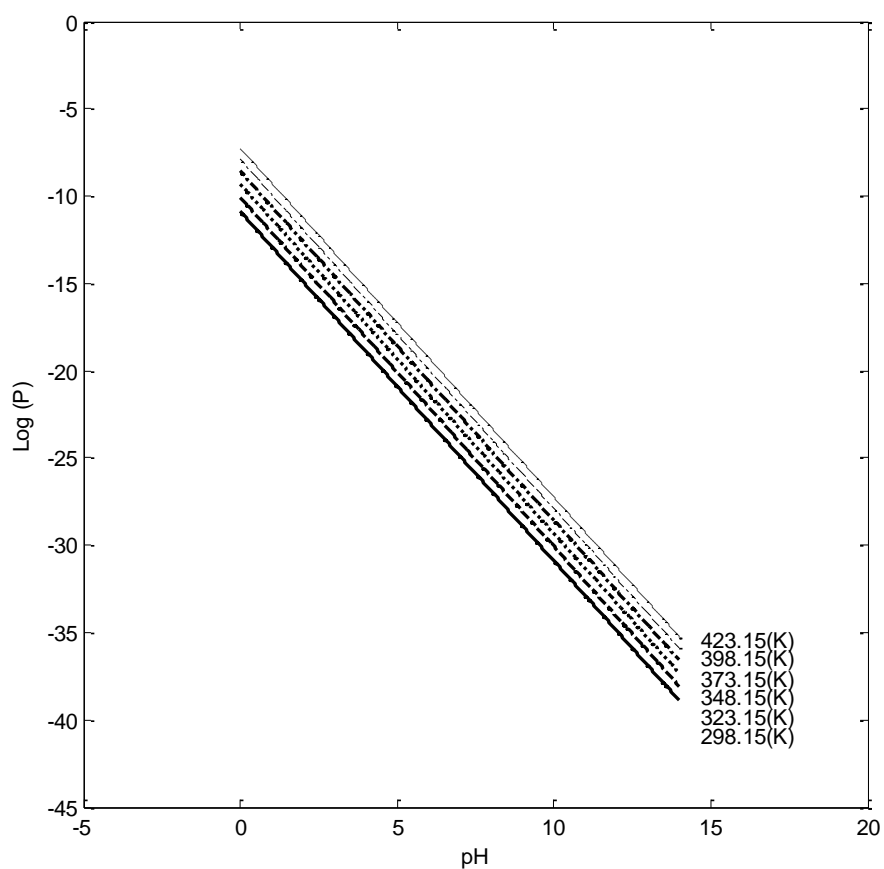
323.15: $\log(p) = -10.08 - 2pH$

348.15: $\log(p) = -9.32 - 2pH$

373.15: $\log(p) = -8.59 - 2pH$

398.15: $\log(p) = -7.91 - 2pH$

423.15: $\log(p) = -7.25 - 2pH$



$$\log\left(\frac{p_{H_2} \times a_{Cu(OH)_2}}{a_{H_2O}^2}\right) = \frac{-\Delta G^0}{2.303RT}$$

298.15: $\log(p) = -27.63$

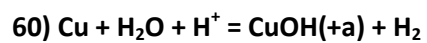
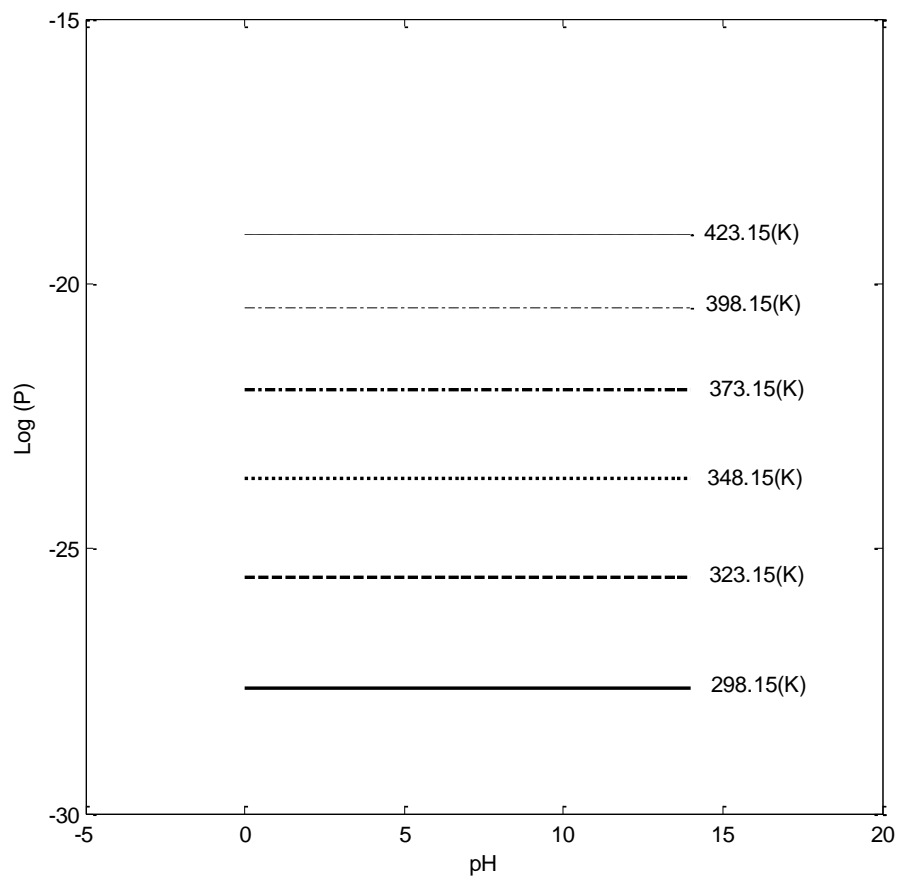
323.15: $\log(p) = -25.53$

348.15: $\log(p) = -23.66$

373.15: $\log(p) = -21.99$

398.15: $\log(p) = -20.47$

423.15: $\log(p) = -19.06$



$$\log\left(\frac{p_{H_2} \times a_{Cu(OH)_2(+)}}{a_{H_2O}}\right) = \frac{-\Delta G^0}{2.303RT} - pH$$

298.15: $\log(p) = -19.35 - pH$

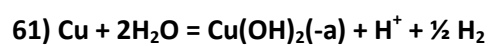
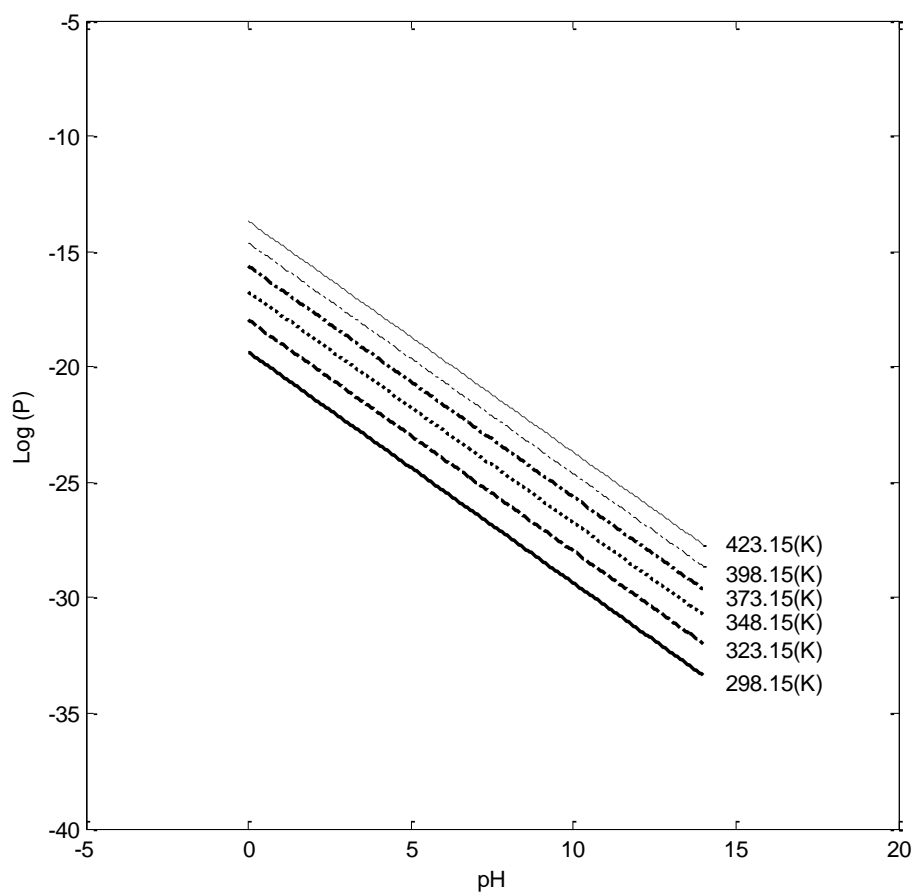
323.15: $\log(p) = -17.97 - pH$

348.15: $\log(p) = -16.74 - pH$

373.15: $\log(p) = -15.63 - pH$

398.15: $\log(p) = -14.62 - pH$

423.15: $\log(p) = -13.69 - pH$



$$\log\left(\frac{p_{H_2}^{0.5} \times a_{Cu(OH)_2(-)}}{a_{H_2O}^2}\right) = \frac{-\Delta G^0}{2.303RT} + pH$$

298.15: $\log(p) = -24.74 + pH$

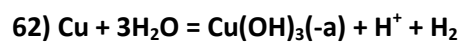
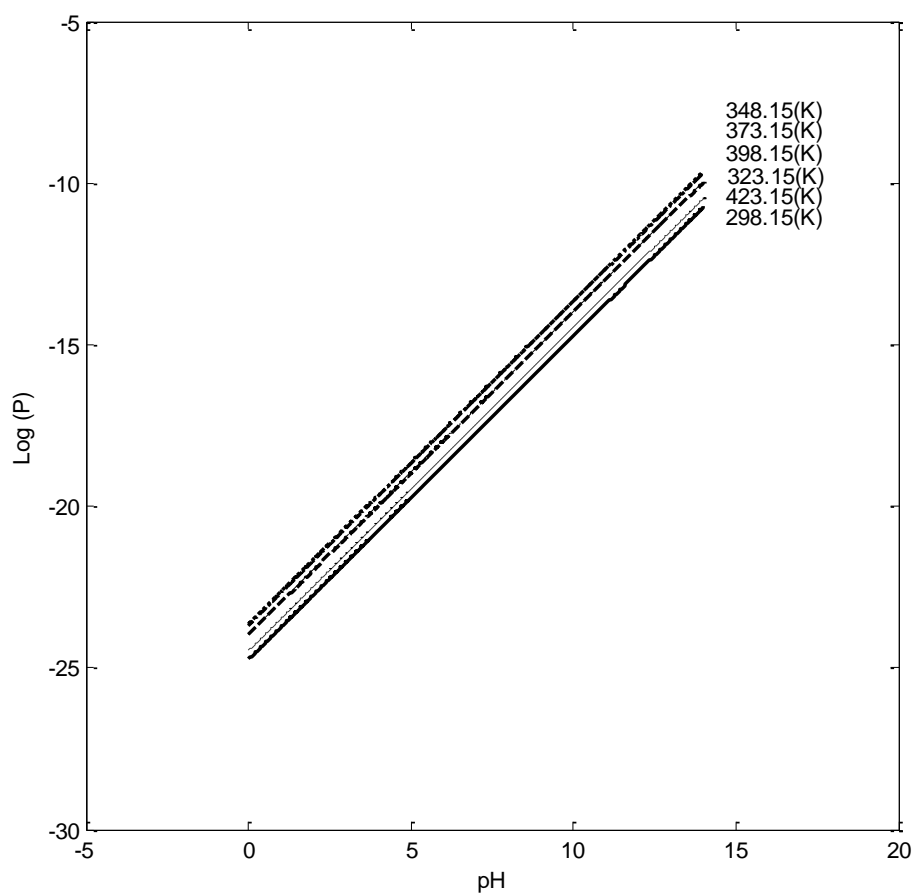
323.15: $\log(p) = -23.98 + pH$

348.15: $\log(p) = -23.65 + pH$

373.15: $\log(p) = -23.67 + pH$

398.15: $\log(p) = -23.96 + pH$

423.15: $\log(p) = -24.47 + pH$



$$\log\left(\frac{p_{H_2} \times a_{Cu(OH)_3(-)}}{a_{H_2O}^3}\right) = \frac{-\Delta G^0}{2.303RT} + pH$$

298.15: $\log (p) = -38.09+pH$

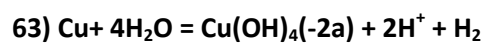
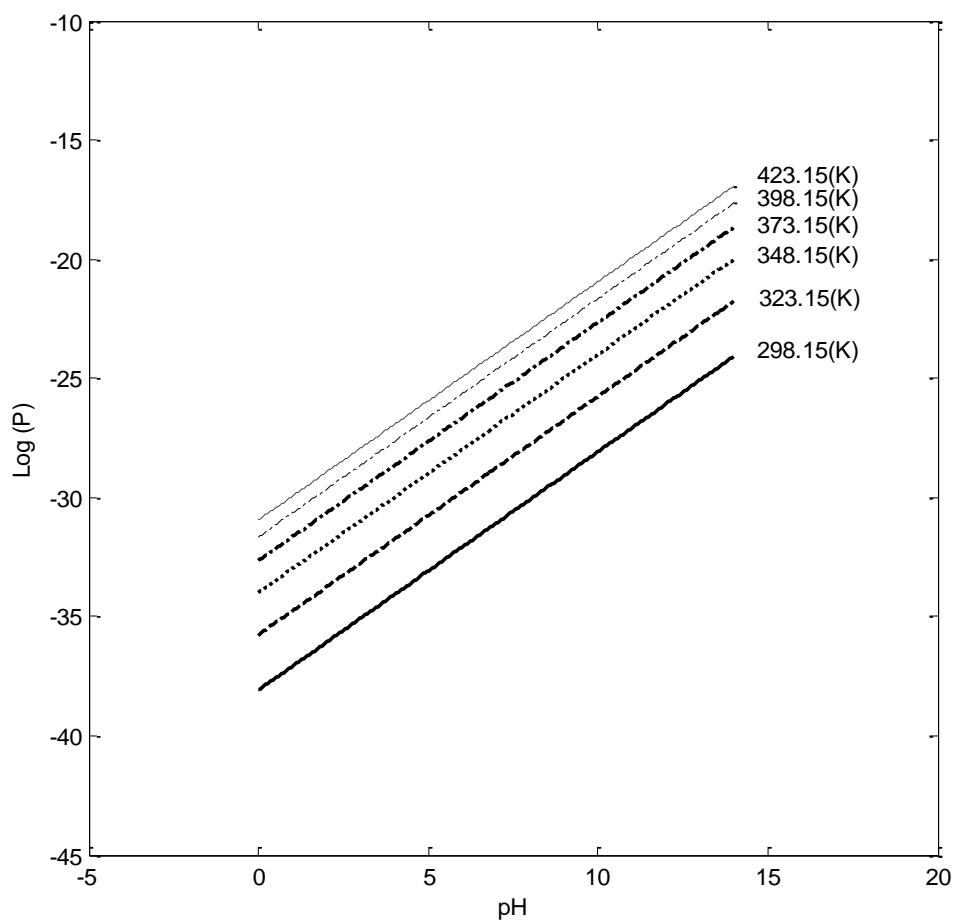
323.15: $\log (p) = -35.77+pH$

348.15: $\log (p) = -34.00+pH$

373.15: $\log (p) = -32.66+pH$

398.15: $\log (p) = -31.66+pH$

423.15: $\log (p) = -30.95+pH$



$$\log\left(\frac{p_{H_2} \times a_{Cu(OH)_4(-2)}}{a_{H_2O}^4}\right) = \frac{-\Delta G^0}{2.303RT} + 2pH$$

298.15: $\log(p) = -50.99 + 2pH$

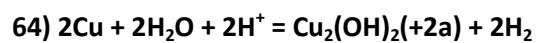
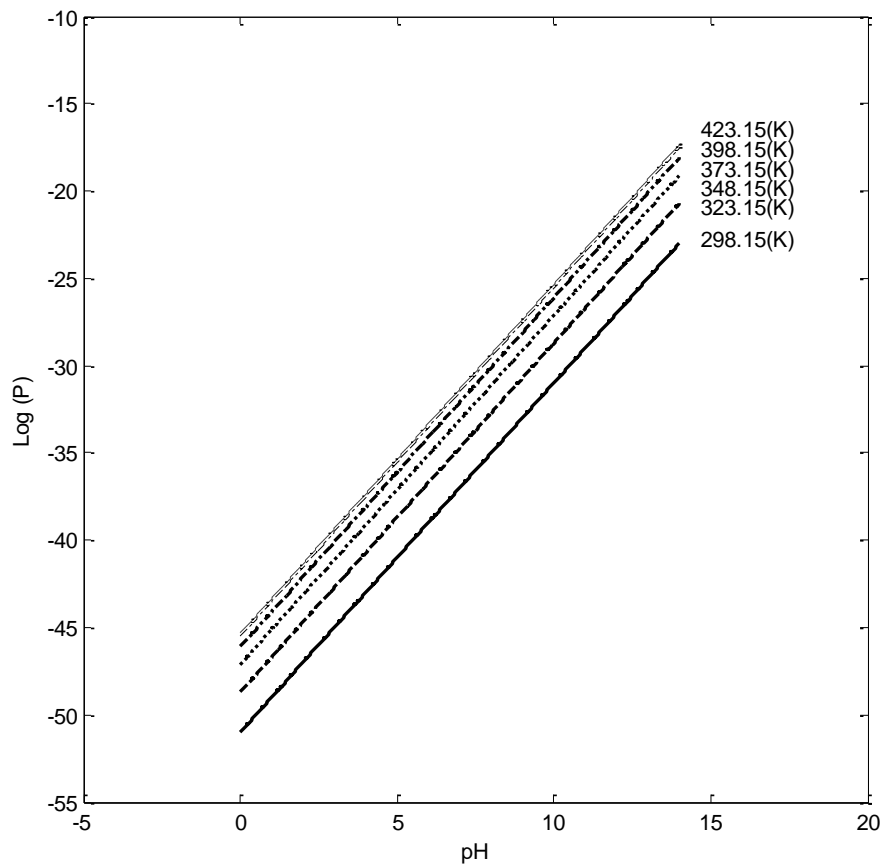
323.15: $\log(p) = -48.70 + 2pH$

348.15: $\log(p) = -47.12 + 2pH$

373.15: $\log(p) = -46.10 + 2pH$

398.15: $\log(p) = -45.53 + 2pH$

423.15: $\log(p) = -45.33 + 2pH$



$$\log\left(\frac{p_{H_2}^2 \times a_{Cu_2(OH)_2(+2)}}{a_{H_2O}^2}\right) = \frac{-\Delta G^0}{2.303RT} - 2pH$$

298.15: $\log(p) = -33.14 - 2\text{pH}$

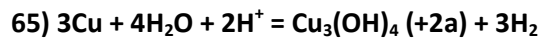
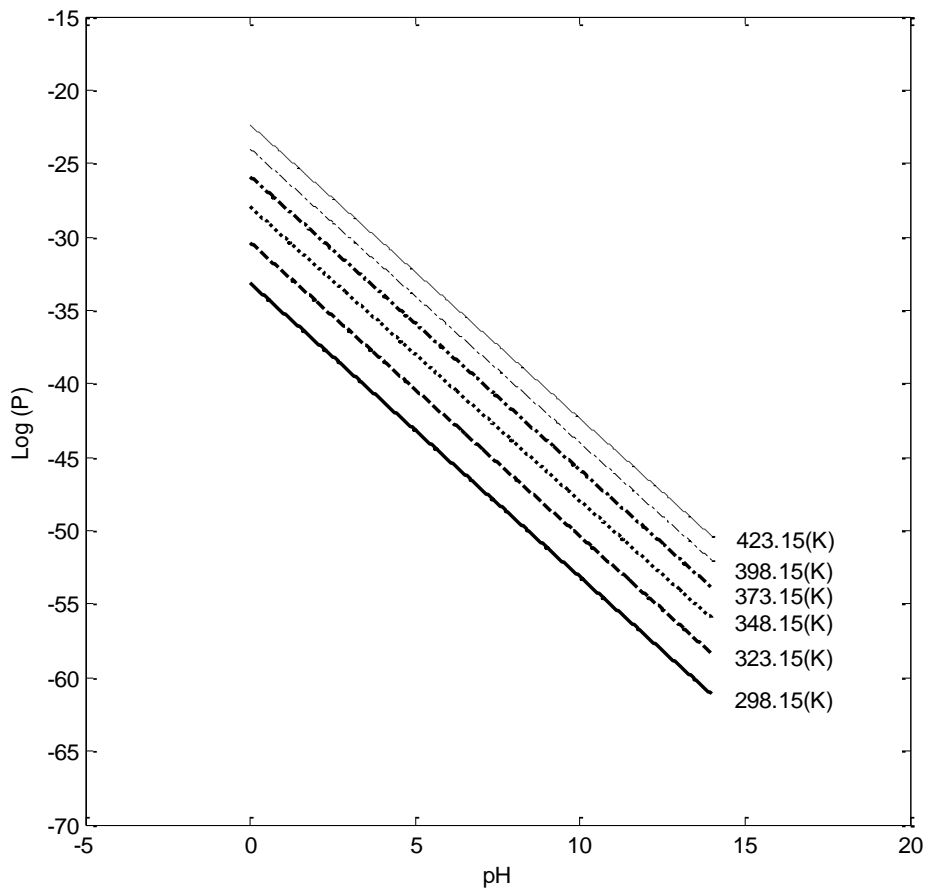
323.15: $\log(p) = -30.36 - 2\text{pH}$

348.15: $\log(p) = -27.96 - 2\text{pH}$

373.15: $\log(p) = -25.86 - 2\text{pH}$

398.15: $\log(p) = -24.01 - 2\text{pH}$

423.15: $\log(p) = -22.36 - 2\text{pH}$



$$\log\left(\frac{p_{\text{H}_2}^3 \times a_{\text{Cu}_3(\text{OH})_4(+2)}}{a_{\text{H}_2\text{O}}^4}\right) = \frac{-\Delta G^0}{2.303RT} - 2\text{pH}$$

298.15: $\log(p) = -55.28 - 2\text{pH}$

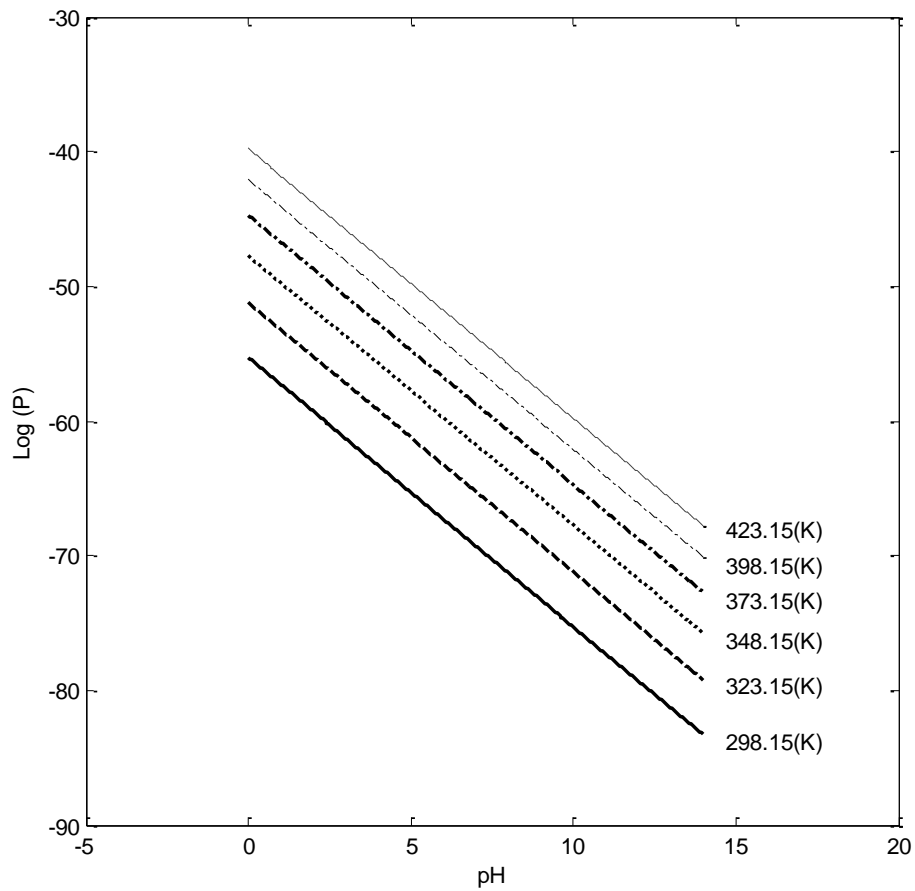
323.15: $\log(p) = -51.20 - 2\text{pH}$

348.15: $\log (p) = -47.72-2pH$

373.15: $\log (p) = -44.72-2pH$

398.15: $\log (p) = -42.09-2pH$

423.15: $\log (p) = -39.78-2pH$



66) $2Cu + 3HS^- + H^+ = Cu_2S(HS)_2 (-2a) + H_2$
 $\log\left(\frac{p_{H_2} \times a_{Cu_2S(HS)_2(-2)}}{a_{HS(-)}^3}\right) = \frac{-\Delta G^0}{2.303RT} - pH$

298.15: $\log (p) = 12.06-pH$

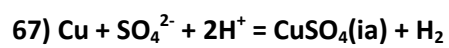
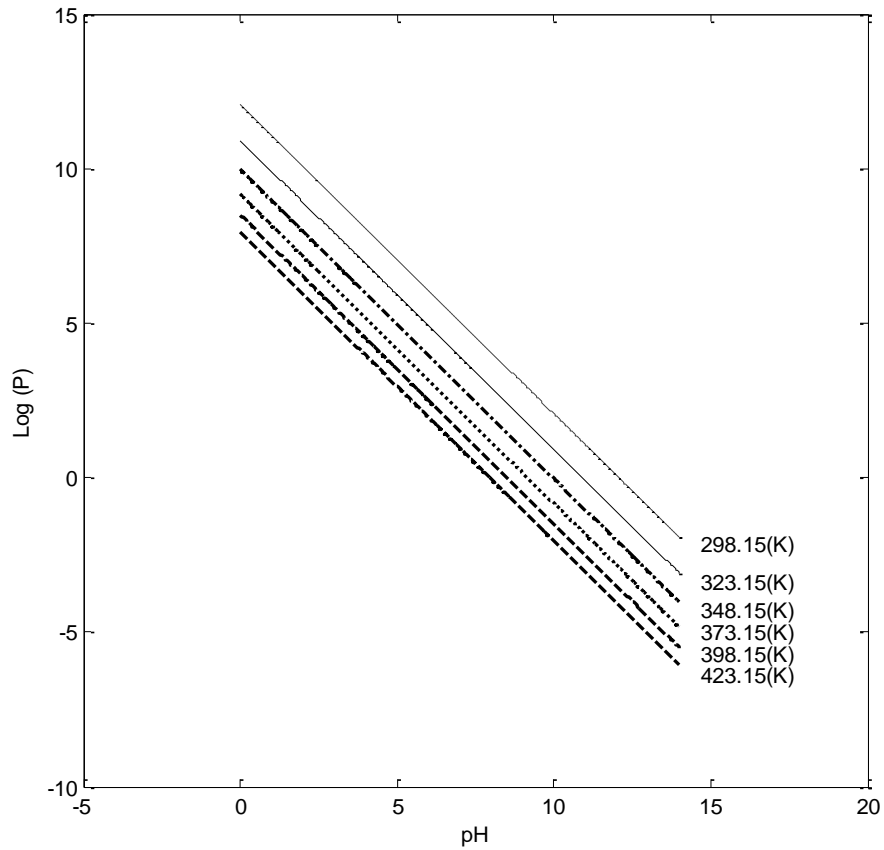
323.15: $\log (p) = 10.91-pH$

348.15: $\log (p) = 9.96-pH$

373.15: $\log (p) = 9.16-pH$

398.15: $\log(p) = 8.50 - pH$

423.15: $\log(p) = 7.95 - pH$



$$\log\left(\frac{p_{\text{H}_2} \times a_{\text{CuSO}_4}}{a_{\text{SO}_4^{2-}}}\right) = \frac{-\Delta G^0}{2.303RT} - 2pH$$

298.15: $\log(p) = -9.15 - 2pH$

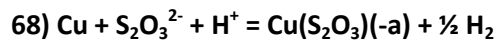
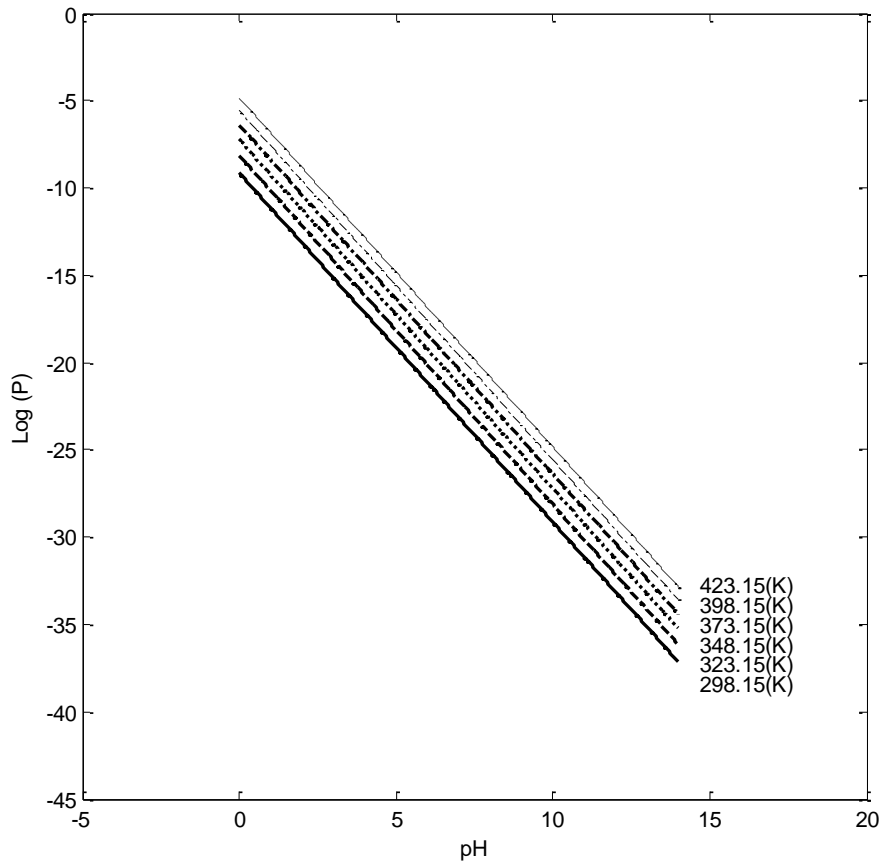
323.15: $\log(p) = -8.15 - 2pH$

348.15: $\log(p) = -7.24 - 2pH$

373.15: $\log(p) = -6.39 - 2pH$

398.15: $\log(p) = -5.59 - 2pH$

423.15: $\log (p) = -4.84-2pH$



$$\log\left(\frac{p_{H_2}^{0.5} \times a_{Cu(S_2O_3)(-)}}{a_{S_2O_3(-2)}}\right) = \frac{-\Delta G^0}{2.303RT} - pH$$

298.15: $\log (p) = 2.23-pH$

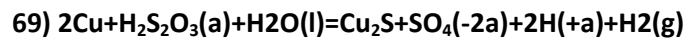
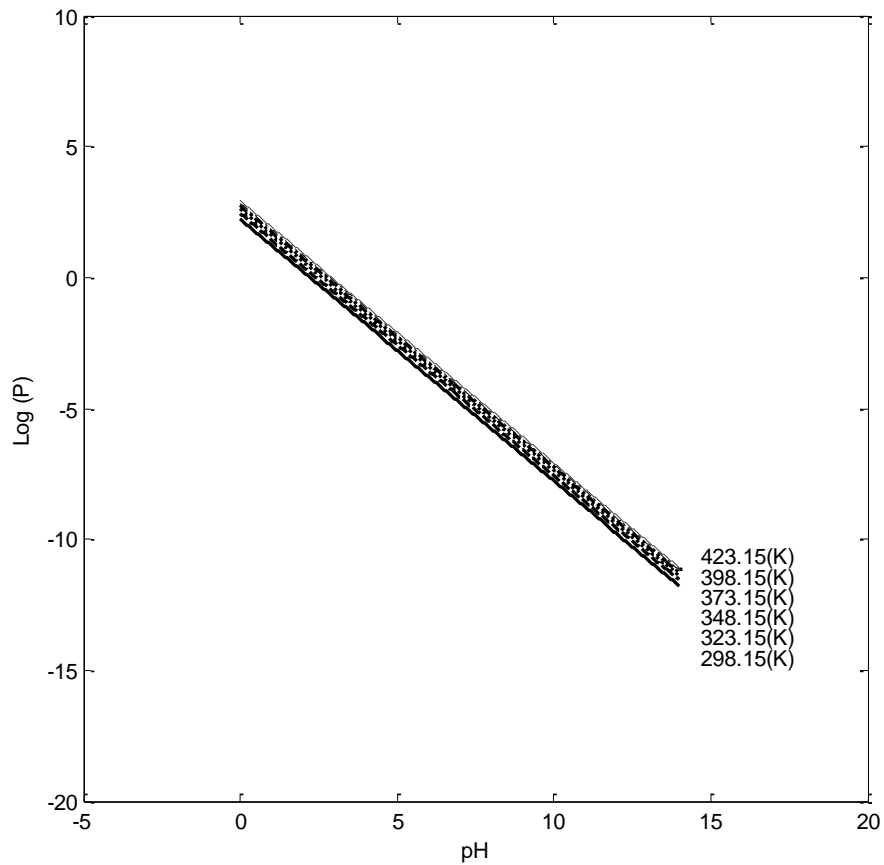
323.15: $\log (p) = 2.44-pH$

348.15: $\log (p) = 2.61-pH$

373.15: $\log (p) = 2.74-pH$

398.15: $\log (p) = 2.84-pH$

423.15: $\log (p) = 2.93-pH$



$$\log\left(\frac{a_{\text{SO}_4^{-2}} \times f_{\text{H}_2}}{a_{\text{H}_2\text{S}_2\text{O}_3}}\right) = \frac{-\Delta G^0}{2.303RT} + 2\text{pH}$$

298.15: $\log (p) = 9.77+2\text{pH}$

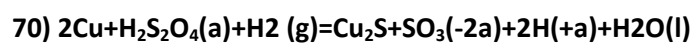
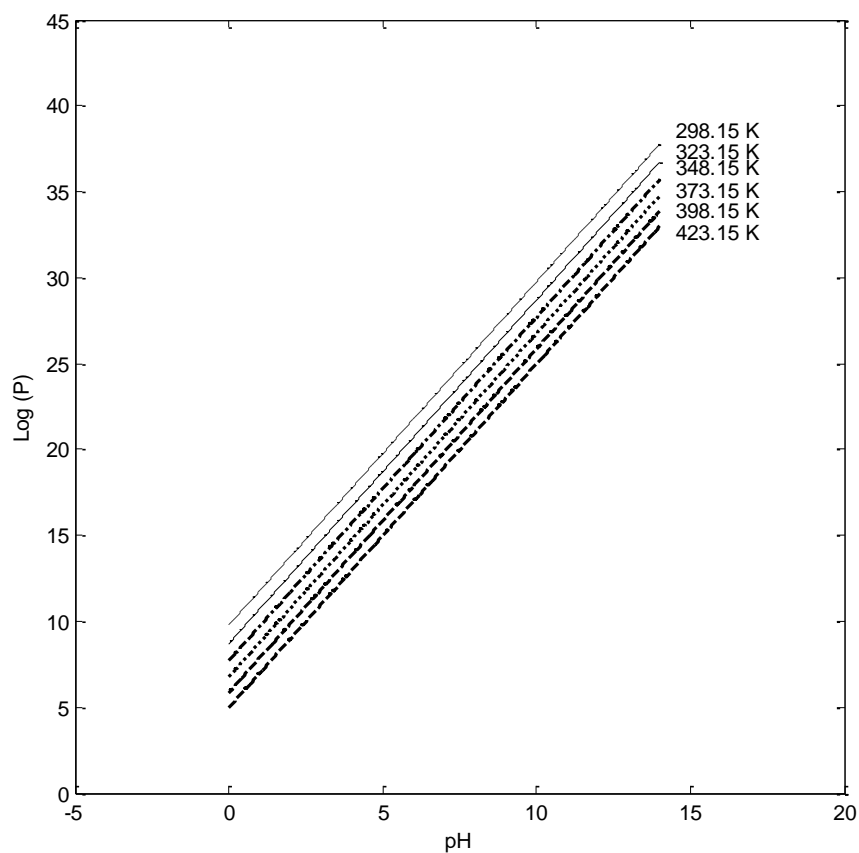
323.15: $\log (p) = 8.71+2\text{pH}$

348.15: $\log (p) = 7.71+2\text{pH}$

373.15: $\log (p) = 6.76+2\text{pH}$

398.15: $\log (p) = 5.86+2\text{pH}$

423.15: $\log (p) = 4.98+2\text{pH}$



$$\log\left(\frac{a_{\text{SO}_3^{-2}}}{a_{\text{H}_2\text{S}_2\text{O}_4} \times f_{\text{H}_2}}\right) = \frac{-\Delta G^0}{2.303RT} + 2\text{pH}$$

298.15: **log (p) = 33.48+2pH**

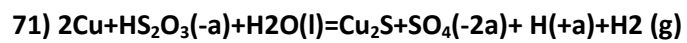
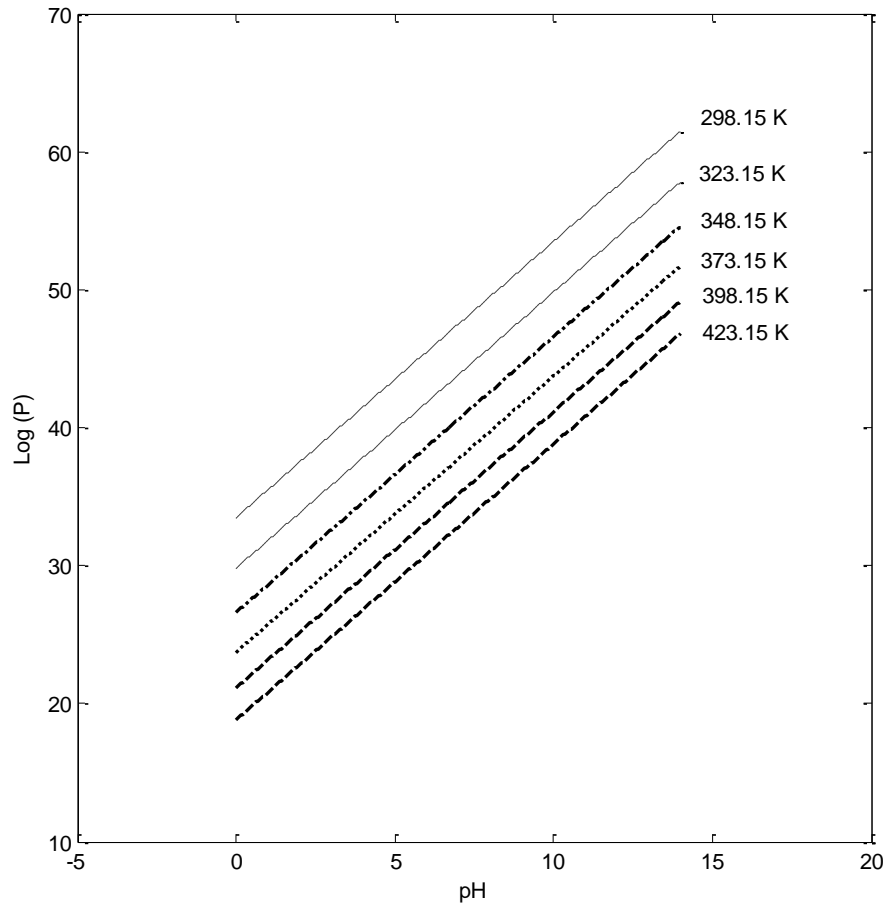
323.15: **log (p) = 29.81+2pH**

348.15: **log (p) = 26.58+2pH**

373.15: **log (p) = 23.71+2pH**

398.15: **log (p) = 21.14+2pH**

423.15: **log (p) = 18.80+2pH**



$$\log\left(\frac{a_{\text{SO}_4^{-2}} \times f_{\text{H}_2}}{a_{\text{HS}_2\text{O}_3^{-}}}\right) = \frac{-\Delta G^0}{2.303RT} + pH$$

298.15: $\log(p) = 10.37 + pH$

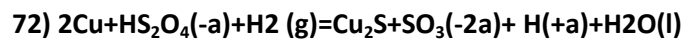
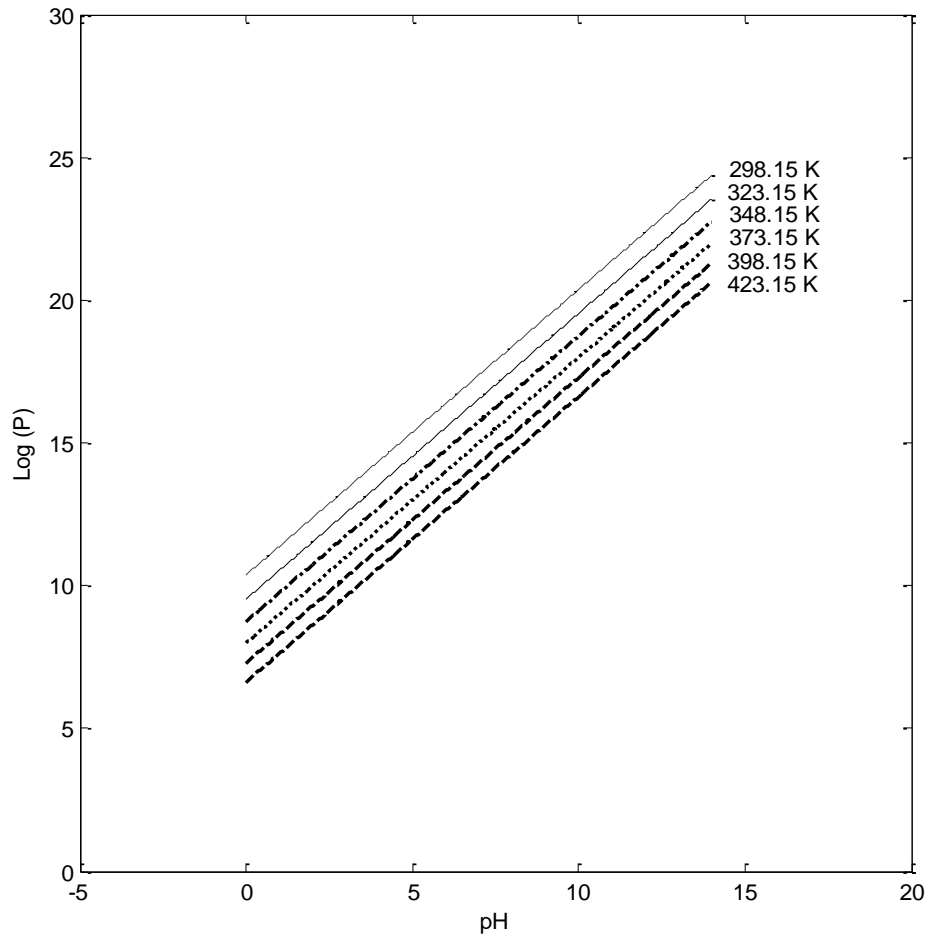
323.15: $\log(p) = 9.53 + pH$

348.15: $\log(p) = 8.74 + pH$

373.15: $\log(p) = 7.99 + pH$

398.15: $\log(p) = 7.29 + pH$

423.15: $\log(p) = 6.62 + pH$



$$\log\left(\frac{a_{\text{SO}_3^{-2}}}{a_{\text{HS}_2\text{O}_4^-} \times f_{\text{H}_2}}\right) = \frac{-\Delta G^0}{2.303RT} + pH$$

298.15: $\log(p) = 33.87 + pH$

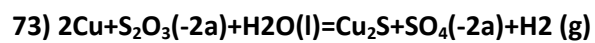
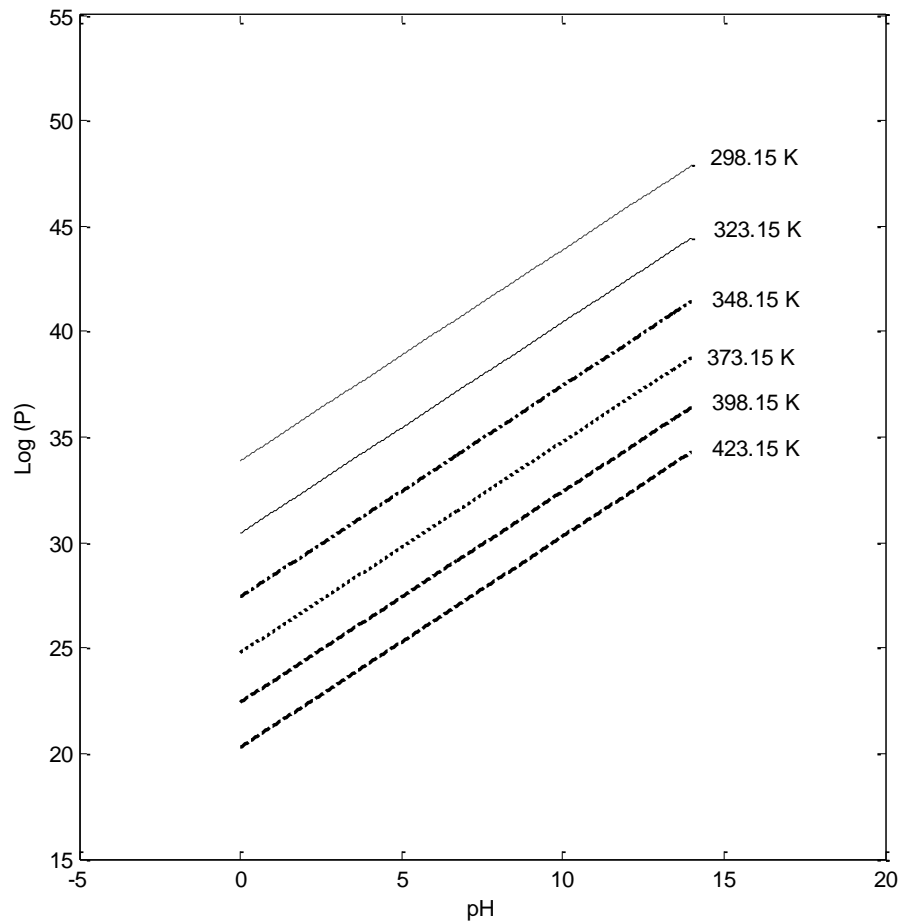
323.15: $\log(p) = 30.43 + pH$

348.15: $\log(p) = 27.42 + pH$

373.15: $\log(p) = 24.77 + pH$

398.15: $\log(p) = 22.41 + pH$

423.15: $\log(p) = 20.28 + pH$



$$\log\left(\frac{a_{\text{SO}_4^{2-}} \times f_{\text{H}_2}}{a_{\text{S}_2\text{O}_3^{2-}}}\right) = \frac{-\Delta G^0}{2.303RT}$$

298.15: **log (p) = 12.73**

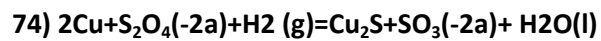
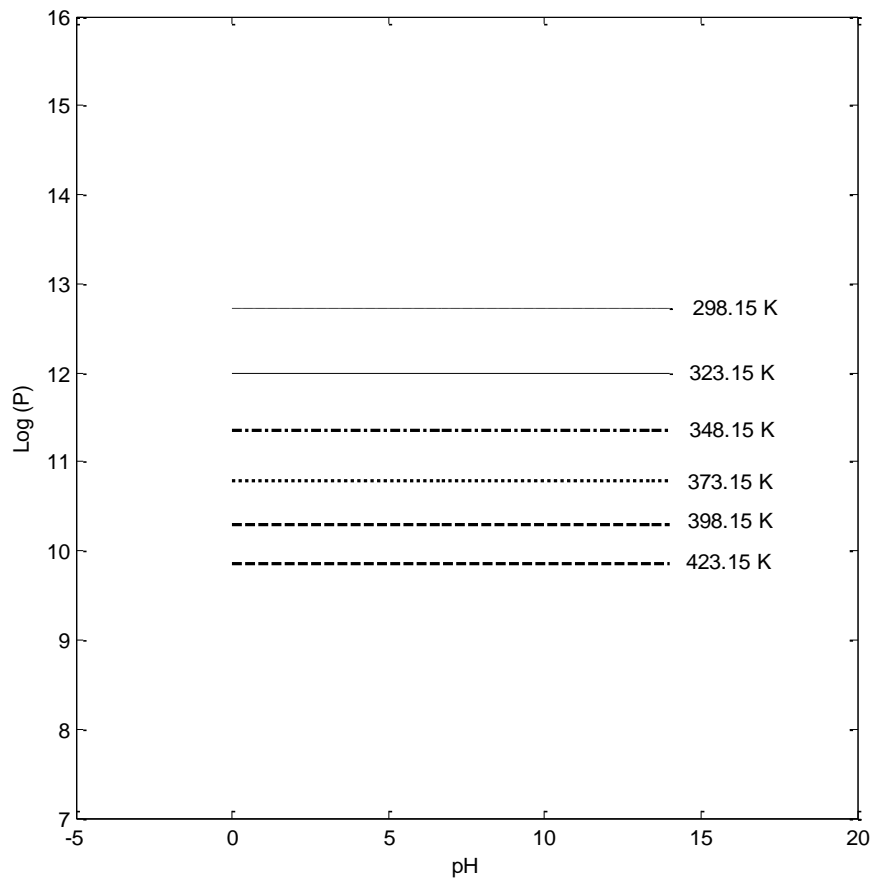
323.15: **log (p) = 11.99**

348.15: **log (p) = 11.35**

373.15: **log (p) = 10.79**

398.15: **log (p) = 10.30**

423.15: **log (p) = 9.86**



$$\log\left(\frac{a_{\text{SO}_3^{-2}}}{a_{\text{S}_2\text{O}_4^{-2}} \times f_{\text{H}_2}}\right) = \frac{-\Delta G^0}{2.303RT}$$

298.15: **log (p) = 36.30**

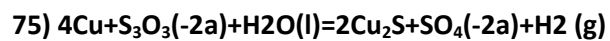
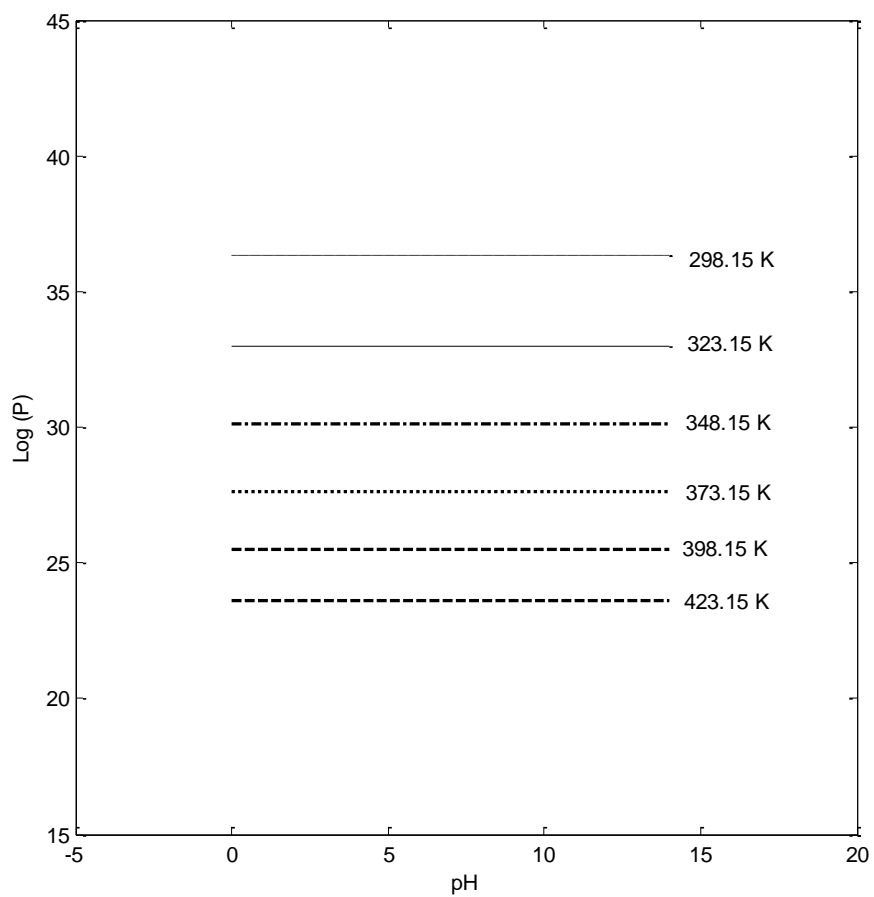
323.15: **log (p) = 32.96**

348.15: **log (p) = 30.10**

373.15: **log (p) = 27.64**

398.15: **log (p) = 25.49**

423.15: **log (p) = 23.59**



$$\log\left(\frac{a_{\text{SO}_4^{-2}} \times f_{\text{H}_2}}{a_{\text{S}_3\text{O}_3^{-2}}}\right) = \frac{-\Delta G^0}{2.303RT}$$

298.15: $\log(p) = -26.58$

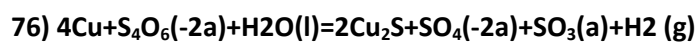
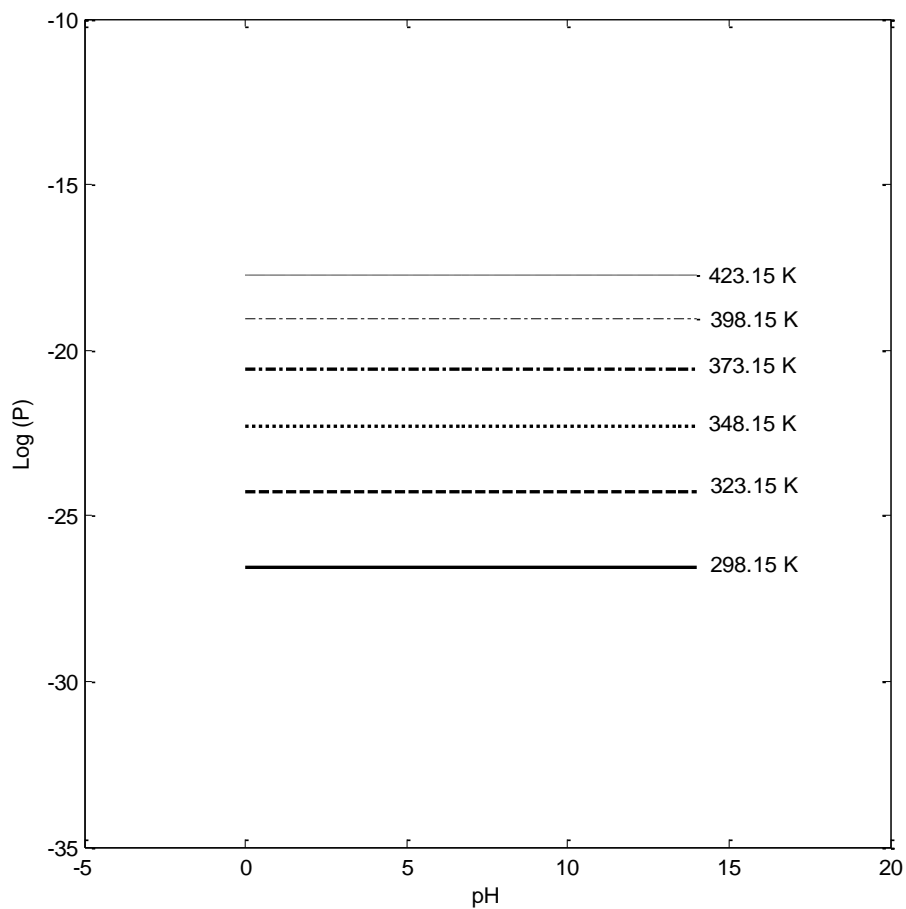
323.15: $\log(p) = -24.28$

348.15: $\log(p) = -22.30$

373.15: $\log(p) = -20.58$

398.15: $\log(p) = -19.06$

423.15: $\log(p) = -17.72$



$$\log\left(\frac{a_{\text{SO}_4^{2-}} \times a_{\text{SO}_3} \times f_{\text{H}_2}}{a_{\text{S}_4\text{O}_6^{2-}}}\right) = \frac{-\Delta G^0}{2.303RT}$$

298.15: $\log(p) = 28.17$

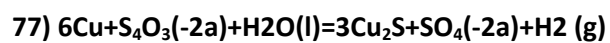
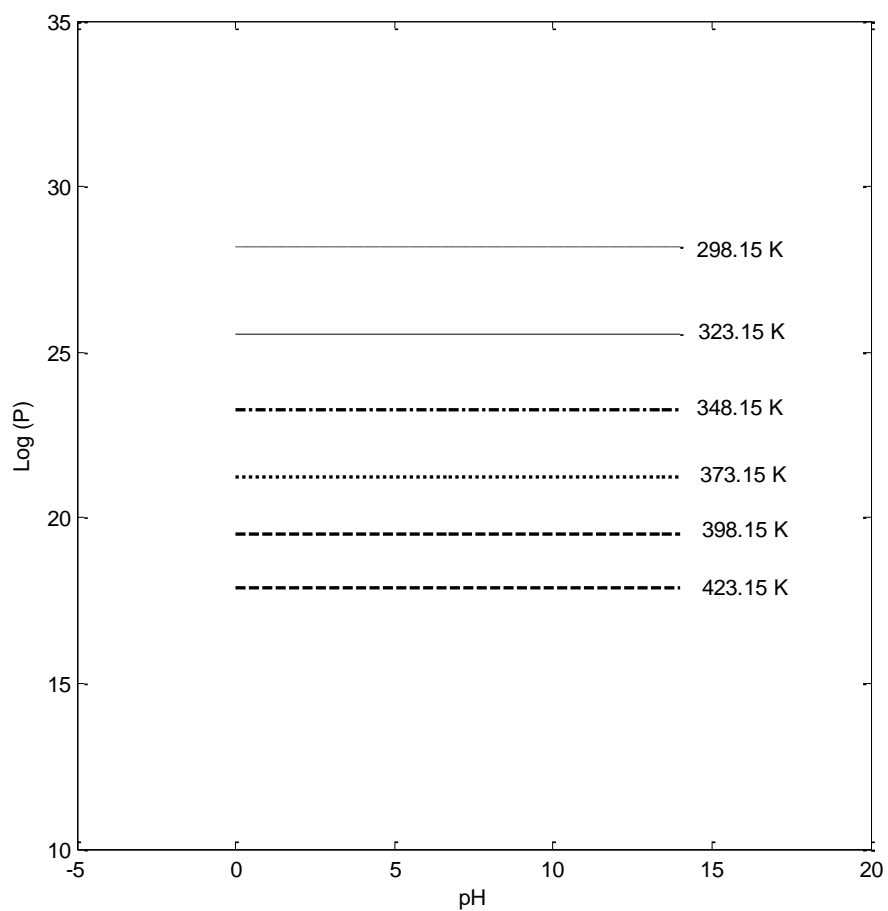
323.15: $\log(p) = 25.54$

348.15: $\log(p) = 23.26$

373.15: $\log(p) = 21.25$

398.15: $\log(p) = 19.49$

423.15: $\log(p) = 17.91$



$$\log\left(\frac{a_{\text{SO}_4^{-2}} \times f_{\text{H}_2}}{a_{\text{S}_4\text{O}_3^{-2}}}\right) = \frac{-\Delta G^0}{2.303RT}$$

298.15: $\log(p) = -34.65$

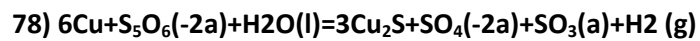
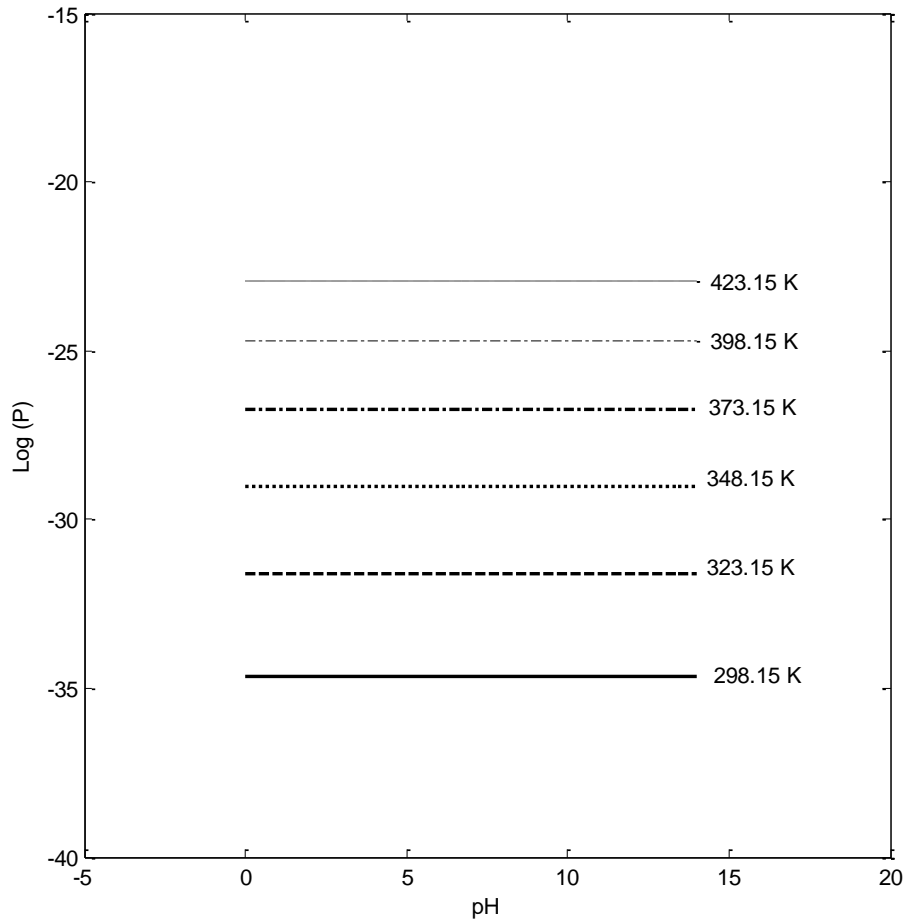
323.15: $\log(p) = -31.61$

348.15: $\log(p) = -29.00$

373.15: $\log(p) = -26.73$

398.15: $\log(p) = -24.73$

423.15: $\log(p) = -22.96$



$$\log\left(\frac{a_{\text{SO}_4^{-2}} \times a_{\text{SO}_3} \times f_{\text{H}_2}}{a_{\text{S}_5\text{O}_6^{-2}}}\right) = \frac{-\Delta G^0}{2.303RT}$$

298.15: **log (p) = 57.78**

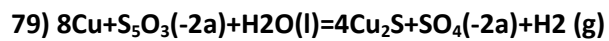
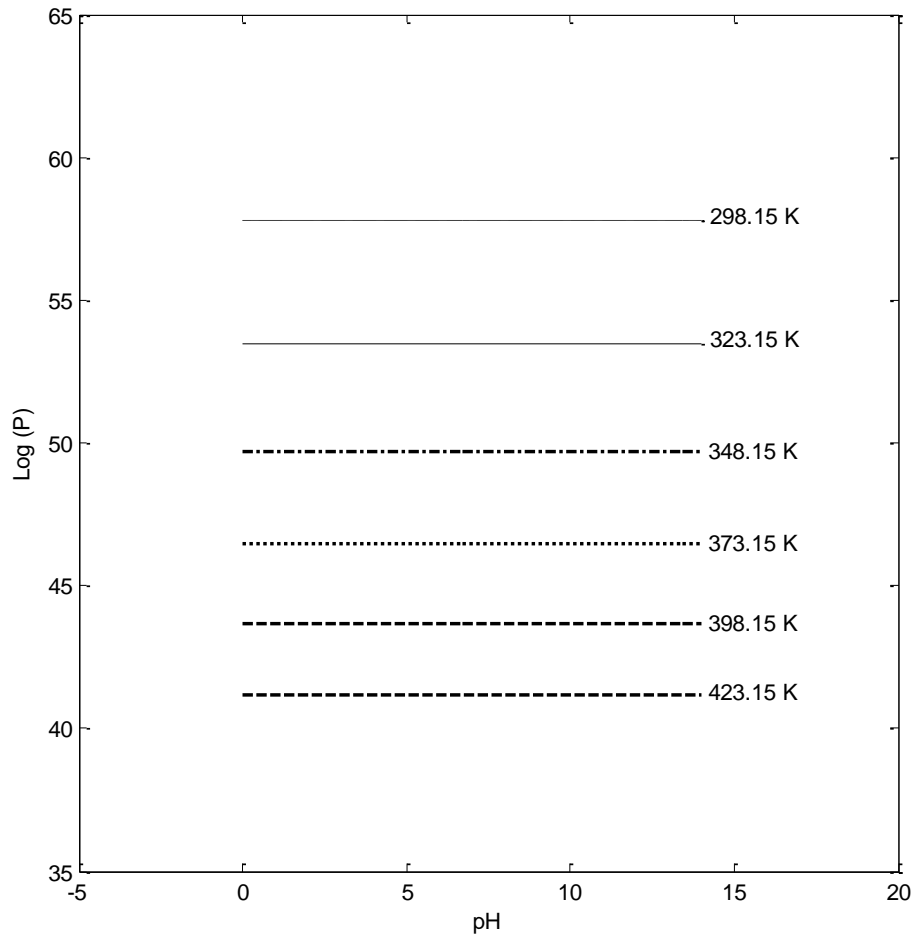
323.15: **log (p) = 53.44**

348.15: **log (p) = 49.71**

373.15: **log (p) = 46.48**

398.15: **log (p) = 43.65**

423.15: **log (p) = 41.16**



$$\log\left(\frac{a_{\text{SO}_4^{-2}} \times f_{\text{H}_2}}{a_{\text{S}_5\text{O}_3^{-2}}}\right) = \frac{-\Delta G^0}{2.303RT}$$

298.15: $\log(p) = -32.66$

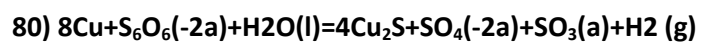
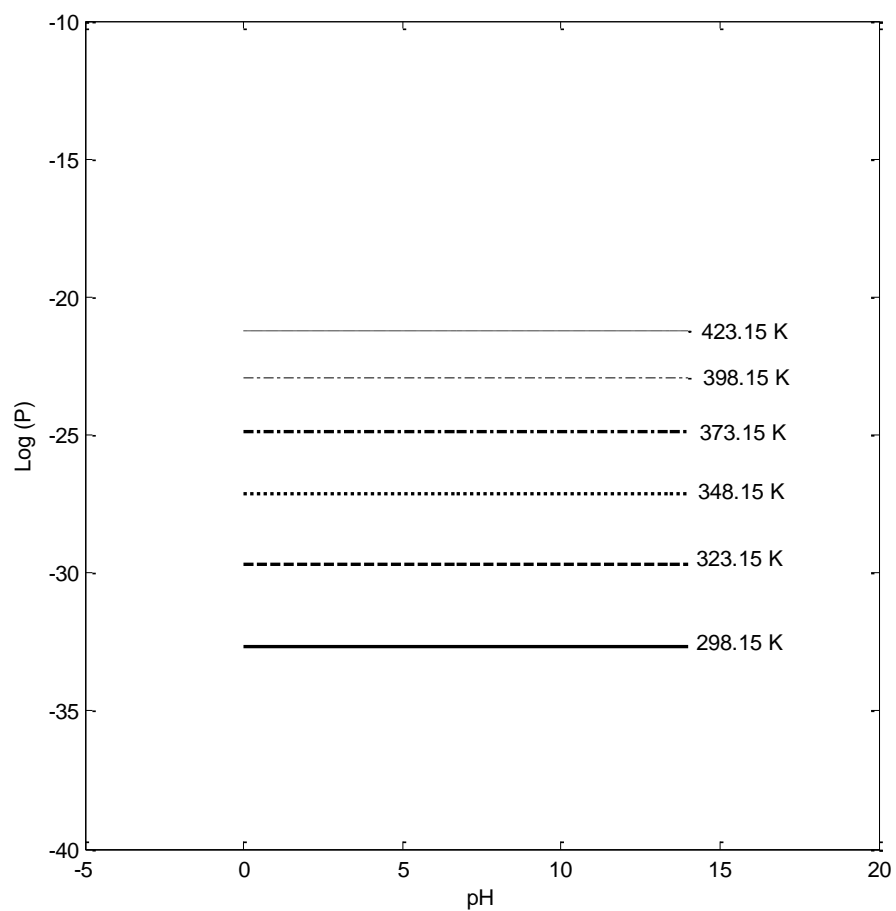
323.15: $\log(p) = -29.67$

348.15: $\log(p) = -27.11$

373.15: $\log(p) = -24.89$

398.15: $\log(p) = -22.94$

423.15: $\log(p) = -21.22$



$$\log\left(\frac{a_{\text{SO}_4^{-2}} \times a_{\text{SO}_3} \times f_{\text{H}_2}}{a_{\text{S}_6\text{O}_6^{-2}}}\right) = \frac{-\Delta G^0}{2.303RT}$$

298.15: **log (p) = 30.19**

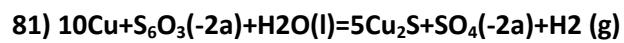
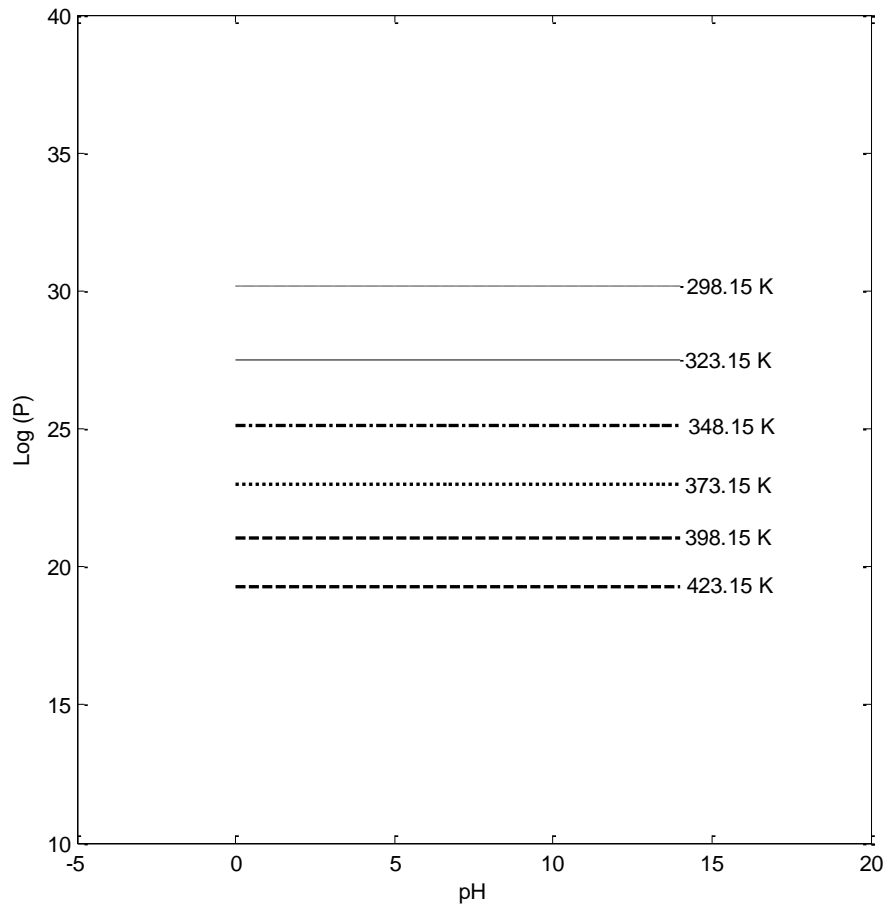
323.15: **log (p) = 27.51**

348.15: **log (p) = 25.13**

373.15: **log (p) = 23.00**

398.15: **log (p) = 21.07**

423.15: **log (p) = 19.29**



$$\log\left(\frac{a_{\text{SO}_4^{-2}} \times f_{\text{H}_2}}{a_{\text{S}_6\text{O}_3^{-2}}}\right) = \frac{-\Delta G^0}{2.303RT}$$

298.15: **log (p) = -25.68**

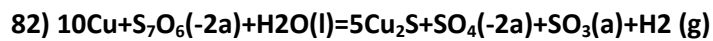
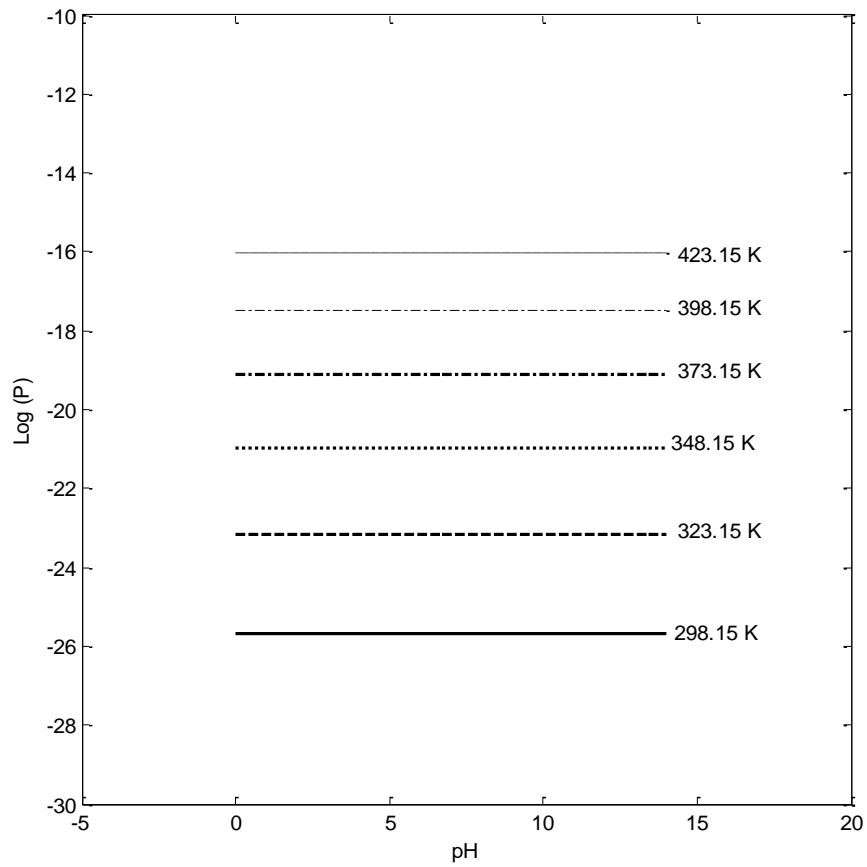
323.15: **log (p) = -23.15**

348.15: **log (p) = -20.99**

373.15: **log (p) = -19.11**

398.15: **log (p) = -17.47**

423.15: **log (p) = -16.03**



$$\log\left(\frac{a_{\text{SO}_4^{-2}} \times a_{\text{SO}_3} \times f_{\text{H}_2}}{a_{\text{S}_7\text{O}_6^{-2}}}\right) = \frac{-\Delta G^0}{2.303RT}$$

298.15: **log (p) = 38.19**

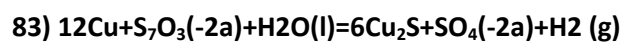
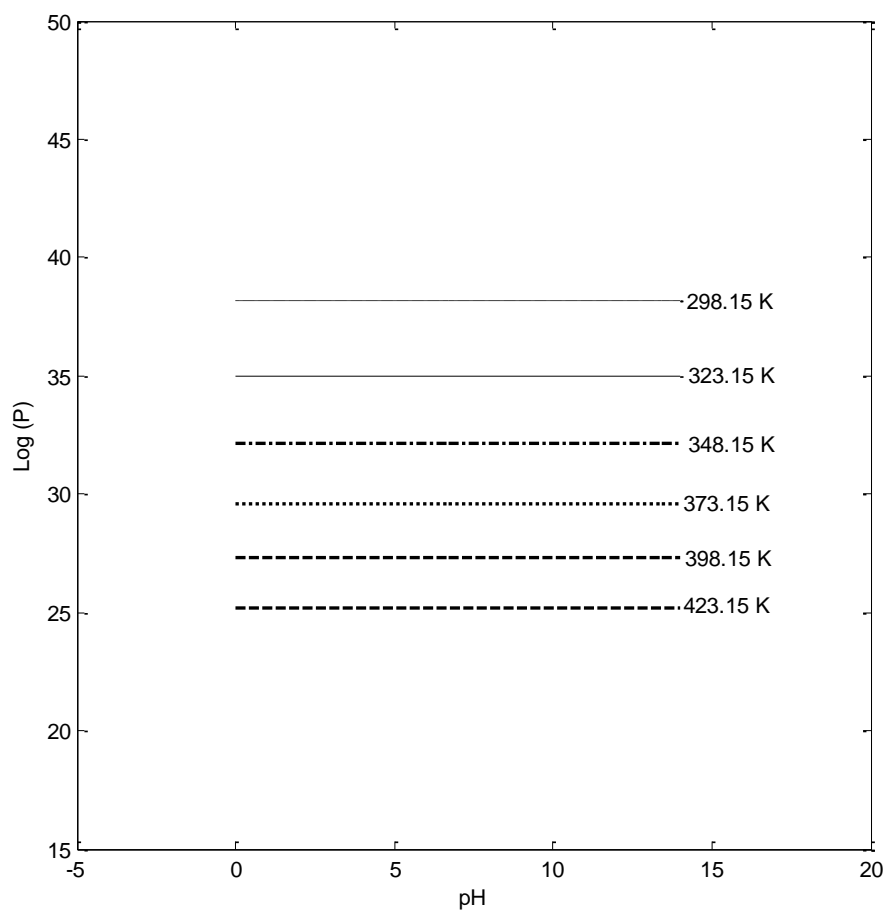
323.15: **log (p) = 34.98**

348.15: **log (p) = 32.14**

373.15: **log (p) = 29.60**

398.15: **log (p) = 27.30**

423.15: **log (p) = 25.20**



$$\log\left(\frac{a_{\text{SO}_4^{-2}} \times f_{\text{H}_2}}{a_{\text{S}_7\text{O}_3^{-2}}}\right) = \frac{-\Delta G^0}{2.303RT}$$

298.15: **log (p) = -16.27**

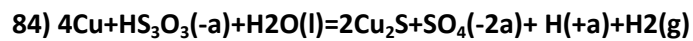
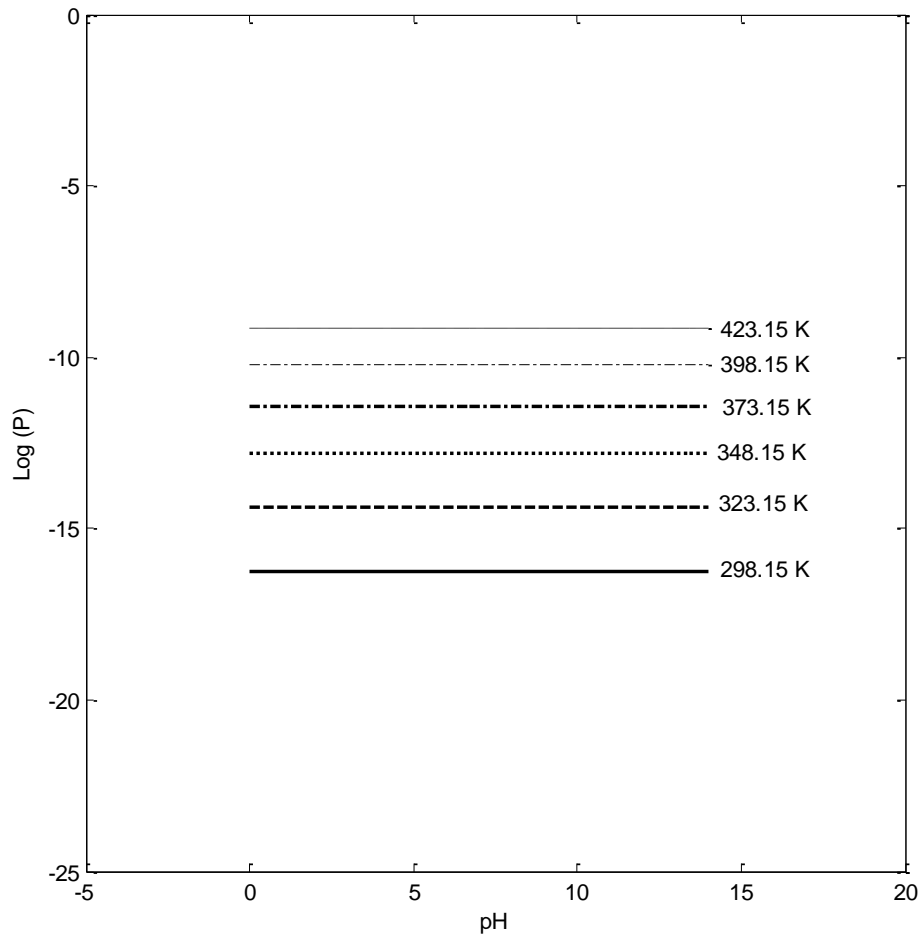
323.15: **log (p) = -14.39**

348.15: **log (p) = -12.79**

373.15: **log (p) = -11.41**

398.15: **log (p) = -10.20**

423.15: **log (p) = -9.15**



$$\log\left(\frac{a_{\text{SO}_4^{-2}} \times f_{\text{H}_2}}{a_{\text{HS}_3\text{O}_3^-}}\right) = \frac{-\Delta G^0}{2.303RT} + pH$$

298.15: $\log (p) = 35.74 + pH$

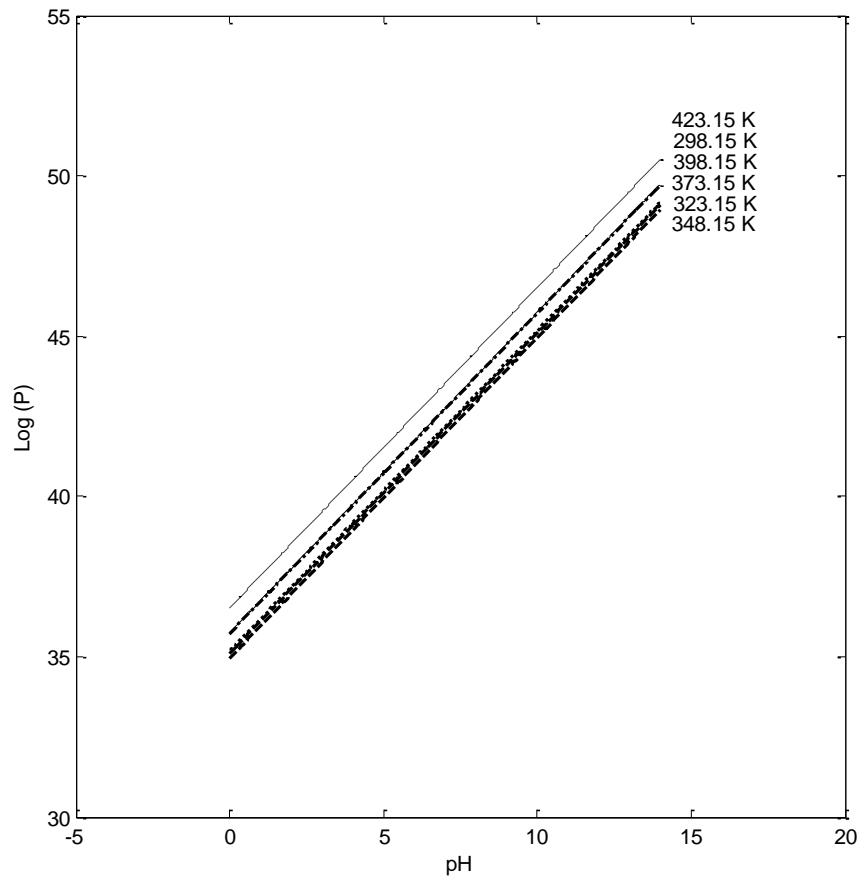
323.15: $\log (p) = 35.10 + pH$

348.15: $\log (p) = 34.94 + pH$

373.15: $\log (p) = 35.16 + pH$

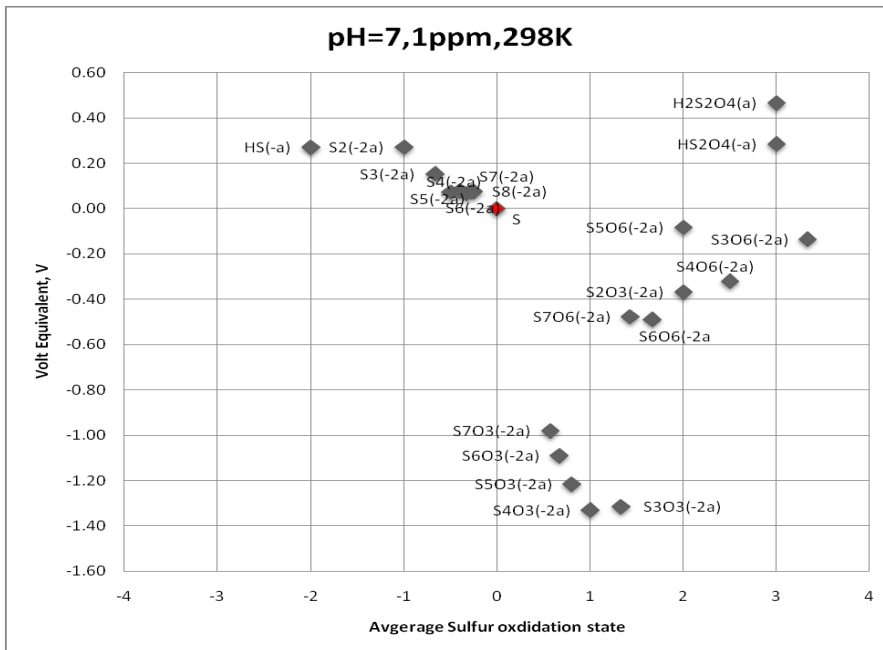
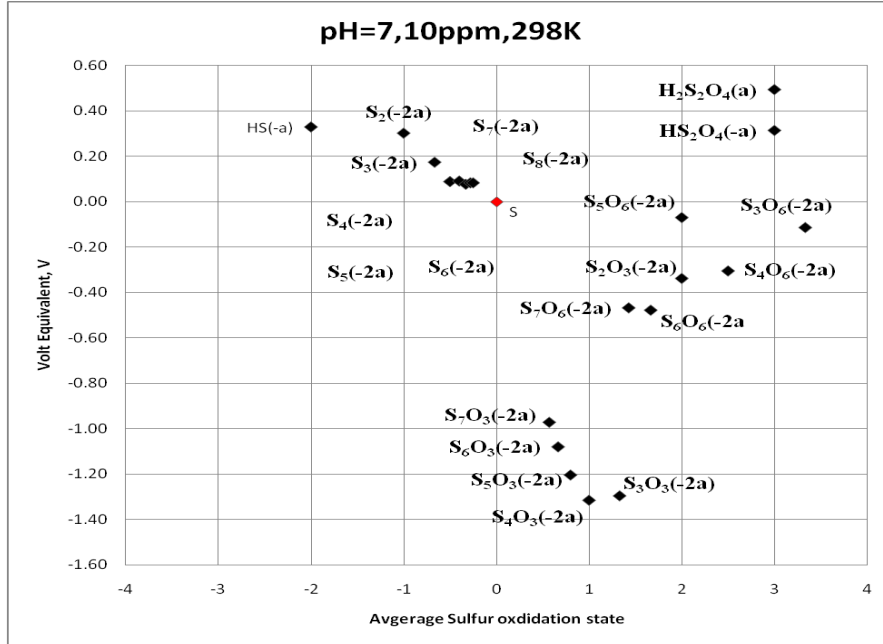
398.15: $\log (p) = 35.71 + pH$

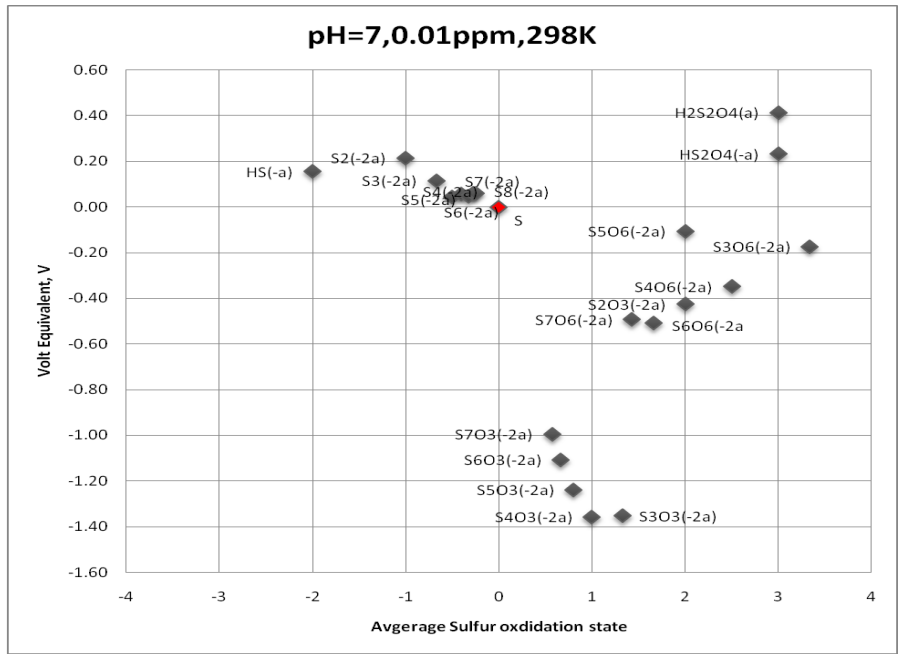
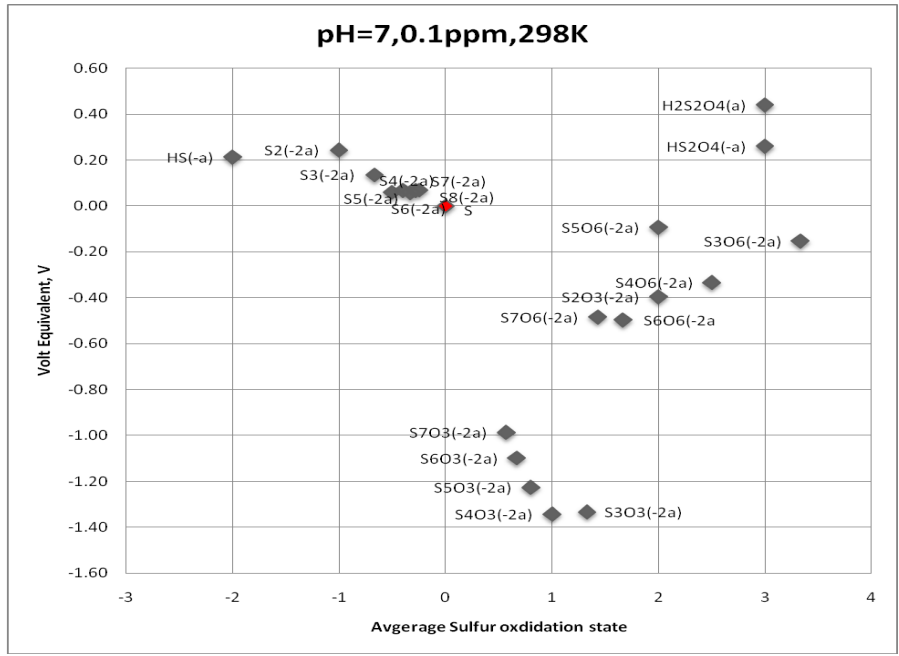
423.15: $\log (p) = 36.51 + pH$

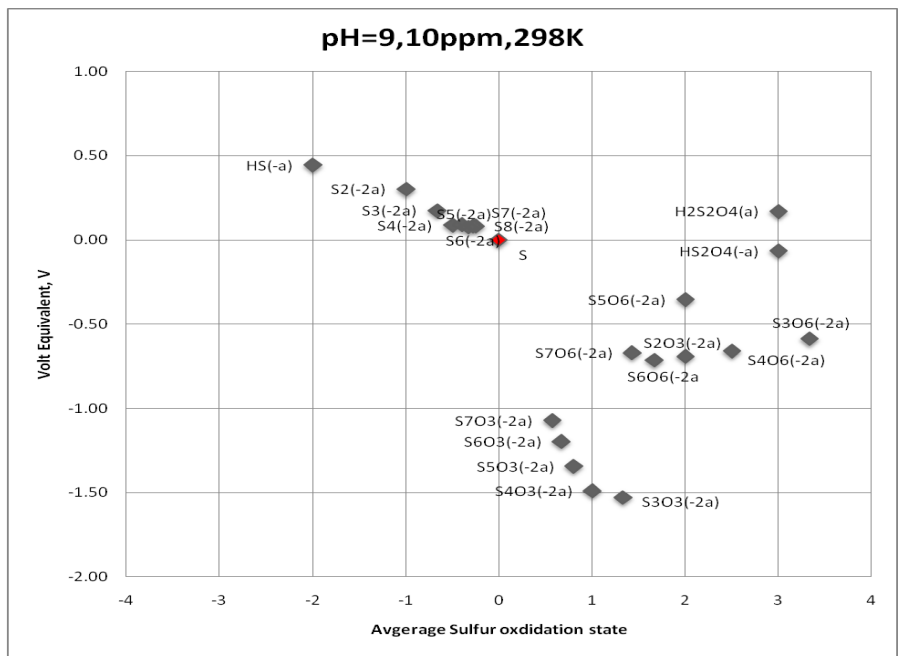
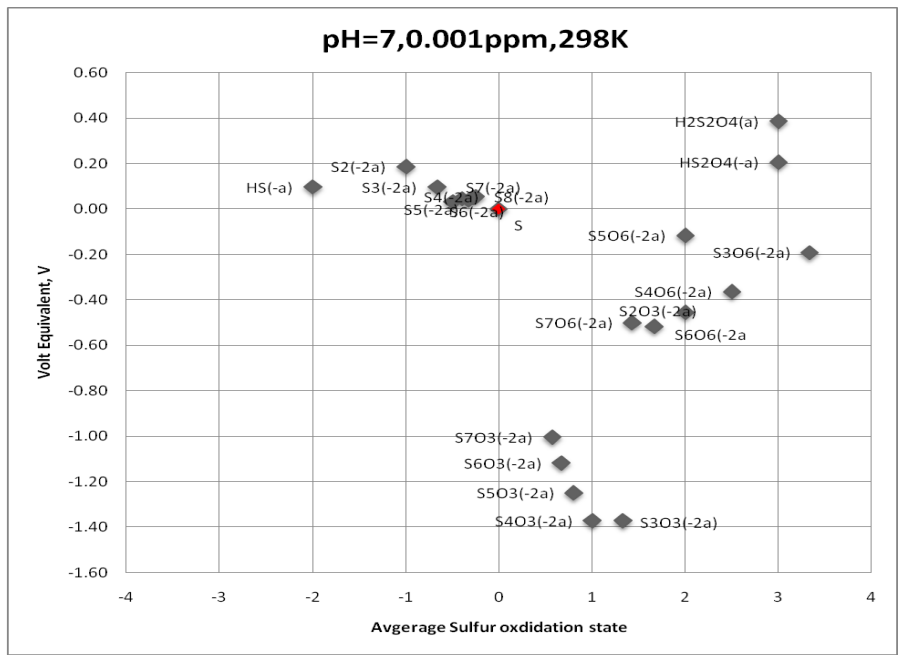


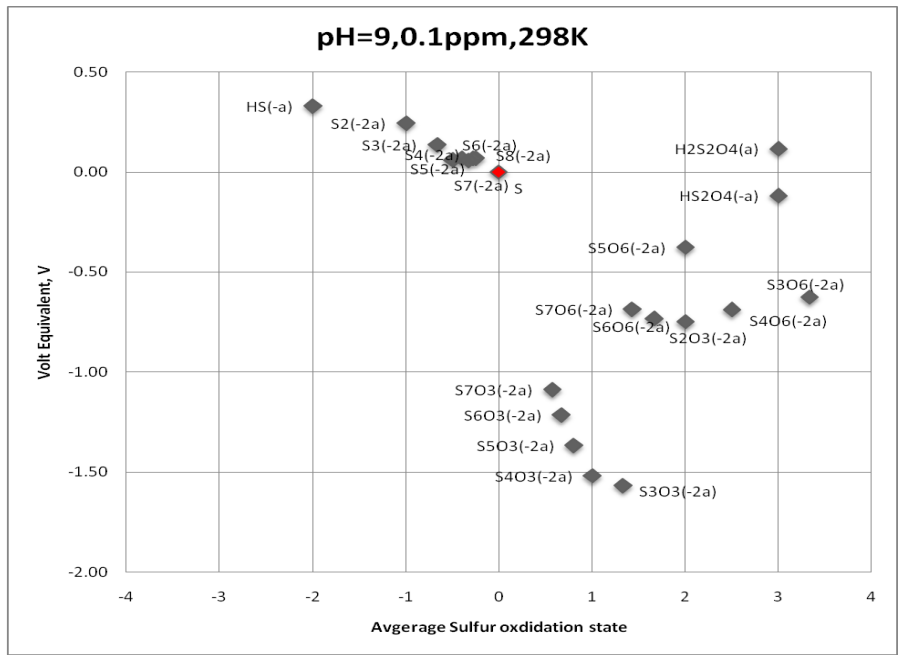
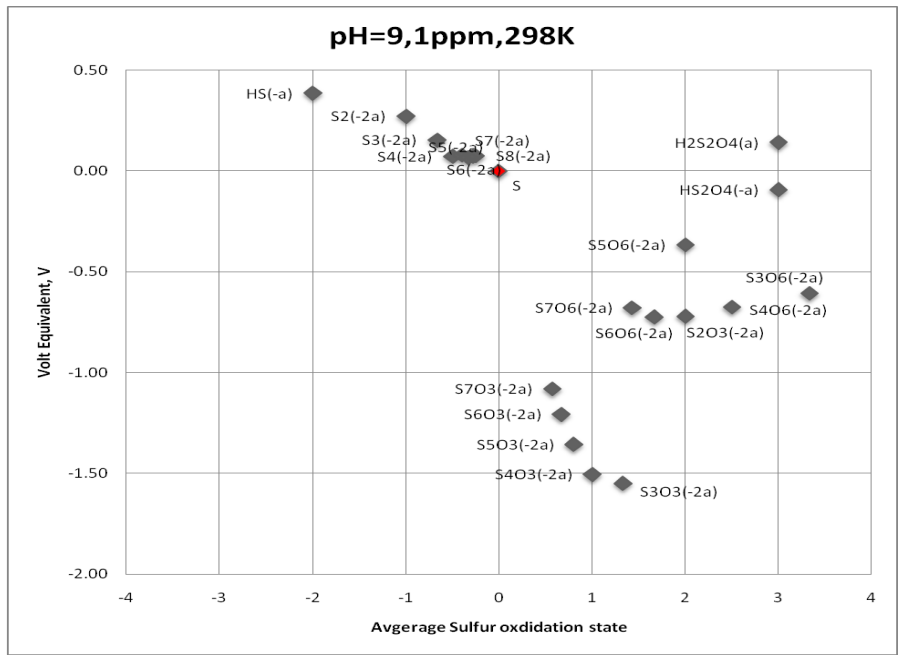
Appendix II

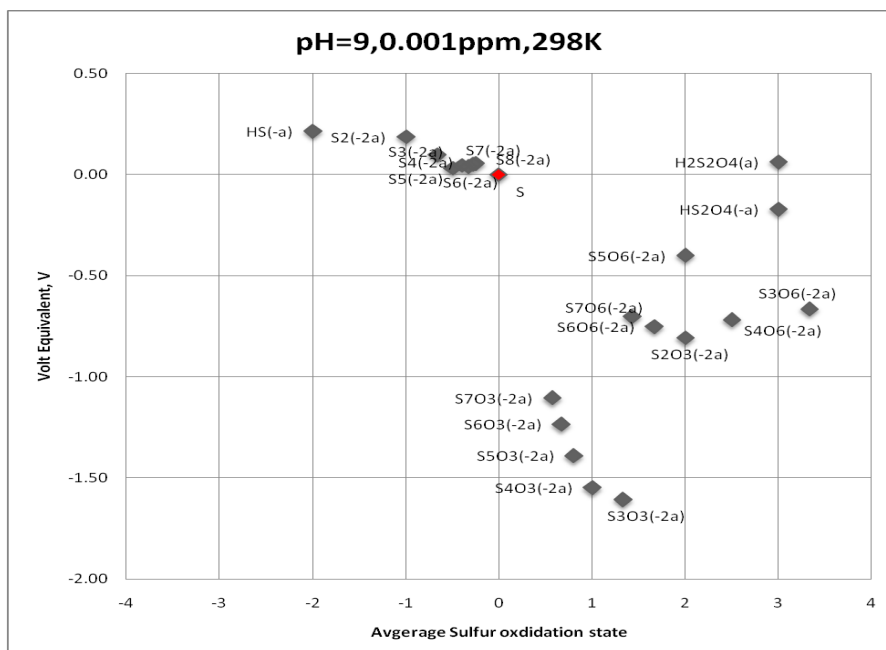
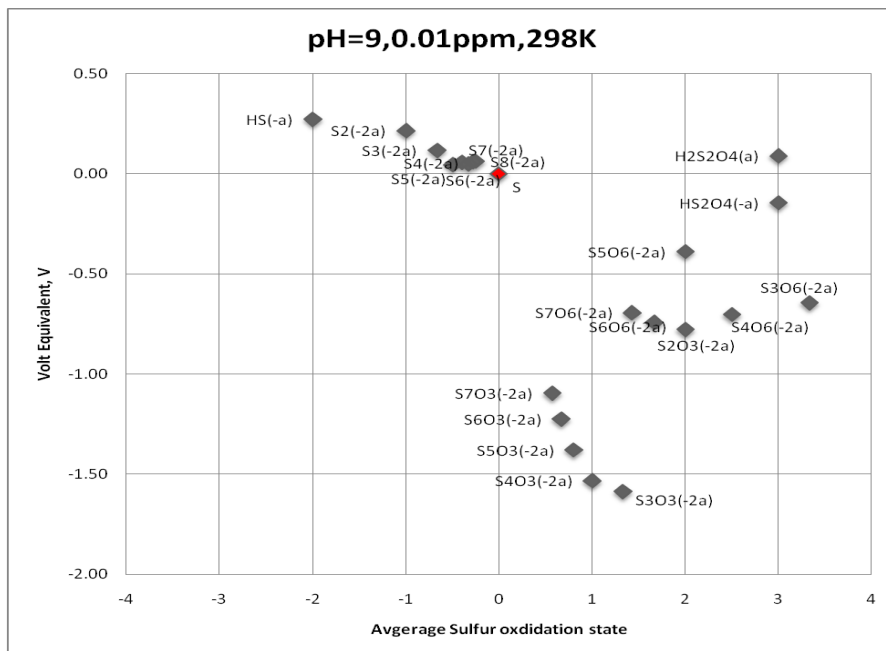
Volt-Equivalent Diagrams

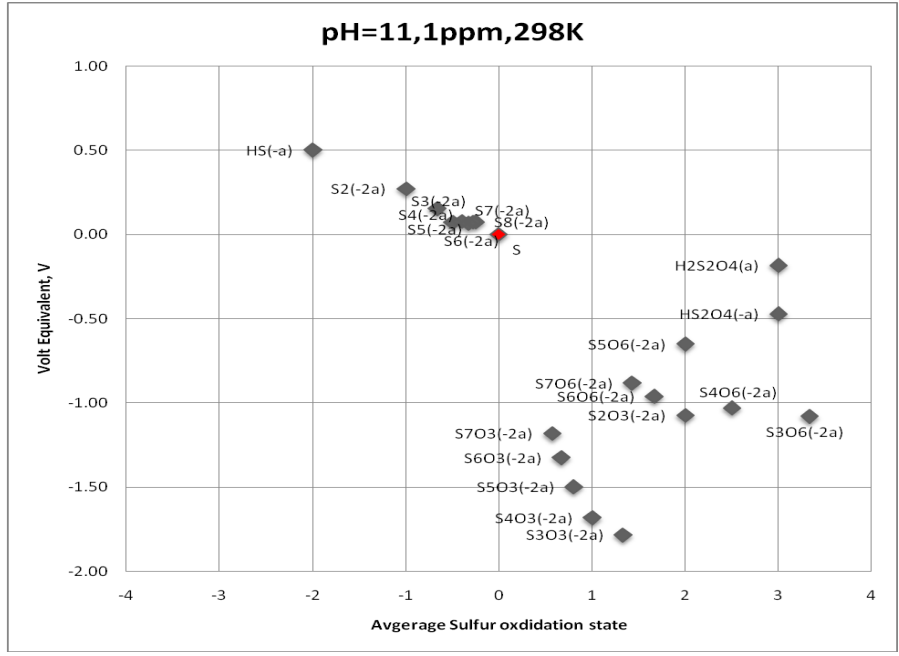
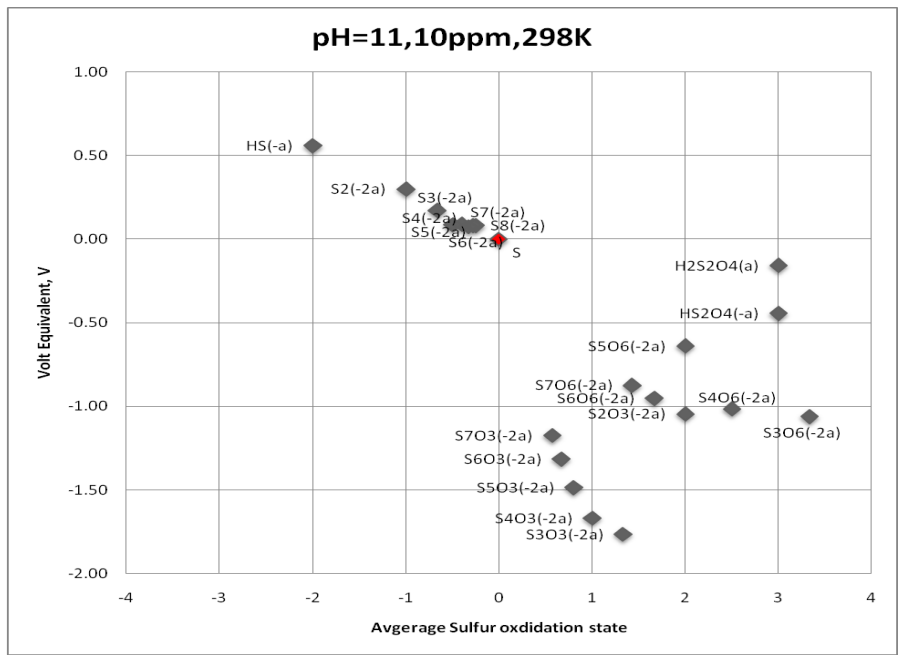


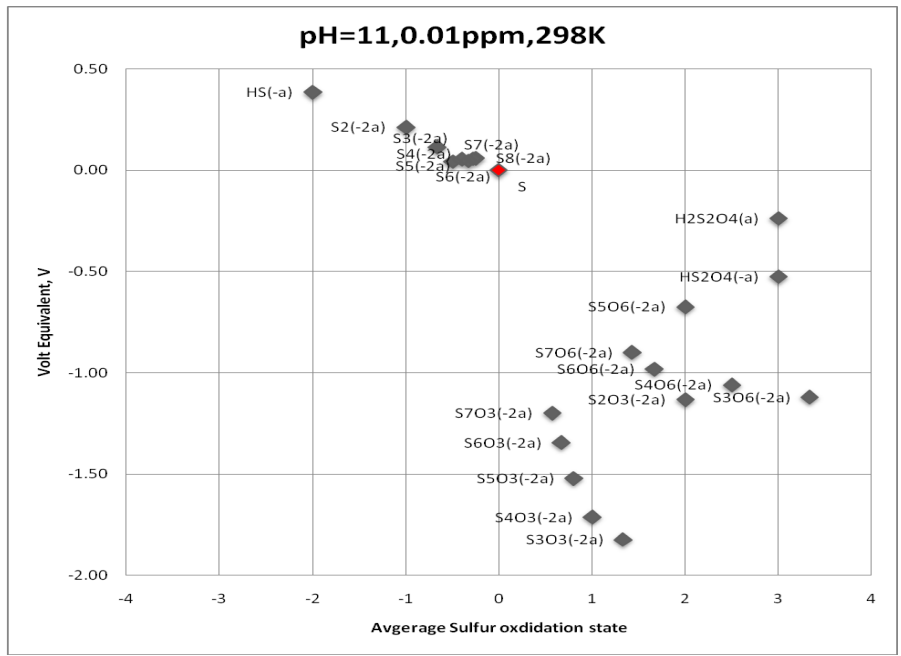
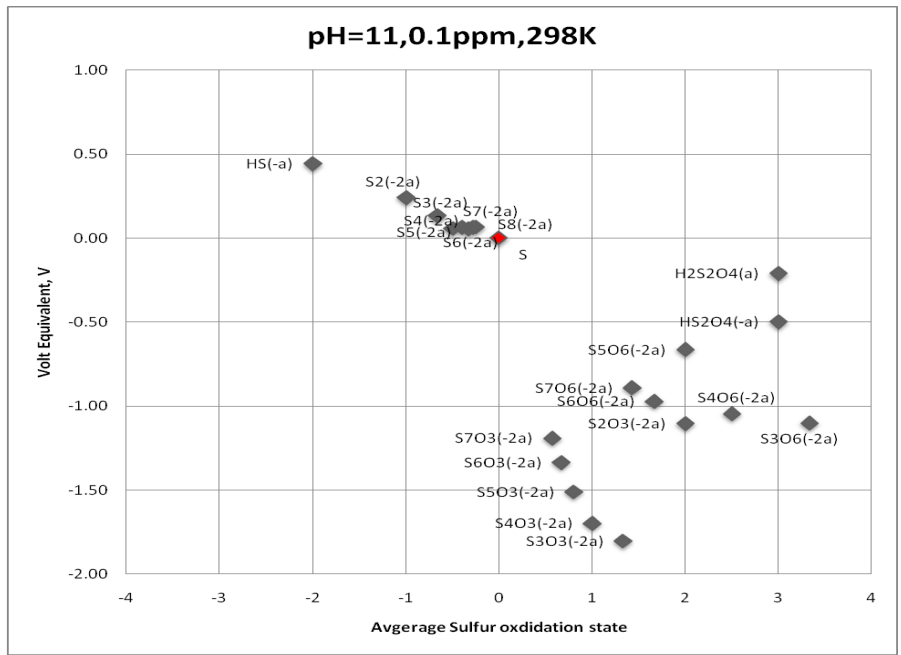


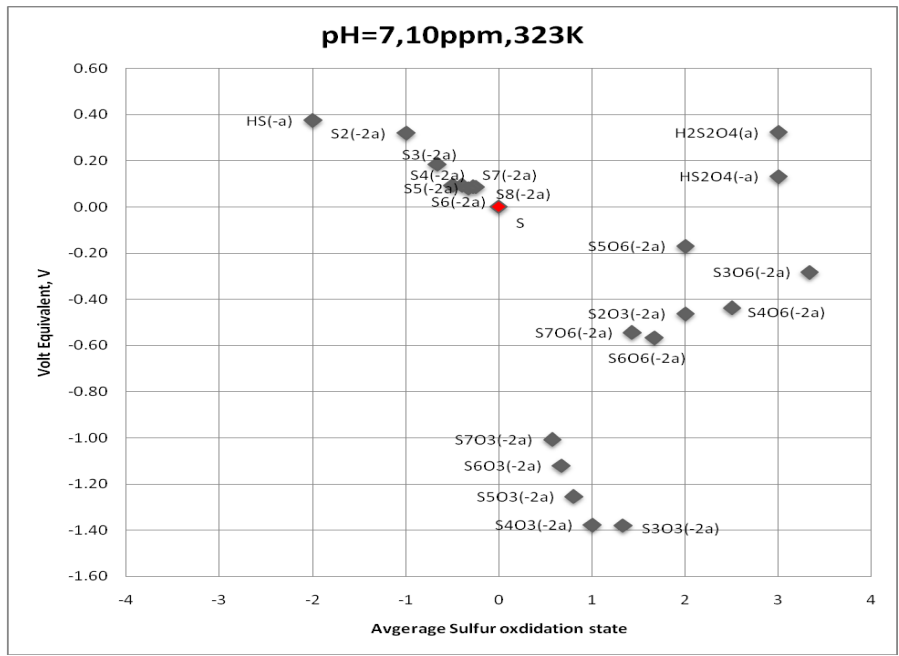
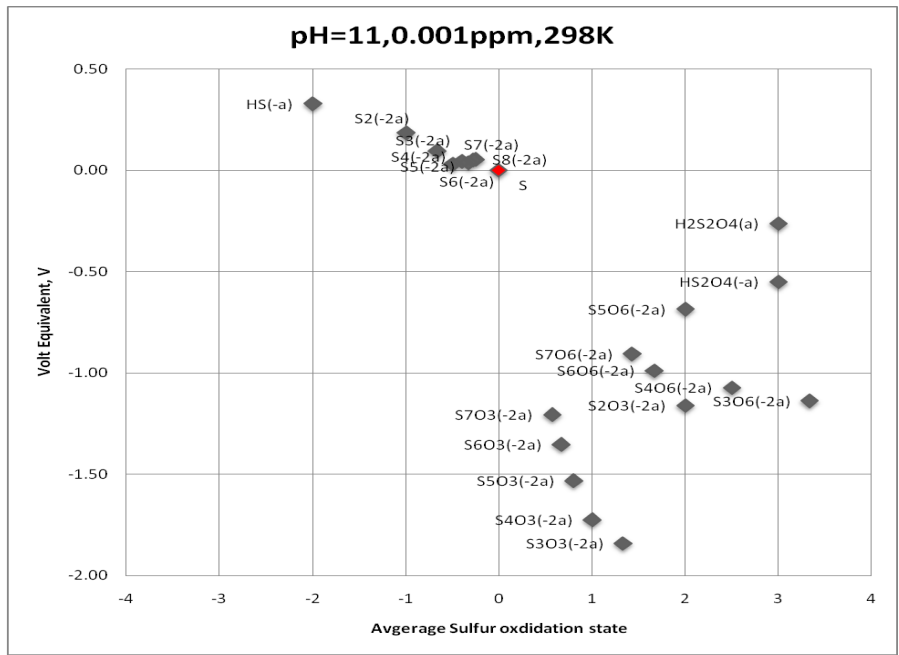


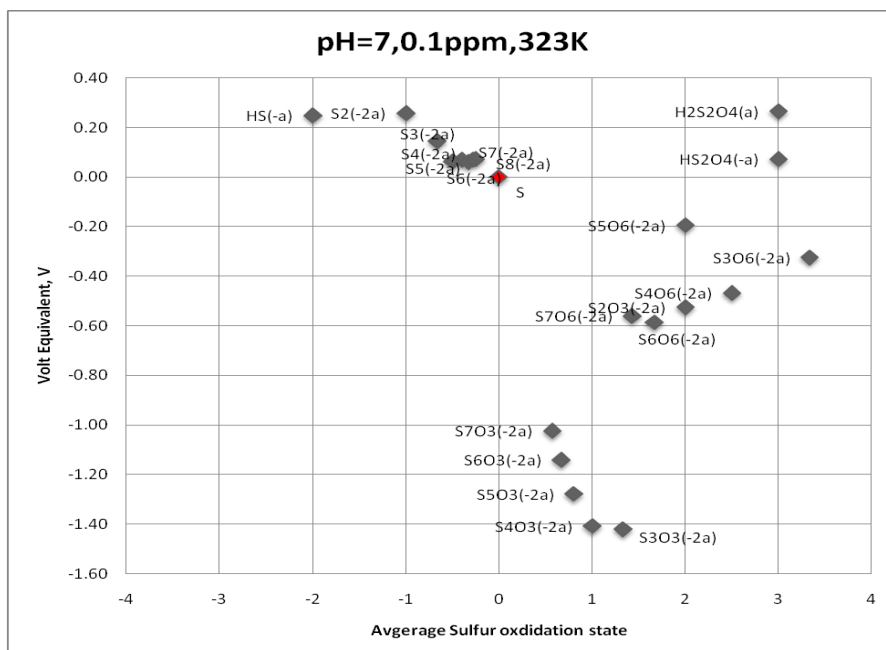
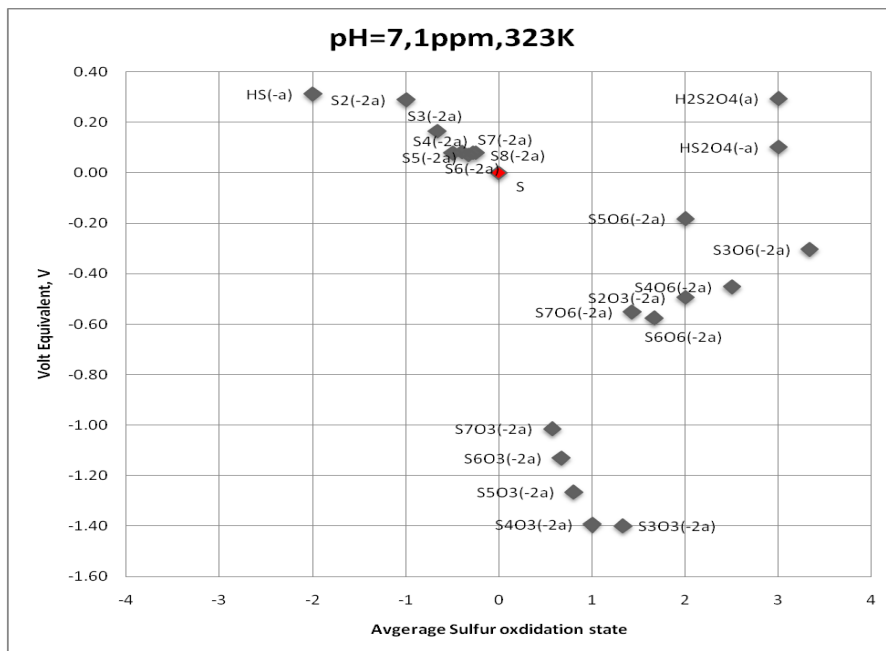


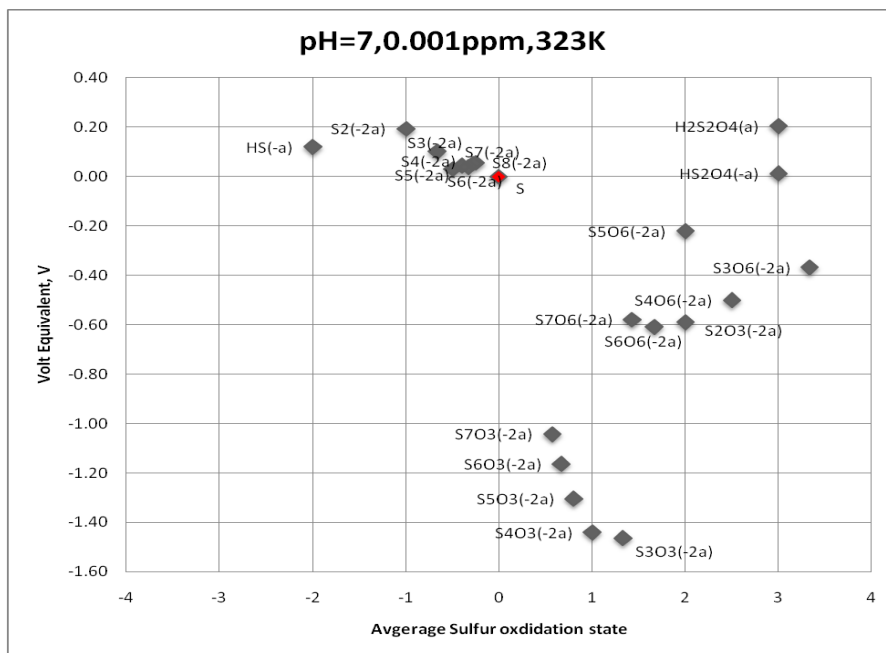
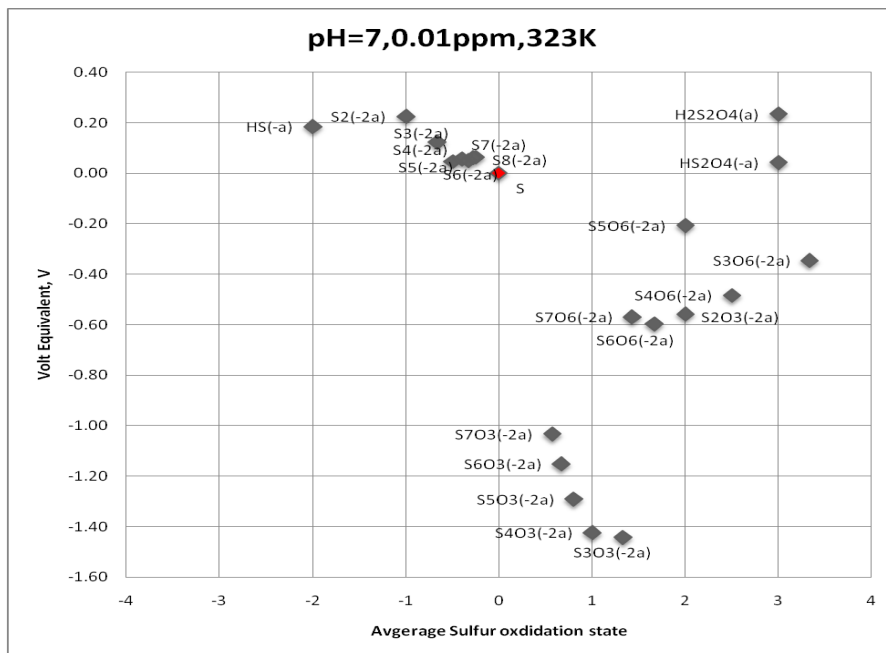


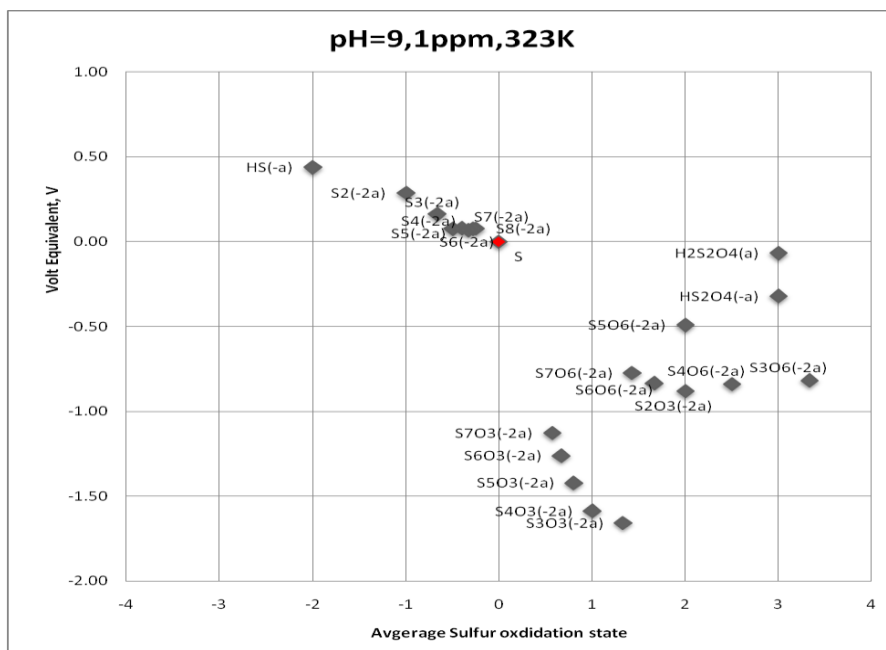
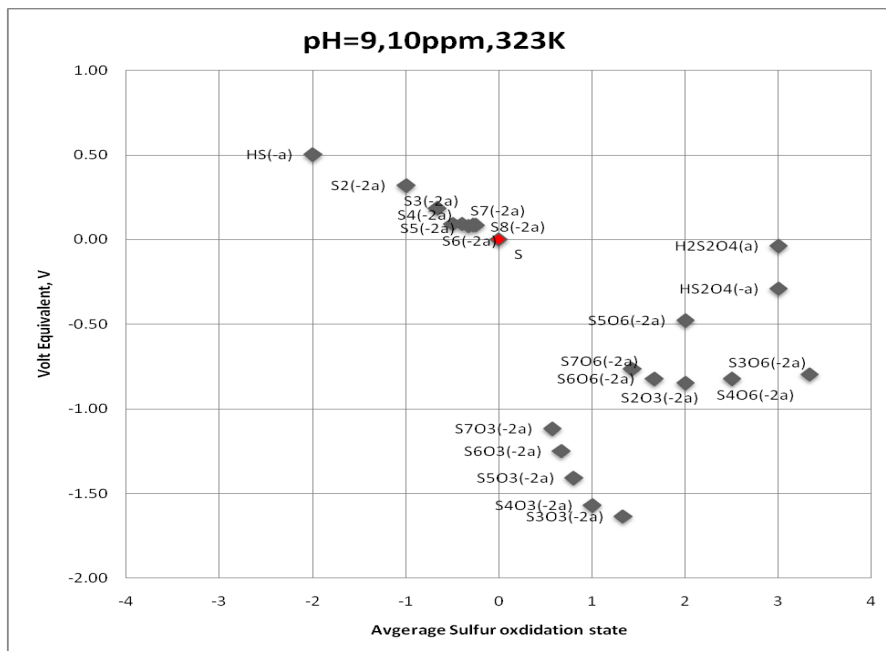


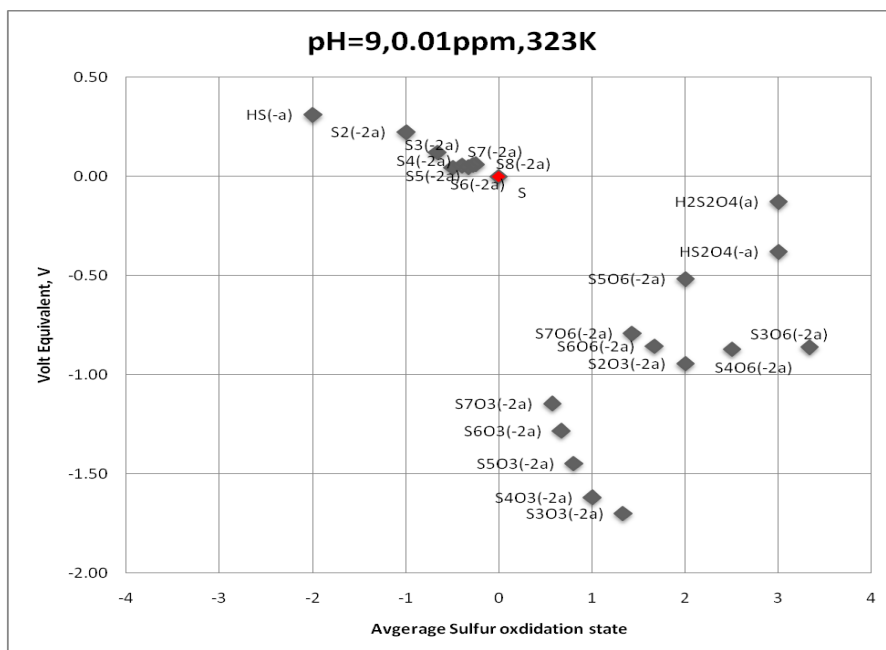
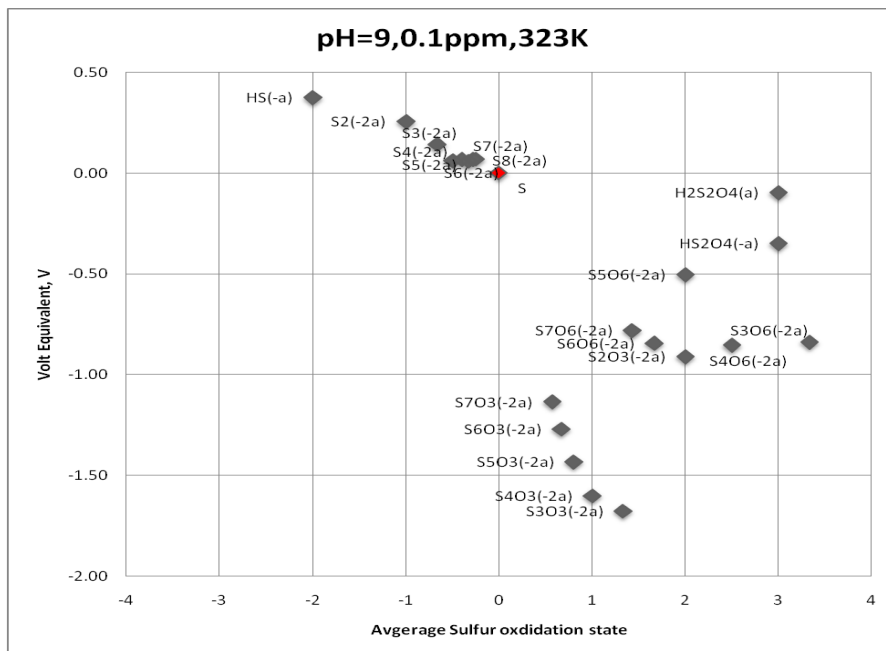


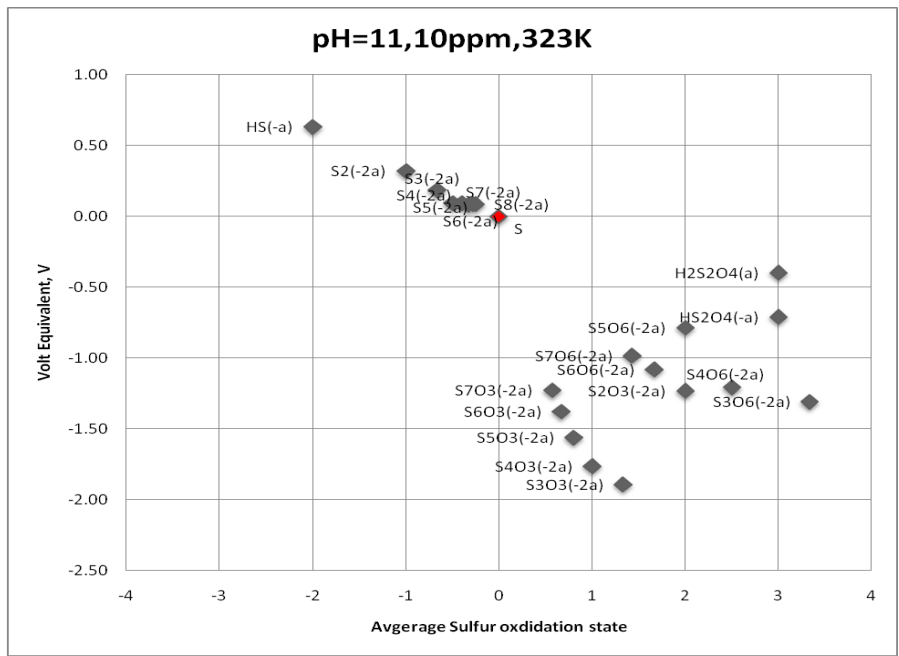
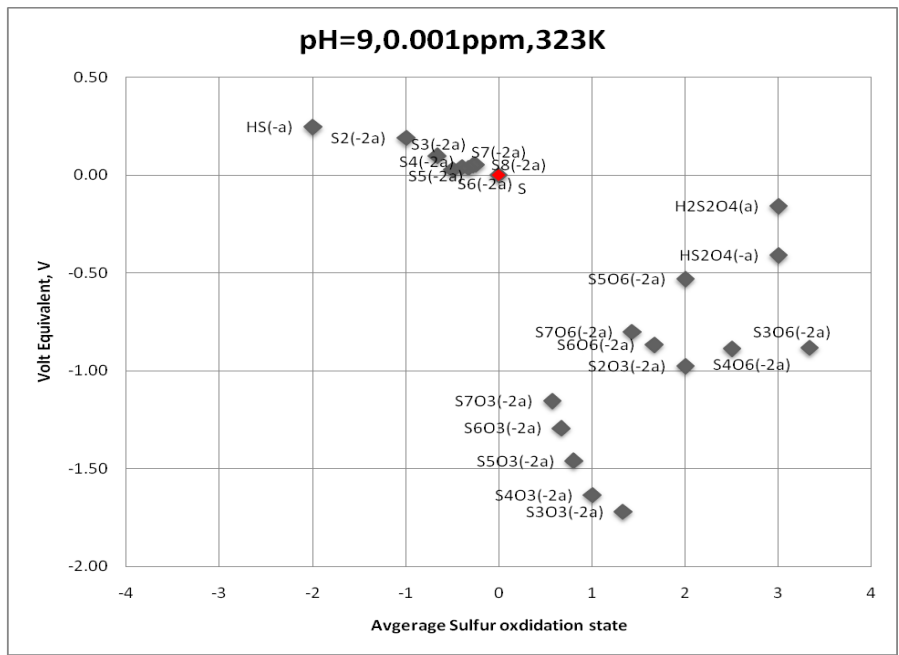


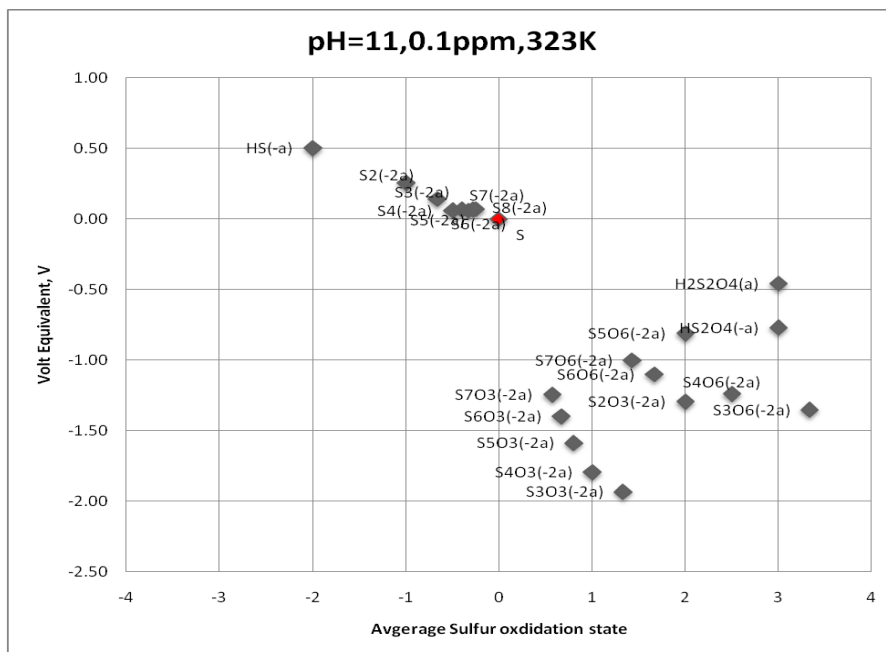
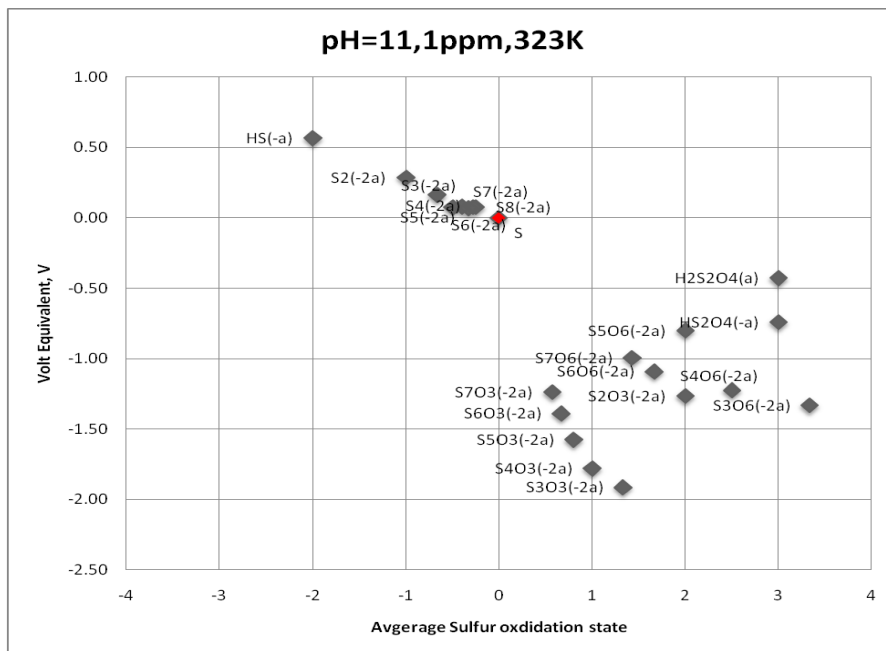


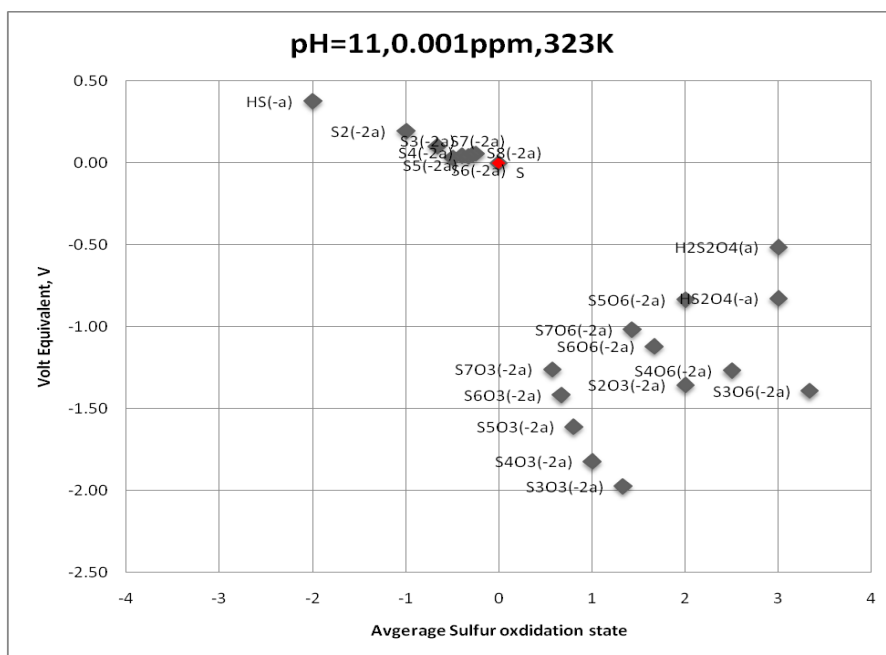
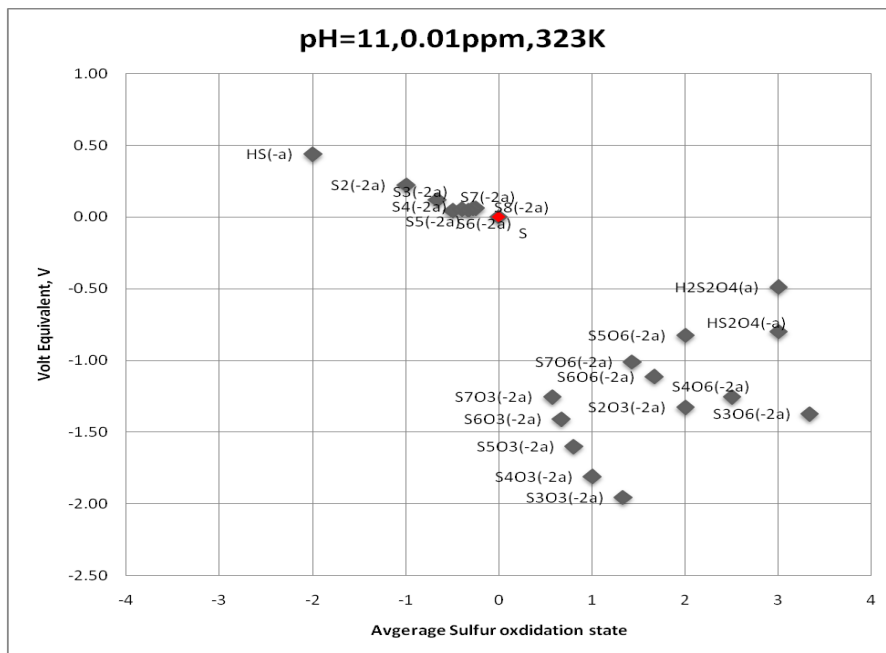


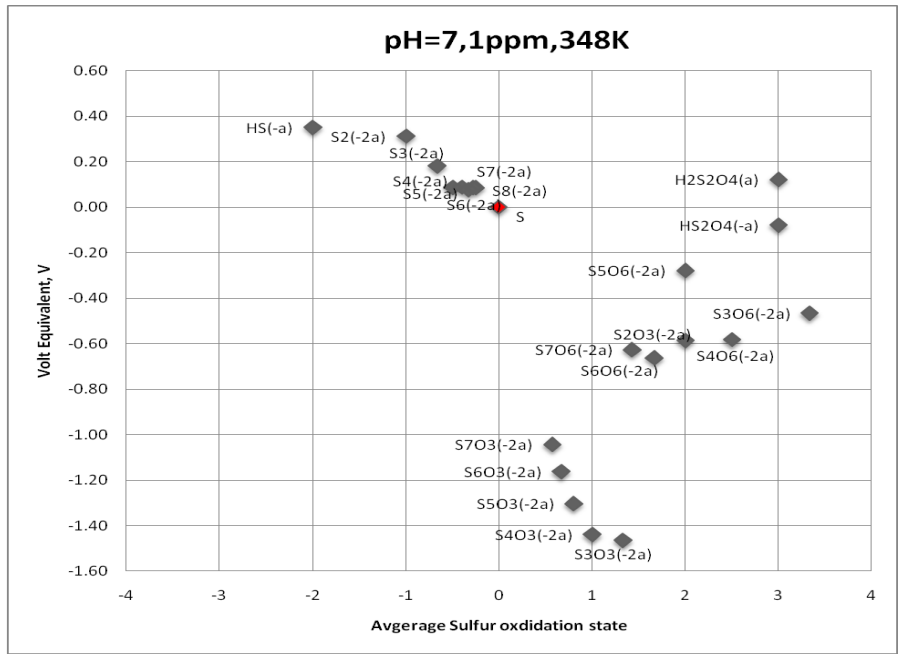
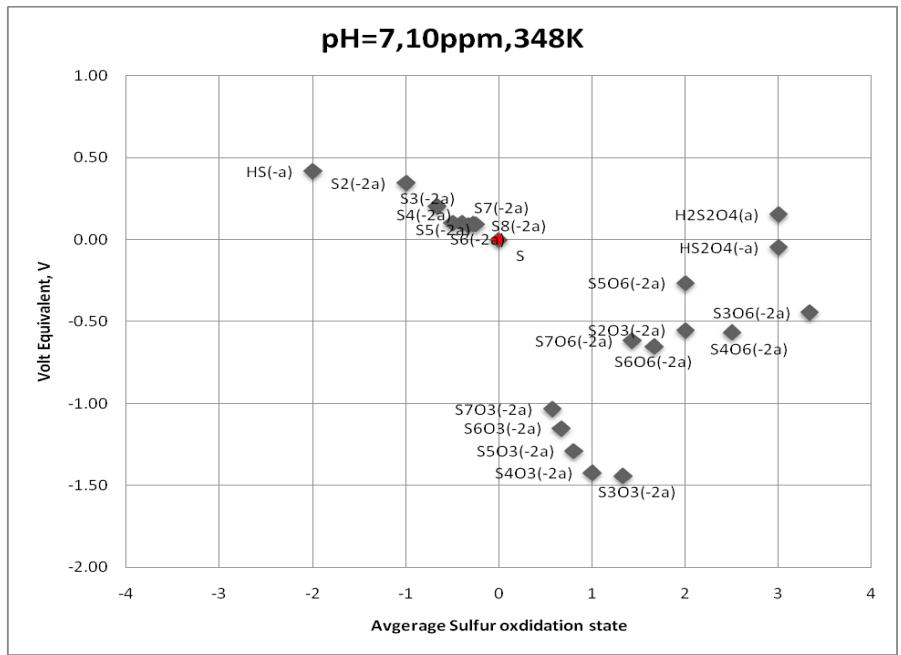


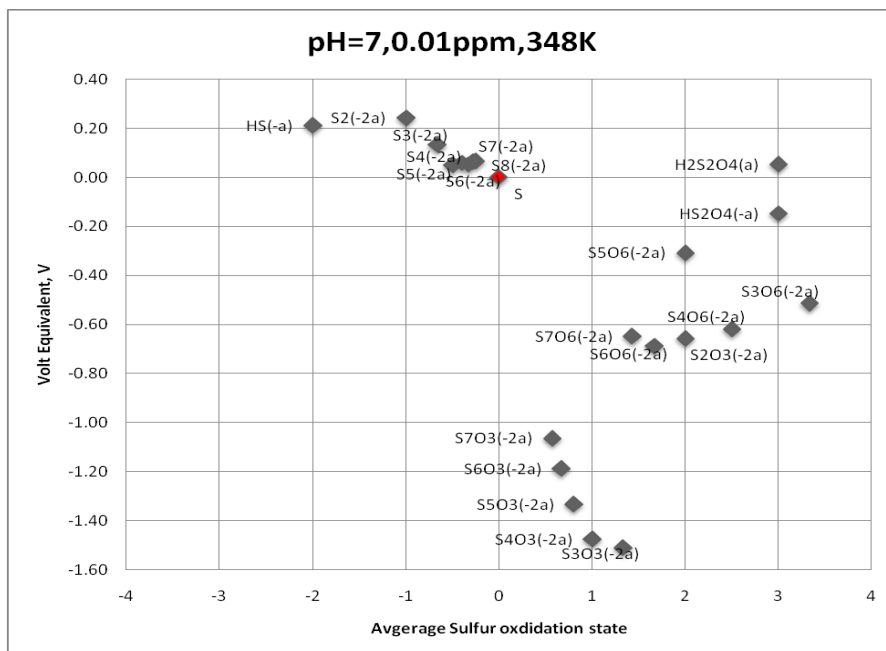
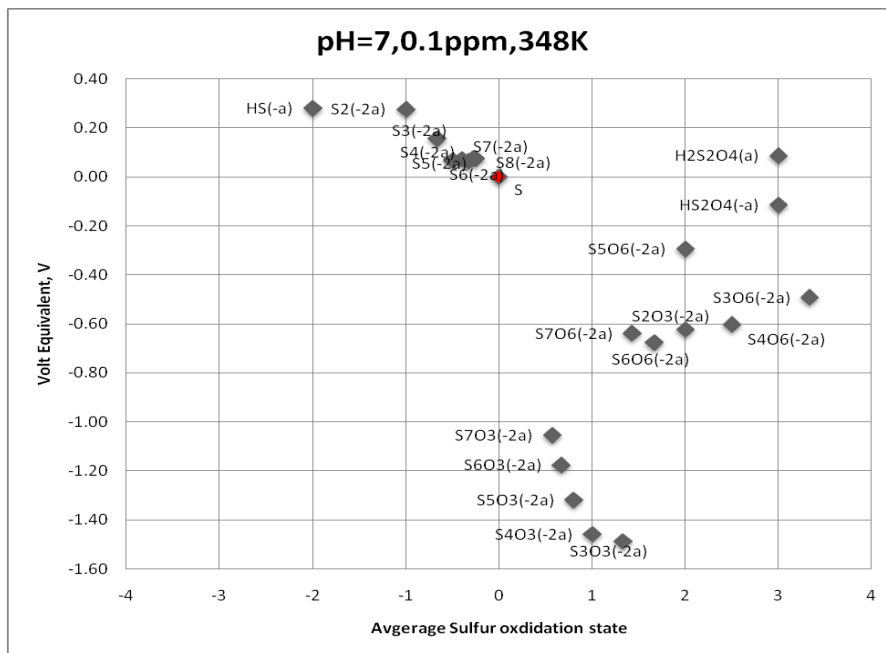


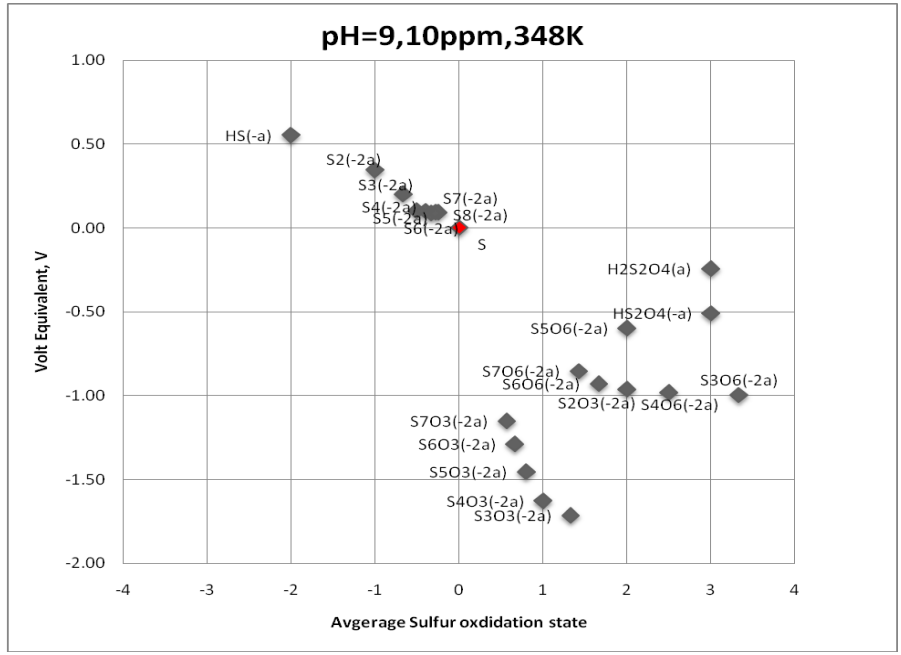
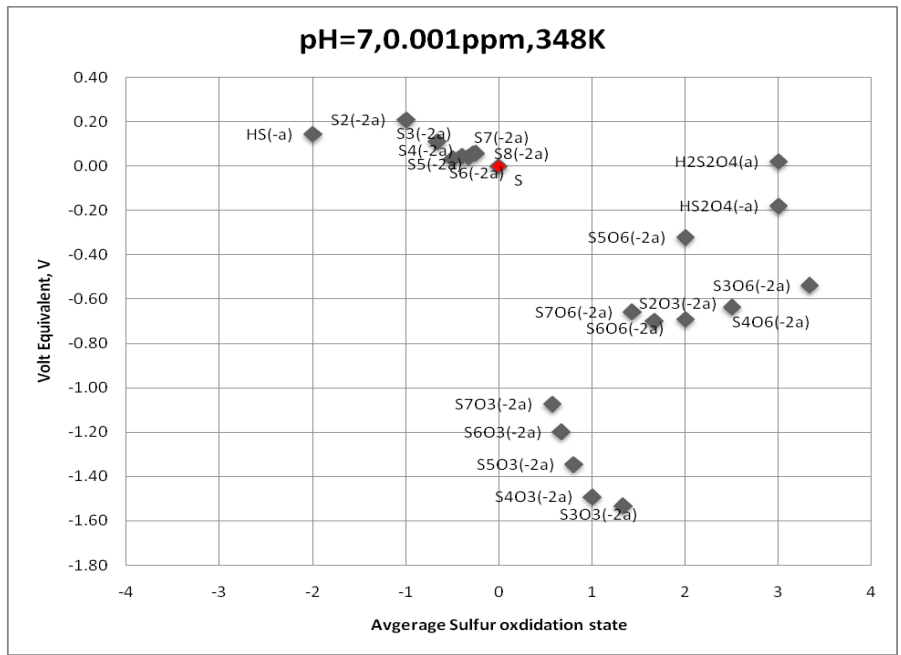


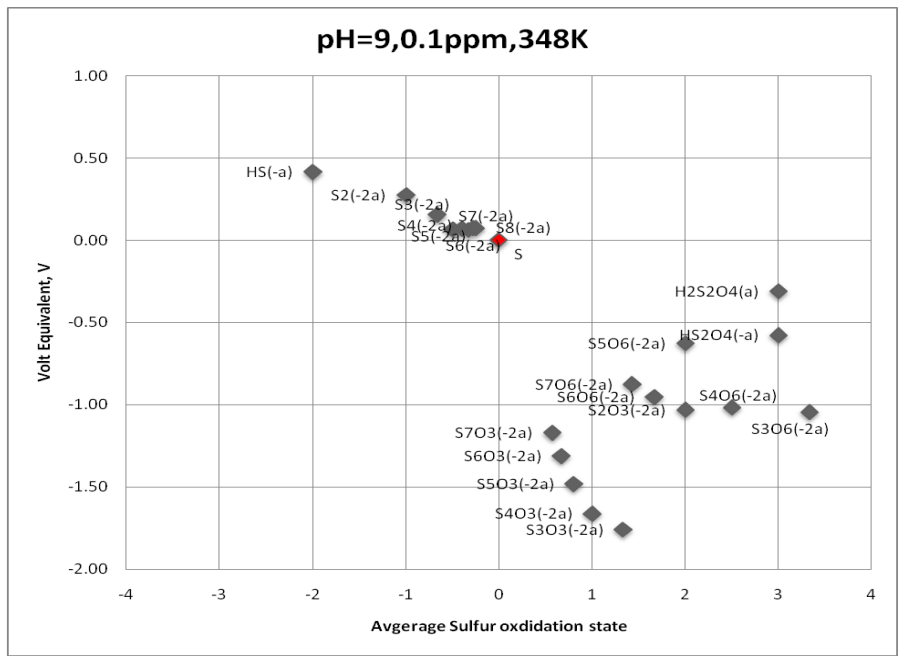
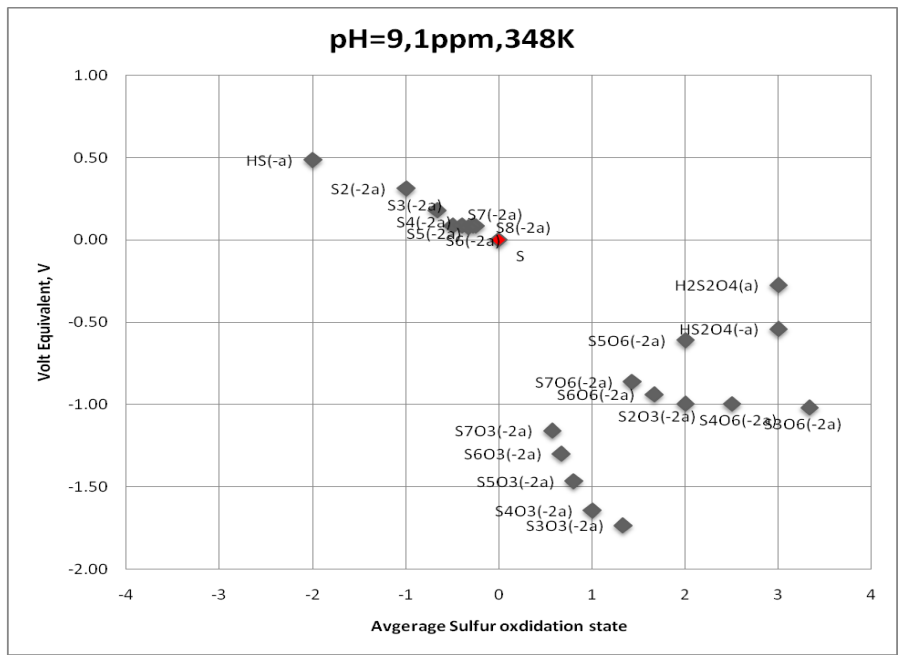


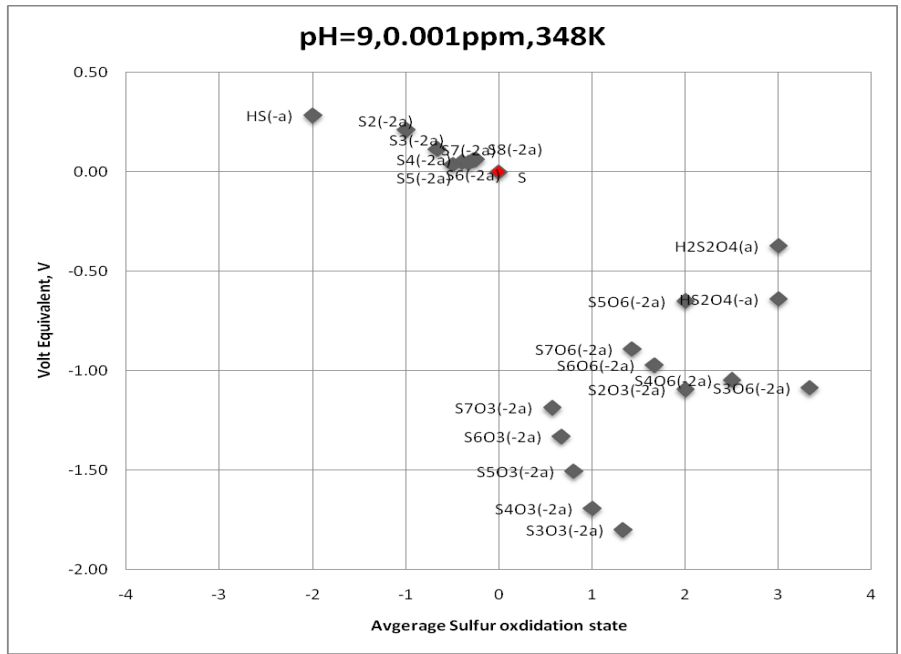
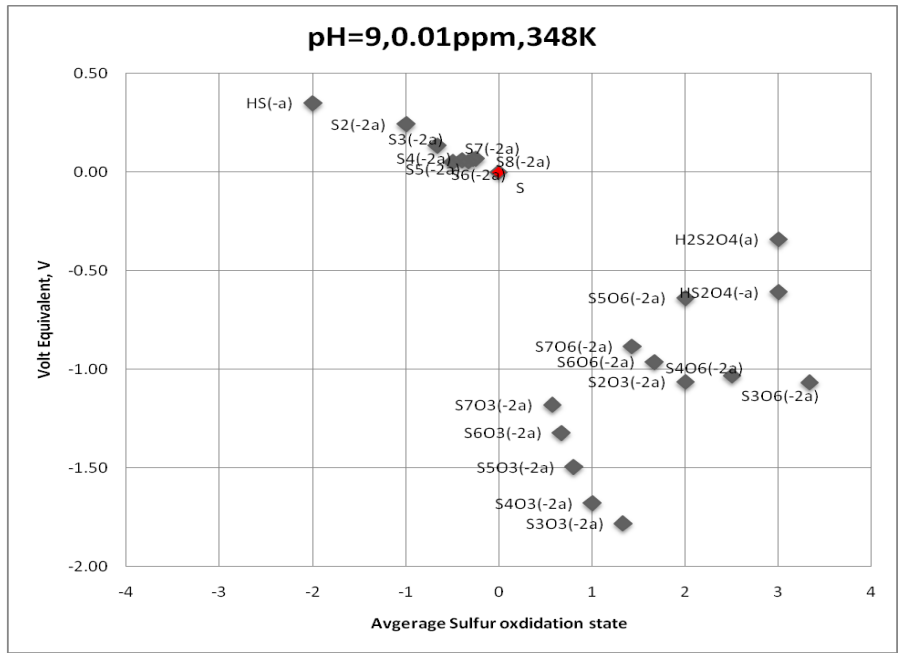


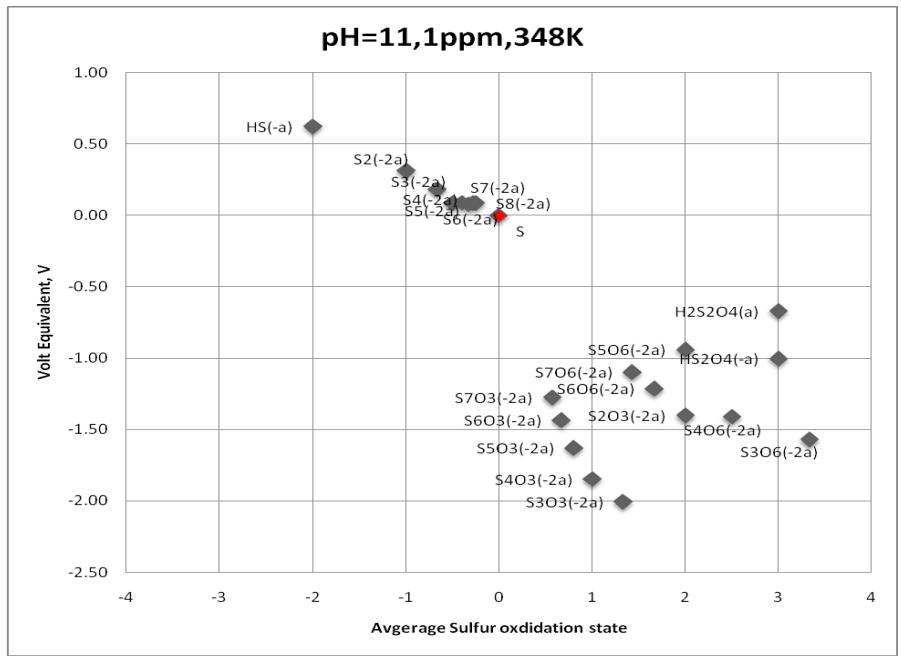
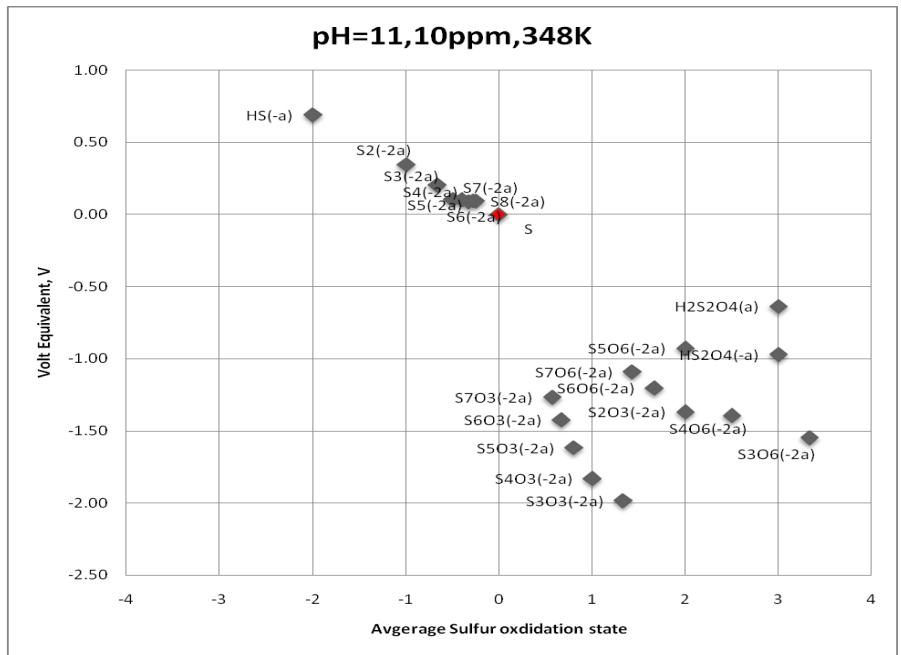


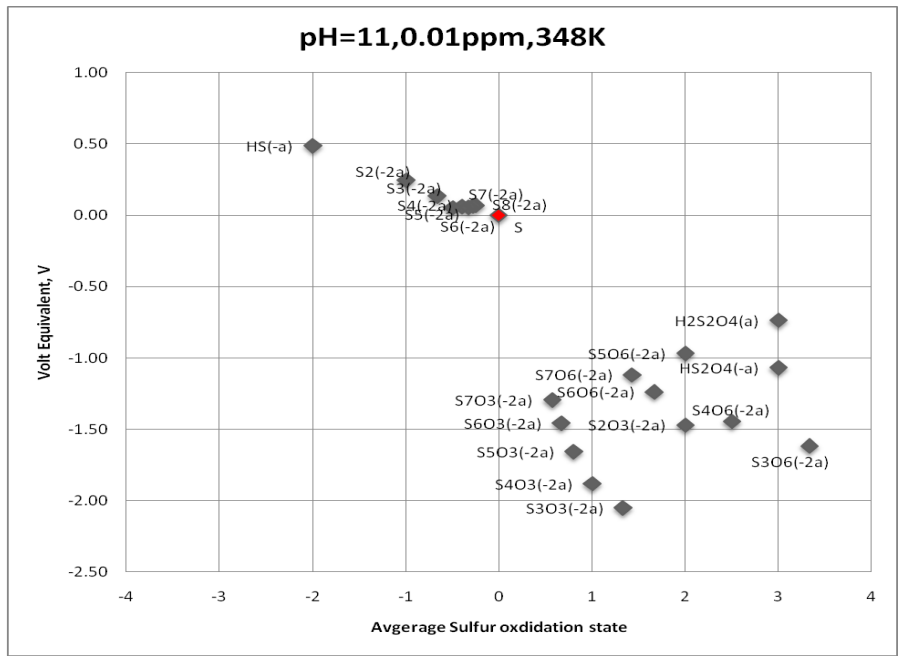
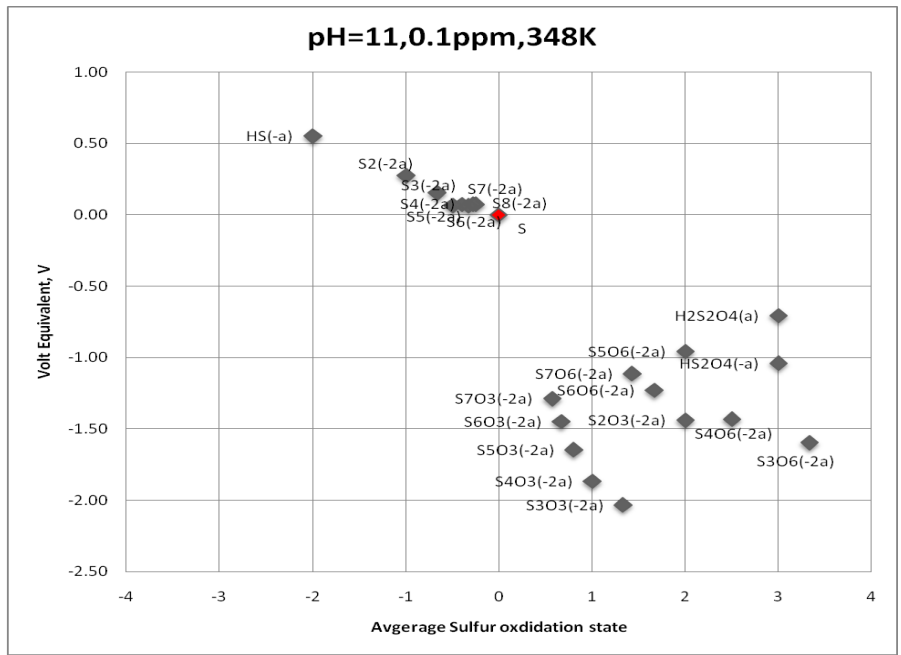


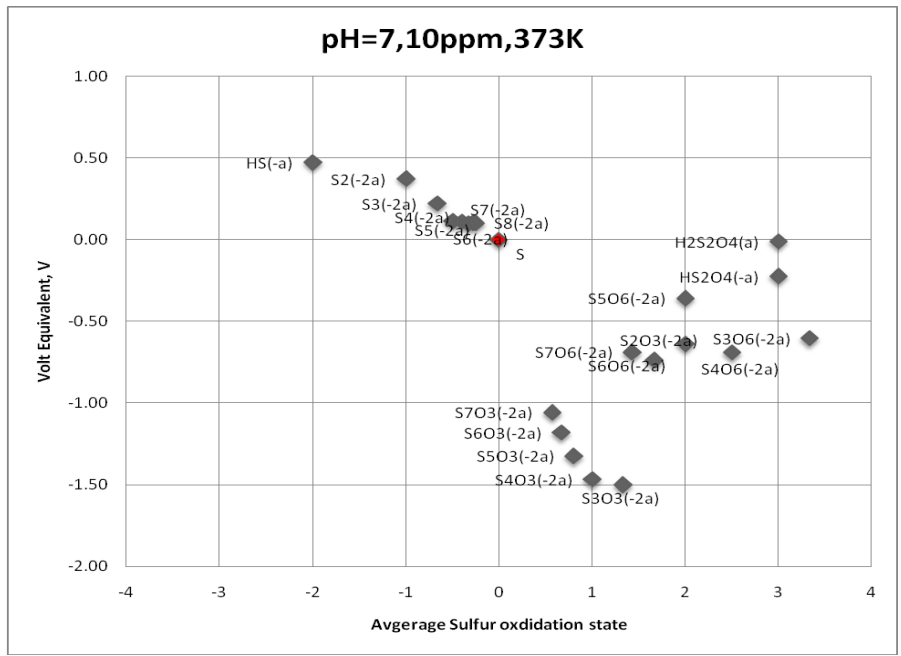
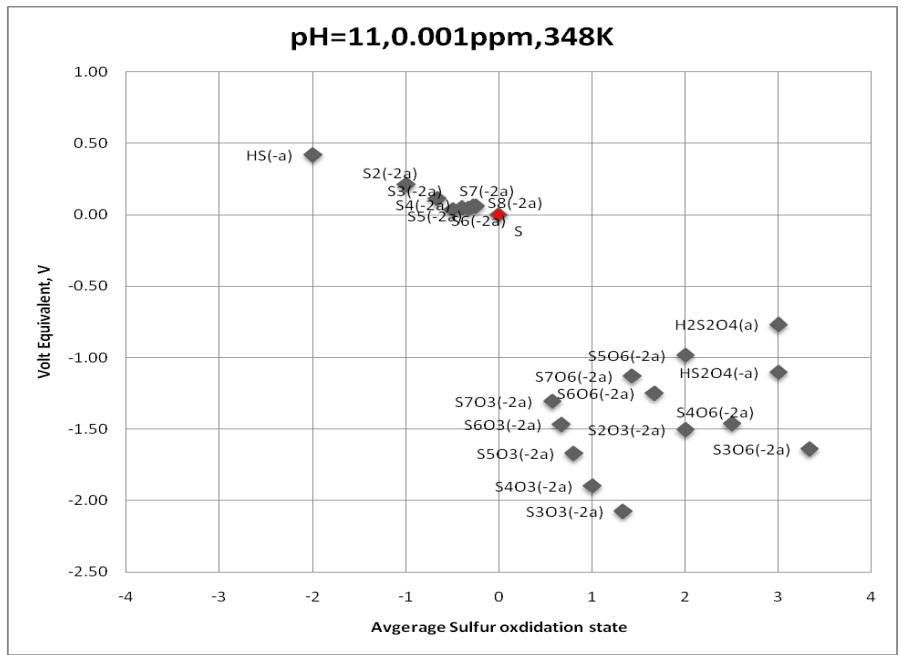


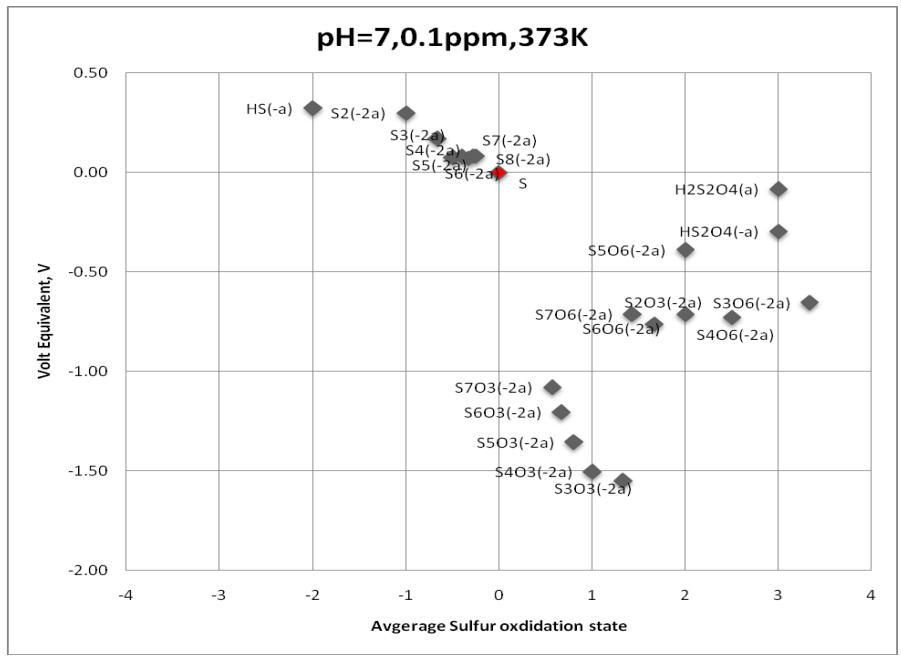
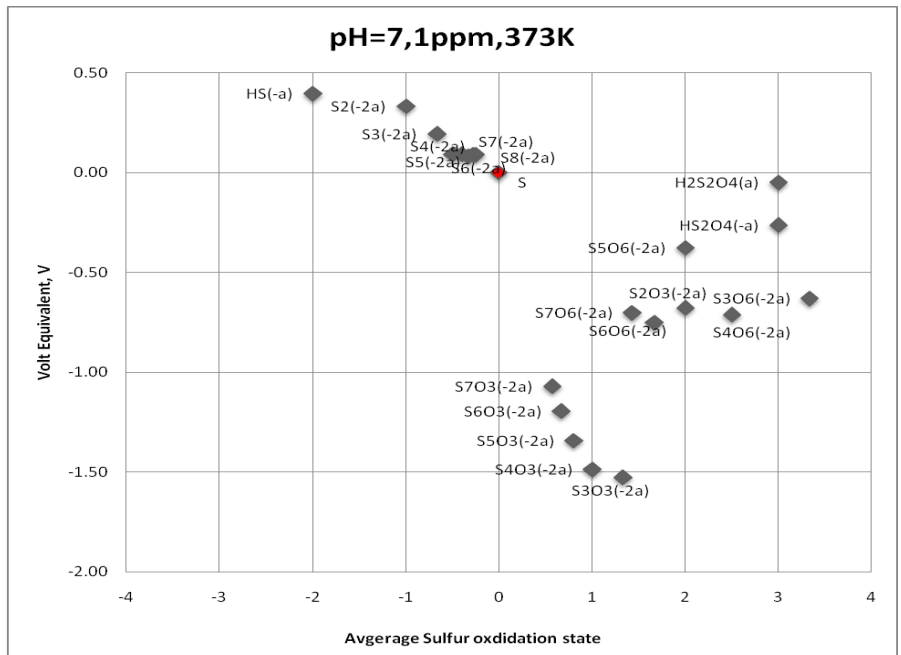


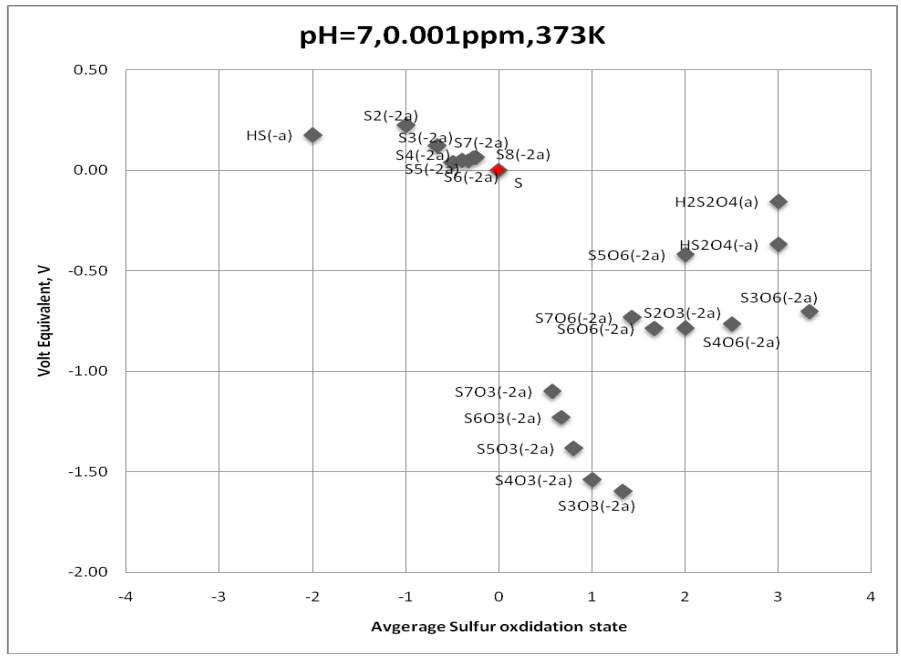
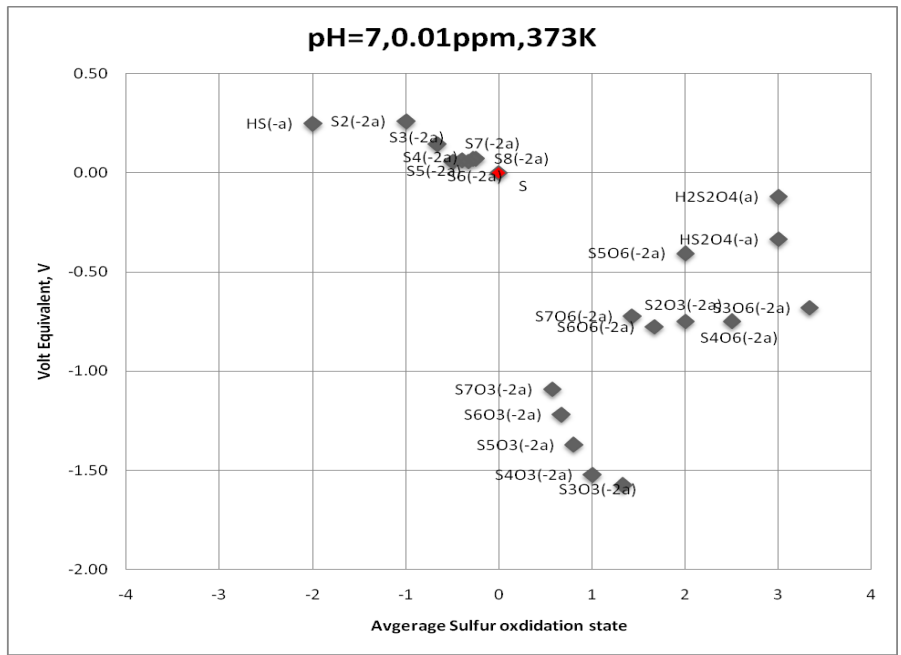


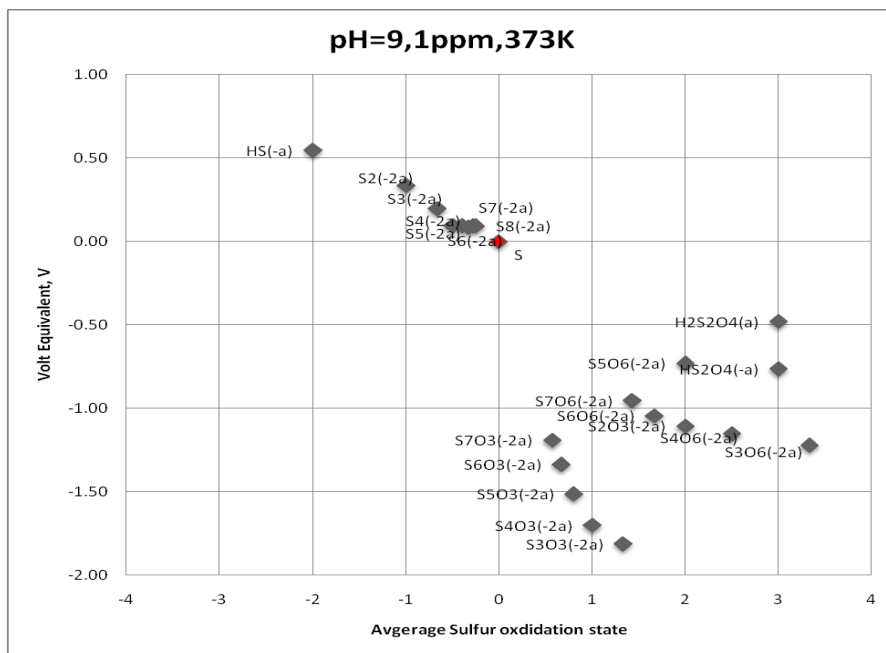
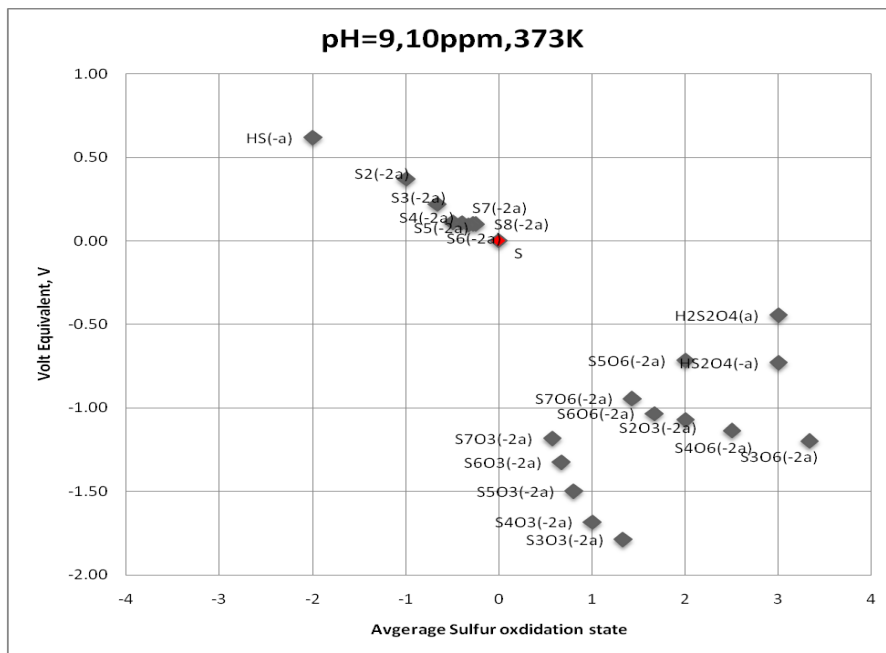


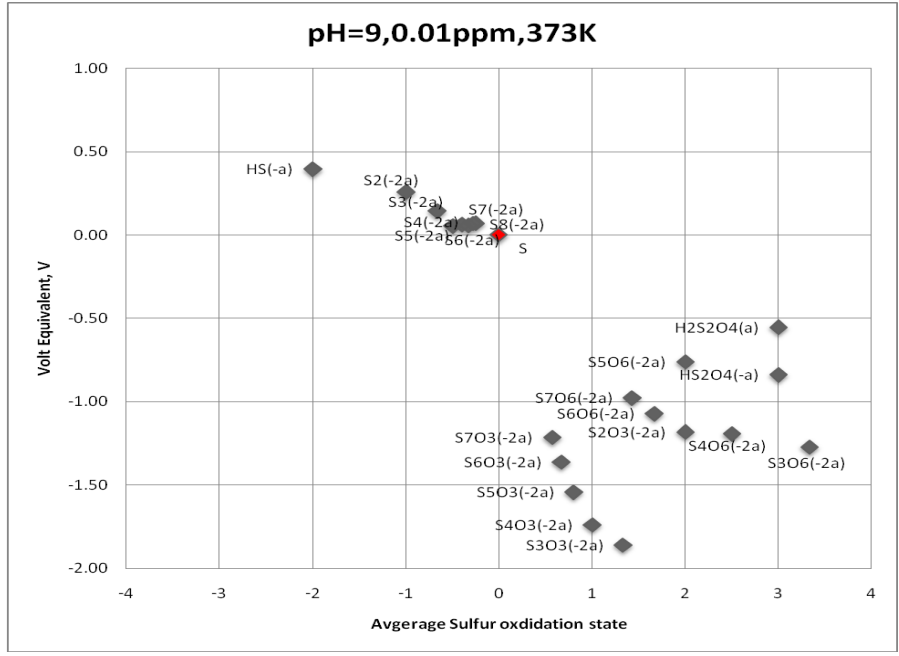
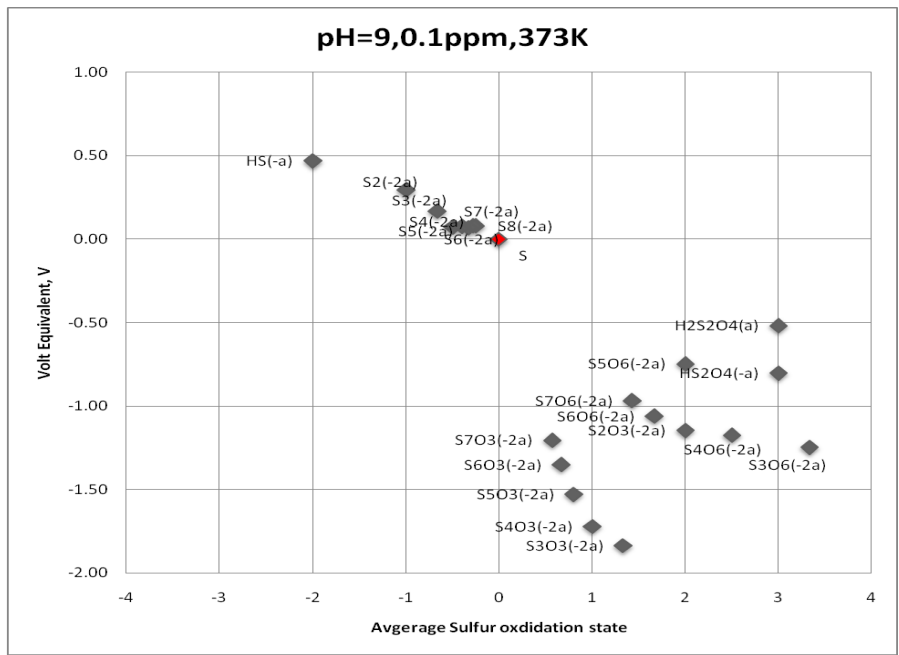


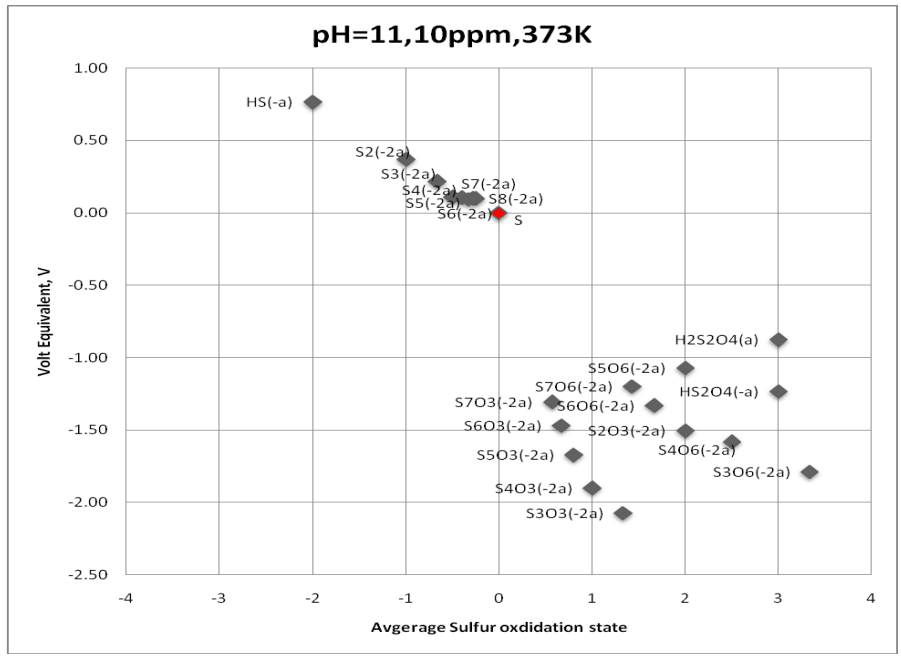
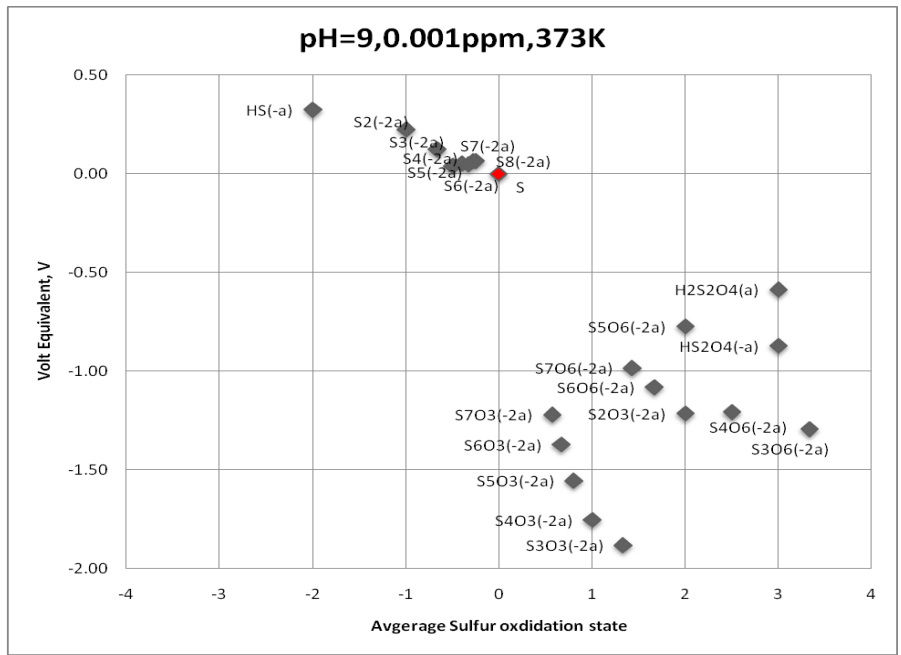


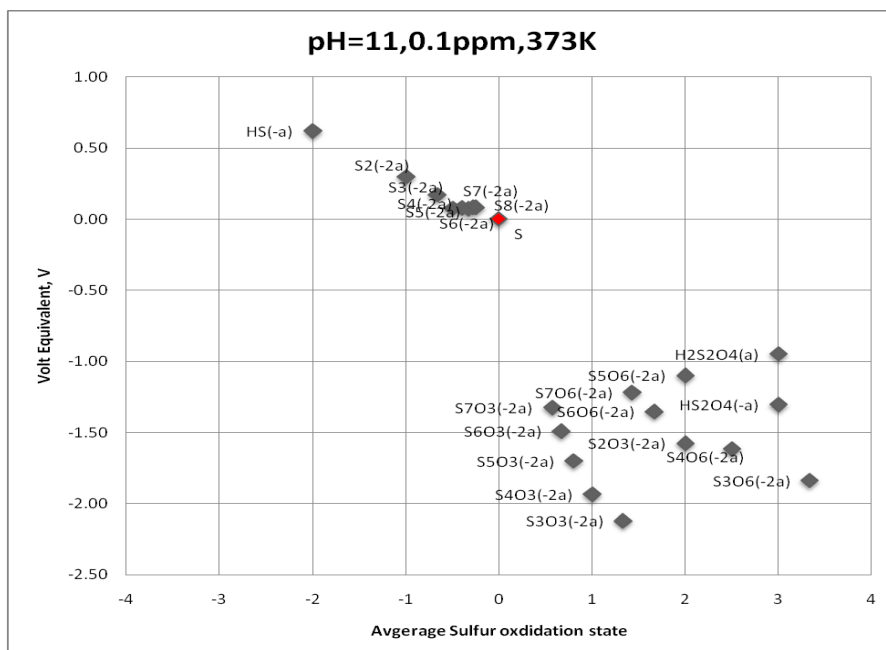
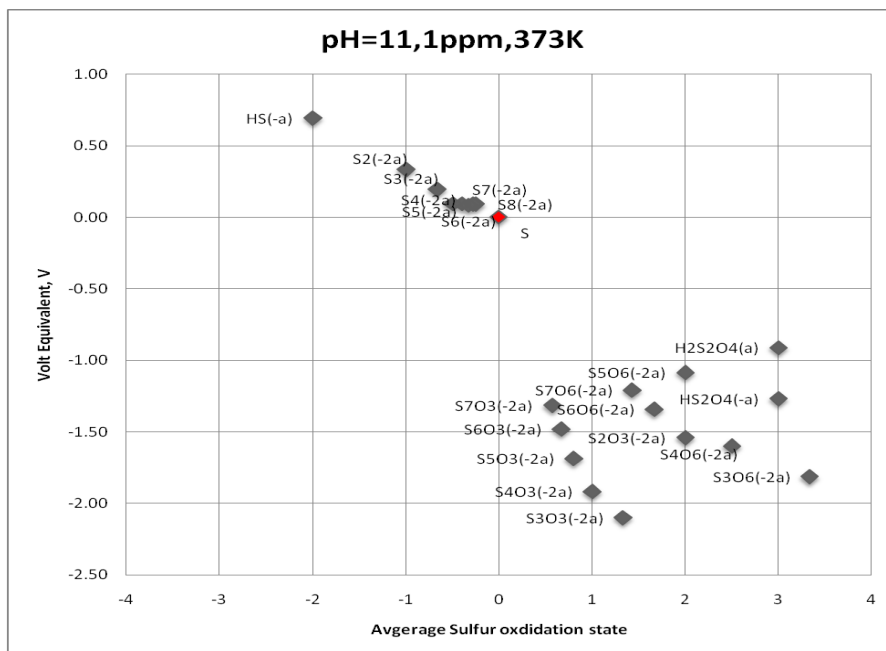


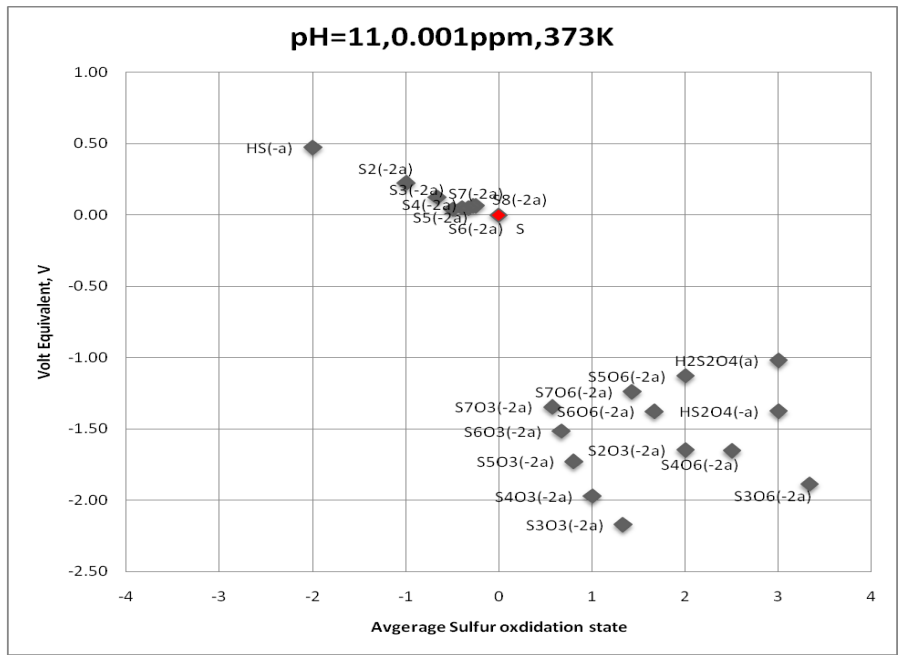
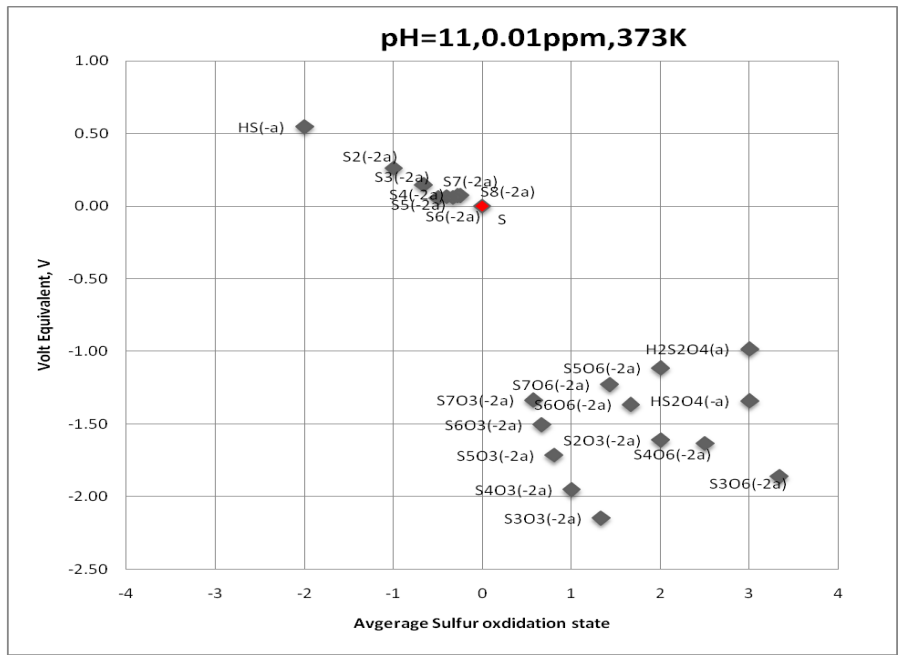


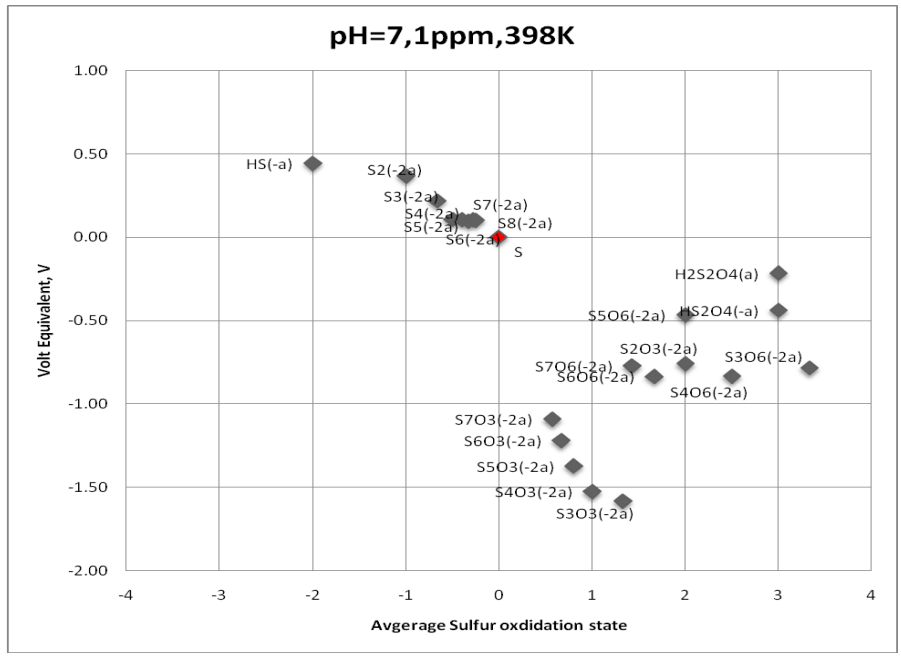
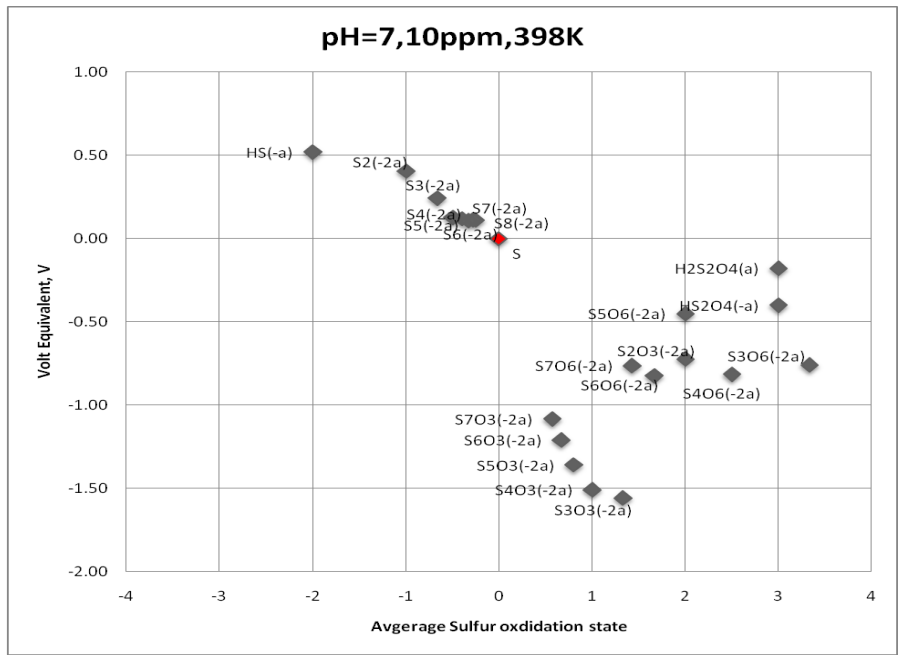


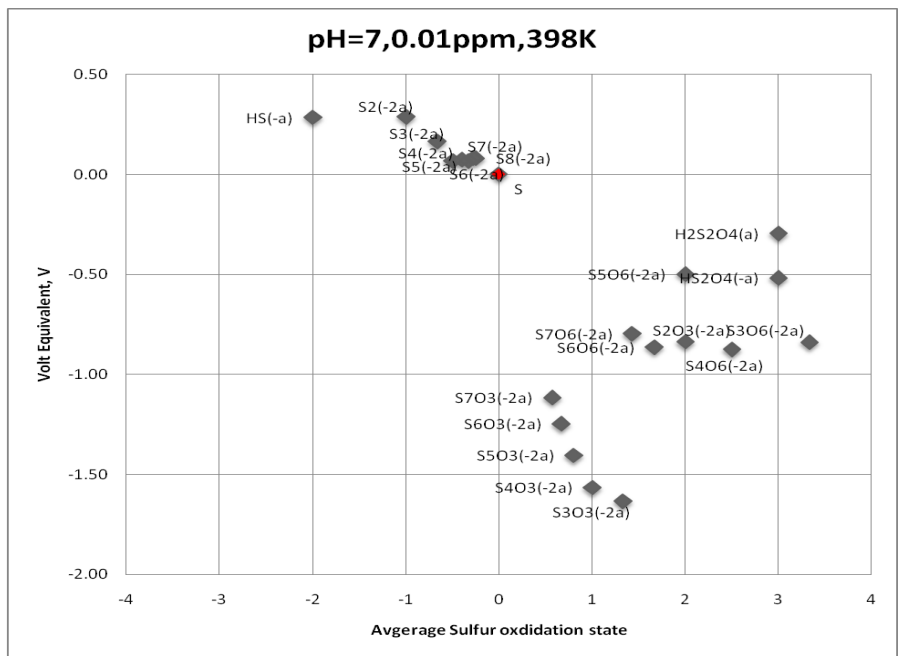
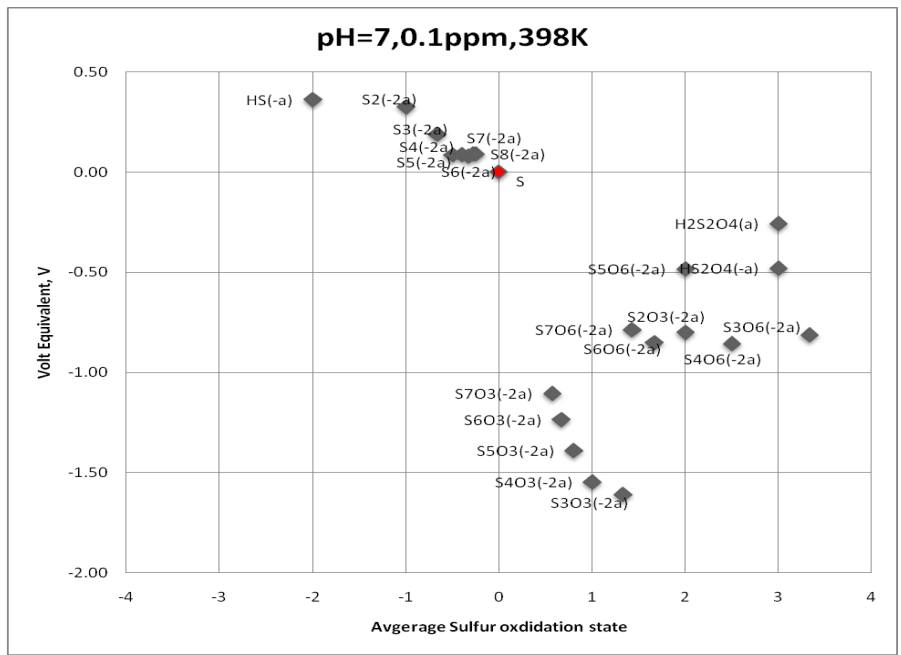


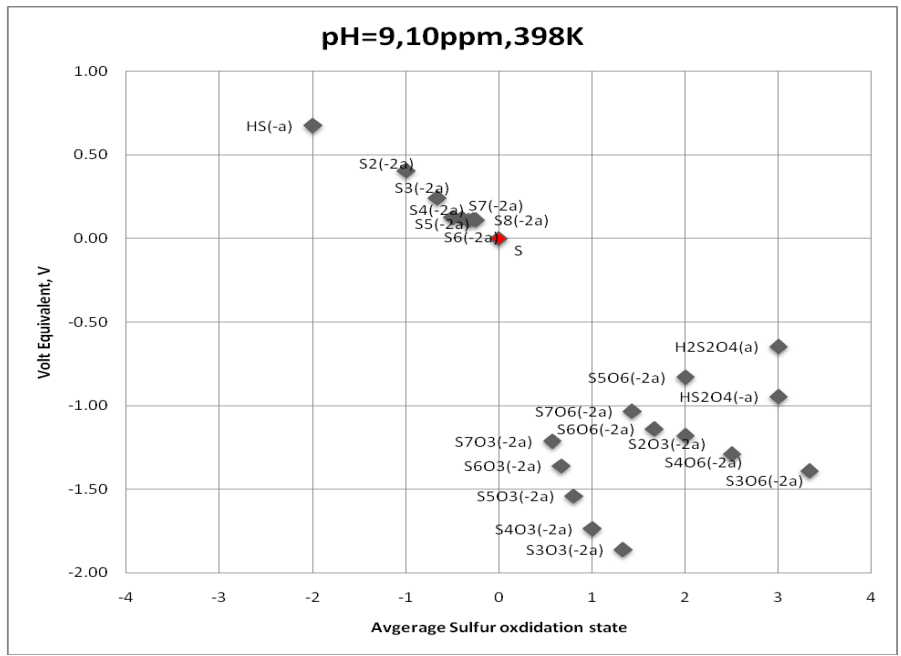
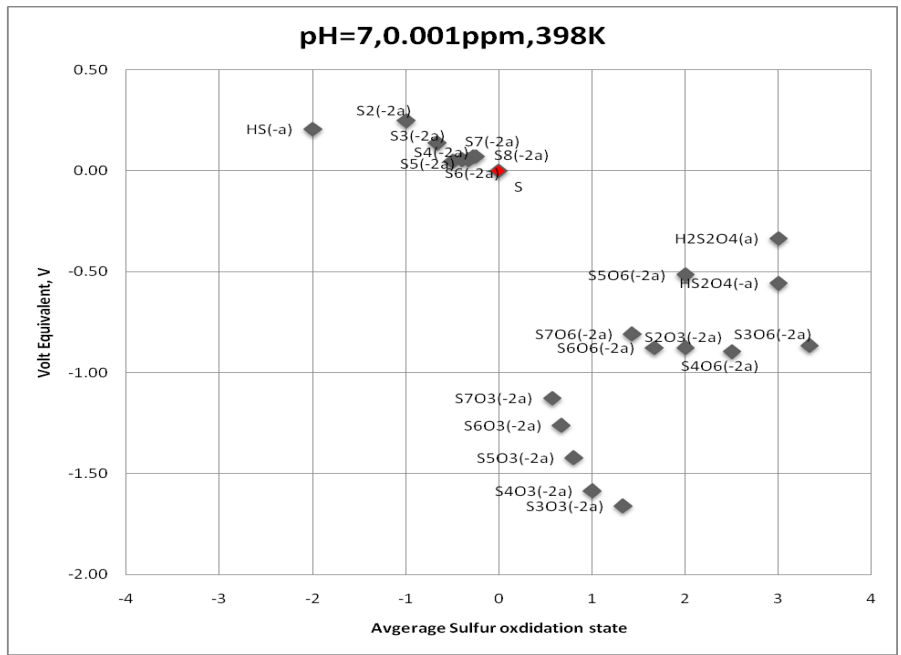


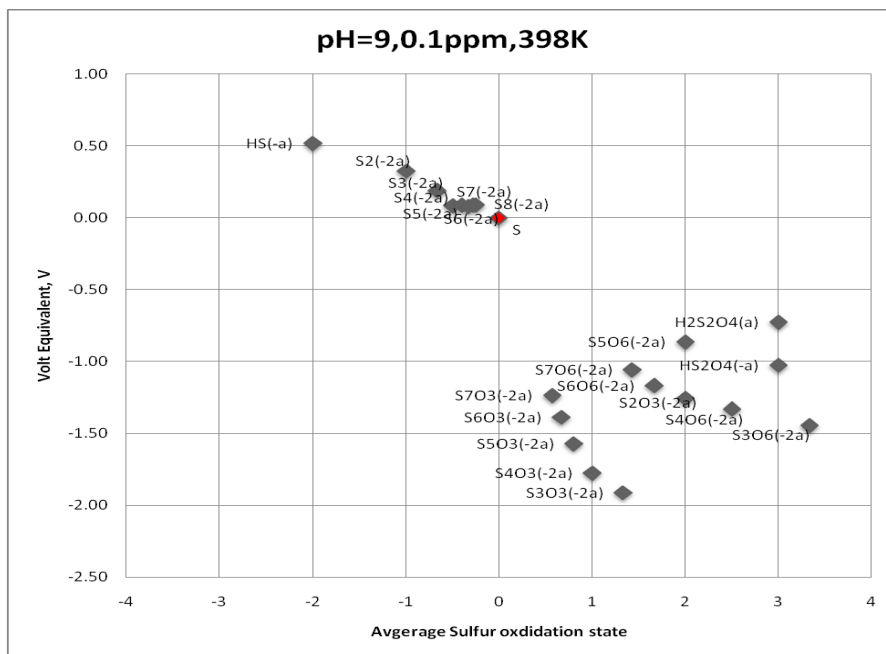
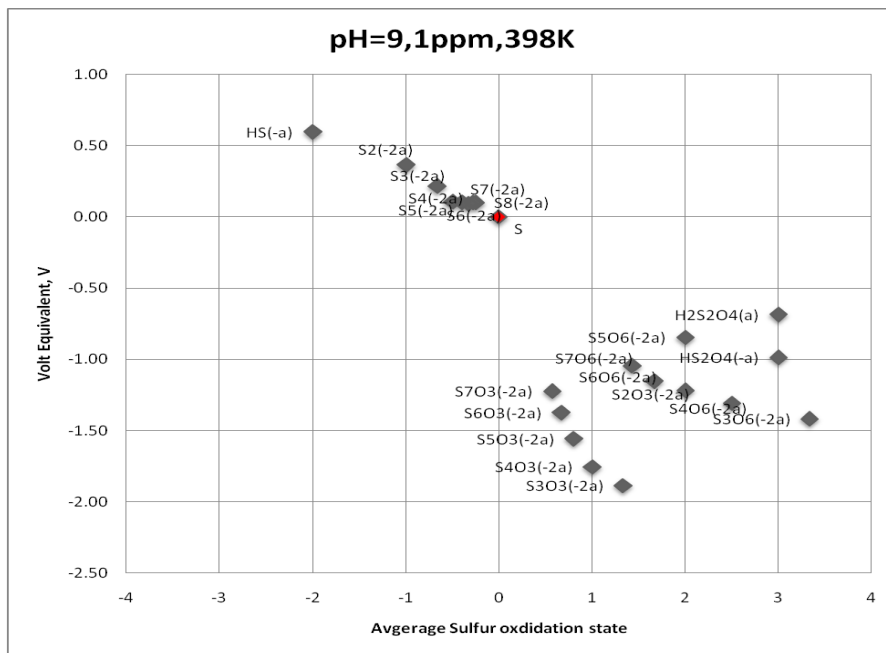


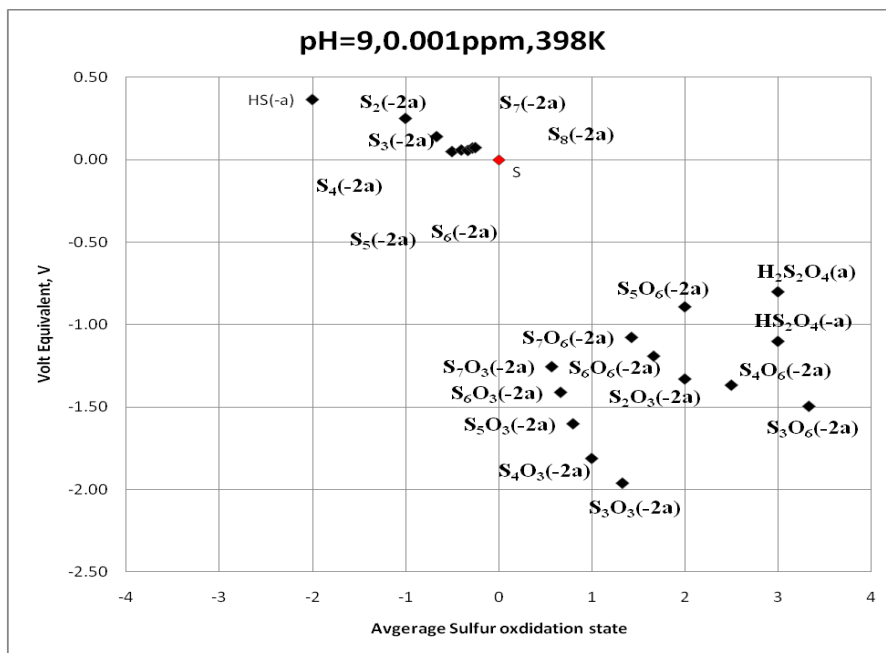
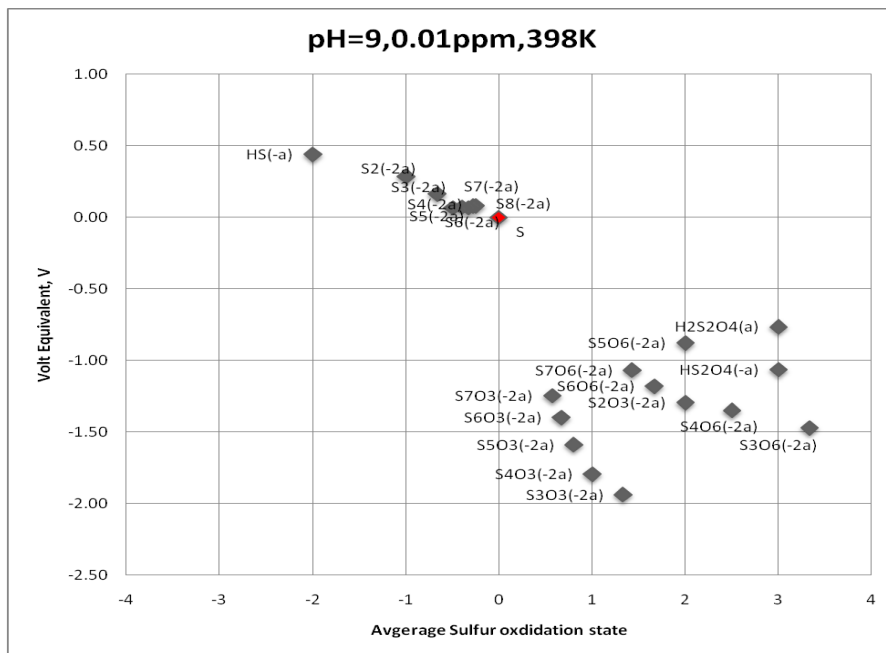


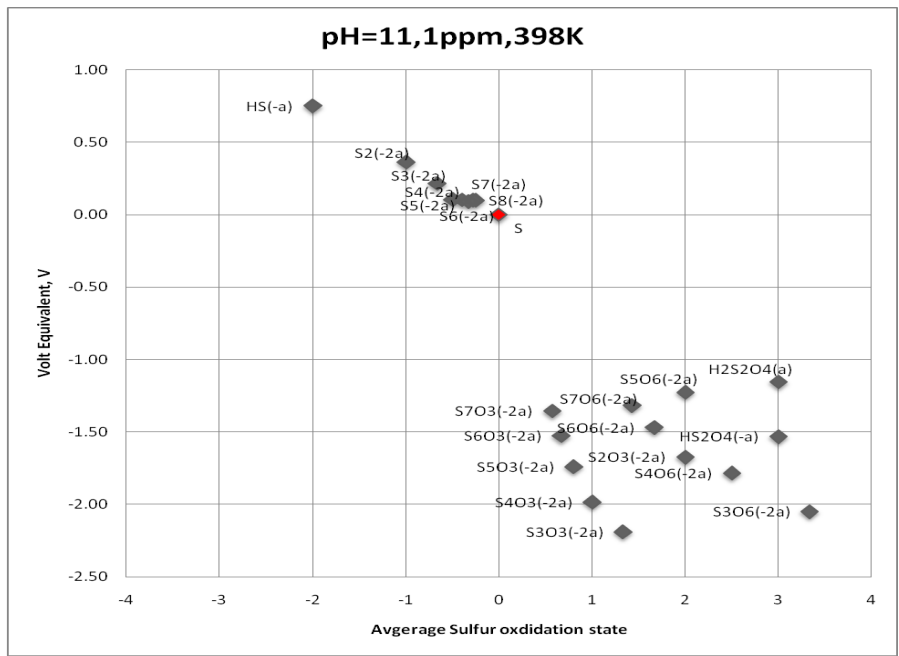
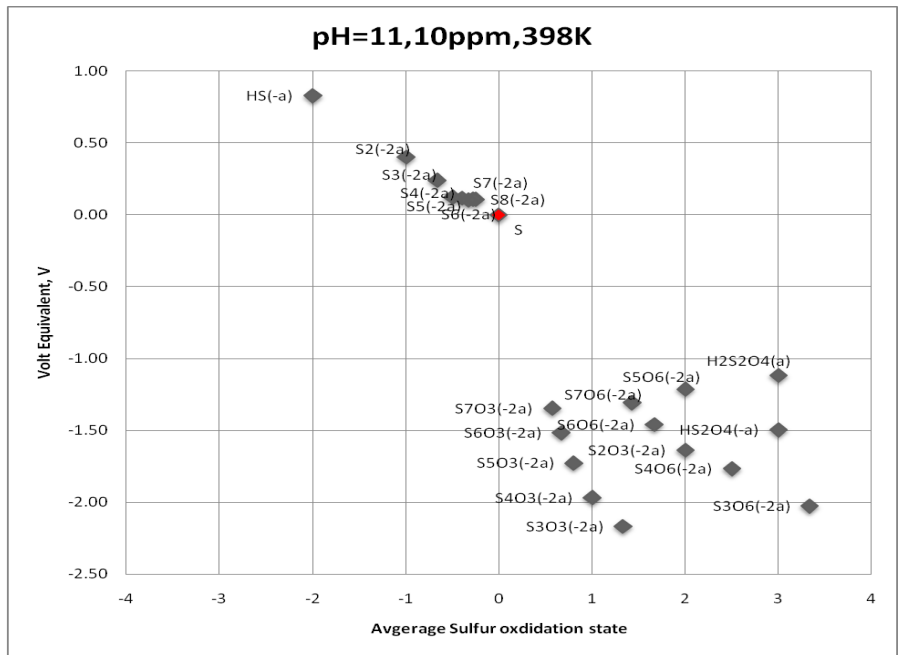


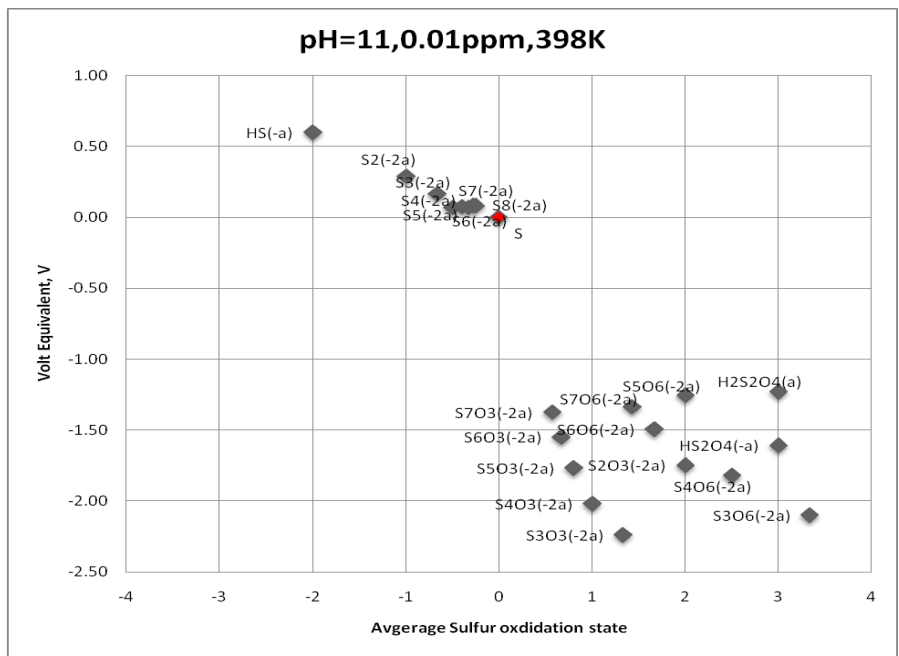
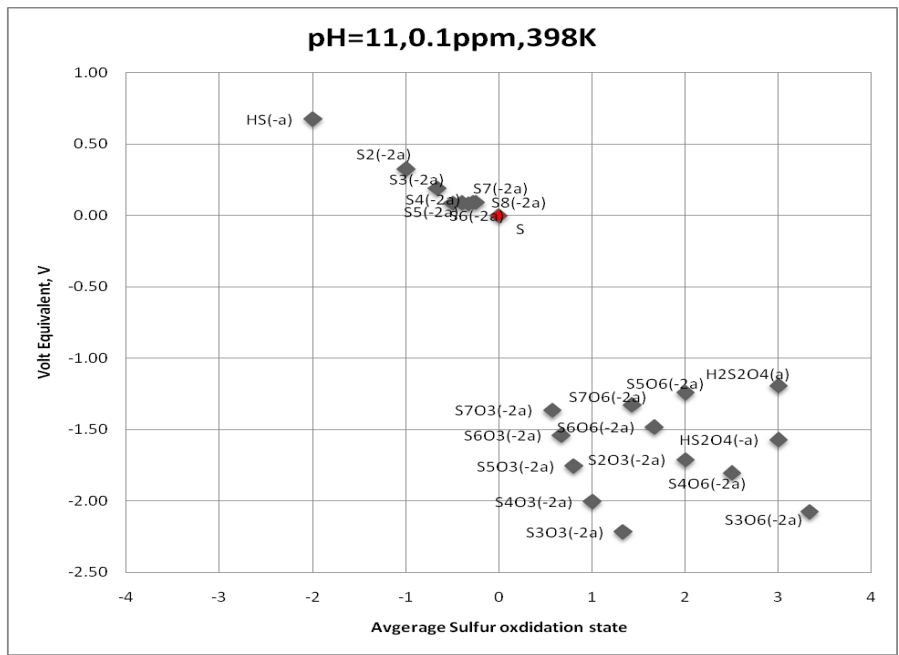


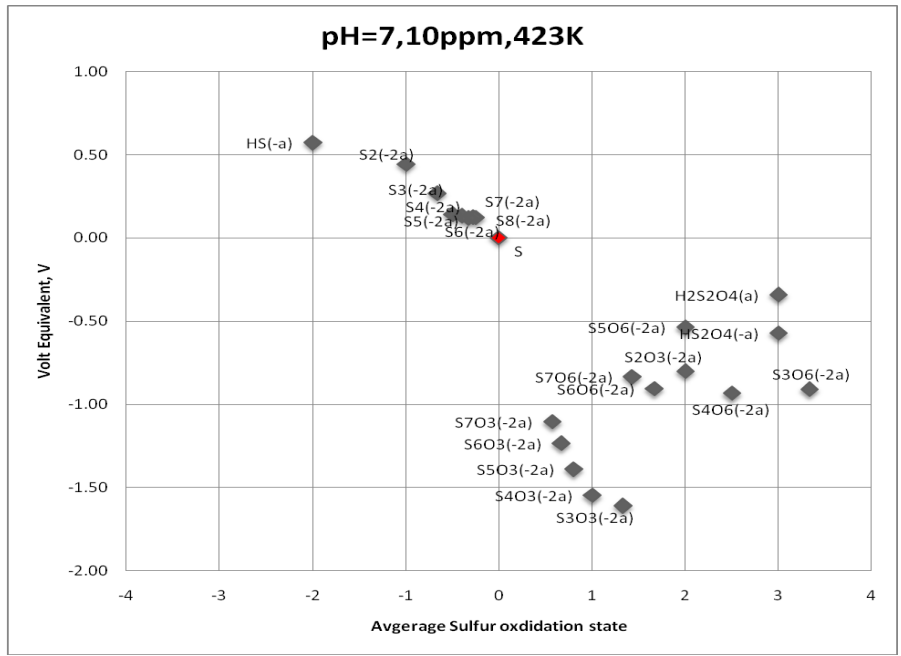
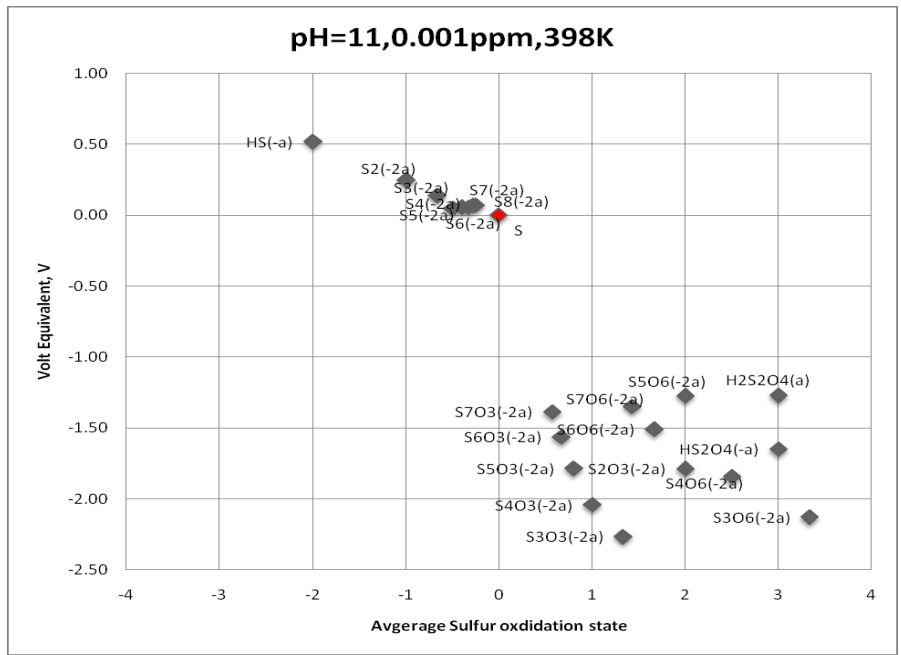


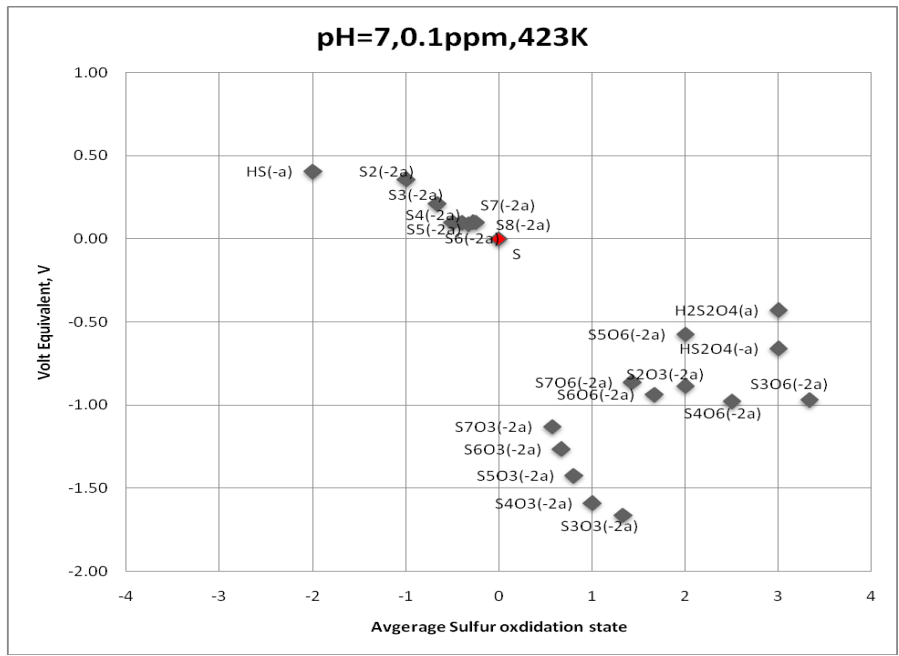
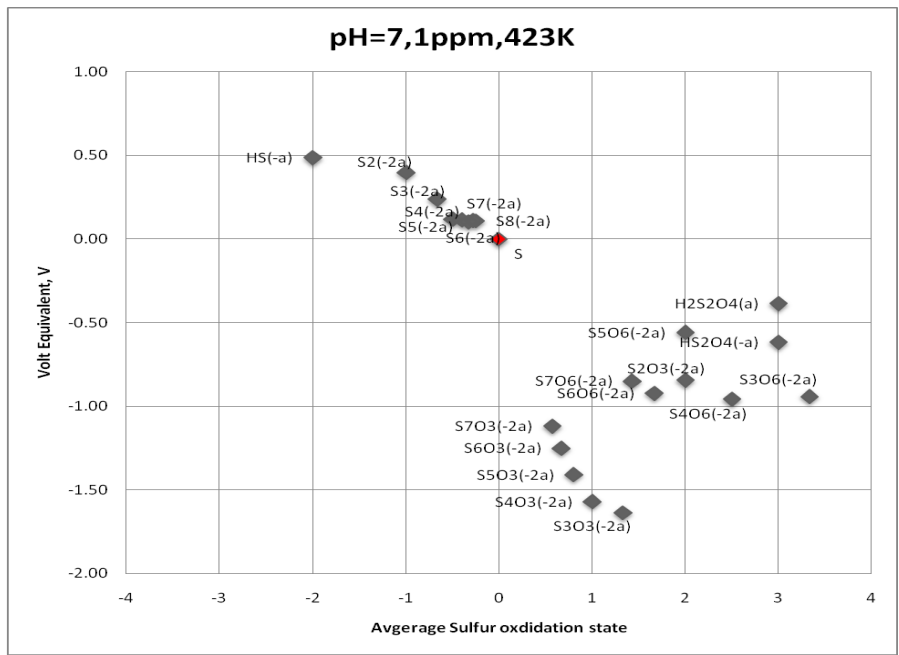


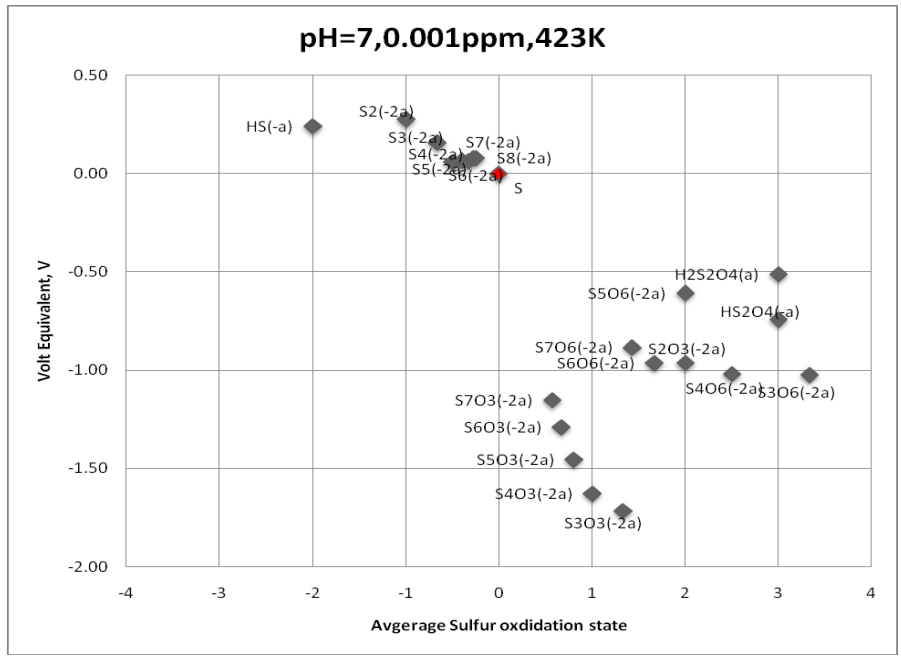
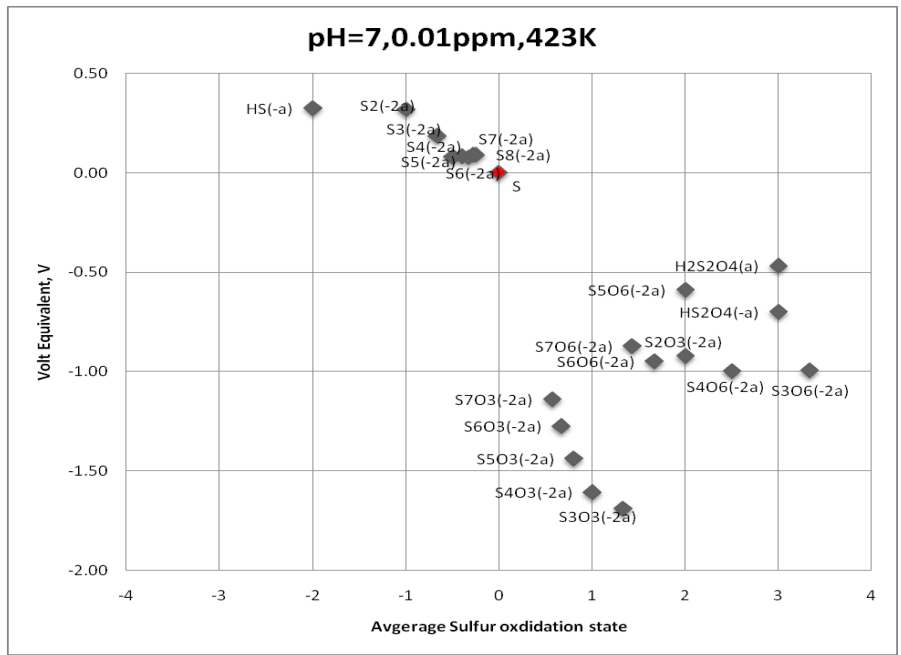


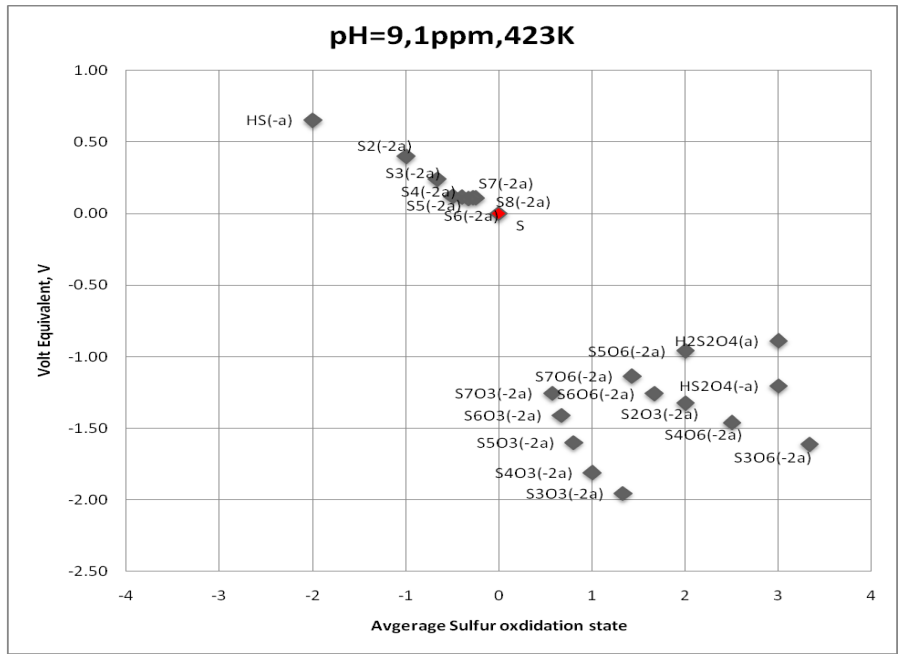
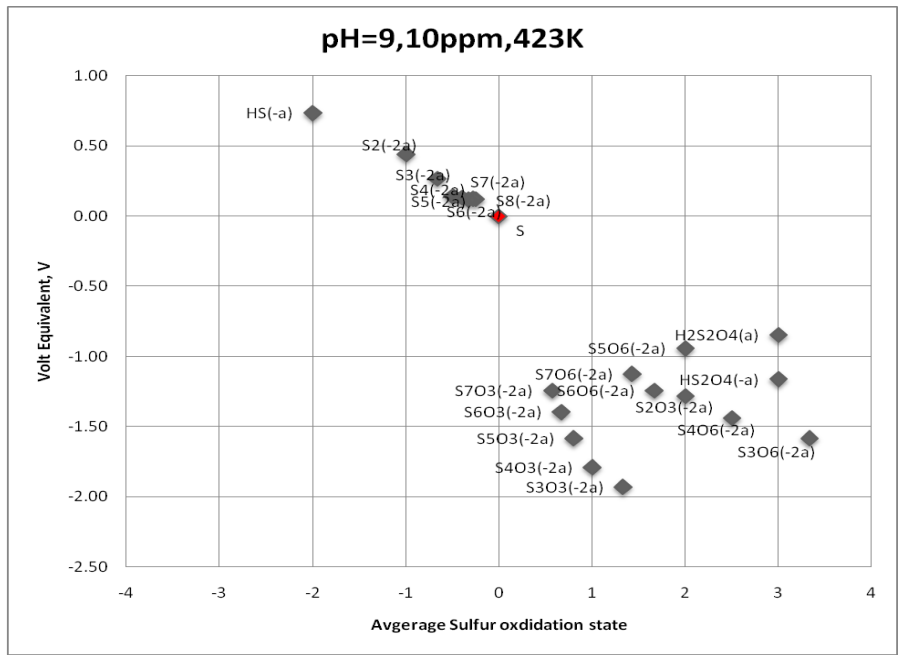


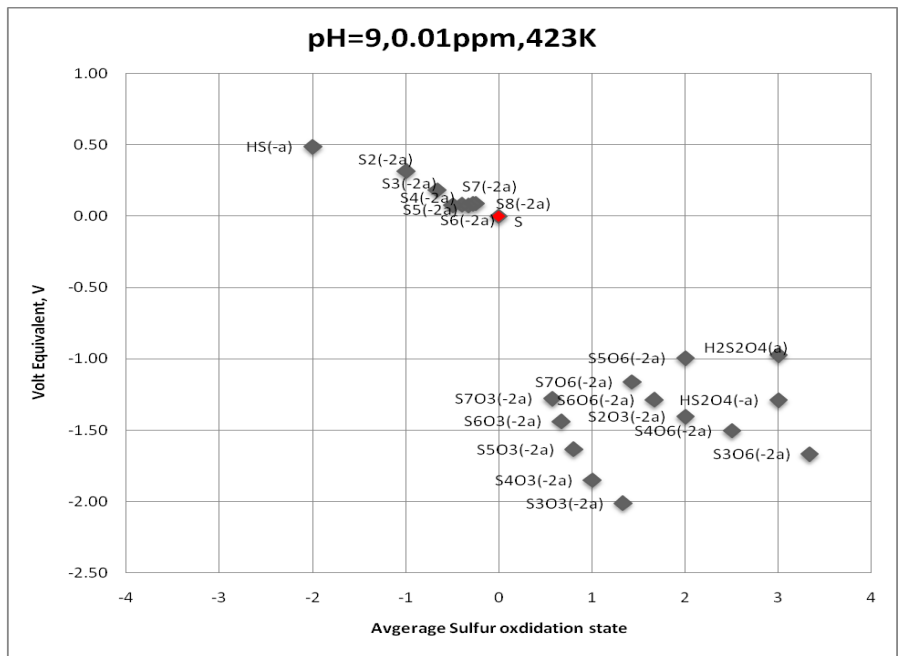
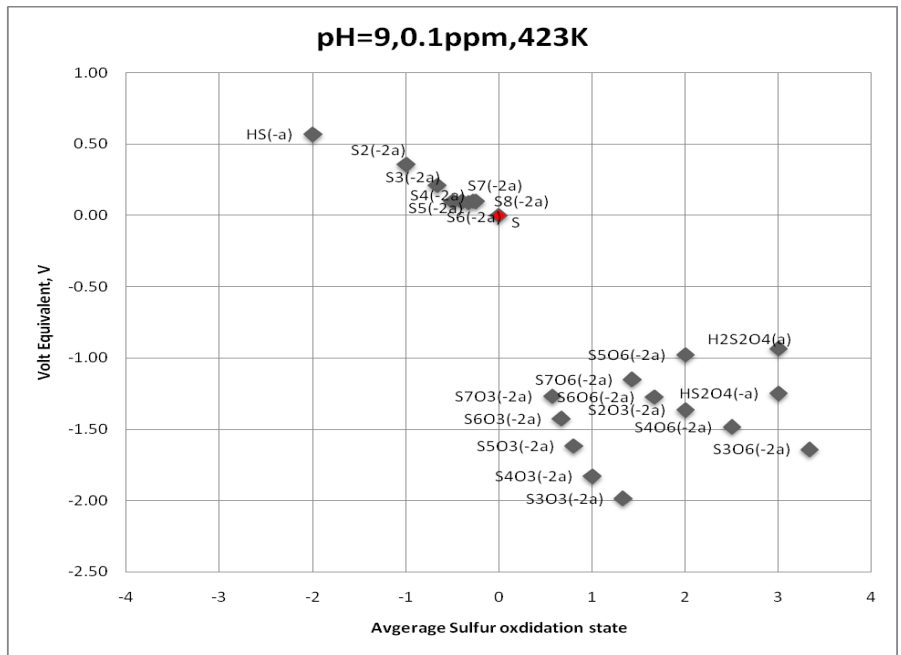


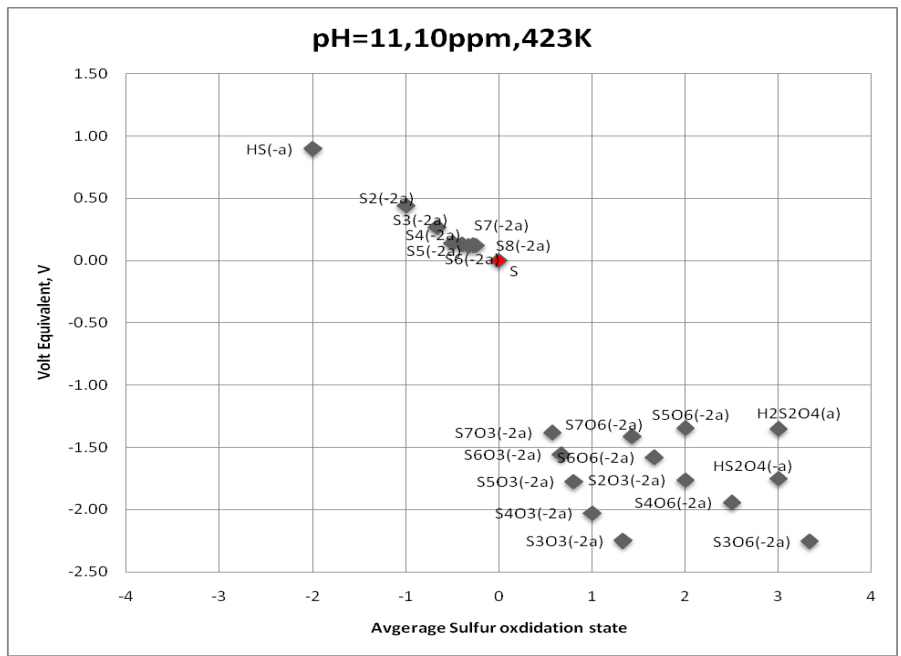
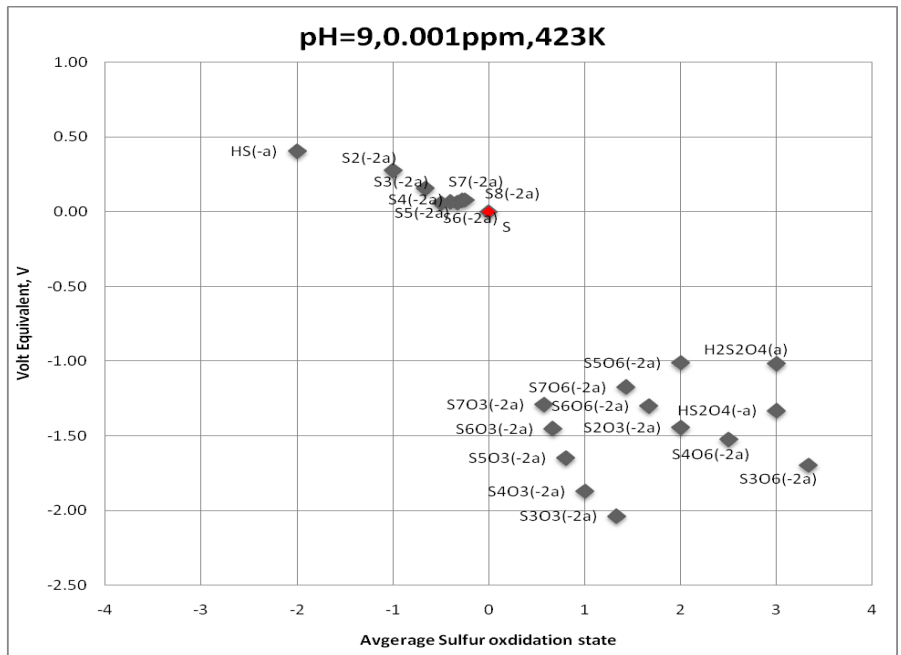


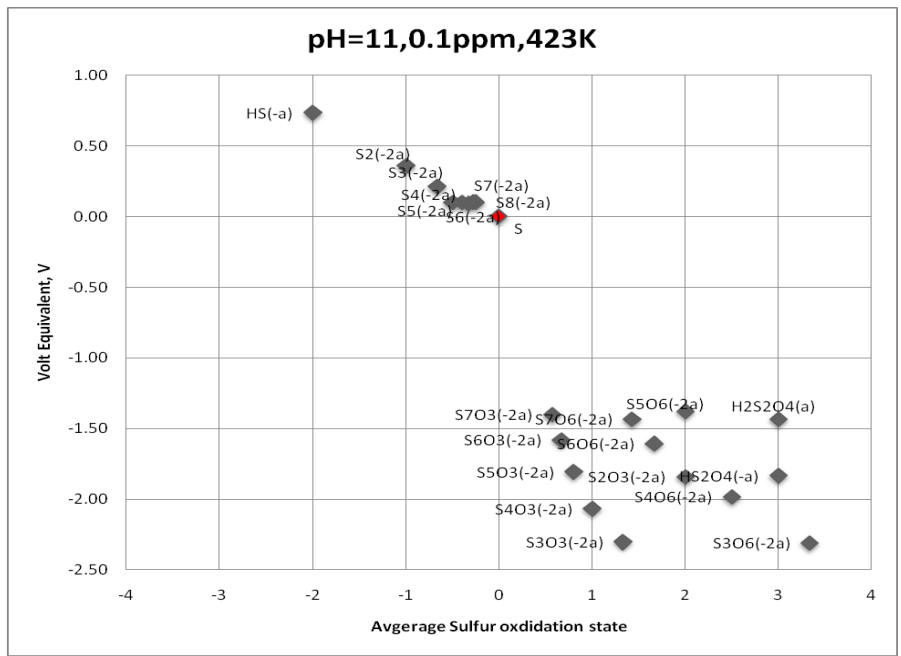
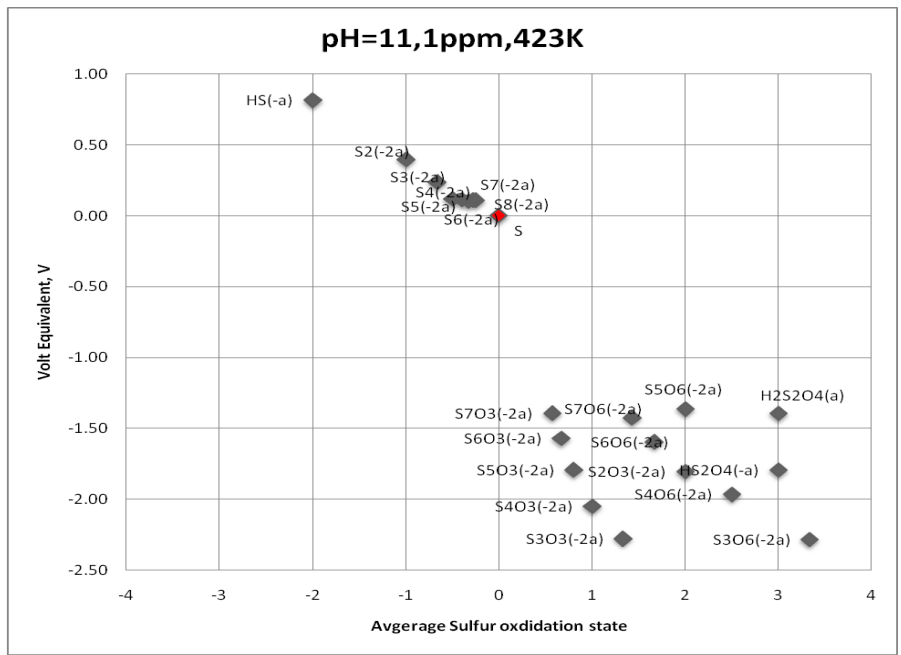


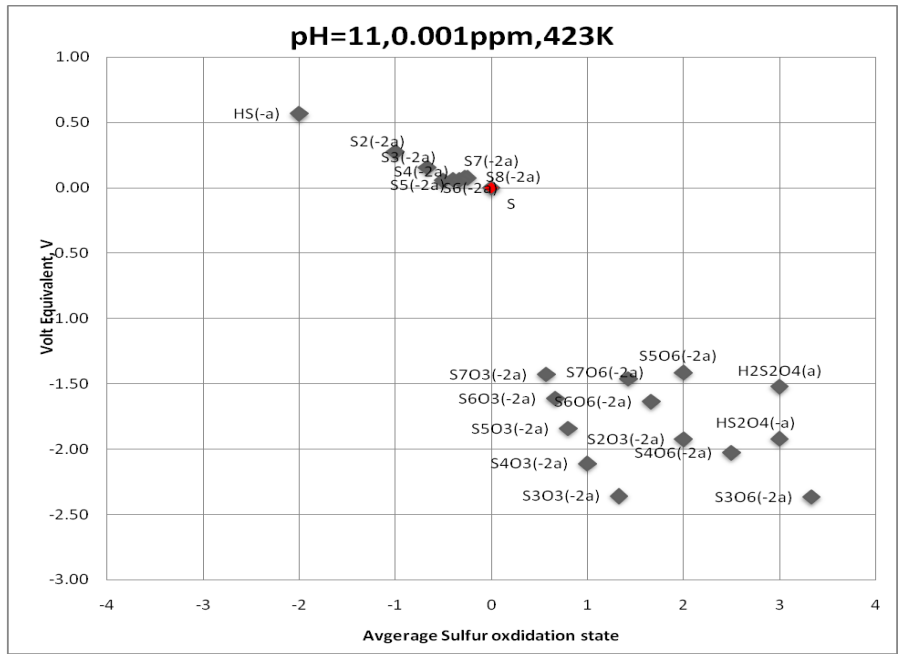
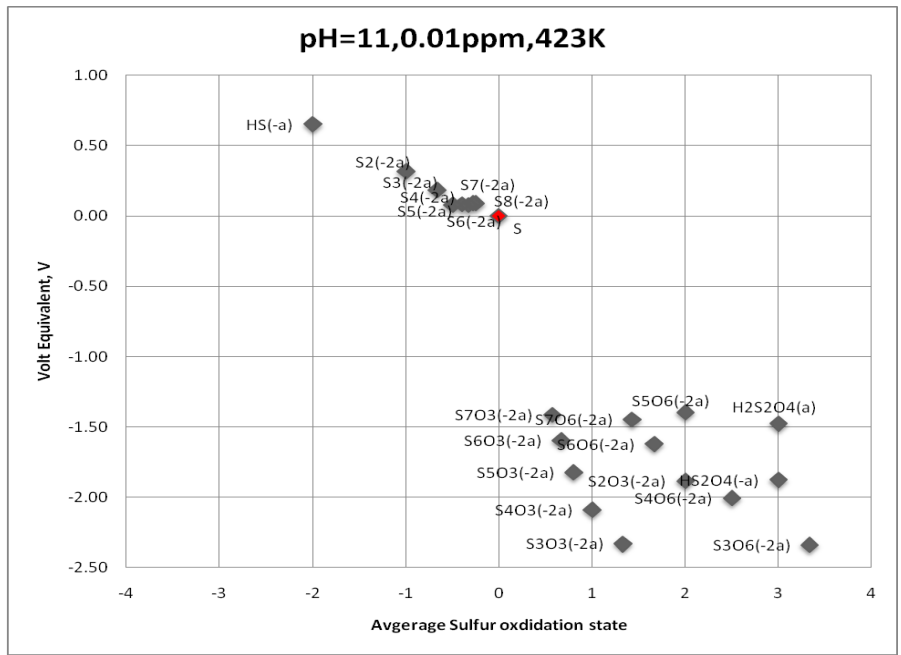












2011:09

The Swedish Radiation Safety Authority has a comprehensive responsibility to ensure that society is safe from the effects of radiation. The Authority works to achieve radiation safety in a number of areas: nuclear power, medical care as well as commercial products and services. The Authority also works to achieve protection from natural radiation and to increase the level of radiation safety internationally.

The Swedish Radiation Safety Authority works proactively and preventively to protect people and the environment from the harmful effects of radiation, now and in the future. The Authority issues regulations and supervises compliance, while also supporting research, providing training and information, and issuing advice. Often, activities involving radiation require licences issued by the Authority. The Swedish Radiation Safety Authority maintains emergency preparedness around the clock with the aim of limiting the aftermath of radiation accidents and the unintentional spreading of radioactive substances. The Authority participates in international co-operation in order to promote radiation safety and finances projects aiming to raise the level of radiation safety in certain Eastern European countries.

The Authority reports to the Ministry of the Environment and has around 270 employees with competencies in the fields of engineering, natural and behavioural sciences, law, economics and communications. We have received quality, environmental and working environment certification.

Strålsäkerhetsmyndigheten
Swedish Radiation Safety Authority

SE-171 16 Stockholm
Solna strandväg 96

Tel: +46 8 799 40 00
Fax: +46 8 799 40 10

E-mail: registrator@ssm.se
Web: stralsakerhetsmyndigheten.se